University of Tuscia

Department for Innovation in Biological, Agrofood and Forest systems (DIBAF)

PhD course in Science, Technology, and Biotechnology for Sustainability – XXXIII cycle

DIACHRONIC ANALYSIS OF LAND COVER USING OPEN SATELLITE IMAGES

AGR/05

PhD Student
Dt. Paolo De Fioravante

PhD Coordinator
Prof. Andrea Vannini

Tutor
Prof. Marco Marchetti

A.Y. 2019/2020

University of Tuscia

Department for Innovation in Biological, Agrofood and Forest systems (DIBAF)

PhD course in Science, Technology, and Biotechnology for Sustainability – XXXIII cycle

DIACHRONIC ANALYSIS OF LAND COVER USING OPEN SATELLITE IMAGES

AGR/05

PhD Student
Dt. Paolo De Fioravante

Signature Paolo De Fioravante

PhD Coordinator
Prof. Andrea Vannini

Signature

Tutor
Prof. Marco Marchetti

Signature Marco Marchetti

A.Y. 2019/2020

Short abstract

The study of land cover and land use dynamics is fundamental to understand causes and effects of the radical changes that human activity is causing locally and globally and to analyse the continuous metamorphosis of the landscape. In the European context, the Copernicus Programme offers several land monitoring tools to users and decision makers, however these are often technically limited complicating analysis, assessment and planning activities.

The first objective of this research examines limits and potential of land cover and land use products available for the Italian territory highlighting significant heterogeneity in terms of formats, spatial resolution, classification systems, reference years and updating frequency. A land cover map was produced integrating the main data analysed, referring to 2012. This study allowed to define the criteria to develop and implement a land cover mapping methodology through the classification of Copernicus Sentinel-1 and Sentinel-2 satellite data. The goal is creating an algorithm which could rapidly process large amounts of data, obtaining products on a national scale with high spatial resolution and update frequency.

The methodology is based on defining decision rules and is designed to be versatile and economically sustainable. Great attention was paid to compatibility with the main activities planned in near future at national and European level. In this sense, a land cover classification system consistent with the European specifications of the EAGLE group has been adopted. The organization of classes follows a modular approach, fully compatible with classification systems of main national and European data. This activity allowed to produce a land cover map for 2018 and the change detection related to forest disturbances and land consumption for 2017-2018. The products have geometric, temporal and thematic characteristics in line with requirements set out in the Space Economy Strategic Plan of the Italian Ministry of Economic Development and with CORINE Land Cover Plus (CLC+). The land cover classification methodology was published in “Land” journal while the change detection methodology was the theme of two publications in “Journal of Maps” and “Remote Sensing” journal. The content of the three publications is taken up and deepened in this thesis.

The rapid and continuous expansion of urban surfaces, often improperly planned and unjustified by population growth, leads to serious environmental, economic and social consequences. Particular attention was therefore paid to transformations related to urbanization phenomena which were studied analysing a set of indicators. In detail, the phenomenon of land consumption was analysed with reference to the new classification system introduced by ISPRA and with respect to elevation, slope, the presence of EUAP protected areas and the distance from the coastline. The analysis on land consumption in coastal area have been published in the "Environmental Engineering and Management Journal". A second level of analysis focused on fragmentation induced on natural areas by land consumption and on the description of spatial evolution of the main Italian metropolitan areas. The study highlighted the presence of strong pressures in coastal area, in plains and close to large metropolitan areas and infrastructures, while the protection regime that applies to EUAP areas is proving effective. The phenomenon of urban sprawl remains, due to the low-density expansion of cities in peripheral areas.

Two United Nations Sustainable Development Indicators (SDGs) were also tested to assess land degradation at a national scale and the correlation between urban growth and population in the main Italian cities. Given the strategic importance of the SDG indicators for environmental monitoring in near future, the estimation of indicators was accompanied by an analysis of how the indicators and their interpretation are affected by the characteristics of input data.

The analysis on land consumption and related phenomena were used in several editions of the ISPRA reports "Land Consumption, territorial dynamics and ecosystem services", "Environmental Data Yearbook" and "Report on Urban Environment Quality".

Keywords

Land cover, Eagle, Copernicus, Sentinel, Sustainable Development Goals (SDGs), CORINE Land Cover, land consumption

Extended abstract

Introduction

Monitoring land cover is a fundamental activity, especially in the European Union, to provide spatial data for comprehensive assessment and mapping of ecosystem services, thus offering a helpful tool to support decision-making activities (Maes *et al.*, 2013).

In the European context, the Copernicus Programme offers many land monitoring tools to users and decision makers, however these are often characterized by technical limitations from a thematic, temporal and geometric point of view. At the national level, the panorama of products to study land cover and land use is fragmented, characterized by data that are often not updated and with inhomogeneous classification systems.

Many initiatives are underway to harmonize spatial data in terms of thematic and geometric characteristics (EAGLE concept, INSPIRE Directive) and to better integrate and compare different datasets (CORINE Land Cover Plus).

The main purpose of this research is to develop a land cover classification methodology that allows to obtain homogeneous data for the entire national territory, with high spatial resolution, high update frequency and accuracy in line with the main Copernicus products. Another essential requirement is linked to the compatibility and continuity with the main national and European initiatives, such as the CLC+ project or the Space Economy Strategic Plan of the Italian Ministry of Economic Development. In this sense, a classification system coherent with the indications of the EAGLE model has been defined, and Sentinel data are used as a geometric reference. The research activity is based on data deriving from Sentinel missions and all analysis are carried out through free software, in fact the methodology is developed on Google Earth Engine and is compatible with the DIAS Onda and with the "SCP" plugin for QGIS.

Materials and methods

The first part of the research involves the definition of a methodology to classify Sentinel data to produce land cover maps on a national scale, with high spatial resolution, high update frequency and EAGLE compliant classification system.

Preliminarily, an analysis of limits and potential of the main spatial data available for the Italian territory was done. This analysis was firstly referred to the data of the Land

Monitoring Service of the Copernicus Program (CLMS), with particular reference to the Pan-European component (CORINE Land Cover, High Resolution Layers) and Local component (Urban Atlas, Riparian Zones, Natura 2000). About national products, National Land Consumption Map of ISPRA and regional land cover and land use maps were considered. Data were selected, standardized in terms of format, classification system and reference system and combined in a 2012 land cover map, which was the reference year for most of the data considered at the time of the research. This analysis allowed to define some of the criteria for developing and implementing a land cover mapping methodology through the classification of Copernicus Sentinel-1 Sentinel-2 satellite data.

The methodology was published on “Land” journal whit the title “Multispectral Sentinel-2 and SAR Sentinel-1 integration for automatic land cover classification” (De Fioravante *et al.*, 2021) and involves the calculation of multi-temporal indices and decision rules that allow to identify land cover classes based on the spectral and backscatter characteristics of pixels. Three distinct sets of decision rules have been developed, one for each of the following land cover macro-classes: abiotic surfaces, biotic surfaces and water surfaces.

In addition, a set of rules has been developed for detecting land cover changes, with reference to the monitoring of forest disturbances and land consumption.

As for land consumption, the variations in NDVI and backscatter were analysed to identify the changes that occurred within a year. This study allowed the creation of a support layer for photointerpretation used by ISPRA in the updating of the National Land Consumption Map (Munafò, 2020) and was published on “Remote Sensing” journal (Luti *et al.*, 2021) and on “Journal of maps” (Strollo *et al.*, 2019). To identify forest disturbances, the change in the median of NDVI and NBR of the areas classified as woody vegetation was observed.

The analysis was conducted for the Italian territory, with reference to 2018 for the land cover and to the period 2017-2018 for land cover changes.

Data produced under this research refer to classification systems developed considering the EAGLE group (EIONET Action Group on Land monitoring in Europe) specification, in order to maintain consistency with future European products and standards.

The land cover map obtained from Sentinel data has a three-level classification system. It consists of land cover classes at the first two levels, while the “biotic-vegetated” class is then further articulated through a third classification level based on EAGLE biophysical characteristics and temporal parameters:

1. Unvegetated-abiotic surfaces (divided into artificial surfaces and natural surfaces);

2. Vegetated-biotic surfaces (distinguished between woody vegetation, subdivided into broad-leaved, needle-leaved, permanent herbaceous vegetation and periodic herbaceous vegetation);
3. Water surfaces (liquid water and solid water).

The land cover map for 2012, obtained merging the available National and Copernicus data, refers to an expanded version of the classification system described above, to maintain the thematic detail offered by input data.

Starting from the maps, surface statistics were elaborated and a comparison was made with the CORINE Land Cover, which is a reference data in the description of land use and land cover on a large scale.

Particular attention was paid to transformations of territory related to urbanization phenomena which were studied analysing a set of indicators. Artificial surfaces have undergone the greatest development in the last few decades and they are associated with the greatest impacts.

First, the evolution of land consumption in Italy was observed using the ISPRA National Land Consumption Map. The phenomenon was analysed with reference to state and evolution at a national level and in specific areas, such as protected areas and with respect to elevation and slope variations. An in-depth analysis was carried out on the evolution of land consumption in the coastal area, which have been published in the "Environmental Engineering and Management Journal" (Riitano *et al.*, 2020). Particular attention was given to the third classification level introduced by ISPRA in 2016 for the characterization of different types of land consumption.

The impact of land consumption was also assessed in terms of the fragmentation it causes on natural areas, through the calculation and interpretation of effective mesh density indicator for the period 2012-2019 (Jaeger and Tappeiner, 2007). The analysis considered land consumption as a fragmenting element and results were returned with respect to a 1 km grid. The analysis was used in several editions of the ISPRA reports "Land Consumption, territorial dynamics and ecosystem services" (Munafò, 2018, 2019, 2020) and "Environmental Data Yearbook" (ISPRA, 2018a, 2018b, 2019b, 2019a).

A third level of analysis involved the study of the forms of urbanization and type of settlements and their evolution in the main metropolitan areas. Appropriate landscape metrics were calculated for the period 2012-2019 (Largest Class Patch Index, Edge Density, Residual Mean Patch Size) (McGarigal, K., SA Cushman, 2012) and the results were published in the ISPRA "Report on Urban Environment Quality" (ISPRA, 2018c, 2019c).

Finally, two of the indicators associated with the United Nations Sustainable Development Goals (SDGs) were tested. The SDG 11.3.1 indicator refers to the "Ratio of land consumption rate to population growth rate". It is particularly useful to understand the link between population variation and land consumption variation, especially in metropolitan areas. The indicator was analysed for 2012-2018. Three input data were compared: CORINE Land Cover, Urban Atlas and the National Land Consumption Map, in order to evaluate the importance of the spatial resolution of input data in describing the phenomenon. Provinces of Bologna, Milan, Neaples, Rome, Venice and Trieste were considered as study areas. A reflection was then conducted on the definition of land consumption to be considered and an interpretation of the indicator was carried out in provinces of those above mentioned capitals.
The SDG 15.3.1 indicator estimates the "Proportion of land that is degraded over total land area". The estimate was carried out for 2012-2019 with reference to the three sub-indicators suggested by the UNCCD (land cover change, land productivity dynamics, soil organic carbon stock) integrated with seven further sub-indicators related to elaborations carried out during this research or taken into consideration by ISPRA to study of the phenomenon. The results related to land degradation were published in the ISPRA report "Land Consumption, territorial dynamics and ecosystem services" (Munafò, 2018, 2019, 2020).

Results and discussion

The 2012 Land Cover Map based on Copernicus and national data reaches an overall accuracy of 90%. The comparison with CORINE Land Cover 2012 and CORINE Change 2012-2018 shows a strong increase in detail in urban areas, which allows to better define the shape of built-up areas and green urban areas and to identify small agglomerations and the road network.
The map clearly distinguishes the patches of trees, permanent crops, herbaceous vegetation and bushes that fall within the CLC mixed and transition areas. The geometry of water bodies and surrounding areas and the identification of small plots of permanent crops among larger agricultural areas is also better than CLC.
This activity allowed to analyse in detail the main data available for the Italian territory at national and European level. CLC is still one of the few data able to guarantee information on land cover and land use for the entire national territory, however it has significant limitations in terms of geometric detail and update frequency. Other Copernicus data offer a higher geometric detail (Urban Atlas, Riparian Zones, Natura 2000) but they are limited to specific territorial areas and they updated with low frequency. The land cover and land use maps

available at regional level in Italy are often based on CLC and are updated in a few cases (Lombardia updated to 2018, Toscana to 2016, Liguria to 2018 and Lazio to 2016). Furthermore, all the aforementioned data still have some thematic critical issues. It is therefore complex to compare different data to conduct studies at different levels of detail, due to the presence of mixed classes and the joint use of land use and land cover definitions.

From the analysis of the 2018 land cover map, it results an overall accuracy of 82%. The map shows a significant improvement in geometric detail compared to CLC. In detail, artificial abiotic surfaces are better identified, especially in agricultural areas and in the CLC classes of "Discontinuous urban fabric" and "Artificial, non-agricultural vegetated areas". Detection of permanent crops and shrubs can improve, while the description of permanent water bodies is accurate. An increase in geometric detail is also visible the description of woody vegetation, mostly in riparian areas, agricultural areas and at CLC mixed classes.

The versatility of the algorithm and the classification system make the methodology suitable for future integrations and adaptation for specific purposes and the products obtainable applying the methodology have thematic, geometric and temporal characteristics that make them consistent and useful in the panorama of the main national and European initiatives for land monitoring. In detail, the products are in line with the requirements set by the Mirror Copernicus as part of the national Space Economy plan of the Ministry of Economic Development, where a Sentinel resolution map with a high update frequency is required to monitor activities at a national scale. It is also compliant with the CLC+ project, in particular with the "CLC+ Core" component, which provides an integration of national and European data harmonized according to an EAGLE classification system to create "instances" to meet specific monitoring needs.

Overall, the analysis of the indicators related to urbanized areas and land consumption showed strong pressure from land consumption and consequent fragmentation and degradation associated with it, especially in coastal areas, in the plains and near large metropolitan areas and infrastructures. The phenomenon of urban sprawl is extremely present close to large cities. The analysis of the SDGs showed the following results:

- SDG 11.3.1 "Ratio of land consumption rate to population growth rate".

  Comparing different input data shows how the spatial resolution, hence the chance to monitor in detail the evolution of consumed land, is fundamental in describing the indicator. In almost all the municipalities considered there is an increase in land consumption, not always connected to population growth.

- SDG 15.3.1 “Proportion of land that is degraded over total land area”.
  Analysis of the sub-indicators considered to evaluate soil degradation shows that between 2012 and 2019 about 90,000 km^2 of territory were affected by the presence of at least one new form of degradation. The areas in which there are more than three forms of degradation cover about 1,600 km^2.

Conclusions and future perspectives

The analysis shows the presence of strong pressures exerted by anthropogenic activity on the natural environment, which require adequate monitoring tools to be understood and managed. This research lays the foundations to create land cover products able to fit within this framework. The proposed methodology has geometric and thematic characteristics compliant with future CLC+ products and with the Space Economy strategic plan. Furthermore, the proposed method consists in defining thresholds and set of rules which can be modified and adapted to different needs. Moreover, the classification system based on EAGLE, allows to introduce new classes and it can be modified for specific purposes, for example with land use attributes to describe agricultural areas. The methodology lends itself to extensions and improvements, such as defining variable thresholds based on altitude, latitude and phytoclimatic characteristics and by exploiting the new free hyperspectral data from the “Hyperspectral Imaging Mission for the Environment” (CHIME). In this way it will be possible to better analyse the phenological characteristics of vegetation to improve mapping of plant species, transition areas and the identification of forest disturbances.

The main limitation in the definition of the change detection algorithms is that the launch of Sentinel satellites took place quite recently and the historical series of images currently available has limited the elaboration of diachronic maps and indicators. Hopefully, in future we could be able to test the algorithm on a larger historical series of data and improve the change detection methodology regarding the description of a larger number of classes.

Despite this, a large set of indicators was analysed, allowing to evaluate the evolution of national territory starting from the analysis of cartographic products based on existing data. The analysis of large-scale land cover changes allowed to describe the main pressures exerted on the natural environment by the territorial dynamics associated with urban areas, land consumption and land degradation.

Acronyms

Abbreviation	Meaning	Abbreviation	Meaning
AAPN	Other National Protected Areas	LCC	Land Cover Components
AAPR	Other Regional Protected Areas	LCCS	Land Cover Classification System
AM	Marine Protected Areas	LCM	National Land Consumption Map
ANN	Artificial neural network	LCPI	Largest Class Patch Index
BI	Burned Index	LCR	Land Consumption Rate
BOA	Bottom Of Atmosphere	LU	Land Use
CAP	Common Agricultural Policy	LUA	Land Use Attributes
CBC	Cross-boundary connections procedure	MAES	Mapping Assessment of Ecosystems and their Services
CH	Landscape Characteristics	Meff	Effective Mesh Size
CHIME	Hyperspectral Imaging Mission for the Environment	MLC	Maximum Likelihood classifier
CLC+	2nd generation CORINE Land Cover	MMU	Minimum Mapping Unit
CLCA	CORINE Land Cover Accounting Layer	MMW	Minimum Mapping Width
CLMS	Copernicus Land Monitoring Service	N2000	Natura 2000
CNN	Convolutional Neural Networks	NBR	Normalized Burn Ratio
CRCS	Italian Research Center on Land Consumption	NDCI	Normalized Difference Coniferous Index
DEF	Economic and Financial Document	NDSI	Normalized Difference Snow Index
DEM	Digital Elevation Model	NDVI	Normalized Difference Vegetation Index
DI	Dispersion Index	NDWI	Normalized difference water index
DLT	Dominant Leaf Type	NIR	Near Infrared
DLTC	Dominant Leaf Type Change	NPP	Net Primary Productivity
DT	Decision tree	PCA	Principal component analysis
DTM	Digital Terrain Model	PGR	Population Growth Rate
EAGLE	EIONET Action Group on Land monitoring in Europe)	PNR	Regional and Interregional Natural Parks
ED	Edge Density	PNZ	National Parks
EEA	European Environment Agency	PRISMA	HyperSpectral Precursor of the Application Mission
EFFIS	European Forest Fire Information System	RF	Random Forest
ETRS	European Terrestrial Reference System	RLCRPGR	Ratio of land consumption rate to population growth rate
EUAP	Official List of Protected Areas	RMPS	Residual Mean Patch Size
EW	Extra-Wide swath	RNN	Recurrent Neural Networks
FAO	Food and Agriculture Organization of the United Nations	RNR	Regional Natural Reserves
FAPAR	Fraction of absorbed photosynthetically active radiation	RNS	State Natural Reserves
FUA	Functional Urban Areas	RUSLE	Revised version of the universal soil loss equation
GHSL	Global Human Settlement Layer	RZ	Riparian Zones
GRA	Grassland Status Layer	SAR	Synthetic Aperture Radar
GRAC	Grassland Change Layer	SBU	Share of Built-up
GRD	Ground Range Detected	SDG	United Nations Sustainable Development Goals
HRL	High Resolution Layers	Seff	Effective Mesch Density
IBU	Imperviousness Built-up	SLC	Single Look Complex
IGM	Italian Military Geographical Institute	SM	Stripmap
IMC	Degree of Imperviousness change	SOC	Soil organic carbon
IMCC	Degree of Imperviousness change classified	SRTM	Shuttle Radar Topography Mission
IMCS	Degree of imperviousness change	SWIR	Short Wave Infrared
IMD	Degree of Imperviousness	TCCM	Tree Cover Change Mask
IMDCL	Confidence layer for the imperviousness	TCD	Tree Cover Density
ISPRA	Italian Institute for Environmental Protection and Research	TOA	Top Of Atmosphere
IW	Interferomatric Wide swath	UA	Urban Atlas
JRC	Joint Research Center	UN	United Nations
LAEA	Lambert Azimuthal Equal Area	WV	Wave
LC	Land Cover	WWPI	Water and Wetness Probability Index

Contents

1 Introduction

The territory is the product of the history of human civilizations, their work, their culture, the system of relations between society and the environment (Magnaghi, 1990). At the same time, it is also a source of resources such as food, biomass and raw materials and provides essential ecosystem services that support production functions, regulate natural cycles, provide cultural and spiritual benefits (Munafò, 2018).

The European Environment Agency introduced the concept of "land system" which defines the territory as the set of terrestrial components which include all the processes and activities related to its anthropic use (Verburg *et al.*, 2013; EEA, 2017f). This concept considers the territory as an integrated system (EEA, 2018a) that combines everything related to land use and land cover. The changes and transformations that occur within the land system lead to consequences on the well-being of humans and the environment at the local, regional and global levels. For this reason, the management of the territory is a fundamental aspect. The study of land cover and land use is essential to understand the causes and effects of human-determined changes (Anderson, 1977). In fact, the transformation of the territory alters the environmental processes and related ecosystem services, which are the benefits that humans obtain directly or indirectly from terrestrial ecosystems (Costanza *et al.*, 1997).

Good land management require effective policies, such as the Community Agricultural Policy (CAP), the "no-net-land-take" of the European Commission by 2050, the Natura 2000 network, the Water Framework Directive (WFD) and the 2020 Biodiversity Strategy. At the international level, a fundamental support to policies for proper land management are the United Nations Sustainable Development Goals (SDGs) and in particular SDG 15[1] and 11[2] (UN, 2016).

This research takes place while a transition is underway in environmental monitoring. The availability of innovative technical solutions and powerful calculation tools has made it possible to have increasingly specific, complex and refined products and solutions for monitoring. Actually these tools are often difficult to interoperate and integrate, leading to a non-optimal management of the resources used for their development. In this sense, a

[1] SDG 15: Protect, restore and promote sustainable use of terrestrial ecosystems, sustainably manage forests, combat desertification, and halt and reverse land degradation and halt biodiversity loss.
[2] SDG 11: Make cities and human settlements inclusive, safe, resilient and sustainable.

process of rationalization of spatial information has begun. Numerous initiatives have been introduced at national and European level in order to make the different products more interoperable from a geometric and semantic point of view, such as the Copernicus Program, the INSPIRE directive and the EAGLE model. This research has a twofold objective. On the one hand, it aims to conduct a synthesis of the main land monitoring tools available for the Italian territory highlighting their criticalities, strengths and limitations. On the other hand, it aims to produce a land cover classification and change detection methodology capable of filling these gaps, maintaining a high level of compatibility with future land monitoring initiatives, such as the CORINE Land Cover Plus or the Space Economy Strategic Plan of the Italian Ministry of Economic Development.

The methodology, analysis and products developed in this research aim to investigate the potential of the free Copernicus Program data by exploiting open source software, in the spirit of sharing and democratizing knowledge.

Particular attention was given to land consumption and the development of urban areas. The harmful role of urban expansion on ecosystem functions is universally recognized in influencing the services they provide to humans and other life on earth (Alberti, 2005). They can lead to hydrological impacts, influencing runoff in urban catchments (Jacobson, 2011), reduces crop production (Ceccarelli *et al.*, 2014). Human pressure on soil is a key driver of the loss of biodiversity and ecosystem services (Haines-Young, 2009). One of the most serious consequences of the urbanization process is the land consumption, which causes the permanent loss of the natural soil, and it is the main cause of land degradation (Munafò, 2020). A set of indicators connected with the state and evolution of land consumption in Italy were therefore investigated, based on the integration of surface statistics, landscape metrics and two of the SDG indicators proposed by the UN for degradation and urban areas monitoring.

2 State-of-the-art

2.1 Regulatory context

European context

The European Union bases itself on the three dimensions of sustainability one of which is the environment. At European level, "thematic strategies" in the environmental field have often been issued, bound by specific Directives and aiming at establishing cooperation measures and guidelines addressed to Member States and local authorities.

The first formal political commitment of the European Commission for soil protection is the 2002 Communication entitled "Towards a thematic strategy for soil protection" (European Commission, 2002). The document highlighted the importance of soil as an essential and non-renewable resource and stressed the need for an integrated European policy to protect it.

In September 2006 the European Commission adopted the Thematic Strategy for Soil Protection, which included the proposal for a Framework Directive (Semikolennykh, 2008). The central themes of the strategy focused on prevention of new soil degradation and the need to implement good practices to reduce the negative effects of land consumption.

In 2011, the Roadmap towards an efficient Europe in the use of resources (European Commission, 2011) included the objective of "no net land take" by 2050 in Europe among the political priorities of the Union.

The net land take is calculated as the balance between land take and the increase in agricultural, natural and semi-natural areas due to restoration or renaturalization (European Commission, 2013).

In detail, to achieve the goal of "no net land take" by 2050 it is required to:

- avoid soil sealing of agricultural and open areas;
- compensate the "unavoidable residual component" through renaturalization of an area of equal or greater extension which may provide the ecosystem services with the amount of consumed natural land.

It is important to underline that this approach limits the phenomenon but does not eliminate it, as the "unavoidable residual component" implies the loss of important portions of resources.

In 2012, the Commission also published the guidelines for achieving the "no net land take" (European Commission, 2013) proposing to implement policies and actions to dicrease, mitigate and compensate land take. These measures would be defined and implemented in detail on a national, regional and local scale by member states.

In 2013, the goal of "no net land take" by 2050 was included in the Seventh Environmental Action Program ("Living well within the limits of our planet") (European Union, 2013). Unlike the 2011 Roadmap, the Environmental Action Program is a regulatory tool.

The proposal for a directive on soil was withdrawn in 2014 following the opposition of some Member States whose clear legislation on the environment conflicted with these new rules.

However, approaching complex problems such as soil protection should be established on integrated measures and policies.

Soil protection, erosion mitigation, landscape protection as well as limitation of the abandonment of agricultural areas are important elements in the Common Agricultural Policy (CAP) 2014-2020 and in the next post-2020 programming. Local land management by farmers and rural populations represents a strategic element (Vrebos *et al.*, 2017) that can significantly contribute to reducing degradation and abandonment of agricultural areas and therefore, indirectly, decrease land consumption.

In 2019, the European Commission launched the European Green Deal which provides indications for efficient management of resources, protection of biodiversity and reduction of pollution. The European Green Deal includes initiatives and measures for soil protection and restoration of degraded soils, in particular the European Union biodiversity strategy for 2030 and the action plan "Towards a Zero Pollution Ambition for air, water and soil - building a Healthier Planet for Healthier People".

The biodiversity strategy ("Bringing nature back into our lives") (European Commission, 2020) was adopted on May 20th, 2020 and sets several objectives:

- increase of land protected areas to 30% (+4%) of the EU surface; among these, one third should become strictly protected;
- an update of the EU thematic strategy for soil in 2021, for organic management of soil that allows to honour the international commitments to achieving land degradation neutrality;
- introduction of legally binding restoration objectives for degraded ecosystems, especially those most capable of capturing and storing carbon and preventing and reducing the impact of natural disasters;

- creation of the European Soil Observatory, included in the 2021-2027 work program of the Joint Research Center of the European Commission.

As for agricultural areas, the strategy has set ambitious objectives:

- use at least 25% of agricultural land for organic farming (we are about 8% in the EU) and increase the spread of agroecological practices;
- reduce the use of pesticides by 50%;
- allocate at least 10% of agricultural areas to characteristic landscape elements with high diversity.

The strategy for biodiversity refers to the strategy for a sustainable environment tackling the issues related to land consumption, soil sealing and regeneration of contaminated sites.

The zero pollution action plan for air, water and soil is driven by the intention to eliminating pollution and toxic substances by 2021.

International context

"The future we want" (UN, 2012) is the report published at the end of the 2012 United Nations Conference on Sustainable Development. It invited governments to pay greater attention to decisions related to land management with respect to environmental, social and economic impacts that cause land degradation.

In 2015, the United Nations Global Agenda for Sustainable Development (UN, 2017) defined the Sustainable Development Goals (SDGs) and indicated, among others, some targets of particular interest for the territory and the soil to be integrated in national programs in short and medium term and to be achieved by 2030:

- ensure that land consumption does not exceed population growth;
- ensure universal access to safe, inclusive and accessible green spaces and public spaces;
- achieve land degradation neutrality, as an essential element for maintaining ecosystem functions and services.

Countries that have signed up to the Agenda (including Italy) have agreed to monitor these objectives, managed by the United Nations Statistical Commission, through a system of indicators related to land consumption, land use and land degradation.

At national level, the National Strategy for Sustainable Development (SNSvS) is the tool that deals with implementing the objectives set by the 2030 Agenda.

The SNSvS 2017-2030 aims at creating a new low-carbon economic model, resilient to climate change and other global changes that cause local crises, such as loss of biodiversity, modification of fundamental biogeochemical cycles and changes in the land use.

In detail, the EU's long-term budget provides a 1074.3 billion euros budget for 2012-2027, 365.4 of which are dedicated to Natural resources and environment. “Funding in this focuses on delivering added value through a modernised, sustainable agricultural, maritime and fisheries policy as well as by advancing climate action and promoting environmental and biodiversity protection” (European Council, 2020).
A temporary instrument was also provided to stimulate immediate recovery: NextGenerationEU (Council, 2020) with 17.5 billion euros provided to the environmental field.

National context

At national level there is no fundamental law to protect the environment, the territory and the Italian landscape. Such an instrument would be indispensable to face challenges such as sustainable development of land use, increasing the resilience of the territory, adaptation to climate change.
In 2012, the first bill to decrease land consumption was presented and entitled “enhancement of agricultural areas and containment of land consumption”; it was not approved due to the early termination of Legislature. A new government-initiated bill was presented in 2014. The text was subject to profound changes and was finally not approved due to the end of Legislature. Several bills have been presented in the past. Some reflect the previous text and other refer to popular initiative proposal, as in the case of C.A.63 “Provisions for the containment of land consumption and for the reuse of built soils” presented by the Save the Landscape Forum in 2018.
The most recent bill is dated April 20, 2021 and is entitled “Regulations for urban regeneration” (Senate Act n.1981). The bill provides financial incentives, both for municipalities and private citizens, to regenerate and reuse abandoned post-industrial areas and surfaces, as well as the agroforestry use of abandoned agricultural land, for the purpose of containing land consumption.
Recently, various non-programmatic legislative interventions on environmental issue have been carried out. The Climate Decree Law (Legislative Decree 14/10/2019, n.111) has introduced many measures to encourage the achievement of sustainability objectives:

- funding an experimental program for reforestation of metropolitan cities is foreseen, for an amount of 15 million euros for both year 2020 and 2021;
- reforestation of riparian belts became one of the criteria to entryst management works of state-owned riparian areas, in order to contrast hydrogeological instability;

- areas that have suffered damage from exceptional climatic events are privileged in planning reforestation interventions and it is forbidden to increase waterproofing in areas with high hydraulic criticality;
- it establishes a fund for safety measures, soil maintenance and reforestation carried out by agricultural and forestry companies in inland areas.

The 2020 budget law (L.27/12/2019, n.160) has several provisions in the environmental field, including the Italian green deal.

The establishment of a fund of about 20.8 billion euros is planned to invest in circular economy, decarbonisation of the economy, reduction of emissions, environmental sustainability and investment programs with high environmental and social sustainability. To this end, a monitoring system of the interventions financed by the Fund is envisaged, with an annual report by the Ministries.

The 2019 Economic and Financial Document (DEF) promoted urban regeneration interventions through simple and binding rules against land consumption. It also indicates measures to prevent and maintain the territory, to update planning tools and intriduce municipal ecological budget.

The DEF 2020 refers to policies on territory protection, even in a new economic framework characterized by the emergency from COVID-19 and the resulting economic and social needs. Specifically, the document focuses on territory vulnerability and indicates an extraordinary plan of interventions of 2.1 billion to fight hydrogeological instability.

2.2 Land cover, land use and the EAGLE concept

The INSPIRE directive (Directive 2007/2/CE) of the European Commission provides the following definitions of land cover and land use.

Land cover

Physical and biological cover of the earth's surface include artificial surfaces, agricultural areas, forests, (semi-) natural areas, wetlands, water bodies.

Land cover (LC) information has to be homogenous and comparable between different locations in Europe.

A land cover dataset consists of a collection of land cover units that can follow two core models: vector data or raster data.

Land use

Territory characterized according to its current and future planned functional dimension or socio-economic purpose (e.g. residential, industrial, commercial, agricultural, forestry, recreational).

Land Use (LU) describes the land in terms of its socio-economic and ecological purpose. For Existing Land Use we mean the description of the actual uses and functions of a territory, while for Planned Land Use we mean the possible utilization of the land in the future, based on the indications of the planning tools.

Land cover and land use are strongly related and for many applications both information are needed (Sallustio *et al.*, 2016). To meet different monitoring needs, data with different characteristics from a spatial, temporal and thematic point of view were introduced. They often adopt specific classification systems, based on different combinations of land cover and land use classes that are difficult to compare and integrate with those of other data.

An example are the Copernicus data. The CLC is a reference in studying land use and land cover, however it adopts a classification system with numerous criticalities:

- presence of land cover and land use classes, with ambiguous or non-exhaustive description of some of them;
- it considers temporal aspects only in some cases and it is not flexible with respect to new phenomena (e.g. energy crop plantations, artificial snowmaking, habitat restoration);
- absence of parameterized information on aspects such as imperviousness or crown cover density;
- unequal representation of landscape types from different bio-geographical regions.

Urban Atlas refers to the CLC classification system describing in greater detail the land cover and land use characteristics of urban areas, while Riparian Zone, Coastal Zone and Natura 2000 use the ecosystem types defined in the Mapping Assessment of Ecosystems and their Services (MAES) (Maes *et al.*, 2013), which are based on the CLC classes too.

In order to coordinate data flows from a thematic point of view, the EAGLE group (EIONET Action Group on Land monitoring in Europe) was created. It aims at defining a conceptual methodology to describe land cover and land use information in a consistent data model.

The EAGLE model aims at separating the land cover and land use components through data modelling systems applicable at different scales and in different contexts, while maintaining compatibility with existing databases.

The data model proposed by the EAGLE group is based on the definition of three blocks, called “categories”. Each block is divided into “segments” that can have different hierarchical levels. Element that stands in the lowest hierarchy level under the segments, are referred to as “types”. The three categories are described below:

- *Land Cover Components (LCC)*

  It refers to the definition of “land cover” provided by the INSPIRE directive 2007/2/CE. The LCCs are mutually exclusive and exhaustive, i.e. an LCC or the combination of several LCCs allows you to describe any kind of land cover. Every level of LCC can be used as a modelling element to semantically describe a class definition or to map landscape.

- *Land Use Attributes (LUA),*

  The LUA follow in principle the Hierarchical INSPIRE Land Use Classification System (HILUCS), with some changes to fit the purpose of the EAGLE concept. The LUA are attached to the Land Cover Unit.

- *Landscape Characteristics (CH),*

  The Characteristics describe further details of the Land Cover Components. The first level of “segments” connected with this “block” distinguishes “Land management”, “Spatial pattern”, “Crop type”, “Mining Product Type”, “Ecosystem Types”, “Height Zone”, “(Bio-) Physical Characteristics”, “General Parameters”, “Status” and “Temporal Parameters”. Each segment then presents further levels.

EAGLE is not a classification system but a tool to describe classes of a given classification system by tracing them to the segments related to the three aforementioned categories. This allows us to better understand the characteristics of the various classes, the overlaps and the possible conversions between different systems. It also provides a basis to define new classification systems.

This allows to enhance the integration between national activities and European land monitoring initiatives encouraging a bottom-up approach in data production.

2.3 Copernicus programme

Copernicus is the European Union program to monitor the environment using space and in-situ data and observations. The European Commission coordinates the Copernicus program. As for infrastructures, the European Space Agency manages the satellite component while the European Environment Agency deals with the in situ surveys. Copernicus provides data on baseline services in topical areas allowing the development of other value-added products for specific public policies or commercial needs. All products and data provided by the Copernicus program are freely and openly accessible to users. Copernicus offers six core thematic services:

- *Atmosphere Monitoring*

  The service monitors air quality and UV forecasts at global and European level, greenhouse gases, climate forcing and emissions. The data available allows developing products and analysis related to the study of the composition of the atmosphere and the understanding of climate change.

- *Land Monitoring*

  It includes monitoring services useful to water management, agriculture and food security, land cover and land use evolution, urban planning, forest monitoring, soil quality and natural protection. It contains four components that will be described later.

- *Marine Environment Monitoring*

  The service provides systematic and regular information on the state of seas and oceans (such as currents, tides, winds, temperature, pollution and salinity). These information supports the development of numerous applications related to the improvement of routes, protection of marine resources, sustainable management of fisheries, monitoring of water quality, coastal erosion, climate change and weather.

- *Emergency Management*

  The service is a tool for subjects entrusted with the management of humanitarian emergencies or natural disasters (such as the Civil Protection Authority). It provides accurate and updated geo-spatial information from satellite and in situ surveys. Data can be integrated with other sources to obtain products to support specific analysis and decision-making processes in all phases of emergency management.

- *Security*

  The service supports European policies in three fundamental areas: border control (migratory phenomena and illegal trafficking at the borders of the European Union), maritime surveillance of the European coasts and Support for External Action of the European Union (which has an important role in the global promotion of principles such as human rights, freedom, democracy and to support third parties in the management of crises or emergencies).

- *Climate Change*

  The service supports other international initiatives to analyse human-induced climate change, in order to expand knowledge and allow the planning of mitigating interventions. The service uses satellite and in situ observations to elaborate numerous indicators (temperature variations, sea level rise, ocean warming, ice melting) and indices (for example those related to precipitation) to perform assessments on the current situation and produce simulations on the future climate evolution.

2.4 Copernicus Land Monitoring Service

Monitoring land cover and its evolution is crucial to define policies to protect the territory. In this respect, initiatives have been developed such as Corine Land Cover which offers data on land cover and land use for numerous European countries since 1990. The purpose of Copernicus Land Monitoring Service[3] (CLMS) is to collect information on the earth's surface and organize it according to criteria that allow to compare different data, the exchange between EU countries and the expansion of the number of users.

CLMS allows to obtain geographic information on soils and on numerous variables related to them (such as the state of the vegetation or the water cycle), supporting applications in a wide variety of sectors such as territorial planning, management of water resources and forests, agriculture and food security.

The Land Monitoring Core Service (LMCS) is composed by four components.

2.4.1 Copernicus Global Land Service (CGLS)

It is technically managed by the European Commission's DG Joint Research Center (JRC).

The global component[4] contains the following elements:

[3] https://land.copernicus.eu/
[4] https://land.copernicus.eu/global/index.html

1. A global systematic monitoring activity which provides near real time bio-geophysical parameters on vegetation state and dynamics and on land cover change at global scale. Production and delivery of parameters take place in a timely manner and the constitution of long term time series is expected. Specific attention is given to continuity and consistency with previous pre-operational activities avoiding gaps in the operational phase and ensuring time consistency of the parameters.
2. A High Resolution Hot Spot Monitoring activity, operating upon request for limited areas. It is based on the creation of land cover and land cover change products based on medium or high resolution images (from 1 to 30 m) with an update frequency between 1 and 10 years. It mainly refers to the sustainable management of natural resources, with an initial focus on Protected Areas or Key Landscapes for Conservation. The classification scheme follows the Land Cover Classification System (LCCS) developed by FAO organized according to a dichotomous (with 8 classes) or modular (up to 30 classes) legend.
3. A service related to Ground-based Observations for Validation, supporting the validation of products based on satellite observations or services and applications.
4. Development of thematic services to address the EU sectoral policies in specific thematic areas. In particular, there is an on-request activity in support of the Global Agriculture Monitoring initiative of the Group on Earth Observation, called Copernicus4GEOGLAM.

2.4.2 Copernicus pan-European component

The European Environment Agency (EEA) coordinates the pan-European component[5]. The main products offered by this service are CORINE Land Cover (CLC) and High Resolution Layers (HRL). Four new High Resolution Snow as Ice products have recently been published as part of the "biophysical parameters" section, providing information on Fractional Snow Cover, Persistent Snow Area, River and Lake Ice Extent and Aggregated River and Lake Ice Extent. In 2021, further products related to phenology and productivity, the European Ground Motion Service and CLC+ are expected to be published.

[5] https://land.copernicus.eu/pan-european

CORINE Land Cover

CORINE Land Cover (CLC) (Büttner *et al.*, 2017) is a vector data related to land cover and land use at European level for years 1990, 2000, 2006, 2012, and 2018. The main characteristics and differences between the versions are reported in Table 1.

Table 1. CORINE Land Cover specifications

	CLC1990	CLC2000	CLC2006	CLC2012	CLC2018
Satellite data	Landsat-5 MSS/TM	Landsat-7 ETM	SPOT-4/5, IRS P6 LISS III	IRS P6 LISS III, RapidEye	Sentinel-2, Landsat-8 (gap filling)
Time consistency	1986-1988	2000 ± 1	2006 ± 1	2011-2012	2017-2018
Geometric accuracy, satellite data	≤ 50 m		≤ 25 m		≤ 10 m (Sentinel-2)
Geometric accuracy, CLC	100 m		better than 100 m		
Thematic accuracy, CLC			≥ 85%		
Thematic accuracy, CHA	-	not checked		≥ 85%	
Production time	10 years	4 years	3 years	2 years	1.5 years
Countries involved	26 (27 with late implementation)	30 (35 with late implementation)	38	39	39

The CLC uses a Minimum Mapping Unit (MMU) of 25 ha and a Minimum Mapping Width (MMW) of 100 m. Change layers with higher resolution than the status layer are also available (MMU of 5 ha). The difference between two status layers will not be equal to the corresponding CLC-Changes layer due to the different MMU and the topological rules defined for updating the polygons.Thanks to the extension and the long historical series, CLC has a wide variety of applications, underpinning various Community policies in the domains of environment as well as agriculture, transport, spatial planning etc.

The data uses a classification system in 44 land cover and land use classes (Table 2).

Table 2. CORINE Land Cover classification system

I level		II level		III level	
1	Artificial surfaces	**11**	Urban fabric	**111**	Continuous urban fabric
				112	Discontinuous urban fabric
		12	Industrial, commercial and transport units	**121**	Industrial or commercial units
				122	Road and rail networks and associated land
				123	Port areas
				124	Airports
		13	Mine, dump and construction sites	**131**	Mineral extraction sites
				132	Dump sites
				133	Construction sites
		14	Artificial, non-agricultural vegetated areas	**141**	Green urban areas
				142	Sport and leisure facilities
2	Agricultural areas	**21**	Arable land	**211**	Non-irrigated arable land
				212	Permanently irrigated land

				213	Rice fields
		22	Permanent crops	**221**	Vineyards
				222	Fruit trees and berry plantations
				223	Olive groves
		23	Pastures	**231**	Pastures
		24	Heterogeneous agricultural areas	**241**	Annual crops associated with permanent crops
				242	Complex cultivation patterns
				243	Land principally occupied by agriculture, with significant areas of natural vegetation
				244	Agro-forestry areas
3	Forest and semi natural areas	**31**	Forests	**311**	Broad-leaved forest
				312	Coniferous forest
				313	Mixed forest
		32	Scrub and/or herbaceous vegetation associations	**321**	Natural grasslands
				322	Moors and heathland
				323	Sclerophyllous vegetation
				324	Transitional woodland-shrub
		33	Open spaces with little or no vegetation	**331**	Beaches, dunes, sands
				332	Bare rocks
				333	Sparsely vegetated areas
				334	Burned areas
				335	Glaciers and perpetual snow
4	Wetlands	**33**	Inland wetlands	**411**	Inland marshes
				412	Peat bogs
		42	Marine wetland	**421**	Salt marshes
				422	Salines
				423	Intertidal flats
5	Water bodies	**51**	Inland waters	**511**	Water courses
				512	Water bodies
		52	Marine waters	**521**	Coastal lagoons
				522	Estuaries
				523	Sea and ocean

High Resolution Layers

The High Resolution layers (HRL) are raster-based datasets that provide information with high spatial resolution for the whole of the EEA-39 area. They are complementary to other Copernicus data and are currently available for 2006, 2009, 2012, 2015 and recently 2018: HRLs refer to the five main themes of the CLC and each HRL corresponds to different products which can be divided into "primary", "derived" and "reference" products.

Imperviousness: It considers the sealed surfaces (e.g. roads and built up areas) and has a historical series that goes from 2006 to 2018 with three-year updates. Versions of this HRL prior to 2018 have a spatial resolution of 20 m (EEA, 2017c).

The following primary and derived products refer to the HRL imperviousness 2018:

- Degree of Imperviousness (IMD), is a raster displaying the degree of imperviousness (1-100%) for the reference year 2018 in 10 m spatial resolution. It is also available a 100 m resolution aggregate version.

- Imperviousness Built-up (IBU) is a raster displaying the built-up component of the imperviousness for 2018 in 10 m spatial resolution. It is in continuity with the European Settlement Map (ESM) which was originally produced by JRC as part of the Global Human Settlement Layer (GHSL). It is also available in aggregate version with 100 m spatial resolution called Share of Built-up (SBU).
- Degree of Imperviousness change (IMC) is a raster displaying the degree of imperviousness change (in percentage) between 2015 and 2018 in 20 m spatial resolution. It is also available in aggregate version with 100 m spatial resolution.
- Degree of Imperviousness change classified (IMCC) is a raster displaying the imperviousness change classified between 2015 and 2018 in 20 m spatial resolution.
- Confidence layer for the imperviousness 10 m status product (IMDCL) is a raster displaying a measure of confidence for the IMD 2018.
- Degree of imperviousness change (IMCS) is a raster displaying decreased and increased imperviousness density due to technical change. It is available at 20 and 100 m spatial resolution.

Forest: This HRL (EEA, 2017a) includes a set of products showing the tree covered surface and its evolution in the EEA-39 countries for 2012, 2015 and 2018. These products provide also details on coverage density and distribution of coniferous and broad-leaved trees. The versions of this HRL prior to 2018 have a spatial resolution of 20 m.
The portfolio of status layers and change products includes:

- Dominant Leaf Type (DLT) is a 10 m resolution raster obtained applying a Random Forest (RF) Classifier to Sentinel-2 images which describes the dominant leaf type (broad-leaved or needle-leaved).
- Tree Cover Density (TCD) is a 10 m raster with grid aligned to the DLT one. It provides information on the percentage of the pixel surface covered by trees;
- Forest Type is a forest product following the forest definition of FAO. It is available in 10 and 100 m spatial resolution.
- Tree Cover Change Mask (TCCM) and Dominant Leaf Type Change (DLTC) are 20 m resolution change layers derived from the binary masks of the corresponding status layers 2015 and 2018.

Grassland: This HRL (EEA, 2017b) includes natural, semi-natural and managed grasslands (according to their origin and utilization) as well as all types of grassland (permanent or seasonal) under highly heterogeneous biogeographic conditions (wet or dry climate, fertile or poor soil). Grass cover within the context of the product is considered as herbaceous vegetation with at least 30% ground cover. HRL grassland includes the following products:

- Grassland Status Layer (GRA) is a 10 m resolution binary raster for 2018 displaying grassland and non-grassland areas. Data are also available for 2015 with a resolution of 20 m and 100 m (aggregate version).
- Grassland Change Layer (GRAC) is a 20 m resolution raster showing changes in grassland vegetation cover between 2015 and 2018 and all unchanged areas with and without grass cover.

Water and wetness: This HRL (EEA, 2017d) maps permanent water, temporary water, permanent wetlands, temporary wetlands and dry areas, based on the water and wetness occurrences in period 2012-2018. Data are available for 2015 (with a resolution of 20 m) and recently also for 2018 (at 10 m and 100 m). The HRL also includes a product called Water and Wetness Probability Index (WWPI) which is a 10 m raster displaying a combined index of water and wetness based on 2012-2018 imagery for 2018, in 10 m spatial resolution.

Small woody features: This HRL (EEA, 2015) provides information on linear structures and little patches of woody features across the EEA39 countries. The dataset is currently available for 2015 reference year only and is produced in three different formats:

- Small Woody Feature Vector Layer, consisting of three classes (Linear elements, Patchy and additional Woody Features);
- Small Woody Feature Raster Layer with a spatial resolution of 5 m which distinguishes small woody features and additional woody features;
- Small Woody Feature 100 m Aggregate Layers, indicating the percentage of pixel surface covered by small woody features.

2.4.3 Copernicus Local component

The European Environment Agency coordinates the Copernicus Local Component. It aims at providing detailed information on critical areas from an environmental point of view, which require specific and detailed monitoring.

Currently, this Copernicus component offers land cover and land use maps in vector format, with high spatial resolution and a 6-year update frequency for four types of areas.

Urban Atlas, Riparian Zones and Natura 2000 were used extensively in this work, while the Coastal Zonea data was not included, since it was published in the final phase of the research.

Urban Atlas

Urban Atlas (UA) (European Commission, 2016) provides land cover and land use information with high spatial resolution for Functional Urban Areas (FUAs) for 2006, 2012 and 2018 (Table 3).

Table 3. Area covered by Urban Atlas

Reference year	Areas of interest
2006	319 Functional Urban Areas with more than 100,000 inhabitants (29 in Italy)
2012	785 Functional Urban Areas with more than 50,000 inhabitants (84 in Italy)
2018	788 Functional Urban Areas with more than 50,000 inhabitants (84 in Italy)

In Italy UA covers an area of 68,137 km^2, equal to 22.6% of the national surface (Figure 1).

Figure 1. Urban Atlas mapping in Italy

The spatial resolution is higher for artificial classes (0.25 ha) than for natural (1 ha).

There are two layers of changes, related to 2006-2012 and 2012-2016, with an MMU of:

- 0.1 ha for changes within class 1 and from natural classes to class 1;
- 0.25 ha for changes between natural classes or restorations.

UA also includes two layers introduced in 2012 and updated in 2018 for some FUAs only:

- Street Tree Layer was created starting from SPOT 5 images. It includes contiguous rows or patches of trees covering 500 m² or more, with a minimum width of 10 m within class 1 UA.
- Building height is a 10 m high resolution raster layer containing height information for core urban areas of 39 European capitals. Height information is based on IRS-P5 stereo images dataset.

UA adopts a four levels classification system which describes in detail (above) all the artificial surfaces (Table 4).

Table 4. Urban Atlas classification system

I level	II level	III level	IV level
1 Artificial surfaces	**11** Urban Fabric	**111** Continuous Urban Fabric (S.L.>80%)	
		112 Discontinuous Urban Fabric (S.L.:10%-80%)	**1121** Discontinuous Dense U.F. (S.L.:50%-80%)
			1122 Discontinuous Medium Density U.F. (S.L.:30%-50%)
			1123 Discontinuous Low Density U.F. (S.L.:10%-30%)
			1124 Discontinuous Very Low Density U.F. (S.L.:<10%)
		113 Isolated Structures	
	12 Industrial, commercial, public, military, private and transport units	**121** Industrial, commercial, public, military and private units	
		122 Road and rail network and associated land	**1221** Fast transit roads and associated land
			1222 Other roads and associated land
			1223 Railways and associated land
		123 Port areas	
		124 Airports	
	13 Mine, dump and Construction sites	**131** Mineral extraction and dump site	
		133 Construction sites	
		134 Land without current use	
	14 Artificial non-agricultural vegetated areas	**141** Green urban areas	
		142 Sports and leisure facilities	
2 Agricultural areas	**21** Arable land (annual crops)		
	22 Permanent crops (vineyards, fruit trees, olive groves)		
	23 Pastures		
	24 Complex and mixed cultivation patterns		
	25 Orchards at the fringe of urban classes		
3 Natural and semi-natural areas	**31** Forests		
	32 Herbaceous vegetation associations (natural grassland, moors...)		
	33 Open spaces with little or no vegetations (beaches, dunes, bare rocks, glaciers)		
4 Wetland			
5 Water bodies			

Riparian Zones

Riparian Zones (RZ) provides land cover and land use information with high spatial resolution in the areas between land and freshwater ecosystems for 2012 (Tamame *et al.*, 2018).

These areas have specific environmental and ecological conditions and provide a wide range of riparian functions (e.g. chemical filtration, flood control, bank stabilization, aquatic life and riparian wildlife support, etc.) and ecosystem services. RZ is a vector data with a MMU of 0.5 ha and a MMW of 10 m and supports many European legal acts and policy initiatives, such as the EU Biodiversity Strategy to 2020, the Habitats and Birds Directives and the Water Framework Directive.

In Italy RZ covers 40,273 km^2, equal to 13.4% of the national surface (Figure 2).

Figure 2. Riparian Zones mapping in Italy

The classification system is composed of 56 classes organized on four levels (Table 5).

Table 5. Riparian Zones classification system

I level		II level		III level		IV level	
1	Urban	**11**	Urban fabric, industrial, commercial, public, military and private units	**111**	Urban fabric (predominantly public and private units)	**1111**	Continuous Urban Fabric (IM.D ≥ 80%)
						1112	Dense Urban Fabric (IM.D ≥ 30 - 80%)
						1113	Low Density Fabric (IM.D < 30%)
				112	Industrial, commercial and military units		
		12	Transport infrastructure	**121**	Road networks and associated land		
				122	Railways and associated land		
				123	Port areas and associated land		
				124	Airports and associated land		
		13	Mineral extraction, dump and construction sites, land without current use	**131**	Mineral extraction, dump and construction sites		
				132	Land without current use		
		14	Green urban, sports and leisure facilities				
2	Cropland	**21**	Arable land	**211**	Arable land		
				212	Greenhouses		
		22	Permanent crops	**221**	Vineyards, fruit trees and berry plantations		
				222	Olive groves		
		23	Heterogeneous agricultural area	**231**	Annual crops associated with permanent crops		
				232	Complex cultivation patterns		
				233	Land principally occupied by agriculture with significant areas of natural vegetation		
				234	Agro-forestry		
3	Woodland and forest	**31**	Broad-leaved forest	**311**	Natural and semi-natural broad-leaved forest		
				312	Highly artificial broad-leaved plantations		
		32	Coniferous forest	**321**	Natural and semi-natural coniferous forest		
				322	Highly artificial coniferous plantations		
		33	Mixed Forest	**331**	Natural and semi-natural mixed forest		
				332	Highly artificial mixed plantations		
		34	Transitional woodland scrub	**341**	Transitional woodland and scrub		
				342	Lines of trees and scrub		
		35	Damaged forest				
4	Grassland	**41**	Managed grassland				
		42	Natural and semi-natural grassland	**421**	Semi-natural grassland		
				422	Alpine and sub-alpine natural grassland		
5	Heathland and scrub	**51**	Moors and heathland	**511**	Heathland and Moorland		
				512	Other scrub land		
		52	Sclerophyllous vegetation				
6	Sparsely vegetated land	**61**	Sparsely vegetated areas				
		62	Beaches, dunes, sands	**621**	Beaches and dunes		
				622	River banks		
		63	Bare rocks, burned areas, glaciers and perpetual snow	**631**	Bare rocks and rock debris		
				632	Burned areas (except burned forest)		
				633	Glaciers and perpetual snow		
7	Wetland	**71**	Inland marshes				
		72	Peat bogs	**721**	Exploited peat bog		
				722	Unexploited peat bog		
8	Lagoons, coastal wetlands	**81**	Coastal wetlands	**811**	Coastal salt marshes		
				812	Salines		
				813	Intertidal flats		
		82	Coastal waters	**821**	Coastal lagoons		

	and estuaries			**822**	Estuaries
9	Rivers and lakes	**91**	Water courses	**911**	Interconnected water courses
				912	Highly modified water courses and canals
				913	Separated water bodies belonging to the river system
		92	Lakes and reservoirs	**921**	Natural water bodies
				922	Artificial standing water bodies
				923	Intensively managed fish ponds
				924	Standing water bodies of extractive industrial sites

Natura 2000

Natura 2000 (N2000) provides high resolution land cover and land use information for areas relevant to protecting rare species and habitats, listed under the Birds Directive and the Habitats Directive (EEA, 2018b).

In Italy N2000 covers 77,703 km^2, equal to 25.8% of the national surface (Figure 3).

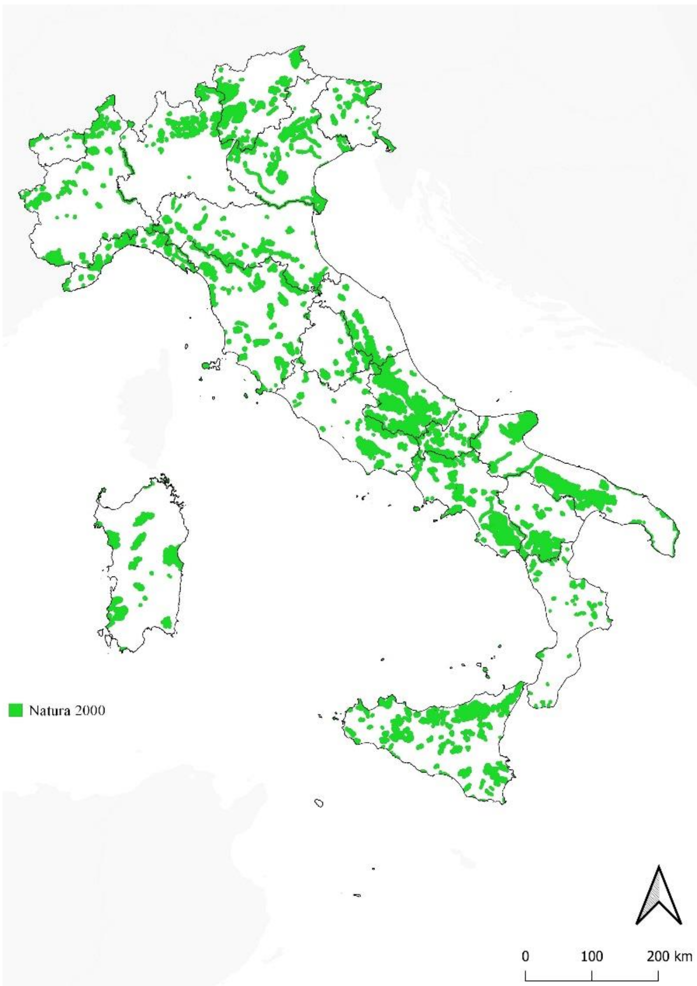

Figure 3. NATURA 2000 mapping in Italy

Data are in vector format, referring to 2006 and 2012, with MMU of 0.5 ha and MMW of 10 m. The N2000 classification system presented 62 classes in 2015 and was subsequently revised in 2017, to align it with those of the other Copernicus Local Component data. Currently the status layer is described by 55 land cover and land use classes (Table 6).
An extension to other habitat types is also foreseen and is currently under discussion.

Table 6. Natura 2000 classification system

Land cover							
I level		**II level**		**III level**		**IV level**	
1	Urban	**11**	Urban fabric, industrial, commercial, public, military and private units	**111**	Urban fabric (predominantly public and private units)		
				112	Industrial, commercial and military units		
		12	Transport infrastructure	**121**	Road networks and associated land		
				122	Railways and associated land		
				123	Port areas and associated land		
				124	Airports and associated land		
		13	Mineral extraction, dump and construction sites, land without use	**131**	Mineral extraction, dump and construction sites		
				132	Land without current use		
		14	Green urban, sports and leisure facilities				
2	Cropland	**21**	Arable land	**211**	Arable land		
				212	Greenhouses		
		22	Permanent crops	**221**	Vineyards, fruit trees and berry plantations		
				222	Olive groves		
		23	Heterogeneous agricultural area	**231**	Annual crops associated with permanent crops		
				232	Complex cultivation patterns		
				233	Land principally occupied by agriculture with significant areas of natural vegetation		
				234	Agro-forestry		
3	Woodland and forest	**31**	Broad-leaved forest	**311**	Natural and semi-natural broad-leaved forest		
				312	Highly artificial broad-leaved plantations		
		32	Coniferous forest	**321**	Natural and semi-natural coniferous forest		
				322	Highly artificial coniferous plantations		
		33	Mixed Forest	**331**	Natural and semi-natural mixed forest		
				332	Highly artificial mixed plantations		
		34	Transitional woodland scrub	**341**	Transitional woodland and scrub		
				342	Lines of trees and scrub		
		35	Damaged forest				
4	Grassland	**41**	Managed grassland				
		42	Natural and semi-natural grassland	**421**	Semi-natural grassland	**4211**	Semi-natural grassland with woody plants (C.C.D. ≥ 30%)
						4212	Semi-natural grassland without woody plants (C.C.D. ≤ 30%)
				422	Alpine and sub-alpine natural grassland		
5	Heathland and scrub	**51**	Moors and heathland	**511**	Heathland and Moorland		
				512	Other scrub land		
		52	Sclerophyllous vegetation				

6	Sparsely vegetated land	**61**	Sparsely vegetated areas		
		62	Beaches, dunes, sands	**621**	Beaches and dunes
				622	River banks
		63	Bare rocks, burned areas, glaciers and snow	**631**	Bare rocks and rock debris
				632	Burned areas (except burned forest)
				633	Glaciers and perpetual snow
7	Wetland	**71**	Inland marshes		
		72	Peat bogs	**721**	Exploited peat bog
				722	Unexploited peat bog
8	Lagoons, coastal wetlands and estuaries	**81**	Coastal wetlands	**811**	Coastal salt marshes
				812	Salines
				813	Intertidal flats
		82	Coastal waters	**821**	Coastal lagoons
				822	Estuaries
9	Rivers and lakes	**91**	Water courses	**911**	Interconnected water courses
				912	Highly modified water courses and canals
				913	Separated water bodies belonging to the river system
		92	Lakes and reservoirs	**921**	Natural water bodies
				922	Artificial standing water bodies
				923	Intensively managed fish ponds
				924	Standing water bodies of extractive industrial sites
10	Sea and ocean				

Coastal zone

Coastal zone provides high-resolution land cover and land use information for a 10 km buffer zone from the coast line. This activity aims at providing a useful tool to coordinate economic growth and maintains a resilient state of the coastal environment, safeguarding coastal protection.

The products have MMU of 0.5 ha and a MMW of 10 m and are based on the coastline derived from EU-Hydro.

The initial production of the Coastal Zones hotspot thematic mapping includes two land cover and land use maps for 2012 and 2018 and a map of changes.

The classification system is composed of 71 classes consistent with those of other Copernicus Local Component products, tailored to the needs of monitoring the coastal area.

2.4.4 Copernicus CLC+

CLC+[6] is a suite of new products developed by the European Environment Agency (EEA) as part of a process called “2nd generation CORINE Land Cover (CLC)” (Kleeschulte *et al.*, 2019).

[6] https://land.copernicus.eu/pan-european/clc-plus

The purpose of the CLC+ is to complements and extents the currently existing CLMS products to better align with increasing requirements for European Land Cover and Land Use monitoring and reporting obligations.

The CLC+ will form the basis for the monitoring of land cover and land use in the years to come and will allow to generate tailored products for different monitoring needs through the creation of specific “instances” to support key EU policy needs through the policy cycle and stakeholders needs. The conceptual model of the CLC+ has four components.

CLC+Backbone

It is a new high spatial resolution vector product that provides a detailed geometric basis for the whole EEA39. This way, it completes the picture formed by the current local component products (Urban Atlas, Riparian Zones and Natura 2000, which cover about ¼ of the territory considered).

CLC+ Backbone will consist of an object-based vector product with 0.5 ha MMU and a 10 m spatial resolution raster product. Data are produced in four steps:

1. Creation of the “hard bones”: stable linear landscape features that act as vector skeleton to support segmentation process of the softbone. They use ancillary data such as OpenStreetMap, EU-Hydro, LUCAS, etc.
2. Creation of the “soft bones” applying segmentation techniques to further detail the hard bones based on the spectral characteristics of the area, Analysed from Sentinel and other VHR data. The process includes regionalization (geographic and thematic domain) and post segment refinements.
3. Producing a 10 m pixel based land cover classification from multi-temporal Sentinel-2 data. It refers to 18 land cover classes consistent with EAGLE.
4. Characterization of the skeleton obtained in step 1 and 2 using Sentinel-1 and Sentinel-2 data to define spectral, textural and backscatter characteristics of the object. The polygons are further attributed using statistical information from the classification from Step 3.

The classification system is limited to basic thematic content (18 classes for vector data and 12 for the raster product, as shown in Table 7 and Table 8). The products are fully compliant with the EAGLE data model and nomenclature can be used as input data for the CLC+ Core database. A data update is expected every 3-6 years.

Table 7. CLC+ Backbone classification system (vector product)

I level		II level		III level	
1	Built-up land	**11**	Very high sealing degree (sealed surfaces > 80%)		
		12	High sealing degree (sealed surfaces 50-80%)		
2	Woodland – needle-leaved trees	**21**	Pure needle leaved > 75%		
		22	Dominantly needle leaved 50-75%		
3	Woodland – broad-leaved trees	**31**	Pure broad-leaved > 75%	**311**	Pure deciduous >75%
				312	Pure evergreen >75%
		32	Dominantly broad-leaved 50-75 %		
4	Shrubland				
5	Permanent herbaceous land (i.e. grasslands)	**51**	Without trees (woody trees ≤10%)		
		52	Few trees (woody trees 10-30%)		
		53	Many trees (woody trees 30-50%)		
6	Periodically herbaceous land (i.e. arable land)				
7	Lichens and mosses land				
8	Partly vegetated land	**81**	Intermediate vegetation cover 30-50%		
		82	Low vegetation cover 10-30%		
9	Non-vegetated (i.e. rock, screes, sand, bare soil)				
10	Water				
11	Snow and ice				

Table 8. CLC+ Backbone classification system (raster product)

Class	Class name
1	Sealed (buildings and flat sealed surfaces)
2	Woody – needle-leaved trees
3	Woody – broad-leaved, deciduous trees
4	Woody – broad-leaved, evergreen trees
5	Woody – shrubs
6	Permanent herbaceous (i.e. grasslands)
7	Periodically herbaceous (i.e. arable land)
8	Lichens and mosses
9	Sparsely vegetated
10	Non-vegetated (i.e. rock, screes, sand, bare soil)
11	Water
12	Snow and ice

CLC+ Core

It is a consistent grid-based Land Cover/Land Use hybrid data repository that integrates and harmonizes land monitoring information. It brings together existing and future European as well as national products using a standardized integration approach in line with the EAGLE data model.

A grid is a spatial model with the appearance of a raster (with a resolution of 100 m in the case of the CLC+ Core), but, instead, it can associate different information to the same pixel. The grid is a more information-rich data model than the raster. The CLC+ Core database will essentially store geospatial and thematic data from sources such as CLC+ Backbone, CLC, Local Component data, HRLs, in-situ as well as information provided by the Member States. Data will be updated dynamically as soon as new information are available.

CLC+ Instances

Instances are products based on a combination of data stored within the CLC+ Core and harmonized with respect to EAGLE. These products are configured according to specific needs and are referenced to the 100 m grid of the CLC+ Core.

This allows combining previously non-harmonized datasets in new ways, for example land cover information coming from CLMS products with specific land use information from the countries. CLC+ shall be understood as a suite of products addressing and replying to various user needs and policy demands. These "instances" can be related to specific nomenclatures (a CLC+ Instance with a 1 ha MMU, a MAES Instance, a national nomenclature instance) or ecosystem types (a wetland Instance, a forest Instance).

An update of the data is expected every 1-3 years.

CLC+ Legacy

The CLC+ Legacy includes appropriate updates of current CORINE Land Cover which already has a well-established and agreed specification. It can be considered as one of the many instances derived from the CLC+ Core database.

2.5 Land consumption

Definition

Land consumption is a process associated with the loss of a fundamental, limited and non-renewable environmental resource, due to the occupation of an originally agricultural, natural or semi-natural surface with an artificial cover (Munafò, 2020). In particular, ISPRA defines land consumption as "variation from a non-artificial cover (unused land) to an artificial cover (consumed land)" (Munafò, 2020).

It is a phenomenon linked to settlement and infrastructural dynamics, then to construction of new buildings and settlements, to expansion of cities, to densification or conversion of land within urban areas, to the infrastructure of territories.

Loss of soil has been described in different ways creating several semantic issues which must be solved to enhance the mapping and accounting efforts made so far and to harmonize future frameworks in one. The European Environmental Agency monitors land consumption at the European scale under the name of Land Take and Soil Sealing.

Land take is often used interchangeably with land consumption or land artificialization as it refers to the increase of artificial surfaces over time. It involves the loss of semi-natural and natural land to urban and other artificial land expansions, as defined by EEA (EEA, 2019). This definition includes both sealed areas, urban green areas, sport and leisure facilities. Considering green urban area as land take it can lead to a widespread overestimation, bringing to a count loss of unsealed areas inside cities. Land take is evaluated through CLC. Due to the data spatial resolution, smaller changes are ignored, even though they contribute quantitatively to the phenomenon as well as increasing the state of fragmentation and degradation. It could be used as a complementary database for thematic insights on the changes but it can lead to an underestimation of land consumption (Siedentop and Meinel, 2004).

The concept of soil sealing considers the permanent covering of soil with artificial materials (such as asphalt or concrete) to create buildings and roads and it constitutes the most evident and widespread form of artificial covering. This concept is employed in HRL impeviousness and excludes the surfaces modified by processes such as soil excavation or compaction, where a natural surface has been replaced by artificial material, or a natural material has been removed from its place of origin (e.g. unpaved parking, dumps and quarries) (EEA, 2017c).

The definition of land consumption adopted by ISPRA is aligned with that of the European Environment Agency and considers the artificial coverage of surfaces (EEA, 2020): "All surfaces where the landscape has been modified or is affected by activities that replace natural surfaces with abiotic 2D/3D artificial structures or artificial materials. The man-made parts of urban and suburban areas, where humanity has established itself with permanent settlement infrastructure, including settlements in rural areas. Green areas in an urban environment should not be considered as artificial surfaces". According to this definition, gardens, urban parks and other green spaces should not be considered in the artificial component of the settlement. On the other hand, artificial surfaces also include those present in agricultural and natural areas.

The ISPRA definition of land consumption excludes natural areas in urban context, which indeed have an important value. On the other hand, it takes into account the land consumption processes related to removal by excavation (including open pit mining activities) and the partial loss, more or less remediable, of the functionality of the soil due to activities such as compaction (e.g. unpaved areas used for parking).

The representation between the concepts of land cover and land use is important in describing land consumption. In terms of land cover, land consumption is expressed as the growing set of areas with artificial coverage (sealed or not). For example, buildings, infrastructures and other constructions, mining areas, landfills, construction sites, paved areas, clay covered with artificial materials, photovoltaic fields, not necessarily in urban areas. This definition includes rural and natural areas and excludes open areas, natural and semi-natural, in the urban environment, which, on the contrary, should be preserved. Urban densification also represents a form of land consumption, if it involves creating new artificial land cover within an urban area. The concept of land use is mainly used for planning. Land use describes how the soil is used for human activities. A land use change may not be accompanied by land consumption and has no effect on the real state of the soil, while in other cases there could be land cover changes that affect soil quality with no land use changes.

Land consumption monitoring

In Italy the law 28 June 2016, n. 132 established the National System for Environmental Protection (SNPA) with the aim of monitoring the territory and providing an annual picture of urban areas transformations and land consumption.

These activities include producing and updating the National Land Consumption Map (LCM), a 10x10 m raster-based product (Figure 4) (Munafò, 2020).

The annual calculations follow a methodology which includes the following phases:

- acquisition of input data (Sentinel-1 and Sentinel-2 data, other available satellite images, ancillary data);
- data preprocessing;
- semi-automatic classification of the complete time series of Sentinel 1 and 2 for the current year and the previous year and production of a preliminary cartography;
- complete multitemporal photointerpretation of the entire territory and detailed scale editing (≥1:5,000) and revision of the historical series;
- rasterization;
- validation;
- production of the national mosaic and reprojection in an equivalent system;
- processing and return of data and indicators;

Data are available for 2012 and for 2015, 2016, 2017, 2018 and 2019, while the update to 2020 is still in progress. The classification system was originally binary (consumed land and non consumed land). Since 2017, two further classification levels have been introduced: the second level distinguishes permanent and reversible land consumption while the third goes further into detail (Table 9).

Table 9. National Land Consumption Map classification system

11 - Permanent land consumption	
111	Buildings
112	Paved roads
113	Railways
114	Airports
115	Ports
116	Other non-built-up sealed/paved areas
117	Permanent paved greenhouses
118	Dump sites
12 - Reversible land consumption	
121	Unpaved roads
122	Construction sites and other clayey areas
123	Not re-naturalized extractive areas
124	Groundwater extractive areas
125	Photovoltaic fields on the ground
126	Other artificial coverings
2 - Non consumed land	

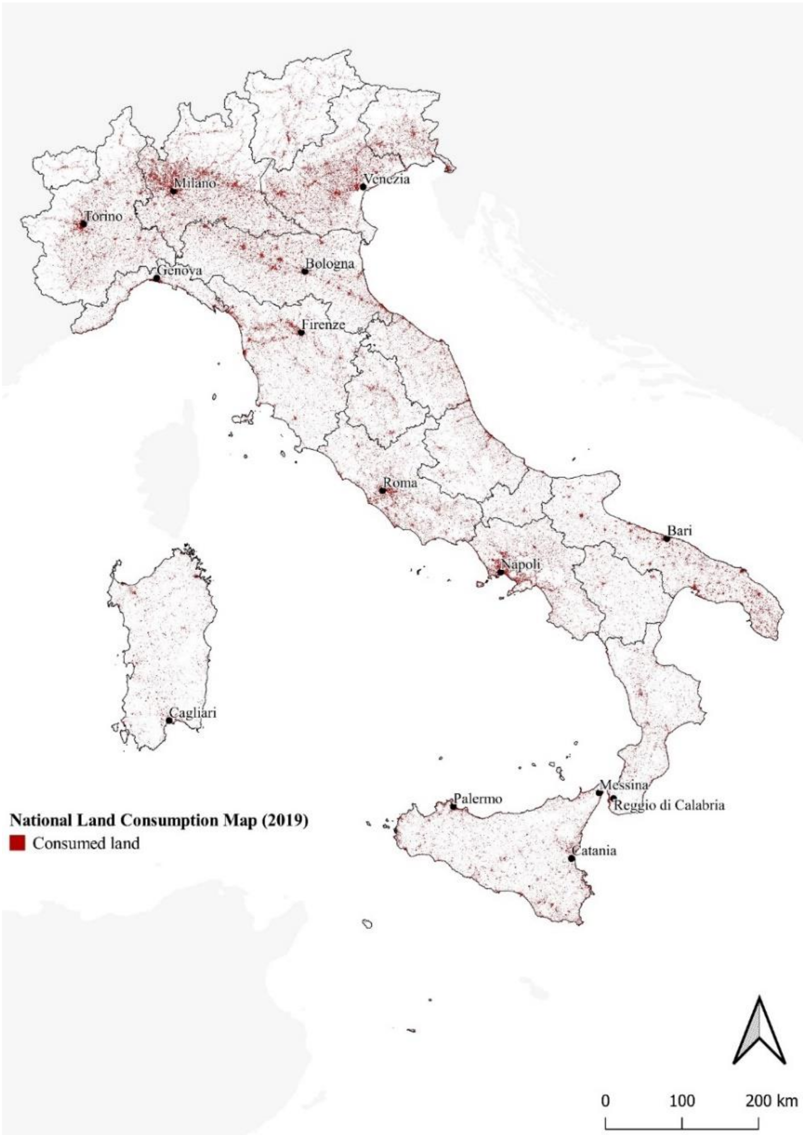

Figure 4. National Land Consumption Map for the year 2019. Source: Munafò, 2020

The classification at the third level currently regards the changes, while only some classes (roads, greenhouses, caevs, landfills) have been fully mapped to the third level. Artificial surfaces are detected only if they are large enough to cover more than 50% of the 10x10 m cell. Therefore, many linear elements of limited thickness are excluded, such as minor infrastructures in agricultural or natural context. Furthermore, the new classification system no longer considers permanent greenhouses as land consumption, excluding paved ones (where detectable). Artificial water bodies (but not groundwater quarries), bridges and tunnel are also excluded.

ISPRA data updated to 2019 show that artificial surfaces at national level are approximately 21,400 km^2. Furthermore, other forms of soil degradation directly linked to the presence of artificial areas could be considered, for example where the size of residual non-artificial spaces is lower than 1,000 m^2 (which occupy approximately 761 km^2 nationwide). The consumed land occupies 7.10% of the national surface and the value has been growing continuously in recent years.

The relation between land consumption and population dynamics confirms an increase in artificial surfaces even in the presence of population stabilization or decrease (Munafò, 2020).

2.6 Land monitoring through remote sensing

Remote sensing is the science and technology that allows to identify or measure the characteristics of an object, without direct contact, through specific sensors (JARAS, 1993). "Earth observation by remote sensing is the interpretation and understanding of the measurements made by aerial or satellite instruments of electromagnetic radiation reflected or emitted by objects on earth, by oceans or by frozen surfaces" (Mather and Koch, 2011).

In this case, remote sensing can be useful to study Earth phenomena which can be monitored and assessed at different spatial and temporal resolutions (Kuenzer *et al.*, 2014; del Río-Mena *et al.*, 2020).

2.6.1 Land cover classification through optical and radar data

Remote sensing studies the characteristics of objects on the earth's surface analysing how an incident electromagnetic radiation is altered by the interaction with the objects themselves.

In detail, electromagnetic radiation interacts with the earth's surface in different ways, depending on the characteristics of the objects (it can be reflected, absorbed or transmitted by the surface).

Remote sensing allows to study these characteristics starting from the analysis of parameters that describe how the incident radiation has been altered by the interaction with the object.

Two families of sensors can be distinguished and both study the behaviour of electromagnetic radiation after its interaction with the earth surface:

- *Active sensors*, which are equipped with instruments that emit the signal that interacts with the surfaces and a sensor to measure the return signal. Active sensors can be used to examine wavelengths that are not sufficiently provided by the sun, such as microwaves. An example of active sensor is the Synthetic Aperture Radar (SAR).
- *Passive sensors*, measure naturally available energy. They generally refer to the solar radiation available during the day. Energy that is naturally emitted (such as thermal infrared) can be detected day and night. Optical data comes from passive sensors;

In this research, optical and radar data were integrated to classify land cover.

Land cover classification through radar data

SAR systems use active sensors that transmit shorts pulses of microwave energy at regular intervals illuminating the surface, while an antenna receives a portion of the transmitted energy, reflected or backscattered from the surfaces.

Radar sensors provide backscatter measurements which indicate the brightness of the objects based on the portion of transmitted energy that is returned back to the receiver. Backscatter can be expressed with positive values if we consider the energy arriving at the receiver, or with negative values if we consider the emitted energy (Moreira *et al.*, 2013).

For each pixel there are two information: phase (in radians) and amplitude (in dB).

For land cover mapping it is necessary to consider some parameters related to the sensor and others related to the surface.

The parameters related to the sensor characteristics are: wavelength, polarization and angle of incidence.

Wavelength is the distance between two consecutive peaks of the wave. Radar sensors operate at specific wavelength and they are classified according to this characteristic (Table 10). Wavelength determines the penetration capacity of the signal and the type of objects with whom they interact; the signal does not see objects much smaller than the wavelength, instead it interacts with objects of wavelength size or bigger.

Table 10. Synthetic Aperture Radar (SAR) sensor classes based on wavelength

Band	Wavelength (cm)
Ka (0.86 cm)	0.8 – 1.1
K	1.1 – 1.7
Ku	1.7 – 2.4
X (3.00 cm)	2.4 – 3.8
C (5.00 cm)	3.8 – 7.5
S	7.5 – 15.0
L (24.00 cm)	15.0 – 30.0
P (68 cm)	30.0 – 100.0

Polarization refers to the plane of signal propagation, with reference to the radiation transmitted and received. The polarization can be horizontal (H) or vertical (V) and there are four combinations based on polarization of the transmitted and received signal (VV, VH, HV, HH).

Incidence angle is the angle between the direction of the incident wave and the earth's surface plane. Low incidence angles indicate a signal almost perpendicular to the surface and are characterized by higher backscatter values and greater penetration. Large angles are more sensitive to surface roughness and penetrate less into canopies. As the angle increases, the energy returning to the sensor decreases and the image become darker. This is important to the classification processes since the classes do not have the same backscatter characteristics in the far range.

The roughness of a surface detected by the radar depends on the characteristics of the surface and the wavelength and incident angle. A surface is smooth if its irregularities are smaller than the wavelength of the signal.

The signal interacts with surfaces in different ways depending on the roughness.

On smooth surfaces, *specular reflection* occurs, i.e. the surface reflects all or most of the signal coming from the sensor. These surfaces appear very dark in radar images. This kind of reflection occurs for example in wavefree water.

Rough surface scatters occur when the surface has a roughness comparable to the wavelength. The energy is dispersed uniformly in all direction and a portion of that energy is back scattered to the radar. In that case, part of energy reaches the satellite and the surface appears brighter. It is typical of bare soil or herbaceous vegetation.

Volume scattering occurs when the radar energy interacts with a volume. It consists of multiple bounces and reflections from different components within the volume and it is the most widespread mechanism in forests. In these areas, using HV or VH polarization will have a higher return then copolarized signal (VV, HH).

Finally, there is *double bounce* when most of the energy is reflected to the radar sensor. It occurs in urban areas, where the vertical surfaces of the buildings reflect the signal.
Factors such as soil moisture and geometric distortions (foreshortening, layover, and shadow) can influence the signal and introduce some ambiguities. In addition, in the SAR data there is spackle noise (a grainy salt and pepper texture in an image) caused by “random constructive and destructive interference from multiple scattering returns that occur within each resolution cell”. The application of specific filters can attenuate the phenomenon however causing a reduction of spatial resolution (Flores-Anderson *et al.*, 2019).

Land cover classification through optical data

Optical sensors acquire information on the earth's surface by exploiting solar electromagnetic radiation (passive sensors). Solar electromagnetic radiation has a wavelength between 230 and 4,000 nm. Part of the energy is absorbed by the atmosphere or undergoes atmospheric backscattering (Camps-Valls *et al.*, 2011). The energy that penetrates through the atmosphere has a wavelength between 10.0 and 12.5 nm and is called the “atmospheric window”. Solar energy passing through the atmosphere interacts with surfaces and is reflected to the sensor. The sensor measures the radiation reflected and emitted from the earth's surface but not the absorbed and transmitted ones. In detail, the sensor measures the radiance, which corresponds to the brightness in a certain direction towards the sensor. Radiance is related to the reflectance of objects which is defined as the percentage of the energy incident on the surface that is reflected.
Different sensors continuously scan the Earth's surface to produce imagery (Camps-Valls *et al.*, 2011) which are composed by a matrix of pixels. Each pixel is associated with a numeric value corresponding to the intensity level of the reflected energy, called “digital number”. The different types of sensors can be classified according to four types of resolution:

- *Spatial resolution* indicates the minimum size of an object that can be detected in an image;
- *Spectral resolution* refers to the number and size of the bands of the electromagnetic spectrum detected by the sensor; each band corresponds to a raster (Congedo, 2016). Based on the number of bands, we define panchromatic sensors (few bands that capture a wide window of the electromagnetic spectrum), hyperspectral sensors (with a high number of bands, each relating to very small intervals of wavelength) and multispectral (with an intermediate number of bands). The most used spectral bands refer to the

wavelengths of the visible (between 380 and 750 nm, in particular blue, green and red and infrared);

- *Temporal resolution* (or revisit time) is the time required to complete orbital cycle and to observe the same area;
- *Radiometric Resolution*: is determined by the number of discrete levels into which signal radiance can be divided. For example, 8-bit image has 256 digital number values.

Each surface interacts with the incident energy in a specific way depending on the wavelength. The behaviour of different materials as the wavelength varies is called the "spectral signature". The spectral signature can be described graphically through the spectral reflectance curve (Figure 5).

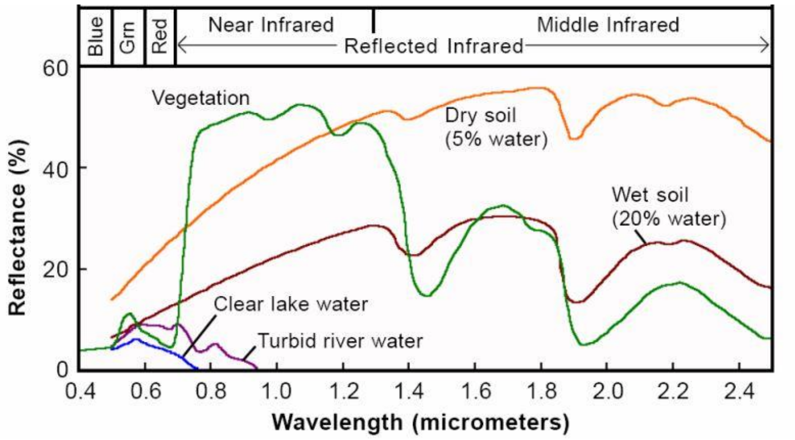

Figure 5. Spectral signature of different surfaces. Source: www.microimages.com

Based on the reflectance value associated with the pixel for a given wavelength, it is possible to determine the material that constitutes the surface represented in the pixel.

From the analysis of Figure 5 we can see the differences between some types of surfaces: Clear water absorbs over 90% of the incident radiation in the visible and 100% of that in the infrared. Turbid water has higher values due to the reflectance of suspended solids in the water. Bare soil reflectance increases with wavelength and in relation to the presence of moisture. The spectral signature of vegetation has several reflectance peaks, the most important of which are in the green (0.50-0.63 nm), one in the near infrared wavelength (0.7-1.1 nm) and two in the medium infrared.

In addition to the analysis of the reflectance values in the single bands, it is possible to combine the values of different bands, obtaining spectral indices. Many indices are developed to highlight the behaviour of vegetation, called vegetation indices.

One widely used vegetation index is the Normalized Difference Vegetation Index (NDVI) (Rouse Jr, 1973):

$$NDVI = \frac{(NIR - Red)}{(NIR + Red)}$$

Where:

NIR = reflectance in the near infrared band;

red = reflectance in the red band.

NDVI varies between +1 and -1, reaching maximum values in the presence of healthy vegetation and minimum values in the presence of water.

Many indexes have been proposed in literature to study specific land cover class or surface characteristics.

The normalized difference water index (NDWI) was proposed to detect surface waters in wetland environments and to allow to measure the water surfaces extent.

McFeeters's NDWI (McFeeters, 1996) is calculated as:

$$NDWI = \frac{(Green - NIR)}{(Green + NIR)}$$

Where:

green = reflectance in the green band.

The Normalized Difference Snow Index (NDSI) (Dozier, 1989) is used for ice detection:

$$NDSI = \frac{(Green - SWIR)}{(Green + SWIR)}$$

Where:

SWIR = reflectance in the short-wave infrared band;

The Normalized Burn Ratio (NBR) (Key and Benson, 1999) is usually used to identify areas burned by fire or to establish the state of the vegetation. NBR index assumes high values at vigorous vegetation and low values in burned areas:

$$NBR = \frac{(NIR - SWIR)}{(NIR + SWIR)}$$

2.6.2 Sentinel satellites

In this research, optical and radar data produced under the Copernicus Program by the Sentinel-1 and Sentinel-2 satellites were used and their characteristics are illustrated below.

Sentinel-1

The mission comprises a constellation of two polar-orbiting satellites, performing C-band SAR imaging. They are able to operate day and night regardless of cloud cover. Considering both satellites, it is possible to have data with a temporal frequency of 6 days at the equator (Torres *et al.*, 2012).

Sentinel-1 data is distributed by ESA in three levels of processing:

- Level-0, raw data for specific usage;
- Level-1, processed Single Look Complex (SLC) data comprising complex imagery with amplitude and phase;
- Level-1, Ground Range Detected (GRD) data with multilooked intensity only;
- Level-2, Ocean data for retrieved geophysical parameters of the ocean.

Level-1 GRD and level-2 data are systematically distributed, level-1 SLC data are distributed by selected areas, while level-0 data are for specific uses.

The Sentinel-1 instrument may acquire data in four modes: Stripmap (SM), InterfeRomatric Wide swath (IW), Extra-Wide swath (EW), and Wave (WV).

Sentinel-1 supports operation in single polarization (HH or VV) and dual polarization (HH+HV or VV+VH). SM, IW and EW products are available in single (HH or VV) or dual polarization (HH+HV or VV+VH), while WV is single polarization only (HH or VV).

Sentinel-2

The Copernicus Sentinel-2 mission includes a constellation of two polar-orbiting satellites placed in the same orbit, phased at 180° to each other. Sentinel-2A was launched in 2015 and Sentinel-2B in 2017. They have wide swath width (290 km) and high revisit time (considering both satellites we arrive at a frequency of 5 days at the equator and two days in the middle latitudes) (Drusch *et al.*, 2012).

Sentinel-2 acquires information for 13 spectral bands in the optical, NIR, SWIR parts of the electromagnetic spectrum, with spatial resolutions ranging from 10 to 60 m (Figure 6):

- 10 m spatial resolution bands: B2 (490 nm), B3 (560 nm), B4 (665 nm) and B8 (842 nm);
- 20 m spatial resolution bands: B5 (705 nm), B6 (740 nm), B7 (783 nm), B8a (865 nm), B11 (1,610 nm) and B12 (2,190 nm);
- 60 m spatial resolution bands: B1 (443 nm), B9 (940 nm) and B10 (1,375 nm).

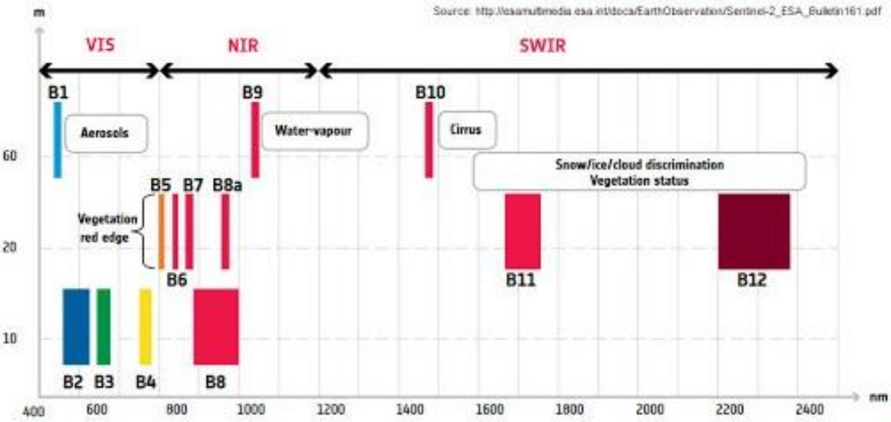

Figure 6. Sentinel-2 spectral bands. Source: ESA

Sentinel-2 data are available in Granules (or tiles) which are 100x100 km^2 squared orthoimages in UTM / WGS84 projection. The Italian territory is covered by about 80 granules (Figure 7).

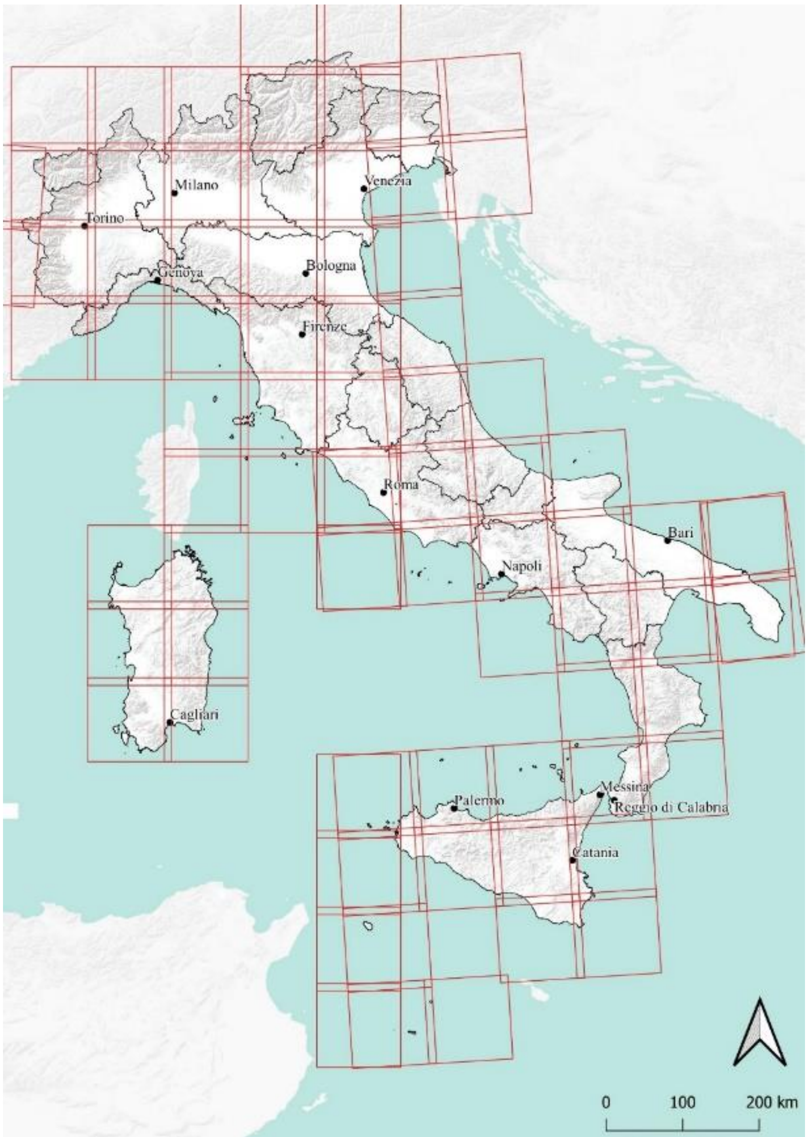

Figure 7. Sentinel-2 granule on Italian territory

Sentinel-2 data are available with different levels of preprocessing:

- Level-2A product provides Bottom Of Atmosphere (BOA) reflectance images;
- Level-1C are provided in Top of Atmosphere (TOA) reflectance with all parameters to transform pixel values into radiances, which require the application of a cloud mask to be used.

In this search, level-1C images were considered, as the archive of level-2A products was not yet complete for the years of interest.

The numerous spectral bands of the Sentinel-2 satellites allow accurate identification of land cover classes, particularly for vegetation; in fact, the infrared bands (Red Edge) are very useful for derivation of vegetation indices and the evaluation of crops (Clevers and Gitelson, 2013).

Sentinel-2C and Sentinel-2D are under construction and will be ready to launch sometimes in 2021.

Four other families of Sentinel Satellites are headed by Copernicus, destined to monitor the sea, the climate, and atmosphere.

- *Sentinel-3*: its main mission is to provide radar and altimetry data for Land Monitoring and Marine Monitoring. It supports the accurate parameterization of such topics as landsurface temperature and land colour and the high accuracy altimetry for measuring global seasurface height.
- *Sentinel-4 and Sentinel-5*: will provide data for atmospheric composition monitoring. They are Meteosat Third Generation satellites and they will be a payload embarked on EUMETSAT.
- *Sentinel-6*: will provide high accuracy altimetry for measuring global seasurface height, primarily for operational oceanography and for climate studies. It is a cooperative mission developed in partnership between Europe (EU, ESA and EUMETSAT) and the U.S. (NOAA and NASA).

In addition, about 30 participating missions managed by national, European and international organizations flank the Sentinel and have already provide a huge amount of data for Copernicus services.

2.7 Land cover classification methods

Identifying specific objects or entities from satellite images can be done manually or through totally or partially automated algorithms. The following approaches could be followed.

Photointerpretation involves manual identification of objects of interest on the image starting from observing parameters such as tone, shape, size, pattern, texture, shadow, and association. The CLC was produced and updated this way and it is an accurate but expensive and timeconsuming methodology to produce land cover maps. As part of this research, photointerpretation was used only to spot a limited number of training areas.

Automatic classification attributes the class to pixels starting from their spectral characteristics. These methods can be divided into supervised and unsupervised depending on the type of learning which the algorithm uses to classify the pixel.

Unsupervised methods involve almost completely automatic procedures. The algorithm groups the pixels into clusters based on their spectral behaviour in different bands. Pixels belonging to a given class have similar spectral behaviour to each other and different from those of pixels belonging to other classes.

One of such methodology is K-means clustering (KMC). Initially the number of classes and clusters is defined, then each pixel is assigned to their nearest cluster based on its spectral characteristics. This way, groups of homogeneous pixels attributed to the different land cover classes (for example) are obtained. The ISODATA method works like K-means, but the number of clusters is defined by the algorithm. Unsupervised methods are often used to reduce dimensionality of datasets and they have great potential.

The supervised classification methods are widely adopted to produce land cover maps. They use training data to define the typical values of each considered land cover class, in the different spectral bands. This type of methodologies include three phases:

1. The training stage: the land cover classes object of the classification are defined, based on the project objectives and characteristics of the available data. For each land cover class, representative training dataset are manually identified.

2. The classification stage: spectral signatures of training datasets related to all the classes considered are calculated. These values (mean and standard deviation) are used as a reference by the algorithm to attribute the class to each pixel.

3. The accuracy assessment stage: an independent set of pixels representative of each class is used to estimate the classification accuracy. The result can be refined by direct editing or by exploiting spectral indices.

Many supervised classification algorithms have been developed ranging from more traditional systems to advanced machine learning algorithms.

Minimum distance

The Minimum Distance algorithm calculates the Euclidean distance between the spectral signature of the pixel and that of the reference classes. The pixel is assigned to the closest distance class.

Maximum Likelihood classifier (MLC)

It is a widely used parametric method. The algorithm assumes that clusters obtained from the training datasets for each category follow a normal (Gaussian) probability distribution (Richards and Richards, 1999; Chang, 2003). This assumption is generally reasonable for common spectral response distributions and allows to describe the distribution of a category response pattern (i.e., the shape of the region in the feature space for that cluster) through a mean vector and the covariance matrix. Starting from these parameters it is possible to compute the statistical probability of a given pixel value to be a member of a particular land cover class. Each pixel will be assigned to the most likely class (highest probability value) or it will be labelled "unknown" if the probability values are all below a minimum threshold set by the operator. To use this algorithm, training areas must be large enough to allow covariance matrix computation.

Artificial neural network (ANN)

The inspiration comes from observing biological learning systems with a strong analogy. "Artificial neural networks are built as an interconnected set of simple units, where each takes a number of real values of inputs (possible outputs of other units) and produces a single output value (which can become the input of many other units)".They are nonparametric classifiers, i.e. they does not require any assumption about the statistical distribution of data and they can incorporate *a priori* knowledge as a realistic constraint, including input data of area of interest. They require a lot of computing power and it is difficult to trace the rules adopted to attribute classes (Black box). However, the Recurrent Neural Networks (RNNs) incorporated in machine learning techniques are still not very efficient in image recognition, highlighting some limitations, mainly related to long processing times and memory limits. Convolutional Neural Networks (CNN) have been developed in these disciplines. These networks are nowadays widely used in classification tasks, where the purpose is to divide the image into subareas using specific filters capable of extracting the most significant features and removing the disturbing ones (Nielsen, 2015).

Decision tree (DT)

"A tree classifier is determined by a finite set of decision rules that are connected and sequentially applied according to a tree topology" (Breiman *et al.*, 1984). These methods can be represented with graphs, where each branch (node) represents a binary choice (yes / no), and the leaves are the result of the series of choices. The classification starts from the roots of the tree and it is divided gradually according to the values of the characteristics (Kotsiantis *et al.*, 2007). The result is a graphical representation of a set of "if-then" rules, easily interpretable. Compared to neural networks, these processes do not involve iterations to reconsider and modify the choices made, but the best version of the tree is immediately sought.

Random forest (RF)

Random forest (RF) algorithm, originally proposed by Breiman (Breiman, 2001), is a machine learning technique based on the decision tree classification model. RF can overcome the drawbacks associated with single decision trees creating many (usually several hundreds) different decision trees, using random subsets of the data (bootstrap dataset) and variables. Once the "forest" has been created, the accuracy of the model can be determined by processing all not included data in the bootstrap dataset (Out-Of-Bag data) and performing a validation.

There are many algorithms to investigate land cover and land use starting from classification of satellite images. Chosing the most suitable method depends on aspects such as the type of data, distribution of classes, research purposes, interpretability of the classifier and also the balance between objectives and the available resources. In general, automatic classification methods are time consuming with the increase of the data dimension and volume, and sometimes data interpretation could be difficult (Chen and Gong, 2013; Gómez *et al.*, 2016).

Supervised classification can be used to analyse a large amount of data; they are based on selecting an adequate number of training samples with known values (Zhu *et al.*, 2016), which are used to predict unknown values of testing data (Holloway *et al.*, 2019). So, it is important to select what completely represents the variability of the characteristics of the analysed territory. During the last years the supervised classification technique increased

(Thanh Noi and Kappas, 2018),thanks to the availability of ancillary data which provide accurate information on ground truth (Colditz, 2015). Ground truth information is also relevant to define thresholds values for the classification; these values are important for isolating objects from the background, in order to improve classification precision (Liu *et al.*, 2011). Threshold methods are used for their simplicity and because they require few parameters (Huang *et al.*, 2019; Xin *et al.*, 2020).

Identification and use of thresholds related to the spectral characteristics and their variation over time is used, for example, to classify land cover (Otukei and Blaschke, 2010) and cover change (Sinha and Kumar, 2013), to define crop phenology to determine the beginning and end of season (Huang *et al.*, 2019), to classify tree species (Persson, Lindberg and Reese, 2018).

Some supervised classification method, for example parametric supervised classifiers (maximum likelihood, minimum distance), are difficult to use for large multitemporal datasets, because they have limited flexibility in decision boundaries. Since these classifiers assume a normal data distribution, they furnish excellent results when data distribution is unimodal but they could be difficult to apply for multimodal dataset analysis (Belgiu and Drăguţ, 2016).

Machine learning (Lary *et al.*, 2016) approaches are largely used in land cover mapping, thanks to their capacity to model class signatures, elaborate many input data and produce higher accuracy compared to traditional parametric classifiers, especially for complex data with many predictor variables (Maxwell *et al.*, 2017). For example, decision trees or random forest are machine learning which focus on decision rules on class boundaries that improve the classification of land cover types with unknown distribution and frequency (Foody and Mathur, 2006; Kulkarni and Lowe, 2016; Liu *et al.*, 2018). On the other hand machine learning is characterized by higher computational intensity, unknown decision rules (black box) and need of input parameters (Rodriguez-Galiano *et al.*, 2012; Gómez *et al.*, 2016); moreover it is not easy to apply it to large areas, because it is characterized by difficult computing, such as the manual choice of a large number of training areas (Sun *et al.*, 2019) and it is negatively influenced by noisy observations and overfitting (Gómez *et al.*, 2016).

2.8 Change detection methods

Change detection can take place through direct identification of changes or comparing two classifications of the same area related to different periods. Change detection methods can be grouped according to different principle. A first distinction is between object-based and pixel-based methods. The choice is related to the type of images used, which depends on the objectives of the research. Object-based methods consider the spatial characteristics and shape of objects, consequently they are more suitable when very high resolution data are available. The pixel-based methods exploit the spectral characteristics of change at pixel level and are more suitable with medium-high resolution images.

The most commonly used algorithms are based on image differencing, image ratioing (Moser and Serpico, 2006), regression analysis, vegetation index differencing, change vector analysis (CVA) (Bovolo and Bruzzone, 2007; Thonfeld *et al.*, 2016), transformation (as principal component analysis, PCA) and tasselled cap transformation machine learning (such as artificial neural networks, support vector machine, decision tree) (Tewkesbury *et al.*, 2015), i.e. those using more than one system.

Image differing or ratioing (Moser and Serpico, 2006) are widely used to create binary maps of change. Accuracy is conditioned by chosing appropriate training areas, which can be selected manually or applying automated algorithms.

Change vector analysis (CVA) (Johnson and Kasischke, 1998; Bovolo and Bruzzone, 2007; Thonfeld *et al.*, 2016) identifies changes defining thresholds on the difference between the values of two information vectors, called "change vector direction" and "multispectral change magnitude". Changed areas are derived as the difference between these two vectors through a threshold to distinguish changed from unchanged pixels. Performance and accuracy are affected by image acquisitions (atmospheric conditions, solar angle) and by the definition of single threshold that could be insufficient for detecting magnitudes of change.

Many studies have tested the combined use of radar and optical data, especially in urban areas (Pesaresi *et al.*, 2016; Haas and Ban, 2017; Celik, 2018; Goldblatt *et al.*, 2018; Sun *et al.*, 2019).

Several classification systems simultaneously classify land cover classes and change classes starting from multitemporal images. They were used for forest change detection and they are widely used in machine learning systems. Many studies highlighted the potential machine learning techniques for change detection (Nemmour and Chibani, 2006; Bovolo *et al.*, 2008; Volpi *et al.*, 2013; Zhu and Woodcock, 2014), although they have limitations: difficulty to find a sufficient number of training areas, user-defined parameters to set the algorithm, effectiveness of variable used.

Researchers have made enormous efforts in developing various change detection methodologies and several reviews have been published (Singh, 1989; Coppin *et al.*, 2004; Lu *et al.*, 2004; Radke *et al.*, 2005; Hansen and Loveland, 2012; Hussain *et al.*, 2013;

Tewkesbury *et al.*, 2015; Ban and Yousif, 2016; Zhu, 2017; Reba and Seto, 2020). However, to identify common guidelines to choose the most suitable methodology algorithm and comparing the accuracy of different technique is a very hard task for several reasons: it depends, among the others, on spatial, spectral and temporal resolution of the sensor used and on the objective of the research itself.

Many of the experiences in literature refer to areas of limited size. Hybrid approaches are often used for large area analyses to exploit the potential of different methods. Other experiences include developing specific algorithms for various land cover change classes, according to specific criticalities.

3 Materials and methods

3.1 Study area

The study area is the Italian territory (Figure 8).

Figure 8. Study area - Italy

The Italian peninsula is located in the middle of the Mediterranean basin between 47°05′ N – 35°29′ N and 6°37′ E – 18°31′ E and has a surface of 302,073 km² (ISTAT, 2014). It is composed of about 23% of flat zones (up to 300 m a.s.l.), 42% of hilly areas (between 300 and 700 m a.s.l.), and 35% of mountains (above 700 m a.s.l.). To the north is the mountain range of the Alps, which exceeds 4,000 m. In this area, the alpine climate prevails, with maximum annual rainfall of 2,500 – 3,500 mm. In the peninsular area there is the Apennine mountain range, reaching its highest peak in Abruzzo with Gran Sasso (2,912 m) and characterized by continental climatic conditions. These areas are covered by clouds for much of the year, making it difficult to find free-clouds optical images. The coastal area has a Mediterranean climate, and average annual rainfall reaches a minimum of 500 mm in Apulia and Molise.

Land cover is characterized by forest, grassland, built up areas and water (both liquid and solid). Herbaceous vegetation is dominated by cropland or pastures and it is concentrated in the coastal area and Po valley, while forests are concentrated in mountain areas. The orographic conformation of the territory heavily affects the urbanization, which is concentrated in the lowland and costal areas. The Italian coastal area extends with almost 8,300 km in the center of the Mediterranean Sea. It is composed for 2,827 km by high coast, while low coast is 5,720 km long and it is most common on the Adriatic side, which consists of long shores and lagoons. All these different types of coastal areas are washed by local seas (Ligurian, Tyrrhenian, Ionanian, Adriatic and the Sardinian and Sicilian seas). Italy has a population of 59,641,488 inhabitants (21/12/2019) (ISTAT, 2020) with a slightly decreasing trend. About 1/4 of the population lives in the 47 cities with over 100,000 inhabitants. The only cities with over 1,000,000 inhabitants are Roma, Milano, followed by Napoli and Torino. The 10% of the population is concentrated in these four cities.

3.2 Production and analisys of land cover maps of Italy

This research deepened two main activities related to land cover monitoring.

The first activity studied the main data available for the Italian territory to evaluate their limits and strengths, analysing aspects such as reference year, update frequency, classification system and spatial resolution. Data were merged into a land cover map for 2012 which was the reference year for most of the data considered at the time of the research. Preliminary versions of the 2012 land cover map were presented through poster communications at the 13th national Statistics Conference of ISTAT and in the ISPRA report "Territorio. Processi e trasformazioni in Italia" (ISPRA, 2018d). The data was also used for the assessment of ecosystem services conducted by ISPRA in the context of the 2018, 2019 and 2020 editions of the report "Land Consumption, territorial dynamics and ecosystem services" (Munafò, 2018, 2019, 2020).

The second activity involved the development of a land cover classification and change detection methodology based on training areas and decision rules for mapping large areas (Houhoulis and Michener, 2000; Berhane *et al.*, 2018), exploiting the potential offered by

Sentinel-1 radar data and Sentinel-2 multispectral images. The methodology aims at ensuring production of a land cover map of the entire Italian territory with a spatial resolution of 10 m with eight land cover classes and four land cover change classes. About change detection, the research focused on identifying changes related to land consumption variations and forest disturbances through the development of specific algorithms for each class of change considered. The methodology makes it possible to produce data that can be updated with high frequency and with characteristics aligned with European indications.

In detail, the maps comply with the EAGLE model for classification systems and are compatible with future Copernicus and national initiatives, such as the Space Economy Strategic Plan of the Presidency of the Council of Ministers and with 2nd generation CORINE Land Cover (CLC+). In addition, this methodology is a step forward compared to existing products in terms of spatial resolution and update frequency. As part of this activity, masks of potential changes were developed to identify variations in artificial abiotic surfaces, which were used in the update of the National Land Consumption Map of ISPRA.

The maps created as part of the two activities refer to an EAGLE compliant classification system, proposed in two variants. The land cover map classification system obtained from Sentinel data has eight land cover classes organized in three levels. The 2012 map obtained from existing data integrates the previous 8-class classification system with the introduction of further classes to distinguish woody vegetation into trees and shrubs and to describe agricultural areas.

The land cover classification methodology based on Sentinel data described below was published in the "Land" journal under the title of "Multispectral Sentinel-2 and SAR Sentinel-1 Integration for Automatic Land Cover Classification" (De Fioravante *et al.*, 2021). The description of the procedures and the results achieved below are an extended version of the analysis presented in the paper.

The procedure for creating masks of potential changes relating to land consumption was the subject of other scientific works published in "Remote Sensing" journal with the title "Land Consumption Monitoring with SAR Data and Multispectral Indices" (Luti *et al.*, 2021) and on "Journal of Maps" whit the title "Land consumption in Italy" (Strollo *et al.*, 2018). Also in this case, the procedures and results presented below take up and extend what is described in the papers.

The research was also presented through two poster communications at the XXIX National Congress S.It.E (Italian Society of Ecology) and at the Earth Technology Expo and included in the next edition of the report "Suolo, servizi ecosistemici e infrastrutture verdi: Metodi, ricerche e progetti innovativi per incrementare il Capitale naturale e migliorare la resilienza urbana” drafted by the Italian Research Center on Land Consumption (CRCS), whit the title “Monitoraggio del consumo e della copertura del suolo tramite immagini Sentinel-1 e Sentinel-2 a cura del Sistema Nazionale per la Protezione dell'Ambiente”.

3.2.1 Definition of an EAGLE compliant classification system

To satisfy the requirements proposed by the European legislation for monitoring activities, both at European and national level, a list of criteria for new data model has been created. The EAGLE concept (Arnold *et al.*, 2013) allows to harmonize the European land monitoring system, unifying land cover and land use information both in topdown and bottomup approaches. It is based on a clear distinction between Land cover and Land use and it is summarized in a matrix composed by three separate descriptors: Land cover components (LCC), land use attributes (LUA) and further characteristics (LCH). The descriptors can be combined in order to create specific classification systems for different needs, or to identify correspondences with existing classes, keeping the three descriptors independent (EAGLE, 2020).

The maps produced are based on two variants of a classification system consistent with the EAGLE specifications (Kleeschulte *et al.*, 2019; EAGLE, 2020).

For the 2018 land cover map obtained from the classification of Sentinel data, an eight classes classification system was defined (Table 11).

Table 11. Land cover classification system

Land cover		
I level	**II level**	**III level**
Abiotic-non vegetated	Artificial abiotic surfaces	
	Natural abiotic surfaces	
Biotic-vegetated	Woody vegetation	Broad-leaved
		Needle-leaved
	Herbaceous vegetation	Permanent
		Periodically
Water surfaces	Water bodies	
	Permanent snow and ice	

The first classification level distinguishes three main land cover classes. It consists of land cover classes at the first two levels, while the “biotic-vegetated” class is further articulated through a third classification level based on LCHs related to biophysical characteristics and temporal parameters.

1- *Abiotic-non vegetated***:** The class includes any unvegetated surfaces, either covered with man-made artificial structures or geologically natural material surfaces (with or without anthropogenic influence or impact). It includes consolidated or unconsolidated unvegetated natural surfaces, such as rocky regions and sands.

   At the second classification level, the class is subdivided into artificial and natural surfaces:

   - *Artificial abiotic surfaces* include impervious surfaces but also reversible land consumption (Munafò, 2020). Impervious and sealed surfaces are mainly covered with features with a certain height above ground (artificial buildings and constructions) or features without a specific height above ground (flat waterproof surfaces) such as artificial surface pavements (e.g. asphalt, concrete). Reversible land consumption includes all areas where natural surface material has been replaced by man-made material or where natural material has been removed, forming a non-impermeable and undeveloped surface, including soil compaction, excavation or temporary impervious cover. For example: unpaved roads, construction sites or courtyards or sports fields, permanent deposits of material, photovoltaic fields, quarries not yet restored. The EAGLE classification system includes quarries and extraction sites in 1211 "bare rock" class, but in this research they are classified as artificial abiotic surfaces since quarries and extraction sites are strongly modified due to compaction and morphology changes caused by material removal. The physical characteristics of these areas are more similar to those of the EAGLE 112 "Non-Sealed Artificial Surfaces" class which includes any open areas where natural surface material has been replaced by artificial material or where natural material removed from its place of origin as result of human activity forms an unsealed and non-built-up surface.
   - *Natural abiotic surfaces* are any kind of surface material that remains in its natural consistence or form, either with or without anthropogenic influence. Consolidated and unconsolidated surfaces include: unvegetated rocky mountainous regions, sand, bare soil.

2- *Biotic-vegetated*: The class includes any terrestrial surface with spontaneous, seminatural or artificial vegetation (e.g. crops, urban parks), with or without anthropogenic influence.

   At the second classification level, biotic-vegetated surfaces are divided into woody vegetation and herbaceous vegetation.

- *Woody vegetation* includes perennial woody plant with single, self-supporting main stem or trunk, containing woody tissue and branching into smaller branches and shoots.

  A third classification level has been defined applying to the land cover class "trees" a LCH related to the "leaf form” allowing to distinguish needle-leaved and broad-leaved trees.
- *Herbaceous vegetation* includes annual, biennial or perennial plants such as most ferns and grasses that do not have a persistent woody stem above ground. On the opposite to woody plants, the buds of herbaceous plants die at the end of the growing season,to regenerate from the tissues left above or below the ground (e.g. bulbs, rhizomes, tubers, seeds).

  A third classification level has been defined applying to the land cover class “herbaceous vegetation” a LCH related to the “temporal parameter” of “duration”. In this way the class is divided on the basis of the persistence of the coverage throughout the year.

  Permanent herbaceous areas are characterized by a continuous vegetation cover throughout a year. No bare soil occurs within a year. These areas are either un-managed or extensively managed natural grasslands or permanently managed grasslands, or arable areas with a permanent vegetation cover or even set aside land in agriculture.

  Periodically herbaceous areas are characterized by at least one land cover change between bare soil and herbaceous vegetation within one year. Depending on the management intensities these areas can change between these two land cover components within a year. Normally these areas are arable areas.

3- *Water surfaces* class includes water in its liquid or solid state of aggregation (snow and ice), both of natural formation (water basins, rivers, streams, stagnant waters, glaciers) and of artificial origin.
   - *Water bodies* are water in liquid state of aggregation regardless of location, shape, salinity and origin (natural or artificial). All types of inland water surfaces without direct interference or interchange with open sea water, regardless of salinity and origin (natural or artificial). Watercourses (flowing water surfaces) come from rivers, streams, canals, waterways. Stagnant waters (water surfaces of non-current waters, mainly lakes and ponds, or meanders of cut rivers) come from natural lakes (both fresh

and salt water), ponds, reservoirs, bottom pools, irrigation ponds, ponds for the production of artificial snow, river banks for the production of hydroelectric energy, ponds for fire fighting.

- *Permanent snow and ice* include the snow cover that persists all year round, above the climatic snow limit and the persistent ice cover formed by the accumulation of snow.

Starting from Sentinel data, a change detection algorithm was developed for changes in artificial abiotic surfaces and for the reduction of woody vegetation caused by forest disturbances. In this sense, four land cover change classes have been defined (Table 12).

Table 12. Land cover change classification system

Land cover change	
Land consumption	
Restoration	
Forest disturbances	Burned areas
	Other disturbances

The land cover change classes include variations of artificial abiotic surfaces in terms of expansion (i.e. land consumption), reduction (i.e. restoration), and the loss of woody vegetation associated with forest disturbances. The changes associated with other land cover classes have not been analysed as the considered period is not wide enough to allow monitoring the woody vegetation increase or distinguish seasonal variations of herbaceous and water classes from the real class changes.

4- *Land consumption* is the replacement of a non-artificial land cover to an artificial land cover, both permanent and reversible. Artificial surfaces that have been changed by, or are under the influence of human activities resulting in a land consumption process, can be sealed or unsealed.

5- *Restoration* is the replacement of an artificial and reversible land cover with a semi-natural land cover where permeable land is back, such as herbaceous (permanent and periodic), woody, urban green.

6- *Forest disturbance* are drastic decreases or disappearances of vegetation, in areas classified as woody vegetation, not associated with land consumption.

  - *Burnt areas*: The class includes natural woody vegetation affected by recent fires. This class includes recently burnt areas of forests, moors and heathlands, sclerophyllous vegetation, transitional forest, shrub formations, areas with sparse vegetation.

- *Other disturbances*: The class identifies the removal of all or most of the trees, large and small, in a surface, following a disturbance event. Virtually all woody vegetation is removed from the site in preparation for the settlement of new wood or another class of biotic vegetation.

The land cover map of Italy based on available data for 2012 refers to an expanded version of the classification system described in Table 13. Compared to the classification system of Table 11, some classes have been introduced to maintain the thematic detail offered by the Copernicus and national input data.
A third classification level is added to the natural abiotic surfaces, with the introduction of two land cover classes related to aggregation of materials: consolidated surfaces (bare rocks scree, cliffs) and unconsolidated (beaches, dunes, sands) surfaces. Woody vegetation is divided into trees and shrubs, while broad-leaved and needle-leaved trees were further articulated at the fifth classification level, exploiting the information provided by the fourth level of CLC.
The fourth and fifth classification level for the other classes are obtained adding to the land cover classes some LCH relating to the "crop type" (olive groves, orchards, vineyard, pastures, arable land and woody plantation).

Table 13. Extended version of the land cover classification system for 2012 land cover map

Land cover									
I level		**II level**		**III level**		**IV level**		**V level**	
1	Abiotic non vegetated surfaces	**11**	Artificial abiotic						
		12	Natural abiotic	**121**	Consolidated (bare rocks scree, cliffs)				
				122	Unconsolidated (beaches, dunes, sands)				
2	Biotic vegetated surfaces	**21**	Woody vegetation	**211**	Trees	**2111**	Broad-leaved		
						2112	Needle-leaved		
						2113	Permanent crops	**21131**	Orchards
								21132	Olive groves
								21133	Wood plantations
				212	Shrubs	**2121**	Vineyards		
						2122	Shrubland		
		22	Herbaceous vegetation	**221**	Periodically	**2211**	Pastures		
						2212	Arable land		
				222	Permanent				
3	Water surfaces	**31**	Water bodies						
		32	Permanent snow and ice						
4	Wetlands								

3.2.2 National Land Cover map based on Copernius and national data

Selection of input data

The land use map for 2012 was produced by the analysis, comparison and integration of the main data available at national level and as part of the Copernicus program for the Italian territory.

In detail, data part of the Local and Pan-European components of the Copernicus Land Monitoring service were considered:

- Copernicus Local Component
  - Urban Atlas (UA)
  - Riparian Zones (RZ)
  - Natura 2000 (N2000)
- Copernicus Pan-European Component
  - Corine Land Cover (CLC) at the fourth classification level
  - High Resolution Layers (HRL) for Grassland (GRA), Dominant Leaf Type (DLT) and Water and Wetness (WAW).

At national level, the National Land Consumption Map (LCM) was used.

The 2012 has been selected as a reference year since the majority of data gathered refer to it. To increase the detail in areas not covered by the high resolution data provided by the Copernicus Local Component, the availability of regional maps was investigated. In detail, regional LU/LC maps related to the reference period were used for Puglia, Lazio, Abruzzo, Veneto, Liguria, Lombardia and Basilicata.

Data preprocessing and map production

Data were projected in the European Terrestrial Reference System 1989 (ETRS-89) and in Lambert Azimuthal Equal Area (LAEA) projection. Then they were converted to raster format, with a spatial resolution of 10 m and cells aligned with LCM and HRLs data (the only two data already in raster format). The production of the map involves the steps described below.

1- *Reclassification of Copernicus UA, RZ, N2000 data*

   The three data have the most extensive coverage and the highest thematic and geometric detail, therefore they were used as a basis for the map. They were first reclassified in the classification system defined in Table 13. For the classes that do not have a direct correspondence with the classification system of Table 13, temporary codes have been introduced (Table 14) and subsequently managed using the HRL data.

Table 14. Temporary codes for mixed land cover classes and land use classes

	Temporary codes	UA	RZ	N2000	CLC
91	Green urban areas	14100			141
92	Annual crops associated with permanent crops		23100	2310	241
	Complex cultivation patterns	24000	23200	2320	242
93	Land principally occupied by agriculture with significant areas of natural vegetation		23300	2330	243
94	Agroforestry		23400	2340	244
95	Transitional woodland and scrub		34100	3410	324
	Damaged forest			3500	
96	Sparsely vegetated areas	33000	61000	6100	333
97	Burnt areas		63200	6320	334
99	Permanent crops (vineyards, fruit trees, olive groves)	22000	22100	2210	
998	Urban areas and artificial surfaces	11100-13400, 14200	11110-14000	1110-1400	111-133, 142
999	Mixed Forest	31000	33100		3131-3132

These areas are classified by Copernicus data in terms of mixed land cover classes (coexistence of trees, shrubs and herbaceous vegetation) or land use classes. Temporary codes have also been attributed to the classes of artificial surfaces and mixed forests, which are detailed later using LCM and HRLs. Reclassification was carried out considering the correspondences, of Table 15 for Natura 2000, of Table 16 for Urban Atlas and of Table 17 for Riparian Zones.

Table 15. Reclassification table for Natura 2000

N2000	Class Name	LCcode	N2000	Class Name	LCcode
1110	Urban fabric (predominantly public and private units)	998	4212	Seminatural grassland without woody plants (C.C.D. ≤ 30%)	93
1120	Industrial, commercial and military units	998	4220	Alpine and subalpine natural grassland	22200
1210	Road networks and associated land	998	5110	Heathland and Moorland	22200
1220	Railways and associated land	998	5120	Other scrub land	21220
1230	Port areas and associated land	998	5200	Sclerophyllous vegetation	21220
1240	Airports and associated land	998	6100	Sparsely vegetated areas	96
1310	Mineral extraction, dump and construction sites	998	6210	Beaches and dunes	12200
1320	Land without current use	998	6220	River banks	12200
1400	Green urban, sports and leisure facilities	998	6310	Bare rocks and rock debris	12100
2110	Arable land	22120	6320	Burnt areas (except forest)	97
2120	Greenhouses	22120	6330	Glaciers and perpetual snow	32000
2210	Vineyards, fruit trees and berry plantations	99	7100	Inland marshes	40000

2220	Olive groves	21132	7210	Exploited peat bog	40000
2310	Annual crops associated with permanent crops	92	7220	Unexploited peat bog	40000
2320	Complex cultivation patterns	92	8110	Coastal salt marshes	40000
2330	Land principally occupied by agriculture with significant areas of natural vegetation	93	8120	Salines	40000
2340	Agroforestry	94	8130	Intertidal flats	40000
3110	Natural and seminatural broad-leaved forest	2111	8210	Coastal lagoons	31000
3120	Highly artificial broad-leaved plantations	2111	8220	Estuaries	31000
3210	Natural and seminatural coniferous forest	2112	9110	Interconnected water courses	31000
3220	Highly artificial coniferous plantations	2112	9120	Highly modified water courses and canals	31000
3310	Natural and seminatural mixed forest	999	9130	Separated water bodies belonging to the river system	31000
3320	Highly artificial mixed plantations	99	9210	Natural water bodies	31000
3410	Transitional woodland and scrub	95	9220	Artificial standing water bodies	31000
3420	Lines of trees and scrub	95	9230	Intensively managed fish ponds	31000
3500	Damaged forest	95	9240	Standing water bodies of extractive industrial sites	31000
4100	Managed grassland	22110	10000	Sea and ocean	31000
4211	Seminatural grassland with woody plants (C.C.D. ≥ 30%)	93			

Table 16. Reclassification table for Urban Atlas

UA	Class Name	LCcode	UA	Class Name	LCcode
11100	Continuous Urban Fabric (>80%)	998	13400	Land without current use	998
11210	Discontin. Dense Urban Fabric (50% - 80%)	998	14100	Green urban areas	91
11220	Discontin. Medium Density Urban Fabric (30% -50%)	998	14200	Sports and leisure facilities	998
11230	Discontinuous Low Density Urban Fabric (10% - 30%)	998	21000	Arable land (annual crops)	22120
11240	Discontinuous Very Low Density Urban Fabric (< 10%)	998	22000	Permanent crops (vineyards, fruit trees, olive groves)	99
11300	Isolated Structures	998	23000	Pastures	22110
12100	Industrial, commercial, public, military and private units	998	24000	Complex and mixed cultivation patterns	92
12210	Fast transit roads and associated land	998	25000	Orchards at the fringe of urban classes	21131
12220	Other roads and associated land	998	31000	Forests	999
12230	Railways and associated land	998	32000	Herbaceous vegetation associations (grassland, moors)	22200
12300	Port areas	998	33000	Open spaces with little or no vegetations (beaches, dunes, bare rocks, glaciers)	96
12400	Airports	998	40000	Wetland	40000
13100	Mineral extraction and dump site	998	50000	Water bodies	31000
13300	Construction sites	998			

Table 17. Reclassification table for Riparian Zones

RZ	Class Name	LCcode	RZ	Class Name	LCcode
11110	Continuous Urban Fabric (IMD ≥ 80%)	998	41000	Managed grassland	22110
11120	Dense Urban Fabric (IMD ≥ 30 - 80%)	998	42100	Seminatural grassland	93
11130	Low Density Fabric (IMD < 30%)	998	42200	Alpine and subalpine natural grassland	22200
11200	ndustrial, commercial and military units	998	51100	Heathland and Moorland	22200
12100	Road networks and associated land	998	51200	Other scrub land	21220
12200	Railways and associated land	998	52000	Sclerophyllous vegetation	21220
12300	Port areas and associated land	998	61000	Sparsely vegetated areas	96
12400	Airports and associated land	998	62100	Beaches and dunes	12200
13100	Mineral extraction, dump and construction sites	998	62200	River banks	12200
13200	Land without current use	998	63100	Bare rocks and rock debris	12100
14000	Green urban, sports and leisure facilities	998	63200	Burnt areas (except burnt forest)	97
21100	Arable land	22120	63300	Glaciers and perpetual snow	32000
21200	Greenhouses	22120	71000	Inland marshes	40000
22100	Vineyards, fruit trees and berry plantations	99	72100	Exploited peat bog	40000
22200	Olive groves	21132	72200	Unexploited peat bog	40000
23100	Annual crops associated with permanent crops	92	81100	Coastal salt marshes	40000
23200	Complex cultivation patterns	92	81200	Salines	40000
23300	Land principally occupied by agriculture with significant areas of natural vegetation	93	81300	Intertidal flats	40000
23400	Agroforestry	94	82100	Coastal lagoons	31000
31100	Natural and seminatural broad-leaved forest	2111*	82200	Estuaries	31000
31200	Highly artificial broad-leaved plantations	2111*	91100	Interconnected water courses	31000
32100	Natural and seminatural coniferous forest	2112*	91200	Highly modified water courses and canals	31000
32200	Highly artificial coniferous plantations	2112*	91300	Separated water bodies belonging to the river system	31000
33100	Natural and seminatural mixed forest	999	92100	Natural water bodies	31000
33200	Highly artificial mixed plantations	999	92200	Artificial standing water bodies	31000
34100	Transitional woodland and scrub	95	92300	Intensively managed fish ponds	31000
34200	Lines of trees and scrub	95	92400	Standing water bodies of extractive industrial sites	31000
35000	Damaged forest	95	10000	Sea and ocean	31000

2- *Creation of the basic mosaic*

The three reclassified data are mosaicized. Where more data are present at the same time, priority is given to UA, then RZ and finally N2000.

3- *Reclassification and insertion of CLC data and regional maps*

The CLC in raster format at 10 m has been reclassified considering the correspondences of Table 18, which also contains the temporary code of Table 14.

Table 18. Reclassification table for CORINE Land Cover

CLC	Class Name	LCcode	CLC	Class Name	LCcode
111	Continuous urban fabric	998	3111-3117	Broad-leaved forest	2111
112	Discontinuous urban fabric	998	3121-3125	Needle-leaved forest	2112
121	Industrial or commercial units	998	3131-3132	Mixed forest	999
1211	Photovoltaic fiends	998	3211	Continuous natural grasslands	22200
122	Road and rail networks and associated land	998	3212	Discontinuous natural grasslands	22200
123	Port areas	998	322	Moors and heathland	21220
124	Airports	998	3231	High mediterranean scrub	21220
131	Mineral extraction sites	998	3232	Low mediterranean scrub, garrigue	21220
132	Dump sites	998	324	Transitional woodlandshrub	95
133	Construction sites	998	3241	Forest harvesting	95
141	Green urban areas	91	331	Beaches, dunes, sands	12200
142	Sport and leisure facilities	998	332	Bare rocks	12100
2111	Intensive nonirrigated arable land	22120	333	Sparsely vegetated areas	96
2112	Extensive nonirrigated arable land	22120	334	Burnt areas	97
212	Permanently irrigated land	22120	335	Glaciers and perpetual snow	32000
213	Rice fields	22120	411	Inland marshes	40000
221	Vineyards	21210	412	Peat bogs	40000
222	Fruit trees and berry plantations	21131	421	Salt marshes	40000
223	Olive groves	21132	422	Salines	40000
224	Woody plantation	21133	423	Intertidal flats	40000
2241	New woody plantation	21133	511	Water courses	31000
231	Pastures	22110	512	Water bodies	31000
241	Annual crops associated with permanent crops	92	521	Coastal lagoons	31000
242	Complex cultivation patterns	92	522	Estuaries	31000
243	Land principally occupied by agriculture, with significant areas of natural vegetation	93	523	Sea and ocean	31000
244	Agroforestry	94			

4- *Use of HRLs for the classification of uncertain classes*

The HRLs DLT, GRA and WAW related to 2012 have been mosaicized and used to assign a land cover class to the uncertain classes of Table 14.

In detail, in the uncertain areas the arboreal component (identified by HRL Forest) was distinguished from the herbaceous component (identified by HRL Grassland) and from areas without vegetation. In relation to the agricultural or natural use of the original classes, the most probable land cover class was therefore attributed, as described in detail in Table 19.

The HRL WAW was used to refine water bodies. In areas covered by high resolution data (UA, RZ, N2000) the water bodies of the HRL WAW are classified as 122 “Unconsolidated natural abiotic surfaces (beaches, dunes, sands)”. This is because the given data report water bodies in more detail than the HRL. In the areas covered only with CLC, water bodies mapped by the HRL were added, as they are smaller than the CLC MMU and MMW.

Table 19. Attribution of classes to temporary codes using HRL

Temp. code	Area covered by DLT	Area covered by GRA	No GRA and No DLT area
91	21131 Orchards	2211 Pastures	2121 Vineyards
92		2212 Arable land	
93		2211 Pastures	2212 Arable land
94	2111 Broad-leaved	2212 Arable land	
95	or	2122 Shrubland	
96	2112 Needle-leaved	222 Permanent	
97		222 Permanent	121 Natural abiotic surfaces
99	21131 Orchards	2121 Vineyards	

5- *Use of HRLs to distinguish broad-leaved and needle-leaved in the mixed forest areas (temporary code 999)*

The mixed forest coming from UA, RZ and N2000 were distinguished in broad-leaved and needle-leaved through a proximity criterion, starting from the Euclidean allocation made on HRL DLT.

6- *Use of the fourth CLC level for the attribution of a more detailed class to broad-leaved and needle-leaved areas*

Broad-leaved and needle-leaved were reclassified to the fifth classification level (not shown in Table 13) on the basis of the fourth CLC level available for the Italian territory. The 2012 broad-leaved and needle-leaved CLC polygons were exported, rasterized and Euclidean allocation was made with respect to the CLC fourth classification level. The Euclidean allocation was used to assign the most detailed class to broad-leaved and needle-leaved pixels of the map, according to a criterion of proximity.

7- *Insertion of LCM and assignment of the class to temporary codes 998*

The LCM for 2012 was superimposed on the map obtained in the previous steps, since it is the most detailed available data. Pixel classified as 998 that do not fall within the LCM are related to urban areas of the Copernicus data without artificial land cover. They have therefore been attributed to class 222 “Permanent herbaceous”.

3.2.3 Development of a supervised land cover classification methodology

3.2.3.1 Overview

The methodology presented in this study uses Sentinel-1 GRD and Sentinel-2 images to map land cover and land cover changes in Italy, on a yearly basis (Figure 9).

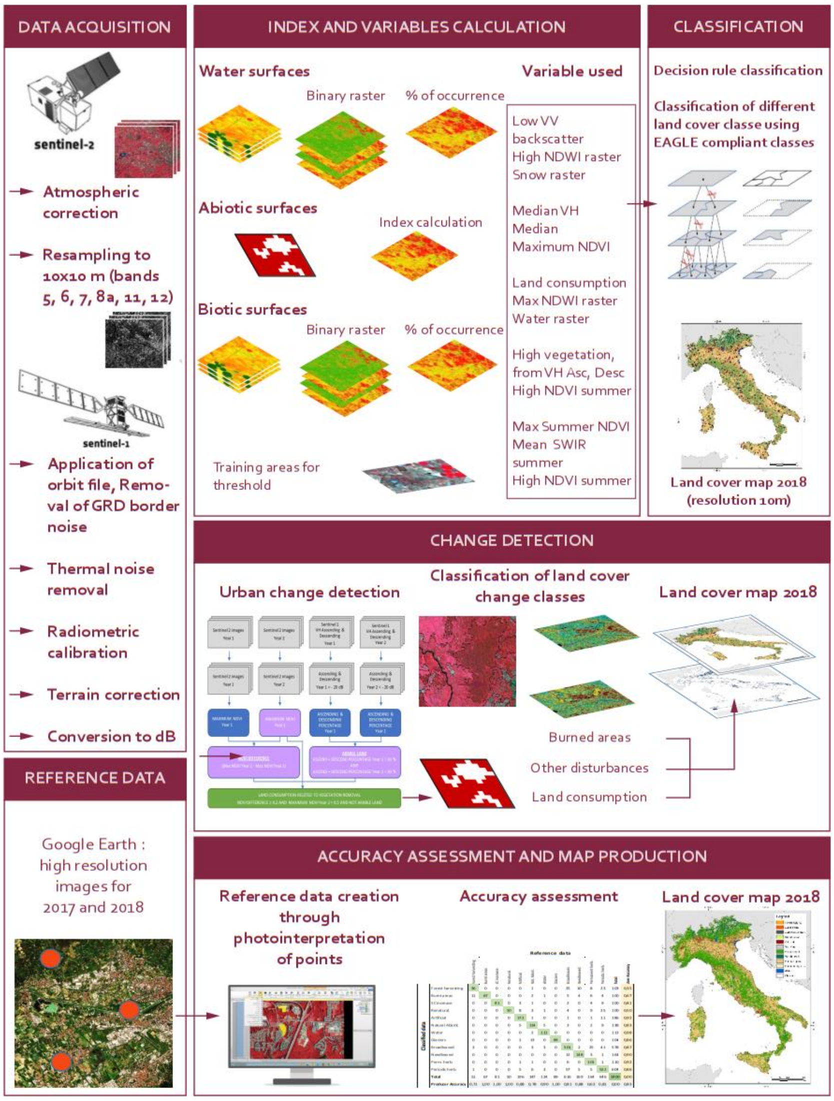

Figure 9. Land cover classification and change detection metodology workflow

Decision rules are defined to identify land cover classes at pixel size of 10 m, setting fixed threshold values on composites (e.g. median, maximum) of multitemporal data. The rules are based on experience, on deep knowledge of literature and on previous analysis of temporal trend of spectral signatures, indexes and backscatter coefficients of each class. Furthermore, the thresholds for vegetation classes were also defined using a collection of training areas. The output classifications were validated through the photointerpretation of very high-resolution images.

The methodology was developed with Google Earth Engine (Javascript language program) but also works on the QGIS Semi-Automatic Classification Plugin and on a DIAS environment[7]. This DIAS experimentation refers to the agreement between Italian Space Agency (ASI) and ISPRA for habitat mapping.

[7] ONDA https://www.ondadias.eu

The classification refers to the land cover classes defined in Table 11 and to the change classes in Table 12.

The methodology was described in a paper published on “Land” journal, entitled “Multispectral Sentinel-2 and SAR Sentinel-1 integration for automatic land cover classification” (De Fioravante *et al.*, 2021). The methodology described below is an extended version of the one presented in the paper.

3.2.3.2 Images preprocessing and training areas collection

Before the classification process, preliminary steps are required to collect training areas and pre-process the input images to obtain the backscatter values for Sentinel-1 GRDs and reflectance values for Sentinel-2 images.

Sentinel-2 L1C images were used in this study. The atmospheric disturbance affecting L1C pixels can increase the uncertainty of spectral signatures and therefore decrease the classification accuracy, however Sentinel-2 L2A historical archive was not available at the time of the research. The input images were cloud masked and pixels affected by clouds excluded from calculations. The cloud mask was made through a simple algorithm based on the quality assessment band as described in Google Earth Engine website[8]. It is worth highlighting that cloud mask products provided with Sentinel-2 images generally underestimate clouds (Coluzzi *et al.*, 2018).

Sentinel-1 GRD images provided in Google Earth Engine are already converted to backscatter values, following the steps described in the website[9], which are:

- Application of orbit file;
- Removal of GRD border noise (low intensity and invalid data);
- Thermal noise removal to reduce discontinuities between sub-swaths;
- Backscatter intensity calculation using radiometric calibration;
- Terrain correction (ortho-rectification using the SRTM 30 m DEM);
- Conversion of backscatter coefficient to dB.

The same preprocess can be applied to the DIAS environment. Sentinel-1 GRD and Sentinel-2 grids are not aligned and have different spatial resolution: in detail, Sentinel-1 GRD have ground range geometry and the preprocessing involves the geocoding to map coordinates. Sentinel-2 images are provided in WGS84-UTM coordinates and cover the Italian territory with about 80 granules. In order to use both images in the same workflow, the spatial

---

[8] https://developers.google.com/earthengine/datasets/catalog/COPERNICUS_S2
[9] https://developers.google.com/earthengine/Sentinel-1

resampling to a common coordinate reference system and spatial resolution is required. In this study, Sentinel-1 data were aligned to the Sentinel-2 grid, in the WGS84-UTM reference system.
Another preliminary operations is the photointerpretation of training areas. These are used to set the thresholds in classifying broad-leaved and needle-leaved vegetation.

3.2.3.3 Classification process

The production of the land cover map involves the calculation of multitemporal indices and decision rules that allows for the separation of land cover classes. A pixel is assigned to a specific class if it has spectral and geometric characteristics that satisfy all the rules and thresholds defined for that class. The classification primarily regards the assignment to each pixel of one of the three classes at the first classification level. This operation provides three masks, to which a more detailed class is subsequently assigned, according to the methodology described below. Table 20 shows the spectral indices used for the classification and calculations on the base of the Sentinel-2 images.

Table 20. Spectral indices used for land cover classification

Satellite	Index name	Brief index formula	Reference
Sentinel-2	Normalized Difference Vegetation Index	$NDVI = \frac{(B8 - B4)}{(B8 + B4)}$	(Rouse Jr, 1973)
	Normalized Burn Ratio	$NBR = \frac{(B8 - B12)}{(B8 + B12)}$	(Key and Benson, 1999)
	Normalized Difference Water Index	$NDWI = \frac{(B3 - B8)}{(B3 + B8)}$	(McFeeters, 1996)
	Normalized Difference Snow Index	$NDSI = \frac{(B3 - B11)}{(B3 + B11)}$	(Dozier, 1989)
	Normalized Difference Coniferous Index	$NDCI = \frac{(B6 - B12)}{(B6 + B12)} * \frac{(B8 - B11)}{(B8 + B11)}$	
	Burned Index	$BI = \frac{\left(1 - (B3 + B4 + B8)\right)}{\left(1 + (B3 + B4 + B8)\right)}$	

3.2.3.4 Water surfaces

Water classes are a required input for the classification of abiotic land cover classes, therefore they must be classified before the other classes (Figure 10).

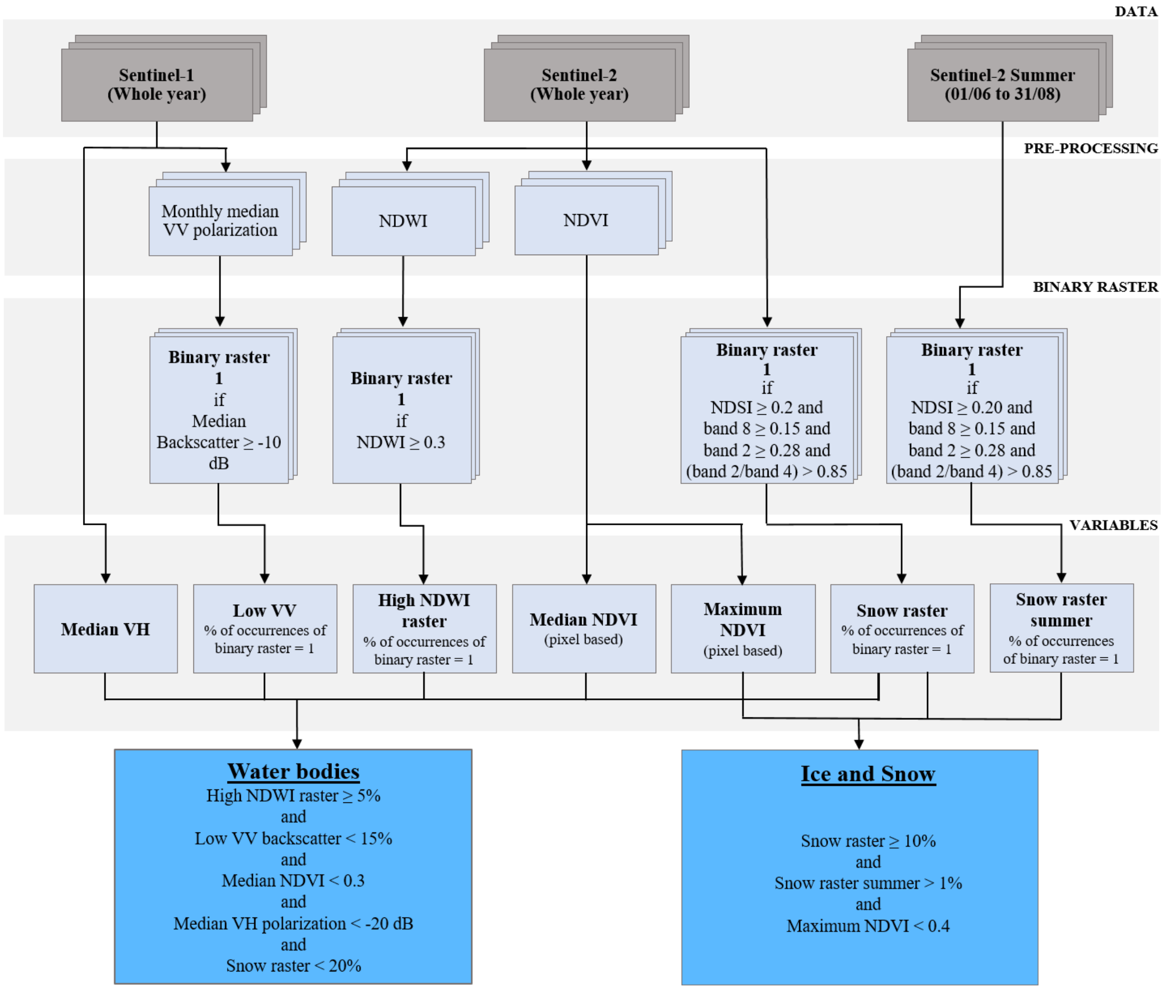

Figure 10. Workflow for the classification of water surfaces

Permanent snow and ice

The classification of permanent snow and ice is based on the definition of rules starting from the NDVI index and the "Snow raster".

The "Snow raster" derives from the methodology developed by ESA (ESA, 2021) to detect snow surfaces, which are identified by reflectance values lower than threshold reported below:

$$\begin{gathered} NDSI \geq 0.2 \\ \text{AND} \\ Band\ 8 \geq 0.15 \\ \text{AND} \\ Band\ 2 \geq 0.28 \\ \text{AND} \\ \frac{Band\ 2}{Band\ 4} > 0.85 \end{gathered} \tag{1}$$

The "snow raster" associates to each pixel the percentage of times in which all the conditions are satisfied during the reporting period.

The conditions are based on NDSI index, which exploits the property of snow surfaces to be very bright in the visible and dark in short-wave infrared (cloud and snow reflectance are similar in band 3 but band 11 reflectance for clouds is very high while it is low for snow). This index allows to detect snow and differentiate it from clouds, with values varying from -1 to 1. As a general rule, positive values define probable areas with snow.

The NDVI is flanked by three “filters” relating to band 8, band 2 and ratio between band 2 and 4. Band 8 threshold eliminates pixels that have high NDSI values and low band 8 (NIR) reflectance: pixels with values over 0.15 are considered as snow. Threshold on band 2 eliminates pixels that have high NDSI values and low band 2 (blue) reflectance; finally, the ratio between band 2 and 4 eliminates pixels that that usually corresponds to water bodies.

The thresholds are those indicated by ESA analysis.

The following three conditions are defined for the identification of permament snow and ice:

1) Snow raster ≥ 10%

For all granules, the snow raster associated with each pixel was calculated, based on the Sentinel-2 annual series, as shown below:

A binary raster was produced for each valid acquisition by attributing to each pixel the value 1 if the conditions of (1) are verified and 0 elsewhere.

Starting from the series of binary rasters for whole year (a binary raster for each valid acquisition), a raster of “percentage of occurrency” (P_{class}) was produced. It considers, for each pixel, the number of times the binary raster assumes the value 1 (N_{occurr}) on the total of valid acquisitions ($N_{cloud\text{-}free}$). It should be highlighted that the number of valid acquisitions can be lower or equal to the total number of available satellite acquisitions, depending on the cloud cover (the percentages obtained from the binary raster will always be calculated in this way unless otherwise specified).

$$P_{Class} = \left(\frac{N_{occurr}}{N_{cloud-free}}\right) * 100$$

Finally, a threshold is defined on the “percentage of occurrency” raster, which is reclassified into into a binary raster. The binary raster takes the value 1 if the “percentage of occurrency” is greater than the threshold and 0 otherwise.

In the following, the concepts of “binary raster” and “percentage of occurrency” raster will refer to the above definition.

In this specific case the “percentage of occurrency” raster is the annual “snow raster”, which is then reclassified in the final binary mask, considering a threshold of 10%. This value allows to eliminate outlier pixels.

2) Snow raster summer> 1%

A second elaboration of the snow raster was carried out for the summer period (1st July - 31st September). The procedure is the same as described above, however a less conservative threshold of 1% has been adopted for the elimination of outlyers.

3) Maximum NDVI < 0.4

A threshold of 0.4 was defined on the maximum NDVI value to exclude areas with the presence of vegetation.

Water bodies

Five conditions were considered in order to identify water surfaces, each of them contributes to reduce possible mistakes between the spectral signature of water and other classes (Figure 10). The first three rules are based on indices derived from Sentine-2 images and the last two used Sentinel-1 GRD data.

1) High NDWI raster ≥ 5%:

It was observed by McFeeters (McFeeters, 1996) that water class has NDWI> 0 while non-water classes have NDWI < 0; a threshold value of 0.3 on NDWI was considered to better isolate water from the built up area and other surfaces (McFeeters, 2013).

For each granule, the Sentinel-2 annual image series was considered and the NDWI of each pixel calculated. A binary raster was processed starting from each image, attributing to each pixel the value 1 if the imposed condition is met (NDWI ≥ 0.3 in this case) and 0 elsewhere.

Starting from the annual series of binary rasters, a raster of “percentage of occurrency” of values 1, called “High NDWI raster” was elaborated. Finally, a threshold of 5% was considered and the “High NDWI raster” was reclassified into a binary raster, assigning a value of 1 to pixels with a percentage of occurrency higher than 5% and 0 elsewhere, in order to exclude outliers from the time series.

2) Median NDVI < 0.3

From the NDVI multitemporal series for the whole year, the median of the NDVI for each pixel was calculated. A threshold of 0.3 was then defined and the possible presence of water bodies was limited to pixels with values below the threshold, in order to eliminate vegetated areas.

3) Snow raster < 20%

As in the case of permanent ice and snow, a “snow raster” was elaborated, relating to how many times the conditions of (1) were verified in each pixel.

A threshold of 20% is defined on the “snow raster”, which is reclassified into a binary mask. The snow raster, in this case, takes the value 1 if the “percentage of occurrency” is lower than the value set by the threshold and 0 otherwise.

4) Median VH polarization < 20 dB

The backscatter values used in this classification are derived from tests carried out on sample areas and from values reported in the literature (Mansaray *et al.*, 2017; Zhou *et al.*, 2017; Gulácsi and Kovács, 2020). The VH band discriminates quite well the different classes presenting backscatter values around 20 db, which remains constant throughout the year. Variations can be due to the wind that makes the water surface rougher and modifies its backscatter. A mask was produced considering all the pixels with an annual median of the VH polarization < 20 dB.

5) Low VV backscatter < 15%

The VV values are generally higher then VH ones. In the case of VV backscatter the value 10 dB was determined as a good threshold for identifying water (Mansaray *et al.*, 2017; Zhou *et al.*, 2017). A binary raster was produced starting from the monthly median (i.e. divided 12), attributing value 0 for values below 10 dB and 1 elsewhere. It was classified as water class when the percentage of value 1 throughout the year is less than 15%.

3.2.3.5 Abiotic surfaces

The workflow for abiotic classes is based on the definition of two rules and requires only Sentinel-2 input images for the whole year. The abiotic surfaces are then distinguished between artificial and natural surfaces (Figure 11).

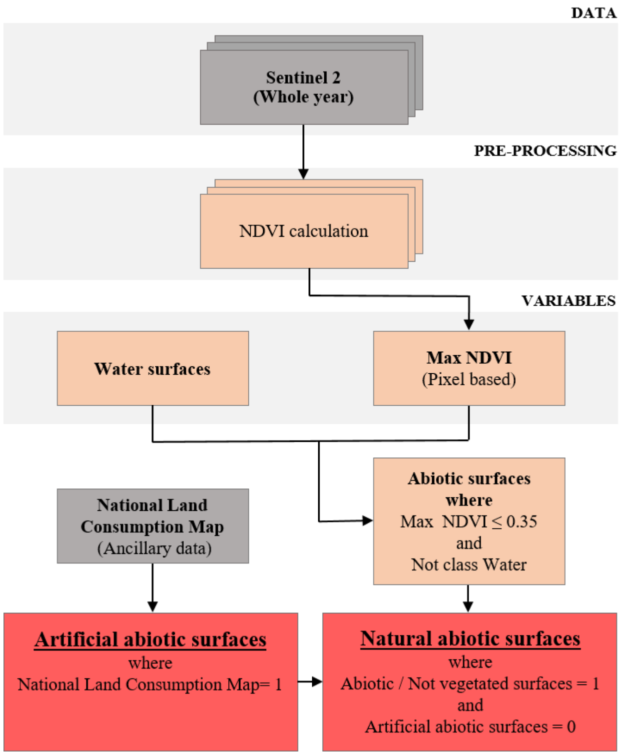

Figure 11. Workflow for the classification of abiotic surfaces

1) *Maximum NDVI ≤ 0.35*

A threshold of 0.35 is defined on the maximum annual NDVI value, in order to exclude areas that may present vegetation during the year. This calculation is in common with the processing of water classes, therefore the same data were calculated only once.

2) *Not Water surfaces*

Both the abiotic surface class and the water surfaces have low maximum NDVI values. To avoid commission errors, this second rule is defined, which excludes pixels previously classified as water surfaces

Artificial abiotic surfaces

The distinction between natural and artificial abiotic classes is based on the National Land Consumption Map (LCM) produced by ISPRA (ISPRA, 2015). The LCM was introduced for 2012 and updated every year from 2015 through photointerpretation.

The LCM for 2012 (10 m resolution) is a product derived from a first classification performed by ISPRA in collaboration with Planetek Italia srl. It was derived from the semiautomatic classification of RapidEye imagery[10] (5 m resolution) acquired in 2011 and 2012 for the whole Italian territory. The production methodology integrates multispectral

[10] https://earth.esa.int/web/guest/missions/3rd-party-missions/current-missions/rapideye

and SAR images, vegetation index (i.e. NDVI), and photointerpretation. To produce the map the Maximum Likelihood classification algorithm was performed, using the five available wavebands of RapidEye imagery and collecting training data of impervious surfaces derived from visual interpretation. Moreover, ancillary data available at the regional level were used, such as regional land cover and land use databases, and OpenStreetMap data to improve the identification of roads. The LCM for the year 2012 was the result of pixel resampling (from 5 m to 10 m) and intensive manual editing, in order to correct omission errors and to improve classification accuracy.

The LCM is yearly updated through an inspection of the national territory and photo-interpretation of the changes. The activity involves the editing of vector polygons at a detailed scale (greater than 1:5,000, MMU 100 m^2) based on the mosaics of Sentinel-2, national orthophotos and other free VHR satellite images (e.g. through Google Earth or Bing services). Then the data were converted into raster format (10 m spatial resolution) by attributing the class to each pixel based on the prevalent coverage that falls within it. The procedure for the production and updating of the LCM is described in the paper published in the "Journal of Maps" entitled "Land consumption in Italy".

The LCM is used in this methodology for the classification of artificial abiotic surfaces since it reaches an overall accuracy of 99.7% (Strollo *et al.*, 2020), which is difficult to achieve with an automatic classification of Sentinel data created from scratch. The high accuracy value is guaranteed by the fact that the LCM is updated by photointerpretation which, however, is an expensive and time-consuming activity. One of the objectives of this research was therefore the creation of a tool to support the annual update of the LCM. Rasters, called "masks", have been created that identify the areas where changes potentially related to land consumption have occurred, in order to reduce the areas to be inspected during photointerpretation and thus reducing the time and costs associated with this activity. (Munafò, 2020). The detailed description of the masks of potential changes is reported in the following paragraphs.

Natural abiotic surfaces

Artificial surfaces and natural abiotic surfaces are very similar from a spectral point of view, so it is difficult to distinguish them only through the use of satellite images.

The natural abiotic surfaces class has been identified considering the pixels classified at the first level as abiotic surface that have not already been classified as artificial abiotic surface.

3.2.3.6 Biotic surfaces

The pixels that are not included in the classes of water bodies and abiotic surfaces are associated to biotic vegetation.

The areas covered by woody vegetation were first identified, and then they were divided into broad-leaved and needle-leaved trees. The land cover of the remaining areas was divided into periodically or permanent herbaceous, according to the EAGLE definition (Kleeschulte *et al.*, 2019) (Figure 12).

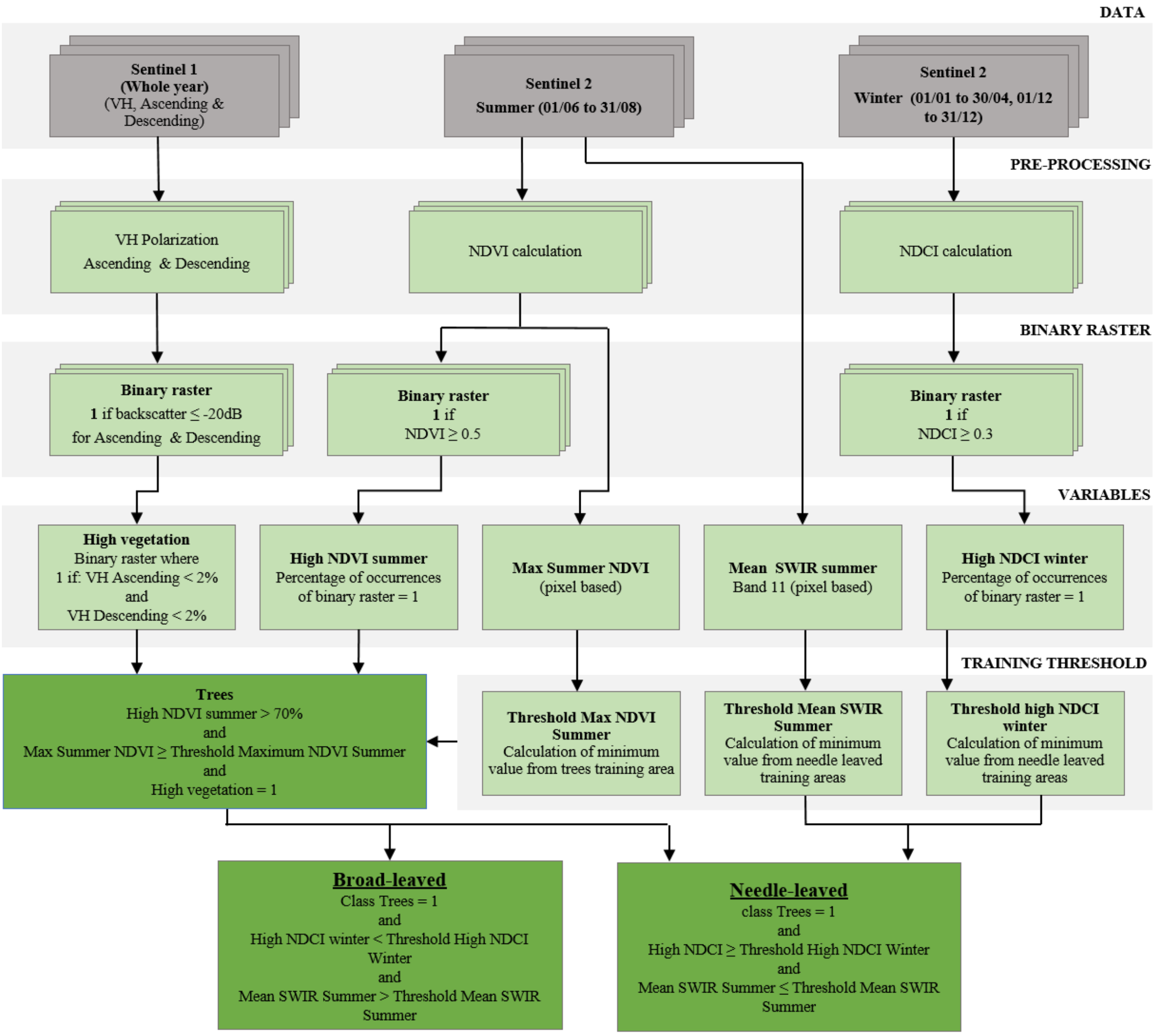

Figure 12. Workflow for the classification of woody vegetation

The classification of biotic surfaces required the Sentinel-1 GRD dataset for the whole year and Sentinel-2 images for the whole year, for the summer period (1st June - 31st August) and for the winter period (1st January - 30th April and 1st December - 31st December). Furthermore, 905 training areas were collected throughout the national territory, for the identification of the woody vegetation and for the distinction of broad-leaved and needle-leaved trees.

Woody vegetation

Woody vegetation was identified through the definition of three rules. The first two rules are relate to information obtained from Sentinel-2 optical images, while the third is based on Sentinel-1 GRD data.

1) *High NDVI summer ≥ 70%*

   The NDVI was calculated for each pixel of all Sentinel-2 summer images. A threshold of 0.5 was defined on the NDVI and a binary raster was created for each image, assigning a value of 1 to pixels with NDVI > 0.5 and 0 elsewhere. Starting from the binary rasters series, a "percentage of occurrency" raster was obtained, called "high NDVI summer". This raster associates to each pixel the number of times (in percentage) that the binary raster has assumed value 1 on the total of valid acquisitions. Finally, a threshold of 70% was defined on the "High NDVI summer" raster, which was reclassified into a binary raster with a value of 1 in the pixels with a frequency above the threshold and 0 elsewhere.

2) *Maximum NDVI summer ≥ Training area threshold*

   The second rule refers to the maximum summer NDVI values of the pixels to be classified. Starting from the series of summer images, the maximum NDVI for each pixel was identified, obtaining a raster of "max NDVI summer". The raster was then reclassified into a binary raster, comparing the values with a threshold obtained from training area. In detail, the maximum summer NDVI was calculated in each pixel of the training areas and the lowest of them was taken as the reference threshold. The binary raster takes a value of 1 if the "Max NDVI summer" of the pixel to be classified is greater than the threshold from the training area and 0 elsewhere.

3) *High vegetation*

   The backscatter of VH polarization for the whole year was used, as it can partially improve the detection between high vegetation (trees) and low vegetation (e.g. crops) (Holtgrave *et al.*, 2020). Since the acquisition orbit influences the view angle, the ascending and descending orbits are considered separately. For the two orbits, two binary rasters were calculated for each acquisition, associating a value of 1 to pixels with backscatter ≤ 20 dB and 0 elsewhere.

The value 20 dB was used as a threshold for distinguishing low vegetation and fallow land that generally have backscatter values lower than 11 dB (Formaggio *et al.*, 2001), from trees that generally have higher backscatter values.

Starting from the binary rasters, a "percentage of occurrency" raster of values 1 was produced.

A threshold of 2% has been defined and the "percentage of occurrency" raster has been reclassified to binary raster, based on this threshold. A pixel has "high vegetation" if both VH ascending and VH descending have a percentage of occurrency lower than 2% of the total acquisitions. The 2% threshold is used to exclude possible outliers from time series of backscatter values.

Broad-leaved and needle-leaved trees

Pixels classified as woody vegetation can be further distinguished in broad-leaved and needle-leaved using Sentinel-2 summer and winter images and training areas.

1) *Woody vegetation raster = 1*

The conditions for distinguishing broad-leaved and needle-leaved are applied only to pixels classified as woody vegetation

2) *Mean SWIR summer ≤ Threshold Mean SWIR summer (needle-leaved trees)*
Mean SWIR summer > Threshold Mean SWIR summer (broad-leaved trees)

The spectral characteristics of needle-leaved and broad-leaved trees are very different in the wavelength of the short-wave infrared (SWIR). Starting from the needle-leaved training area the mean of the SWIR was calculated on summer images (1st June – 31st August) and the maximum value was set as a threshold. Needle-leaved trees pixels will have mean SWIR summer values lower than or equal to the threshold, while broad-leaved trees higher.

3) *High NDCI winter > Threshold high NDCI winter (needle-leaved trees)*

The third condition exploits a new index developed in this research and called "Normalized Difference Coniferous Index" (NDCI) (Table 20). NDCI is calculated on the winter subset of Sentinel-2 images (1st January - 30th April and 1st December - 31st December) and is the multiplication between two normalized difference index: the first is based on band 6 (red edge, 740 nm) and band 12 (short wave infrared band, 2,190 nm), the second is based on band 8 (infrared, 842 nm) and band 11 (short wave infrared band, 1,610 nm).

These bands show a more pronounced difference between needle-leaved and broad-leaved trees in winter than in summer due to the fall in the spectral response of broad-leaved trees compared to needle-leaved which don't drop their leaves in senescence period (Persson *et al*., 2018).

NDCI was calculated for all winter images. A threshold of 0.3 was then defined for the NDCI and a binary raster was associated with each image, with a value of 1 if the NDCI was above the threshold and 0 elsewhere. A "percentage of occurrency" raster of 1 values was processed from the binary rasters. Finally the "percentage of occurrency" raster was compared with a threshold obtained from the training areas relating to needle-leaved trees, considering the minimum value of the winter high NDCI. Needle-laved pixels will have "percentage of occurrency" values lower than or equal to the threshold, while broad-leaved higher.

Herbaceous vegetation

Herbaceous vegetation relates to pixels not previously assigned to other land cover classes. These areas meet the following conditions:

1) *Maximum NDVI > 0.35*

As seen for the identification of abiotic surfaces, the condition distinguishes the vegetated areas from the unvegetated ones.

2) *Non-Woody vegetation*

Areas with vegetation cover but which do not respect the rules for falling into woody vegetation are considered as herbaceous.

Permanent and periodically herbaceous

The pixels of herbaceous vegetation can be divided into permanent and periodically herbaceous by defining conditions on the NDVI calculated on the annual series of Sentinel-2 images (Figure 13).

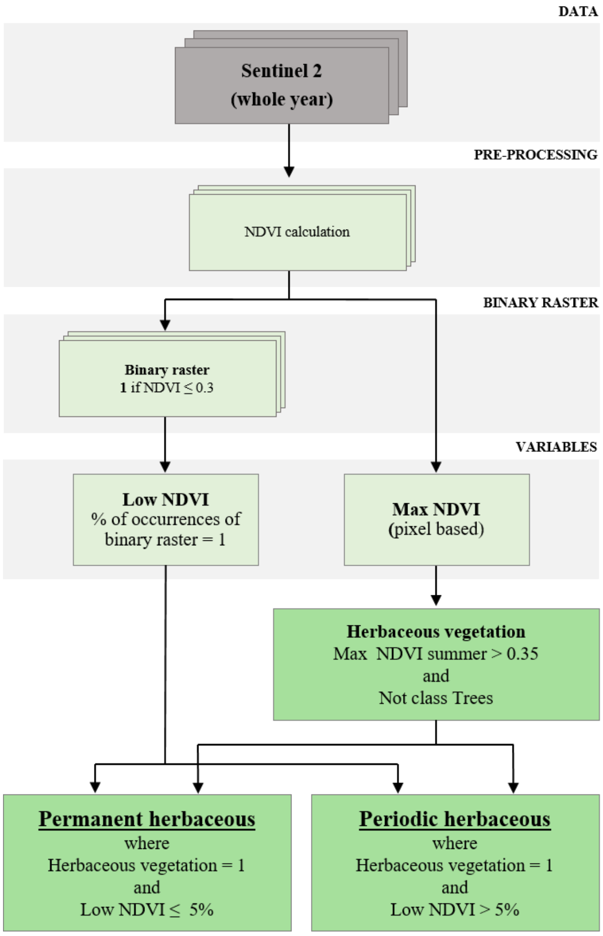

Figure 13. Workflow for the classification of herbaceous classes

1) *Low NDVI > 5% (periodic herbaceous)*

   Low NDVI ≤ 5% (permanent herabceous)

A threshold value of 0.3 was defined for the NDVI values of the Sentinel-2 images for the whole year. Each image has an associated binary raster with a value of 1 in the pixels with the NDVI greater than the threshold and 0 elsewhere. A raster of "percentage of occurrency" of the values 1 of the binary rasters is elaborated, called "low NDVI". Finally a threshold of 5% is set and compared with the values of the "low NDVI" raster. The permanent herbaceous has low NDVI values below the threshold of 0.3 for less than 5% of the observations, otherwise the pixel is classified as periodically herbaceous.

The condition "Low NDVI" ≤ 5% implies a very constant presence of vegetation during the year, such as permanent grass, while the condition "Low NDVI" > 5% implies that vegetated cover was replaced by non-vegetated cover for several periods of the year (i.e. more than 5% of valid acquisitions). It is worth noticing that non-vegetated cover could also be snow cover.

3.2.3.7 Land cover change

Forest disturbance monitoring

A specific methodology for mapping forest disturbance was developed, which also allows to distinguish burned areas from other kinds of changes like forest harvesting (Figure 14).

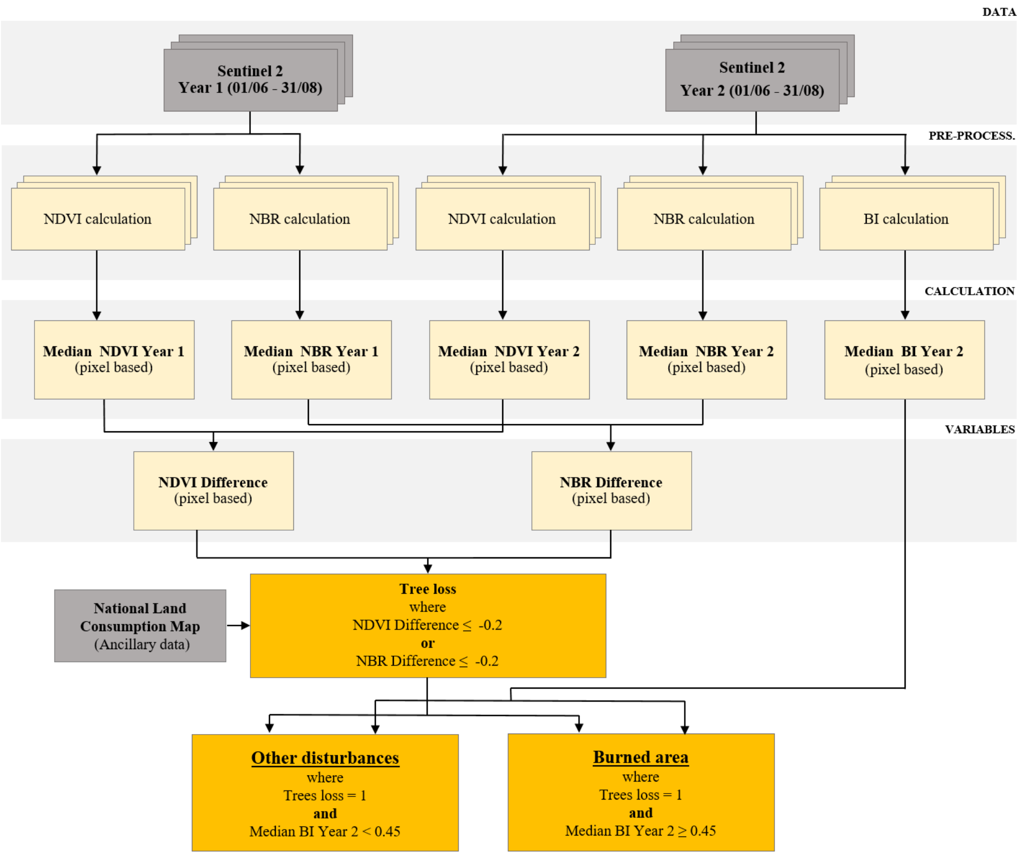

Figure 14. Workflow for the classification of tree loss

The methodology is applied to woody vegetation class, which acts as a mask for the delimitation of the forest area of year 1, where the search for changes takes place.

Other input data are the Sentinel-2 summer images (from 1st June to 31st August) for the two reference years. In this research, the changes that took place between 2017 and 2018 were analysed.

Two spectral indices were calculated for the two reference years: NDVI and NBR (Chirici *et al.*, 2020) (Table 20).

NBR is useful for identifying areas that have been burned in the reference period. Actually, healthy vegetation has very high near-infrared reflectance and low reflectance in the shortwave infrared portion of the spectrum, while recently burned areas have a low reflectance in near infrared and a high reflectance in the shortwave infrared band.

The NDVI values are is high in vegetated areas, while it decreases if there are reductions in vegetation cover.
To identify a forest disturbance, at least one of the following two conditions must be verified.

1) *NDVI median difference ≤ 0.2*

The median of the summer NDVI is calculated for the two reference years and then the difference between the two values is considered:

$$NDVI\ difference = Median\ NDVI\ year\ 1 - Median\ NDVI\ year\ 2$$

If the difference is greater than 0.2, the NDVI variation indicates the presence of a change

2) *NBR median difference ≤ 0.2*

The difference between the median of the summer NBR of the two reference years is considered:

$$NBR\ difference = Median\ NBR\ year\ 1 - Median\ NBR\ year\ 2$$

The threshold value 0.2 was identified empirically as optimal value for detecting tree loss and avoiding errors caused by phenological variations.

Distinction between "burned areas" and "other forest changes"

Starting from the pixels classified as forest disturbance, a distinction was made between "burned areas" and "other forest changes", through an innovative Burned Index (BI) (Table 20). The BI is higher for dark or brown pixel, as in case of burned areas.
The median of BI of year 2 was calculated, obtaining a raster of "Median Burned index Year 2". Pixels already classified as forest disturbance can be further detailed in fires if Median BI Year 2 ≥ 0.45
The threshold value 0.45 was determined empirically as optimal value for distinguishing burned areas and avoiding errors due to shadow areas where pixels tend to be dark.

Land consumption monitoring

The methodology uses Sentinel-1 GRD and Sentinel-2 images to automatically detect land cover changes caused by potential land consumption and it was publisched in 2021 on "Remote Sensing" journal with the title "Land consumption monitoring with SAR data and multispectral indices" (Luti *et al.*, 2021) (Figure 15). This publication was preceded by another on the same theme in the journal "Journal of maps" with the title "Land consumption in Italy" (Strollo *et al.*, 2020). The methodology reported below takes up and extends what is described in the two publications.

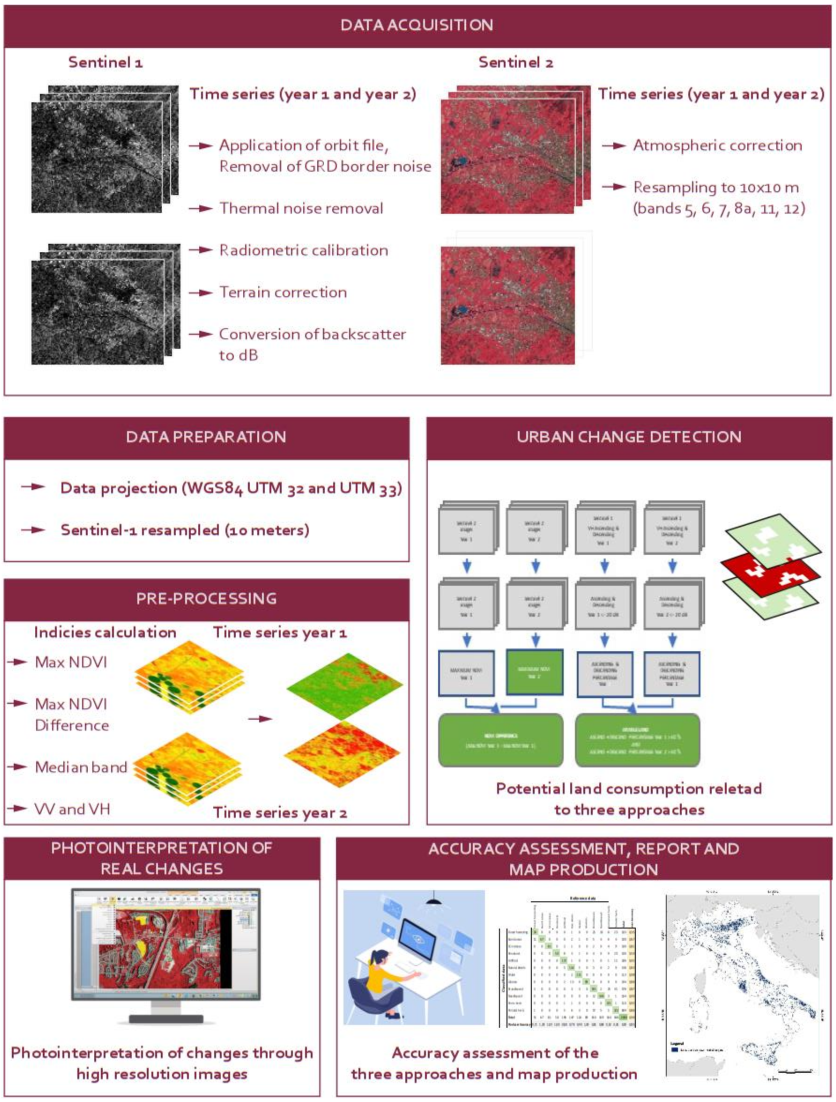

Figure 15. workflow for the production of the mask of potential land consumption

The methodology is based on the following assumptions, as well as on observation of test areas and literature:

- Land consumption can follow the removal of vegetation, if present before the change, and therefore causes a decrease of vegetation indices, such as NDVI;
- Built-up areas such as buildings, infrastructures, or even construction sites, are characterized by high backscattering values, because of multiple reflections or double-bounce effect (Cao *et al.*, 2014). Therefore, land consumption can increase the backscatter if the land cover was characterized by low or intermediate roughness like low-vegetation and bare soil before changing.

Land consumption can be detected if at least one of the above assumptions is verified.

Based on these assumptions, a fully automatic workflow was developed, using multitemporal acquisition of Sentinel-1 GRD and Sentienel-2 images, in order to detect yearly changes occurred in the study area of Italy. Sentinel-1 imagery allows to calculate of backscatter in the polarizations VV and VH, which are influenced by several factors such as geometry, dielectric properties, and roughness of surfaces (Nezry, 2014). Sentinel-2 images allow to evaluate spectral characteristics of land surface, related to land cover materials.

Decision rules are defined to estimate changes at pixel size of 10 m, setting fixed threshold values on composites (e.g. median, maximum, differences, etc.) of multitemporal images. This method does not require any training area. A Digital Terrain Model (DTM) was used to calculate the slope and refine the calculation to avoid errors related to the morphology of mountain areas.

It is worth pointing out that these classifications of changes are intended to be used to support the ISPRA monitoring of land consumption, in order to reduce the time of photointerpretation as well as reducing the area to be manually analysed.

As the acquisition orbit influences the angle of view of Sentinel-1 images, the ascending and descending orbits are considered separately, to preserve the information related to object configuration and orientation on the ground.

The backscatter of VH polarization can partially improve the detection of low vegetation or crop (Holtgrave *et al.*, 2020), while the VV polarization can be more sensitive to soil variations (Hoskera *et al.*, 2020) although these considerations should be further investigated for buildings and infrastructures. The output classifications were validated through the photointerpretation of very high-resolution images that allowed to identify of real changes.

According to the assumptions of this study related to land consumptions changes, the following methods were used:

- Sentinel-2 images allow to calculate NDVI differences in the two years for changes involving the removal of vegetation cover; Sentinel-1 GRD was also used to improve the detection.
- Sentinel-1 GRD allow to calculate differences in backscatters caused by buildings, infrastructures, or construction sites.

For the sake of simplicity, these two methods are explained in two separate paragraphs even though the model is unique.

Land consumption related to the removal of vegetation

The identification of land consumption is conducted by ISPRA through photointerpretation. In order to produce the composites, the acquisition periods between 1st March and 31st July (periods must be the same in the 2 years) were considered. In this period, vegetation in Italy is at its maximum vegetative growth guaranteeing the distinction between land consumption and bare soil. In addition, the range is large enough to ensure the availability of cloud-free images.

Since Sentinel-2 images are provided as granules (the minimum partition of the image with size 10,000 km^2), the steps in the workflow are intended to be performed for each granule. Italy is covered by about 80 granules in the WGS 84 UTM 32 and UTM 33 coordinates.

Three experimental versions were developed and tested (called “approaches”), to assess the benefit of different periods, conditions and thresholds, although the basic approach is the same. In detail, two basic conditions were defined for the detection of changes based on NDVI values, which were used in all three approaches alone or accompanied by other rules:

In the first approach, potential changes related to the application of only the two basic conditions are identified for the period between 1st March and 31st July.

In the second approach, a third condition is added, in order to filter commission errors related to seasonal variation of vegetation cover in agricultural areas. The reference period is still between 1st March and 31st July.

The third approach applies the two basic conditions varying the reference period to evaluate how its amplitude influences the identification of changes. In detail, in addition to the period between 1st March and 31st July, the period from 1st June to 31st December is considered.

The first two approaches are based on thresholds already tested in bibliography (Spadoni *et al.*, 2020), while for the third approach different thresholds were tested to distinguish the most probable changes (relative to more restrictive NDVI values, called “main range”) from less probable ones (relative to a less restrictive “additional range” of NDVI). The three approaches are detailed below.

The *first approach* considers that land consumption related to removal of vegetation has NDVI difference values greater than 0 between the two years and NDVI lower in the second year. Starting from these considerations, the following two conditions were defined:

$$NDVI\ difference\ \geq 0.2$$

AND

$$MAX\ NDVI\ year\ 2 < 0.5$$

The first condition implies a reduction of vegetation cover, while the second condition verifies the scarcity of vegetation. The threshold values are conservative and derive from literature and empirical testing (Strollo *et al.*, 2020). Pixels with NDVI values that meet these conditions have a probable change in land cover caused by land consumption.

Sentinel-2 images were processed according to these steps:

1. NDVI was calculated for every image;
2. MAX NDVI value per pixel was calculated for each year obtaining two raster (MAX NDVI raster);
3. These two MAX NDVI raster were used to calculate a third raster of NDVI difference between the 2 years (NDVI difference = MAX NDVI year 1 - MAX NDVI year 2);
4. Starting from the products of points 2 and 3, a binary mask was created where both conditions are met.

The *second approach* (Figure 16), in addition to the two conditions defined before, uses Sentinel 1 data to identify agricultural areas. Actually, these areas can be erroneously classified as land consumption due to their spectral behavior (e.g. fallow land cultivated the first year, and uncultivated the second year). An ARABLE LAND filter was defined and tested to identify agricultural areas to be excluded from change detection rules as defined in the first approach.

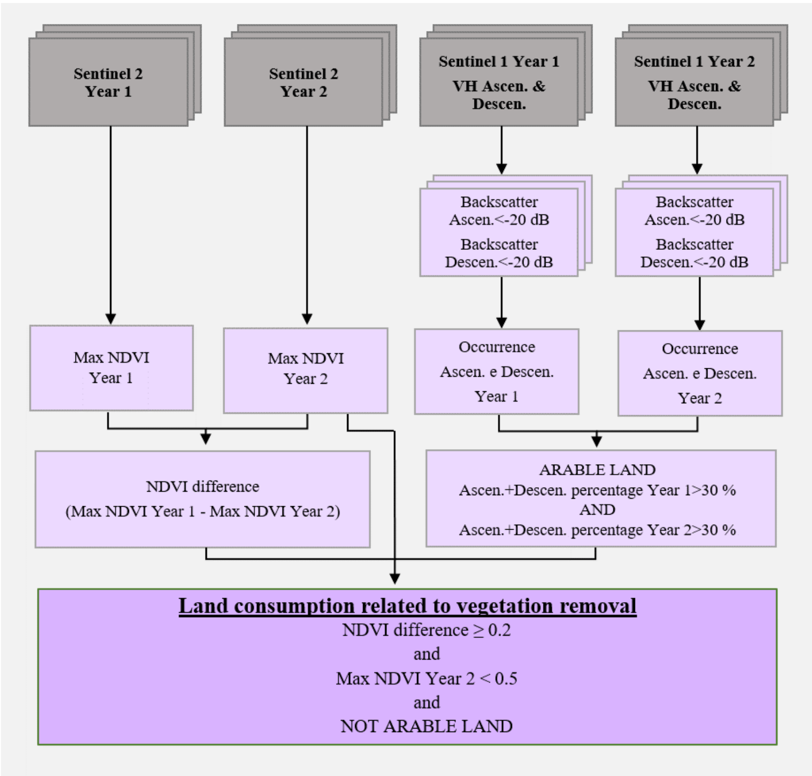

Figure 16. Land consumption related to vegetation removal with arable land filter

In order to create this raster, Sentinel-1 images with polarization VH were used, according to the following steps:

1. Four collections of Sentinel-1 VH images were distinguished by ascending and descending orbit for the 2 reference years:

   - Ascending year 1
   - Ascending year 2
   - Descending year 1
   - Descending year 2

   The sum of ascending percentage and descending percentage allows to consider both as viewing geometries which can cause shadowing and therefore affect backscatter values (Ballère *et al.*, 2021). The 2 years images are not used to estimate any difference but to verify the same condition in both years; this could fail the detection of fallow land that exhibits low backscatter values in one year.

2. A raster has been created for each of the four collections, indicating the number of times (as percentage) the backscatter was < 20 dB for each pixel.
   The 20 dB value is conservative, as fallow land is characterized by backscatter values lower than 11 dB. This value entails the presence of commission errors (agricultural areas with backscatter values higher than 20 dB), but limits the omission errors that would occur excluding land consumption associated with low backscatter values from the masks. Commission errors will be eliminated during the manual digitization of the changes while omission errors would not be considered during photointerpretationas it focuses on inspecting the masks of potential changes.
   Four rasters were obtained:

   - Ascending percentage year 1
   - Ascending percentage year 2
   - Descending percentage year 1
   - Descending percentage year 2

3. A raster ARABLE LAND is calculated according to the following condition (threshold was defined by trial and error):

$$(\text{Ascending Percentage Year 1} + \text{Descending Percentage Year 1}) \geq 30\%$$
$$\text{AND}$$
$$(\text{Ascending Percentage Year 2} + \text{Descending Percentage Year 2}) \geq 30\%$$

The ARABLE LAND layer is a binary raster whose pixels have value 1 if the above conditions are verified and zero elsewhere. The areas where the condition is verified will be excluded from the masks of potential change as it cound be agricultural areas.

It is worth pointing out that the ARABLE LAND layer is not designed for classifying arable land in general but detecting the portion of arable land that can be confused with land consumption because of temporary removal of vegetation.
In the second approach ARABLE LAND condition it is added to the two previous ones:

$$NDVI\ difference \geq 0.2$$

AND

$$MAX\ NDVI\ year\ 2 < 0.5$$

AND

$$ARABLE\ LAND = 0$$

The third condition (i.e. ARABLE LAND = 0) has the purpose to exclude false changes occurred in arable land.

The *third approach* considers that the amplitude of the reference period influences the identification of changes (Figure 17).

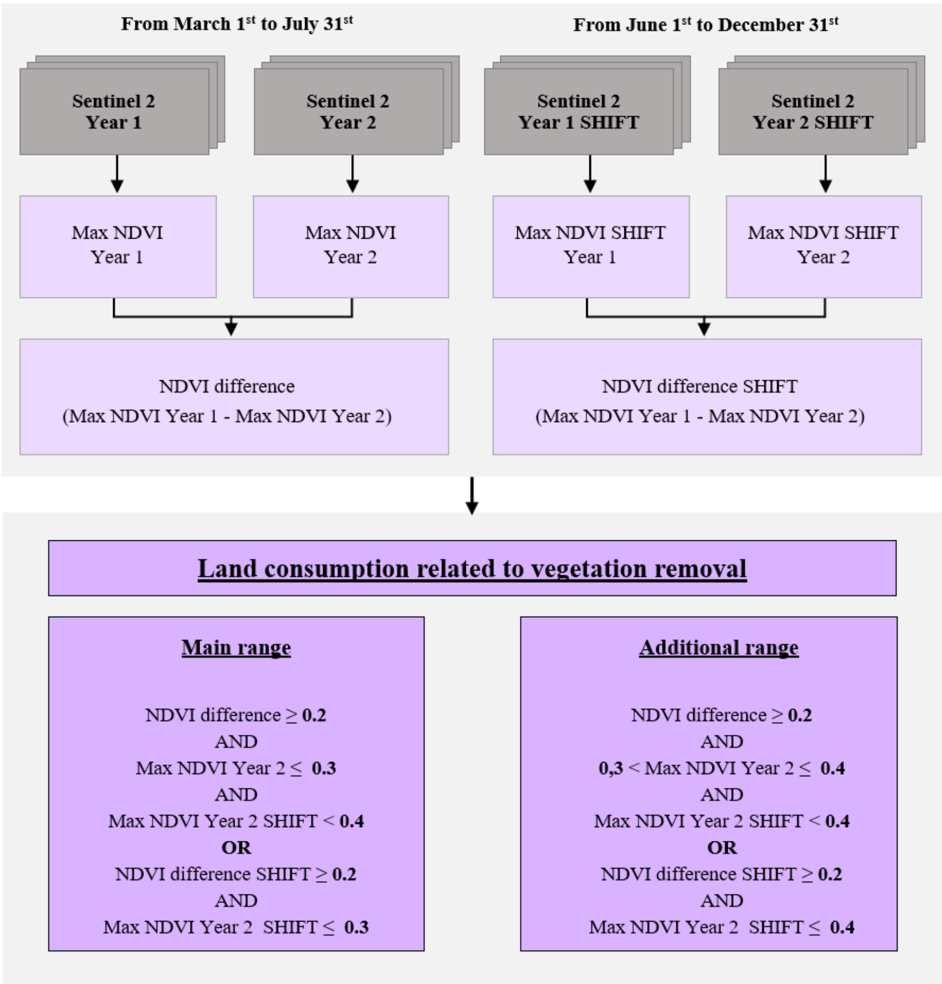

Figure 17. Workflow of the methodology of land consumption related to vegetation removal with the Shift period

Specifically, following the conditions defined in the first two experiments, it is not possible to identify the changes occurred during the reference interval of the second year as, if the period is particularly large, the omitted changes can be numerous. If a change occurred between the start of year 1 (Start date 1) and the start of year 2 (Start date 2) these can be detected because the MAX NDVI year 2 is lower than year 1 and the difference between the two MAX NDVI raster is positive (Figure 18).

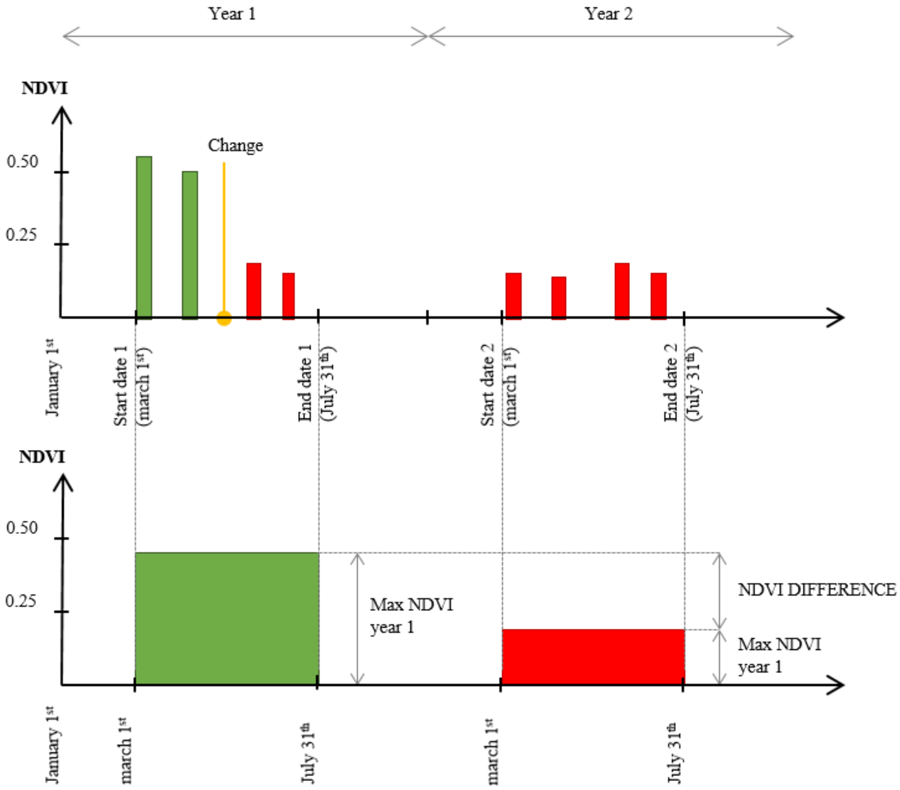

Figure 18. Scheme of change occurred between Start date 1 and Start date 2 and detected by the methodology; the upper chart represents the NDVI values of a pixel at different acquisition times; the lower chart represents the Maximum NDVI value resulting from the acquisition periods of the 2 years.

If the change occurred after the start of year 2 (i.e. between March and June) (Figure 19), it is not detected because even if the NDVI values decrease during the second year, the MAX NDVI year 2 is affected by the NDVI values before the change, and the difference between the two MAX NDVI rasters is not sufficient to check the conditions. This change will be detected the following year (e.g. comparing year 2 and year 3) because it happens between the start of year 2 and the start of year 3 as illustrated in the previous example (Figure 18).
The third approach aimed at detecting the changes occurred between March (i.e. Start date 2) and June (i.e. Start date 2 shift) of year 2, as illustrated in Figure 19. To this end, a second observation period was defined between 1st June and 31st December, called SHIFT PERIOD.

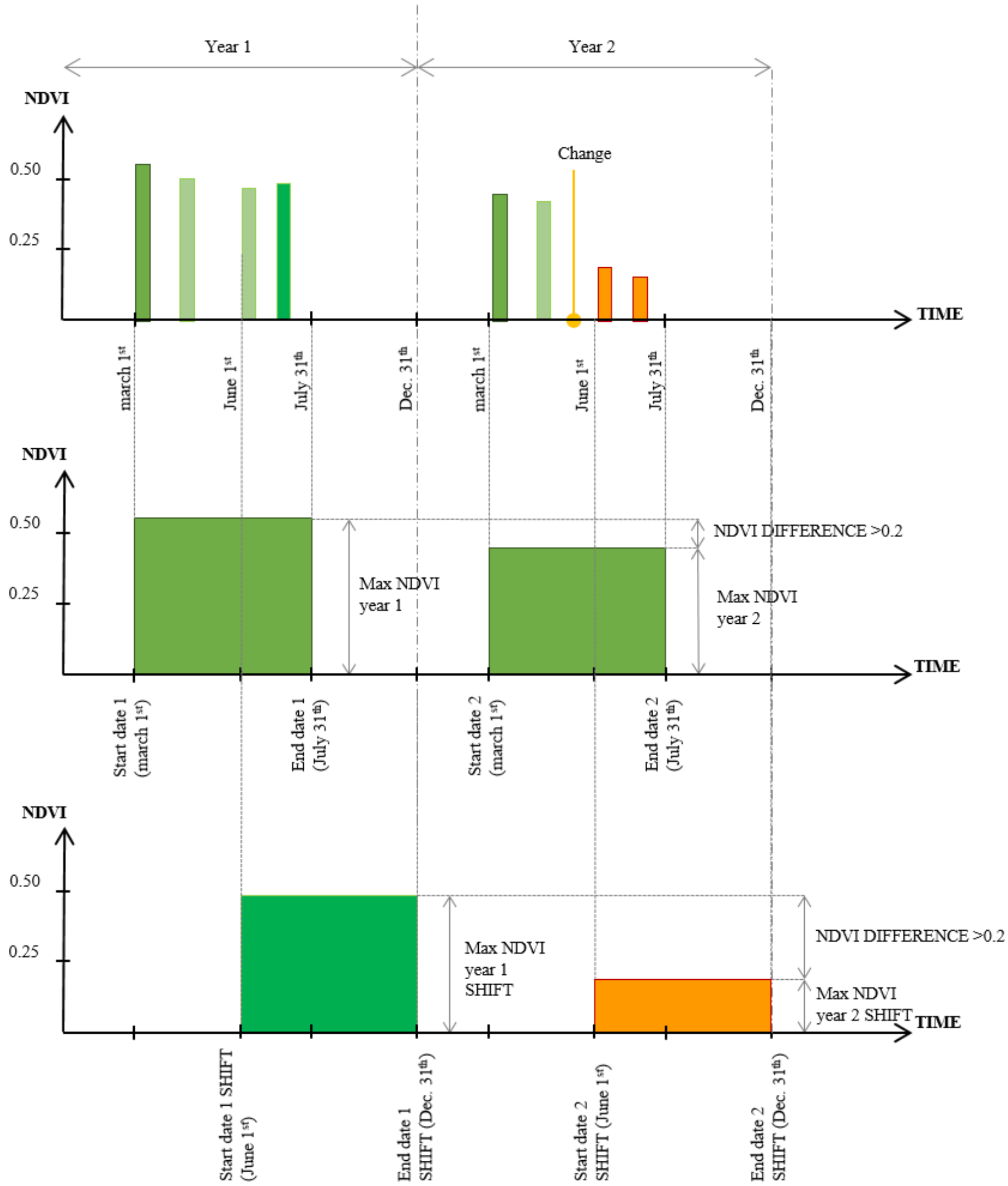

Figure 19. Scheme of change occurred after Start date 2 that can be identified with the Shift period

Moreover, a different set of NDVI thresholds were tested, in order to differentiate possible changes from NDVI variations due to agricultural practices (Figure 19). In detail, the "main range" refers to "NDVI max year 2" values lower than 0.3, while the "additional range" refers to "NDVI max year 2" values between 0.3 and 0.4. This distinction allows to distinguish more probable changes (main range) from less probable ones (additional range), attributing two distinct codes to the two types and increasing the flexibility in the use of masks during photointerpretation. The thresholds were established through trial and error.

The changes occurred between March and June of year 2 were detected with the following condition:

$$NDVI\ difference\ SHIFT \geq 0.2$$

AND

$$MAX\ NDVI\ year\ 2\ SHIFT \leq 0.3$$

The first condition (i.e. NDVI difference SHIFT ≥ 0.2) describes a change in NDVI max linked to a possible change that occurred before 1st June of the second year. The second condition (i.e. MAX NDVI year 2 SHIFT < 0.3) confirms the absence of vegetation after 1st June of the second year.

The definition of the shift period allows to introduce a further condition in addition to the two basic ones of the first experiment. The changes of the standard period (i.e. occurred before the 1st March of year 2) were identified according to the following conditions:

$$NDVI\ difference \geq 0.2$$

AND

$$MAX\ NDVI\ year\ 2 \leq 0.3$$

AND

$$MAX\ NDVI\ year\ 2\ SHIFT < 0.4$$

The third condition considers that the reduction of NDVI associated with the appearance of the change exists even after the reference period.

Possible changes related to the NDVI values of the additional range for the second year (between 0.3 and 0.4, characterized by more uncertainties because occurred in partially vegetated areas) were also analysed, modifying the initial thresholds. The identification of changes occurred between March and June of year 2 relating to the additional range of NDVI, takes place through the following conditions:

$$NDVI\ difference\ SHIFT \geq 0.2$$

AND

$$MAX\ NDVI\ year\ 2\ SHIFT \leq 0.4$$

Changes of standard period (i.e. occurred before the 1st March of year 2) relating to the additional range of NDVI, were identified according to the following conditions:

$$NDVI\ difference \geq 0.2$$

AND

$$0.3 < MAX\ NDVI\ year\ 2 \leq 0.4$$

AND

$$MAX\ NDVI\ year\ 2\ SHIFT < 0.4$$

Land consumption related to buildings and infrastructures

Land cover changes related to buildings and infrastructures can increase the backscatter values, although these values are influenced by several factors such as height and orientation of buildings. The developed workflow tries to exploit the availability of Sentinel-1 data in order to compare backscatter variations of two periods (Figure 20).

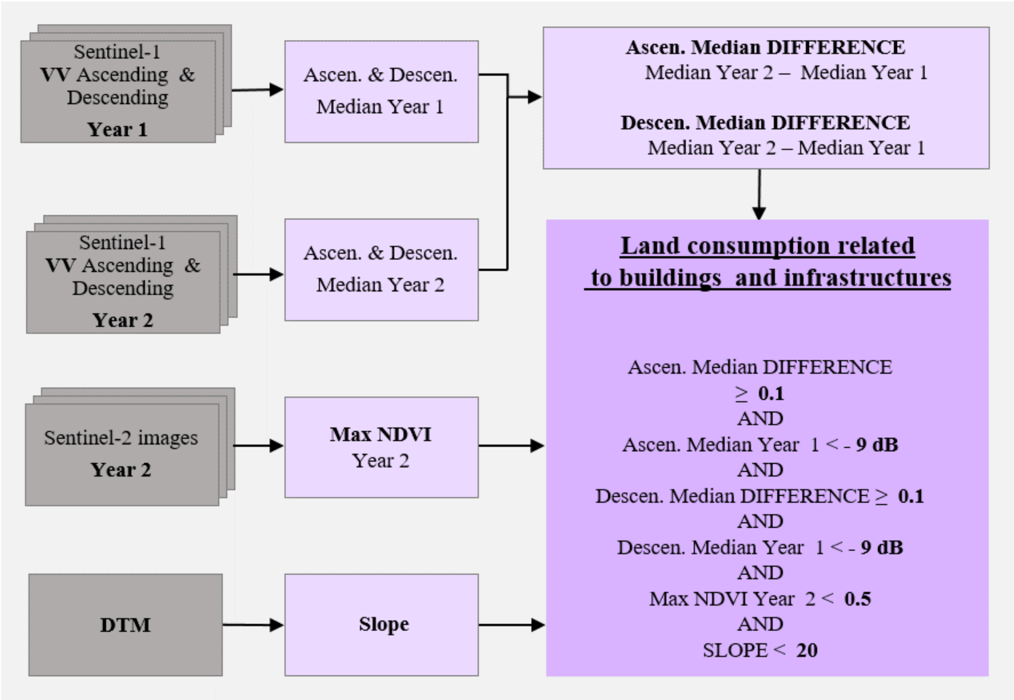

Figure 20. Workflow related to the detection of land consumption associated with buildings and infrastructures

It is worth highlighting that roads or squares without buildings have generally lower backscatter values which are, therefore, not detected with this method. VV polarization of Sentinel-1 data was used because it could be more suitable for building detection, since it emerge from the background more than VH polarization (Koppel *et al.*, 2017).

The calculations involve the following steps:

1. Four collections of Sentinel-1 VV images were distinguished (by ascending and descending orbit and for the two reference years).
2. For each collection, the median was calculated and converted the dB to natural values, obtaining 4 rasters:

   - Ascending median year 1
   - Ascending median year 2
   - Descending median year 1
   - Descending median year 2

3. The differences between the median values of the two years were calculated for the ascending and for the descending orbit:

$$\text{ASCEND. MEDIAN DIFFERENCE} = (\text{Ascend. median year } 2 - \text{ Ascend. median year } 1)$$

$$\text{DESCEND. MEDIAN DIFFERENCE} = (\text{Descend. median year } 2 - \text{ Descend. median year } 1)$$

   Difference values greater than 0 mean that backscatter values increased during this period.
4. Slope in degrees was calculated from the SRTM-DEM (Shuttle Radar Topography Mission) Version 4 (Jarvis *et al.*, 2008), in order to exclude areas whose backscatter values are influenced by high slope.

The following conditions were defined to detect land consumption related to buildings and infrastructures:

$$\text{ASCENDING MEDIAN DIFFERENCE} \geq 0.1$$

AND

$$\text{ASCENDING MEDIAN year } 1 < -9 \text{ dB}$$

AND

$$\text{DESCENDING MEDIAN DIFFERENCE} \geq 0.1$$

AND

$$\text{DESCENDING MEDIAN year } 1 < -9 \text{ dB}$$

AND

$$\text{SLOPE} < 20$$

AND

$$\text{MAX NDVI Year } 2 < 0.5$$

The threshold values of 0.1 and 9 dB were evaluated by trial and errors as optimal values to distinguish real changes. The concurrent conditions for ascending and descending orbits aims at excluding partial increase of backscatter values related to variations of vegetation and the particular geometry of objects on the ground. The condition ASCENDING (DESCENDING) MEDIAN DIFFERENCE ≥ 0.1 allows to identify variations in backscatter related to the construction of a new buildings, while the condition ASCENDING (DESCENDING) MEDIAN year 1 < 9 dB excludes areas that are already build in the first year (therefore having high backscatter values), such as buildings under construction or restoration. This could potentially exclude land consumption over forested areas (characterized by high backscatter values), yet these changes should be detected in the methodology described in the previous paragraph considering the NDVI difference.

In addition, areas having slope values > 20° are excluded because usually urbanization affects flat areas and also backscatter values are badly affected by high slope.

The last condition (MAX NDVI Year 2 < 0.5) uses the NDVI calculation from Sentinel-2 described in the previous paragraph, aiming at excluding vegetated pixels that had a backscatter increase due to forest growth.

The changes derived with this method are therefore combined with those identified in the previous paragraph using Sentinel-2, producing three maps (one for each approach) of possible changes related to land consumption. The three masks were compared to assess which approach is the most effective.

3.2.3.8 Accuracy assessment

The validation involved the 2012 land cover map and the 2018 land cover map integrated with the 4 land cover change classes.

First, a qualitative verification was carried out, through a systematic visual search for macroscopic errors. An Accuracy assessment on the base of Olofsson methodology was then performed (Olofsson *et al.*, 2014). This approach is widely used in literature (Stehman and Czaplewski, 1998; Olofsson *et al.*, 2014; FAO, 2016; Stehman and Foody, 2019)

For validation, a sample of points was photointerpreted using very high resolution images. The points were then compared with the values of the land cover map. The sample size (n) was calculated using the equation reported by Olofsson (Olofsson *et al.*, 2014) and referred to 5.25 in (Cochran and William, 1977).

$$n = \frac{(\sum W_i S_i)^2}{[S(\hat{O})]^2} \tag{2}$$

where:

W_i = area proportion of each classes derived from the map classification

S_i= standard deviation of stratum i, $S_i = \sqrt{U_i(1 - U_i)}$ ((Cochran and William, 1977), Eq. 5.55)

U_i= user accuracy of class *i*

$S(\hat{O})$= target standard error.

S_i influences the sample size and his value is related to the U_i, that is unknown. A conservative scenario was assumed, considering U_i= 0.6 for all classes.

$S(\hat{O})$ was assumed to be 0.01 as suggested by Olofsson (Olofsson *et al.*, 2014), that corresponds to a confidence interval of 1%.

The application of (2) gives a sample of size 2,400 for both land cover maps (Table 21, Table 22).

Table 21. Parameters for calculating the sample size (land cover map 2012)

Land cover class	Area (ha)	W_i	U_i	S_i	W_i*S_i
Artificial abiotic surfaces	2,102,288	0.070	0.6	0.49	0.034
Consolidated(bare rocks scree, cliffs)	802,539	0.027	0.6	0.49	0.013
Unconsolidated (beaches, dunes, sands)	59,325	0.002	0.6	0.49	0.001
Broad-leaved	7,805,217	0.259	0.6	0.49	0.127
Needle-leaved	2,167,261	0.072	0.6	0.49	0.035
Orchards	619,759	0.021	0.6	0.49	0.010
Olive plantation	1,088,099	0.036	0.6	0.49	0.018
Wood plantations	46,356	0.002	0.6	0.49	0.001
Vineyards	689,746	0.023	0.6	0.49	0.011
Shrubland	1,375,125	0.046	0.6	0.49	0.022
Pastures	1,372,790	0.046	0.6	0.49	0.022
Arable land	9,183,519	0.305	0.6	0.49	0.149
Permanent herbaceous	2,337,826	0.078	0.6	0.49	0.038
Water bodies	402,830	0.013	0.6	0.49	0.007
Permanent snow and ice	37,000	0.001	0.6	0.49	0.001
Wetlands	50,295	0.002	0.6	0.49	0.001
Total	30,139,975				1
$S(\hat{O})$ overall accuracy		0.01			
Total number of points		2,400			

Table 22. Parameters for calculating the sample size (land cover map 2018)

Land cover class	Area (ha)	W_i	U_i	S_i	W_i*S_i
Artificial abiotic surfaces	2,127,999	0.071	0.6	0.490	0.035
Natural abiotic surfaces	953,574	0.032	0.6	0.490	0.015
Broad-leaved	12,006,500	0.398	0.6	0.490	0.195
Needle-leaved	1,607,582	0.053	0.6	0.490	0.026
Permament herbaceous	12,657,900	0.420	0.6	0.490	0.206
Periodically herbaceous	239,834	0.008	0.6	0.490	0.004
Water bodies	337,737	0.011	0.6	0.490	0.005
Permanent snow and ice	111,773	0.004	0.6	0.490	0.002
Other disturbances	78,490	0.003	0.6	0.490	0.001
Bured areas	11,106	0.000	0.6	0.490	0.000
Land consumption	6,600	0.000	0.6	0.490	0.000
Restorations	906	0.000	0.6	0.490	0.000
Total	30,139,974				1
$S(\hat{O})$ overall accuracy		0.01			
Total number of samples		2,400			

Sample size calculation according to Olofsson (Olofsson et al., 2014). The required inputs are the areas of each class and the expected user's accuracy for the sample. The points were divided among the land cover classes through a stratified sampling. The number of points attributed to each class assumed to be equal to the average between equal and area proportional distribution[11] (Table 23, Table 24).

[11] https://fromgistors.blogspot.com/2019/09/AccuracyAssessmentofLandCoverClassification.html

Table 23. Allocation of points (land cover map 2012)

Classes	Allocation		
	Equal	Proportional	Final
Artificial abiotic surfaces	150	167	159
Consolidated(bare rocks scree, cliffs)	150	64	107
Unconsolidated (beaches, dunes, sands)	150	5	100
Broad-leaved	150	622	386
Needle-leaved	150	173	162
Orchards	150	49	100
Olive plantation	150	87	119
Wood plantations	150	4	77
Vineyards	150	55	103
Shrubland	150	109	130
Pastures	150	109	130
Arable land	150	731	441
Permanent herbaceous	150	186	168
Water bodies	150	32	91
Permanent snow and ice	150	3	77
Wetlands	150	4	77
Total	**2,400**	**2,400**	**2,427**

Table 24. Allocation of points (land cover map 2018)

Classes	Allocation		
	Equal	Proportional	Final
Artificial abiotic surfaces	200	169	185
Natural abiotic surfaces	200	76	138
Broad-leaved	200	956	578
Needle-leaved	200	128	164
Permament herbaceous	200	1,008	604
Periodically herbaceous	200	19	110
Water bodies	200	27	113
Permanent snow and ice	200	9	104
Other disturbances	200	6	103
Bured areas	200	1	100
Land consumption	200	1	100
Restorations	200	0	100
Total	**2,400**	**2,400**	**2,400**

Points were photointerpreted with very high-resolution images from Google Earth, considering 2018 as the reference year for the land cover classes and 2017 and 2018 for the land cover change classes. The photointerpretation followed a pixel-based approach, assigning to each point the class on which it falls exactly

3.3 Land consumption in Italy and related phenomena

In recent decades, the transformations of the territory have been dominated by the growth of artificial surfaces, new transport infrastructures or new constructions. These areas have increased more than 180% compared to the 1950s (ISPRA, 2018d). Part of this research focused on the state and evolution of artificial areas in Italy through the calculation and observation of a set of indicators.

The first part of the paragraph analyses spatial distribution and temporal evolution of land consumption in Italy with respect to the new classification system introduced by ISPRA for the description of the phenomenon. In the second part, the fragmentation of the territory caused by land consumption was assessed and the third section focuses on the development of the main Italian urban areas between 2012 and 2019 through the calculation and interpretation of landscape metrics.

The concluding section describes the United Nations Sustainable Development Indicators (SDGs) for assessing degradation (SDG 15.3.1) and the relationship between urban and population growth (SDG 11.3.1). Various input data were tested and an interpretation of the indicators was conducted on the Italian territory (for 15.3.1) and on the main Italian cities (for 11.3.1).

3.3.1 Spatial distribution and evolution of land consumption

The spatial distribution and the temporal evolution of land consumption in Italy have been studied in the context of two research activities.

A first activity focused on the third classification level introduced by ISPRA in 2016 for the characterization of the different types of land consumption (Munafò, 2018). The phenomenon was analysed on a national scale for the period 2016-2019, with reference to elevation, slope and the presence of EUAP areas. The analysis described below are an in-depth analysis of the results presented in the publication “Land Consumption in Italy” of Journal of Maps (Strollo *et al.*, 2020), in the 2018 and 2019 editions of the ISPRA “Environmental Data Yearbook” (ISPRA, 2018a, 2018b, 2019b, 2019a) and in the 2018, 2019 and 2020 editions of the ISPRA “Land Consumption, territorial dynamics and ecosystem services” report (Munafò, 2018, 2019, 2020).

The second analysis describes land consumption in coastal areas, for the period 2012-2018. This study was published in the “Environmental Engineering and Management Journal” with the title “Land consumption in Italian coastal area” (Riitano *et al.*, 2020).

3.3.1.1 Land consumption at the third classification level

The analysis of land consumption at the third classification level required the use of following input data:

- *National Land Consumption Map (LCM)*

  As described in the previous chapter, the data is a raster with a spatial resolution of 10 m, updated every year by ISPRA. The rasters relating to 2016, 2017, 2018 and 2019 were used, with changes classified at the third classification level (Munafò, 2020).
- *EUAP protected areas*

  The Official List of Protected Areas (EUAP) was established by law 394/91 (Framework law on protected areas) and currently it is in its sixth update (approved with Ministerial Decree 27/04/2010 and published in the Official Gazette no. 31/05/2010). The list includes: National Parks (PNZ), Marine Protected Areas (AM), State Natural Reserves (RNS), Other National Protected Areas (AAPN), Regional and Interregional Natural Parks (PNR), Regional Natural Reserves (RNR), Other Regional Protected Natural Areas (AAPR).

  The "Nature and Sea Protection Directorate" is the department of the Ministry of the Environment and the Protection of the Territory and the Sea, which is responsible for updating the list. The list is constantly updated for PNZ, AM, RNS and AAPN, while for regional protected areas (PNR, RNR and AAPR) the last update is of 27/04/2010.

  In this research the terrestrial EUAP were considered, therefore the AM and AAPN (which refer to marine areas) were excluded.
- *Tinitaly/01 DEM*

  Tinitaliy/01 is a Digital Elevation Model (DEM) presented in 2007 (Tarquini et al., 2007) for the whole Italian territory. Tinitaly/01 is freely available as a 10 m cell size grid, in WGS 84-UTM 32 projection system.

To analyse the changes occurred yearly, each of the four consumed land rasters was combined with the one related to the following year, obtaining three maps of changes which describe the class assumed by each pixel in the two years.

National Land Consumption Map 2016
→ Changes map 2016-2017
National Land Consumption Map 2017
→ Changes map 2017-2018
National Land Consumption Map 2018
→ Changes map 2018-2019
National Land Consumption Map 2019

The three rasters of changes were used to produce surface statistics related to the evolution of the phenomenon at national level. They were then intersected with data related to EUAP protected areas, elevation and slope, according to the specific procedures described below.

- *EUAP protected areas*

  EUAP areas were considered as a whole and disaggregated into five layers related to each of the five typologies (marine protected areas were excluded). Data were converted into raster files and combined with the three layers of changes. The following products were obtained, which were then analysed:

  - three raster of changes (referring to the periods 2016-2017, 2017-2018 and 2018-2019), for the entire portion of the national territory with the presence of EUAP areas.
  - three raster of changes for each of the five types of EUAP areas.

- *Tinitaly/01 DEM*

  Tinitaly/01 DEM has been reclassified into three classes (Table 25) (Munafò, 2020):

Table 25. Elevation classes obtained from the reclassification of Tinitaly/01 DEM

Class	Name	Altimetric range
1	Plain areas	< 300 m a.s.l.
2	Hill areas	between 300 and 600 m a.s.l.
3	Mountain areas	> 600 m a.s.l.

Starting from the Tinitaly/01 DEM, the slope values for each cell were obtained. The slope data were then reclassified into two classes: high slope areas (> 10%) and low slope areas (< 10%).

Cross referencing was then carried out between elevation, slope and the three raster of changes. This way, land consumption was analysed with reference to the six combinations of elevation and slope.

3.3.1.2 Land consumption in Italian coastal area

The main research goal is to observe land consumption in relation to the distance from the coast in Italy. The methodology described below is taken from the paper "Land consumption in Italian coastal area" published on "Environmental Engineering and Management Journal". The coastline data produced in accordance with the methodology proposed by Barbano *et al.* (2006) have been used. The coastline has been digitized by ISPRA and Planetek, starting from orthophotos acquired during IT2000 flight and cartography made by the Italian Military Geographical Institute (IGM) at scale 1:25000.

For land consumption, the LCM relating to 2012 and 2018 was used at the first classification level (consumed land/non-consumed land) (Munafò, 2020).

Using GIS techniques, starting from the coastline up to 10 km, a raster has been built assigning to each cell its Euclidean distance (called "distance raster"). Raster spatial resolution is 10 m and its grid is aligned to the LCM aiming at speeding up and improving the process. Combining the distance raster, reclassified in 10 m zones starting from the coast (value = 0), with the LCM, it was produced a new raster providing in a unique attribute both of the abovementioned informations. Results are then aggregated into five distance ranges (100 m, 300 m, 500 m, 1 km, 10 km).

Permanent water bodies and wetlands were excluded from the spatial analysis, since administrative boundaries used as spatial reference for the LCM (ISTAT, 2018) include water bodies located outside the coastline, like the Venice Lagoon.

The analysis considered the distribution of variables in the five distance ranges at national and regional level (NUTS1) and for the three coastal typologies: high, low and other. The latter class includes artificial coastal manufacts (ports, docks, riverbanks, piers, connections, etc.). Lastly, the demographic variation in the municipalities with coastline access were considered using ISTAT databases aligned with the reference period to correlate land consumption and demographic variation.

3.3.2 The fragmentation of the territory

The degree of fragmentation was assessed through the effective mesh density (S_{eff}) (EEA, 2017e), defined as:

$$S_{eff} = \frac{1}{m_{eff}} * 1000$$

It represents the density of territorial patches (meshes), expressed in number of meshes per 1,000 km^2. S_{eff} is based on the calculation of the effective mesh size (m_{eff}), whose definition was introduced by Jaeger (2000), and then modified according to the "cross-boundary connections (CBC) procedure" (Jaeger and Tappeiner, 2007). The m_{eff} is evaluated within a reference area called "reporting unit" and it is related to the probability that two random points in a given area are located in the same territorial particle (mesh). In this sense, it measures the obstacle to movement between two points within the reporting unit, due to the presence of barriers, called “fragmenting elements”. The choice of the most appropriate fragmenting elements is guided by the aims and objectives of the analysis.

The index has the following expression:

$$m_{eff}^{CBC} = \frac{1}{A_{total}} * \sum_{i=1}^{n} A_i * A_i^{compl}$$

where:

n = the number of patches;

A_i = size of patch *i* inside the boundaries of the reporting unit (i = 1, 2, 3, …, n);

A_i^{compl} = area of the complete patch that A_i is a part of, i.e., including the area on the other side of the boundaries of the reporting unit up to the physical barriers of the patch;

A_{total}= total area of the reporting unit.

S_{eff} index is a more intuitive measurement of territorial fragmentation than m_{eff}. In this research, the S_{eff} was calculated for the entire Italian territory, considering as a reporting unit a regular grid of 1 km^2 and as fragmenting elements the National Land Consumption map, suitably integrated with the vector information of OpenStreetMap, in order to improve the identification and continuity of linear infrastructures. The m_{eff} values were then aggregated into 5 classes (Table 26), according with the indications from the European Environment Agency.

Table 26. Classes of fragmentation in relation to S_{eff} values

Classes of fragmentation	**S_{eff} (number of meshes per 1000 km^2)**
Very low	0 – 1.5
Low	1.5 – 10.0
Medium	10.0 – 50.0
High	50.0 – 250.0
Very high	> 250.0

The national fragmentation data for 2012 and 2019 were then combined with:

- The regional administrative boundaries;
- EUAP protected areas;
- The elevation and slope ranges obtained from DEM;
- The coastal area.

The results obtained from the application of the methodology were used in the 2018, 2019 and 2020 editions of the ISPRA report “Land Consumption, territorial dynamics and ecosystem services” (Munafò, 2018, 2019, 2020) and in the “biosphere” section of the 2018 and 2019 editions of the ISPRA "Environmental Data Yearbook" (ISPRA, 2018a, 2019a). The data were also presented in two poster communications at the "World Forum on Urban Forests" in Mantua (Italy) and at the ISTAT 13th national Statistics Conference.

3.3.3 Urbanization forms and the type of settlement

Knowing the different forms of urbanization and the type of settlement is essential to address the issues of urban sustainability and resilience, as they describe the organization of the cities functionalities in terms of accessibility and capacity of transformation and adaptation.
The analysis is based on the calculation and interpretation of four landscape metrics calculated starting from the LCM for 2012 and 2019.

Largest Class Patch Index (LCPI)

LCPI is an indicator of compactness, which indicates the extension of the largest polygon of the artificial class compared to the overall extension of the class. It is expressed as a percentage and assumes high values in cities with a large urban area, while low values correspond to widespread urbanization.

Residual Mean Patch Size (RMPS)

RMPS is an indicator of diffusion, which expresses the average width of the residual artificial polygons, excluding the largest one. RMPS is expressed in ha and provides the size of the spread of cities around the central core. High RMPS values correspond to low diffusion conditions, for example in polycentric urban areas, while low RMPS values characterize widespread urban areas.

Edge Density (ED)

It is the ratio between the total sum of the perimeters of the polygons of the urbanized areas and their surface, expressed in $\left[\frac{m}{ha}\right]$. It provides information on the dispersion of urban borders. The ED value is low in urban areas with compact shape and with regular borders and rises in areas with more indented borders.

Dispersion Index (DI)

It is the ratio of high-density areas to high and low areas density. It is an indicator of territorial dispersion which assumes high values in low-density areas and low values in more compact areas.

The LCM with binary classification system (consumed land/non-consumed land) was used to calculate the ED.

A “focal density” realized on the LCM at a distance of 50 m was used for the calculation of RMPS and LCPI. It has been reclassified based on the average urbanized surface around each pixel and makes it possible to limit the disturbance of isolated buildings or linear infrastructures.

To evaluate the increase in degradation associated with the dispersion index, ISPRA data were used, based on the land consumption density map and the population density map (Munafò, 2020). The map has four classes:

- High density urban centers (Class 1). Areas with population density greater than 1,500 inhabitants per km^2 and density of consumed land higher than 50%;
- Medium density urban groups (Class 2). Areas with population density between 300 and 1,500 inhabitants per km^2 and density of consumed land between 10% and 50%;
- Rural areas (Class 3). All areas with low densities of both population and consumed land;
- High density of consumed land (higher 50%) and population densities lower than 300 inhabitants per km^2 (Class 4).

The ID was calculated as the ratio between classes 1 and 4 and classes 1, 2 and 4.

The calculation of the landscape metrics was done through Fragstats software (McGarigal, K., 2012) considering the administrative boundaries of the Italian provincial capitals as reference areas.

The results obtained from the application of the methodology were used in the 2018, 2019 editions of the ISPRA report “Report on Urban Environment Quality” (ISPRA, 2018c, 2019c).

3.3.4 Sustainable Development Goals

The 17 Sustainable Development Goals (SDGs) are the main elements of the 2030 Agenda for Sustainable Development which has been adopted by all the United Nations Member States in 2015. These Goals indicate the path for all countries which adhered to be followed urgently, in a global partnership. The UN have recognized through this system the need to strategize to end poverty, improve health and education, tackle climate change and work to preserve the environment. This research moves from two indicators related to SDGs 11 and 15.

As the SDG 11 states that the goal is to “Make cities and human settlements inclusive, safe, resilient and sustainable” the target 11.3 specifies the need to improve “By 2030, inclusive and sustainable urbanization and capacity for participatory, integrated and sustainable human settlement planning and management in all countries”. Following this statement 11.3.1 indicators was deepened, namely “Ratio of land consumption rate to population growth rate” (UN, 2016).

The indicator was calculated for some large Italian cities to study the variation in land consumption in relation to population, analyse the input data currently available at national level and evaluate a more suitable definition of land consumption.

As the SDG 15 refers to “Protect, restore and promote sustainable use of terrestrial ecosystems, sustainably manage forests, combat desertification, and halt and reverse land degradation and halt biodiversity loss” and its target 15.3 states: “By 2030, combat desertification, restore degraded land and soil, including land affected by desertification, drought and floods, and strive to achieve a land degradationneutral world”. Indicator 15.3.1 refers to this target: “Proportion of land that is degraded over total land area” (UN, 2016).

The analysis followed the methodology presented by ISPRA (Munafò, 2019) which integrates the three subindicators proposed by the UNCCD (Sims *et al.*, 2017) with a set of additional 7 subindicators developed within this research and further ISPRA activities. The assessment provided a first estimate of the extent and distribution of the phenomenon in Italy for the period 2012-2019.

3.3.4.1 SDG indicator 11.3.1 Ratio of land consumption rate to population growth rate

The “Ratio of land consumption rate to population growth rate” (RLCRPGR) indicator refers to the variation in land consumption with the variation in population in a reference period. In detail, it is defined as the ratio of land consumption rate (LCR) to population growth rate (PGR) (UN, 2021):

$$\text{RLCRPGR} = \text{LCR/PGR} = \left[\frac{\left(\frac{CL_{t+n}-CL_t}{CL_t}\right)}{n}\right] \Bigg/ \left[\frac{\ln\left(\frac{Pop_{t+m}}{Pop_t}\right)}{m}\right] \quad (3)$$

Where:

CL_t= Total areal of the consumed land for first year

CL_{t+n}= Total areal of the consumed land for last year

n = Number of years between CL_t and CL_{t+n}

Pop_t = Total population in the first year

Pop_{t+m} = Total population in the last year

m = Number of years between the two measurement periods

The rate of change in land consumption and population have positive values if the two quantities increase in the reference period ($CL_t < CL_{t+n}$, $Pop_t < Pop_{t+n}$), vice versa they will be negative.

The land consumption rate of large areas or urban areas can always be considered positive or null (LCR ≥ 0), in this way the sign of the RLCRPGR indicator is linked to population variation (PGR). In this case RLCRPGR can assume the following values:

- RLCRPGR = 0

  Land consumption did not vary in the considered period
- RLCRPGR > 0
  - 0 < RLCRPGR < 1

    Both rates of change are positive, but the population increases more than land consumption
  - RLCRPGR > 1

    Both rates of change are positive, but land consumption increases more than the population
- RLCRPGR < 0
  - 0 > RLCRPGR > 1

    The rate of population change is negative and the absolute value of the population decrease is greater than the value of land consumption increase.
  - RLCRPGR < 1

    The rate of population change is negative and the absolute value of the decrease in population is lower than the increase in land consumption.

In rural areas, negative land consumption rates can occur (LCR < 0), for example due to restoration of a road construction site. Again, the sign of the RLCRPGR indicator will depend on the rate of change of the population:

- RLCRPGR > 0
  - 0 < RLCRPGR < 1

    Both rates of change are negative, but the population decreases more than land consumption

- RLCRPGR > 1

  Both rates of change are negative, but land consumption decreases more than the population

- RLCRPGR < 0
  - 0 > RLCRPGR > 1

    The rate of population change is positive and the absolute value of the population increase is greater than the in land consumption decrease.

  - RLCRPGR < 1

    The rate of population change is positive and the absolute value of the increase in population is less than the decrease in land consumption.

As for the interpretation of the indicator it should be kept in mind the sign of LCR and PGR, since the same RLCRPGR value can be associated with different dynamics (for example a negative RLCRPGR value can derive from an increase in PGR and a decrease of LCR or from an increase in LCR and a decrease in PGR).

The indicator was analysed for the period 2012-2018 referring to three different analysis (Figure 21).

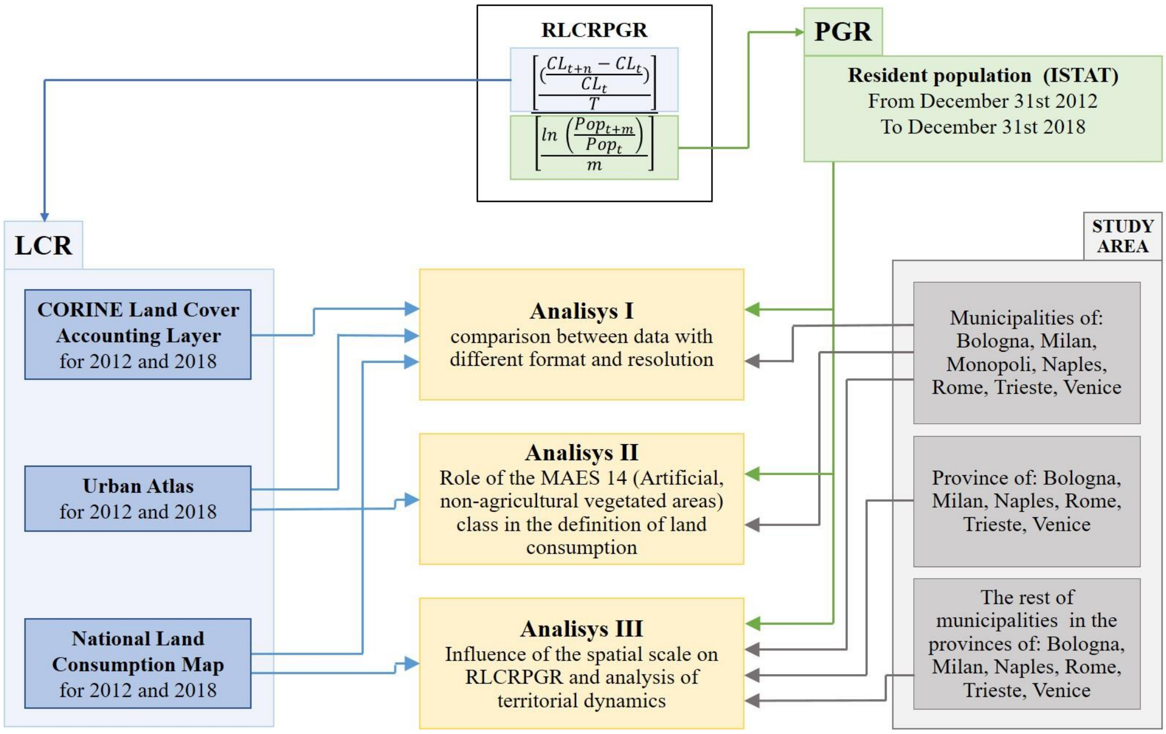

Figure 21. Flow chart outlining steps of calculation, input data sources, and scale level

Analysis I: Calculation of the RLCRPGR using different input data

The first analysis compares three data for the calculation of the LCR. In detail, the National Land Consumption Map (LCM) produced by ISPRA (Munafò, 2020) and the two Copernicus data CORINE Land Cover Accounting Layer (CLCA) and Urban Atlas (UA) (European Commission, 2016) were considered (Table 27). As for population, official ISTAT data were used. This analysis allowed to evaluate how the indicator varies using data with different spatial resolution and format for the description of land consumption.

The analysis refer to the territory of seven Italian municipalities: Bologna, Napoli, Venezia, Trieste, Roma, Milano and Monopoli.

Table 27. Main characteristics of the input data for the calculation of Land Consumption Rate (LCR)

Data	**CORINE Land Cover Accounting Layer**	**Urban Atlas**	**National Land Consumption Map**
Coverage	EU 39	788 FUAS	Italy
Type of information	Land use/land cover map	High-resolution land use/land cover map	Land consumption map
Format	Raster	Vector	Raster
MMU	1 ha	Urban classes 0.25 ha Rural classes 1 ha Urban classes 0.1 ha (changes) Rural classes 0.25 ha (changes)	0.01 ha
Reference year	1990, 2000, 2006, 2012, 2018	2006, 2012, 2018	2012, 2015-2019

Analysis II: Green urban areas in the calculation of the RLCRPGR

The second analysis focuses on the class 14 "Artificial, non-agricultural vegetated areas", which is present in the UA and CLCA classification systems. The analysis was carried out on Urban Atlas data, which was more sensitive to land consumption variations than CLCA. The purpose of the study is to analyse one of the main differences between the definition of land consumption provided by ISPRA (which excludes these areas from land consumption) and by the EEA (which includes them). It was assessed how the class affects the value of the RLCRPGR indicator and whether it has suitable characteristics to be considered as land consumption.

Analysis III: Evolution of the provincial territory starting from the RLCRPGR

A third analysis referred to the variations in land consumption starting from to the National Land Consumption Map (Munafò, 2020), extending the study area to the whole provincial territory of Bologna, Napoli, Venezia, Roma, Milano and Trieste. The objective is to evaluate the dynamics of those territories in terms of population and land consumption variation, starting from the interpretation of the RLCRPGR indicator.

The three input data were compared in their native format, i.e. raster for SC and CLCA and vector for UA. For the SC the first level of classification was considered, while for CLCA and UA class 1 “Artificial surfaces” was extracted. For the UA data, the polygons for years 2012 and 2018 have been integrated with the “Urban Atlas Change 2012-2018” data, in order to take into account the smallest changes.

Data were clipped on the extent of the considered municipalities and the RLCRPGR was calculated, as defined above.

For UA data, the calculation was performed a first time by considering the entire class 1 as land consumption and a second time by separating the contributions related to class 14 “Artificial, non-agricultural vegetated areas”.

In the second analysis, the UA data for years 2012 and 2018 were considered, integrated with the “Urban Atlas Change 2012-2018” data. The extension of class 1 over the two years and the variation between 2012 and 2018 were calculated. The component related to class 14 was therefore separated, in order to assess its extension with respect to the entire class 1 surface and the flows of change that involved the class.

The polygons of class 14 to 2018 were then combined with the LCM to evaluate the presence of consumed land (according to the ISPRA definition) within the class 14 areas of UA. For this comparison, the two sub-classes at the third classification level of class 14 were considered: 141 “green urban areas” and 142 “sport and leisure facilities”

For the third analysis, only the LCM data was used. Starting from these data, RLCRPGR indicator were calculated for all municipalities belonging to the provincial territory of the six capitals. All the processing was done on Qgis software and data were then reorganized on a spreadsheet.

3.3.4.2 SDG indicator 15.3.1 Proportion of land that is degraded over total land area

The land degradation assessment was carried out on a national scale, for the period 2012-2019. The analysis followed the methodology presented by ISPRA (Munafò, 2019), which is based on the UNCCD (Sims *et al.*, 2017). The calculation primarily involves the combined use of three subindicators:

- Land Cover change;
- Land Productivity dynamics, evaluated starting from the NDVI index and using a NASA model based on the calculation of three indicators (trajectory, status and performance);
- Soil organic carbon stock.

Due to the complexity of the topic and the absence of a consolidated methodology, the UNCCD suggests integrating the basic set of indicators with other specific ones at national level. In detail, ISPRA introduces seven further sub-indicators:

- Fragmentation, evaluated in terms of mesh density variation;
- Soil erosion, calculated using the revised version of the universal soil loss equation (RUSLE) (Renard, 1997);
- Reduction in size of natural spaces, in terms of increasing natural spaces smaller than 1000 m^2 in the reference period;
- Potential impact area, considering a buffer of 60 m from the consumed land;
- Density of artificial areas, considering high and medium density areas;
- Burned areas;
- Loss of habitat quality.

The details about the above mentioned indicators are illustrated below. For the calculation of the three basic indicators, the Trends.Earth platform (Conservation International, 2020) was used, which allows the monitoring of land change using earth observations in a desktop and cloud-based system. The additional sub-indicators refer to elaborations carried out within this research activity (soil erosion, fragmentation) and data produced by ISPRA (potential impact area, loss of habitat quality, density of artificial areas, burned areas).

A binary raster map was produced for each cause of land degradation, indicating the areas with increasing degradation in the period 2012-2019. The overall degradation was assessed by superimposing the binary raster according to the criterion of "The One Out, All Out". "In other words: if there is a decline in any of the indicators at a particular pixel, then that pixel is mapped as being degraded" (Conservation International, 2020). The evaluation is partial, as degradation phenomena such as salinization, compaction and contamination have not been considered.

The map indicates whether one or more causes of deterioration persist in the same area.

The degradation map was analysed on a national scale and combined with further data: regional administrative limits (NUTS 1), EUAP protected areas, elevation, slope and coastal area.

Land Cover change

Land cover reflects the use of land resources (i.e., soil, water and biodiversity) for agriculture, forestry, human settlements and other purposes (Herold, 2009). Land degradation related to land cover changes was assessed starting from the land cover maps obtained by combining the National Land Consumption Map for 2012 and 2019 with CORINE Land Cover data (Figure 22). The CLC 2012 and CLC 2018 data were first integrated with the CLC Change 12-18 layer (to include the changes with MMU of 5 ha, against the 25 ha of the CLC data) and rasterized at 10 m resolution. The two land cover maps were then reclassified according to the categories adopted by the UNCCD for the environmental reporting processes (forests, meadows and pasture, agricultural areas, artificial areas, bare soil, water bodies and wetlands).

A transition matrix was created (Table 28) defining land degradation variation associated with each change between land cover classes that occurred between 2012 and 2019.

The land cover changes that lead to increased degradation are shown in red, those that reduce degradation in green and those that do not affect degradation in grey.

Table 28. Transition matrix for the evaluation of the degradation associated with land cover changes (red = increase in degradation, green = decrease in degradation, gray = no variation)

		To						
		Forests	Meadows and pasture	Agricultural areas	Artificial areas	Bare soil	Wetlands	Water bodies
From	Forests	0	-	-	-	-	-	0
	Meadows and pasture	+	0	-	-	-	-	0
	Agricultural areas	+	+	0	-	-	-	0
	Artificial areas	+	+	+	0	+	+	0
	Bare soil	+	+	+	-	0	+	0
	Wetlands	-	-	-	-	-	0	0
	Water bodies	0	0	0	0	0	0	0

The elaborations were carried out using the Trends Earth model, which allows to process historical series of indices and variables from satellite images.

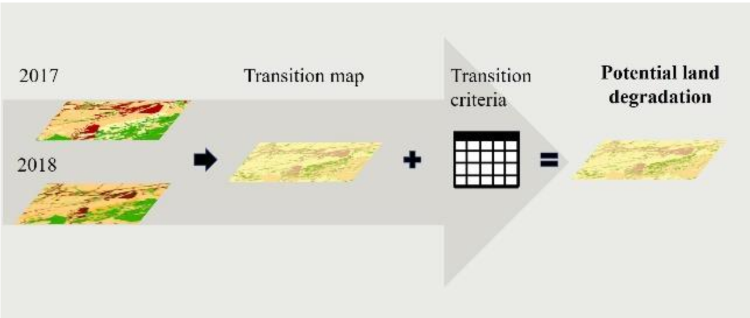

Figure 22. Land degradation related to land cover change - workflow

Land Productivity dynamics

Land productivity is the biological productive capacity of the land, the source of all foods, fiber and fuel that sustain humans (Sims *et al.*, 2017).

Land productivity can be measured across large areas through earth observations in terms of Net Primary Productivity (NPP). NPP is the net amount of carbon assimilated after photosynthesis and autotrophic respiration over a given period (Clark *et al.*, 2001) and is typically represented in units such as kg/ha/year (annual NPP or ANPP).

The largescale estimate of NPP is time consuming and expensive, but it can be indirectly evaluated starting from NDVI measurements, exploiting the correlation between the fraction of absorbed photosynthetically active radiation (FAPAR) and plant growth vigor and biomass (Sims *et al.*, 2017).

The estimation of the degradation associated with the loss of NPP was conducted through the Trends.Earth model, exploiting the NDVI time series data obtained from MODIS and AVHRR data to compute three measures of change: trajectory, state and performance.

The *trajectory* indicator measures the rate of change in primary productivity over time, calculated through a linear regression at the pixel level on the NDVI values. Positive trends indicate a potential improvement in soil conditions, while negative ones indicate potential degradation. The analysis was carried out using MODIS data (1 km of spatial resolution) for the period 2001-2019.

The *status* indicator evaluates the recent changes in primary productivity occurred in a period of interest, called the "comparison period", compared to the primary productivity in a reference period, defined as the "baseline period".

The analysis uses MODIS data, with reference to a "comparison period" between 2012 and 2019 and a "baseline period" between 2001 and 2012.

The NDVI values for the "baseline period" were calculated and the probability distribution was created and then divided into 10 percentile classes.

The mean NDVI was then calculated for the "comparison period" and the "baseline period" and the two means were associated with the corresponding percentile class in which they fall.

If the difference between the "comparison period" percentile class and the "baseline period" percentile class is lower than -2, the pixel is potentially degraded, if it is between -1 and 1 it is stable, while if the value is greater than 2 the level of degradation in the pixel is improving.

The *Performance* indicator measures local productivity related to other similar vegetation types in similar land cover areas or bioclimatic regions throughout the study area (Figure 23). The model defines “units”, i.e. ecologically similar classes on the basis of soil type (soil taxonomy units, using USDA system provided by SoilGrids at 50 m resolution) and land cover classes (full 37 land cover classes provided by ESA CCI at 300 m resolution). The probability distribution of the mean NDVI of each “unit” is created, and the 90th percentile of the distribution is identified as a reference value.

To evaluate the degradation in a pixel, its mean NDVI value is compared with the reference value of the corresponding unit. The pixel is considered degraded if its mean NDVI is < 0.5 mean NDVI at the 90th percentile (reference value).

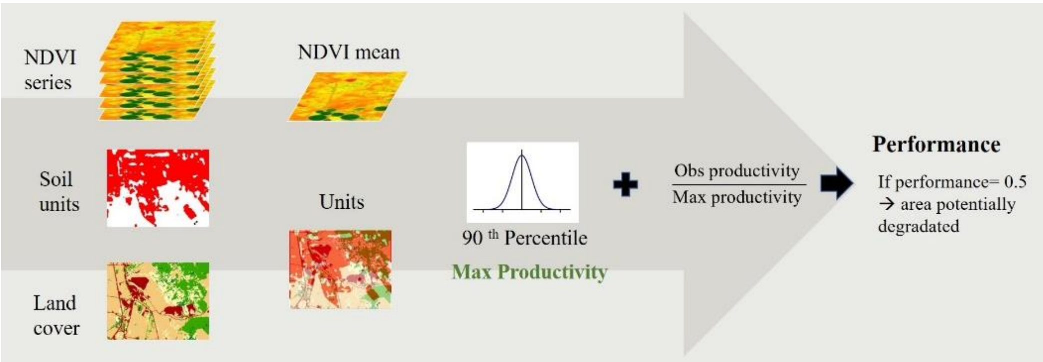

Figure 23. Land degradation related to land productivity dynamics - workflow

The values obtained for trajectory, status and performance were then combined (Table 29), allowing to identify the pixels with an increase in degradation linked to the loss of productivity.

Table 29. Aggregating the productivity subindicators (red = increase in degradation, green = decrease in degradation, gray = no variation)

Trajectory	+	+	+	+	+	+	0	0	0	0	0	0	-	-	-	-	-	-
State	+	+	0	0	-	-	+	+	0	0	0	0	+	+	0	0	-	-
Performance	+	-	+	-	+	-	+	-	+	-	+	-	+	-	+	-	+	-
Productivity	**+**	**+**	**+**	**+**	**+**	**-**	**0**	**0**	**0**	**-**	**-**	**-**	**-**	**-**	**-**	**-**	**-**	**-**

Changes in soil organic carbon

The third subindicator for monitoring land degradation assesses the changes in soil organic carbon (SOC) over a reference period.

Changes in SOC are difficult to assess due to the high spatial variability of soil properties, the different frequency of monitoring as well as the different survey methodologies.

The assessment of the loss of organic carbon occurred at national level in the first 30 cm of soil, was conducted through trends.earth for the period 2012-2019.

The SOC was evaluated starting from the national map of organic carbon, obtained from the analysis of 6,748 stratigraphic profiles collected from 1990 to 2013 on the national territory as part of the Global Soil Partnership (FAO and ITPS, 2020).

The 7-class land cover map used to estimate the degradation caused by land cover change was therefore considered. The map was resampled to 50 m resolution and conversion coefficients were introduced to evaluate the carbon stock variations associated with land cover changes. The coefficients were the result of a literature review performed by the UNCCD and are presented in the Table 30.

Table 30. Conversion coefficients for the evaluation of carbon stock variations (red = increase in degradation, green = decrease in degradation, gray = no variation).

	Forests	Grasslands	Croplands	Wetlands	Artificial areas	Bare lands	Water bodies
Forests	1	1	0.8	1	0.1	0.1	1
Grasslands	1	1	0.8	1	0.1	0.1	1
Croplands	+	+	1	1/0.71	0.1	0.1	1
Wetlands	1	1	0.71	1	0.1	0.1	1
Artificial areas	2	2	2	2	1	1	1
Bare lands	2	2	2	2	1	1	1
Water bodies	1	1	1	1	1	1	1

Areas which experienced a loss in SOC of 10% of more during the reporting period will be considered potentially degraded, and areas experiencing a gain of 10% or more as potentially improved.

Fragmentation

The degradation due to the fragmentation of the territory was evaluated starting from the variation of mesh density which took place between 2012 and 2019 (discussed previously). Pixels with an increase in mesh density greater than 10 (n. of meshes per 1,000 km^2) in the reference period were considered as degraded.

Soil erosion

Land degradation caused by water erosion was evaluated for the period 2012-2019 using the universal equation of soil loss (USLE) (Wischmeier and Smith, 1978) and its revised version (RUSLE) (Renard, 1997). This is based on an empirical model tested on standardsized experimental particles, providing quantitative results on potential soil loss, expressed in t/ha/year. The equation is based on climatic, pedological, morphological, vegetation and land use parameters:

$$E = R * K * C * LS * P$$

Where:

E = estimate of soil loss due to water erosion;

R= rainfall erosivity factor;

K= soil erodibility factor;

C= cover-management factor;

LS= slope length and slope steepness factor;

P= support practices factor.

Parameter values refer to Panagos et al. (2015). The K factor is based on the chemical-physical characteristics of the soils described by the LUCAS soil survey database 2010 (Panagos *et al.*, 2014); the R factor uses the European database of rainfall erosivity, based on high-resolution temporal rainfall data collected from 1,541 precipitation stations across Europe (REDES) (Panagos *et al.*, 2015). The LS factor is obtained from the high-resolution (25 m) DEM of the European Union (EUDEM) (Panagos *et al.*,2015), while a conservative value of 1 has been set for the P factor, since there are no databases with a satisfactory coverage for the Italian territory.

For the calculation of the C factor, the LANDUM model (Panagos *et al.*, 2015) was applied. The model provides an estimate of the coefficient for arable lands and non-arable land, while artificial areas, wetlands, water bodies, bare rocks, beaches and glaciers are not considered in the evaluation.

The C factor for arable lands is calculated according to the formula proposed by Panagos et al. (2015), which takes into account the correlation between degradation and land management methods and the crop type:

$$C_{arable} = C_{crop} * C_{management}$$

C_{crop} is the C-factor based on the crop type. The C_{crop} values for the CLC classes of arable land (21 class) are reported in the literature; in this work the value of 0.5 was considered for rice fields and 0.30 as the average value for all other crops.

$C_{management}$ is a corrective factor related to management practices on soil erosion reduction (reduced tillage, cover crop and crop residues). The information on production methods by municipality was obtained from the last ISTAT agricultural census, which indicates: methods of management of the area, types of crops and the use of crop residues capable of reducing erosive phenomenon. No corrective factors were applied in municipalities without such information.

For non-arable lands, values from studies carried out in Italy, Belgium, Slovakia, Greece, Bulgaria, France, Switzerland, Portugal and Spain were used (Panagos *et al.*, 2015). The influence of vegetation in these areas was estimated through the F-Cover index of the Copernicus program, which considers the percentage of vegetation cover within each pixel (Baret and Weiss, 2018).

The coefficient assumes values between 0 and 1 based on the erosion tendency of the class and is represented on a 10 m grid.

Potential impact area

The impacts of land consumption affect surfaces with artificial cover but also neighbouring areas, for example through noise disturbance, local contamination, the spread of alien species.

To provide a first estimate of the phenomenon, ISPRA defines a criterion based on distance, identifying the areas located at 60, 100 and 200 m from the perimeter of the consumed land identified by the National Land Consumption Map (Munafò, 2020).

The increase in degradation was associated with the expansion of the area of potential impact between 2012 and 2019, considering the first 60 m from the consumed land. Data were represented in a 10 m resolution raster.

Burned areas

The degradation associated with burned areas was assessed by ISPRA starting from the official data provided by the national fire register. The framework law n. 353/2000 indicates that the municipalities are responsible for monitoring the burned areas, with the support of the Carabinieri Command Unit for Forestry, Environmental and Agrifood Protection, which maintains, manages and updates the database.

The database covers the national territory, excluding the regions with special status (Valle d'Aosta, Trentino-Alto Adige, Friuli Venezia Giulia, Sardegna and Sicilia).

Burned areas between 2012 and 2019 were associated with the value 1 of a 10 m resolution binary raster, which indicates the new land degradation.

Reduction in size of natural spaces, in terms of increasing natural spaces smaller than 1,000 m^2 *in the reference period*

The surface of continuous natural patches was calculated starting from the National Land Consumption Map for 2012 and 2019. The number of patches smaller than 1000 m^2 was then compared between the two years, classifying as degraded the areas in which the large natural patches have given way to small patches (smaller than 1000 m^2). This trend is a form of degradation as it reduces the ecological connectivity of natural areas.

Areas with increasing degradation were represented in a 10 m resolution raster.

Density of artificial areas, considering high and medium density areas

To evaluate the increase in degradation associated with the expansion of urban areas, ISPRA data were used, based on the land consumption density map and the population density map (Munafò, 2020). The map has four classes:

- high density urban centers (Class 1). Areas with population density greater than 1,500 inhabitants per km^2 and density of consumed land higher than 50%;
- medium density urban groups (Class 2). Areas with population density between 300 and 1,500 inhabitants per km^2 and density of consumed land between 10% and 50%;
- rural areas (Class 3). All areas with low densities of both population and consumed land;
- industrial areas (Class 4). All areas with high density of consumed land (higher 50%) and population densities lower than 300 inhabitants per km^2.

The increase in degradation between 2012 and 2019 was associated with the expansion of high and medium density classes in the reference period. Areas with increasing degradation were represented in a 10 m resolution raster.

Loss of habitat quality.

Degradation due to the loss of habitat quality linked to the loss of ecosystem services was estimated starting from the data produced by ISPRA for 2012 and 2019 (Munafò, 2020). The difference between the maximum value of the habitat quality index between the two years was calculated, considering degraded areas with a reduction of the value of 0.1%.

The analysis conducted on soil degradation were published in the ISPRA report "Land Consumption, territorial dynamics and ecosystem services" (Munafò, 2018, 2019, 2020) and in the "biosphere" section of the ISPRA "Environmental Data Yearbook" (ISPRA, 2018a, 2019a). Also, a synthesis of the methodology was presented at the VII AIQUAV conference, with the title "Indicators and mapping of urban dynamics and land degradation".

4 Results and discussion

4.1 Land cover maps of Italy

4.1.1 National Land Cover map for 2012

The map produced by the integration of the main available data is shown in Figure 24.

Figure 24. Land Cover Map (2012)

The map was used as a part of the report “Land Consumption, territorial dynamics and ecosystem services” (Munafò, 2018, 2019, 2020) and “Territory. Process and trasformation in Italy” (ISPRA, 2018d) published by ISPRA, as an ancillary data for the production of new Copernicus CLC Plus layers and for the estimation of ecosystem services in Italy.

Accuracy assessment

Accuracy assessment was conducted on the map of Figure 24 and provides the results shown in Table 31. The map has an overall accuracy of 90%. The omission error is less than 20% in all classes and slightly higher than this value for permanent snow and ice and wetlands. The commission error is just over 20% in 2 of the 16 classes, while it is less than 3% for the artificial abiotic surfaces, beaches, dunes and sands, olive plantation and permanent snow and ice.

Table 31. Confusion matrix (land cover map 2012)

	Reference data																		
Classified data	**Artificial abiotic surfaces**	**Consolidated abiotic**	**Unconsolidated abiotic**	**Broad-leaved**	**Needle-leaved**	**Orchards**	**Olive plantation**	**Wood plantations**	**Vineyards**	**Shrubland**	**Pastures**	**Arable land**	**Permanent herbaceous**	**Water bodies**	**Permanent snow and ice**	**Wetlands**	**Total**	**User's Accuracy (%)**	**Commission error (%)**
Artificial abiotic surfaces	135	0	0	0	0	0	0	0	0	1	0	0	1	1	0	0	138	**0.98**	**0.02**
Consolidated abiotic	0	92	0	4	0	0	0	0	0	3	0	0	3	0	1	0	103	**0.89**	**0.11**
Unconsolidated abiotic	0	1	99	0	0	0	0	0	0	0	0	0	0	2	0	0	102	**0.97**	**0.03**
Broad-leaved	0	0	0	326	0	0	0	0	0	3	3	20	4	0	0	0	356	**0.92**	**0.08**
Needle-leaved	2	3	0	0	156	0	0	0	0	2	1	3	10	0	0	0	177	**0.88**	**0.12**
Orchards	0	0	0	5	1	89	5	0	0	1	2	3	2	0	0	0	108	**0.82**	**0.18**
Olive plantation	0	0	0	0	0	0	108	0	0	2	0	0	0	0	0	0	110	**0.98**	**0.02**
Wood plantations	0	0	0	0	0	0	1	76	5	0	2	0	0	0	0	0	84	**0.90**	**0.10**
Vineyards	1	0	0	2	0	9	2	0	95	1	0	6	5	0	0	0	121	**0.79**	**0.21**
Shrubland	0	0	1	10	0	0	0	1	0	113	0	0	8	0	0	1	134	**0.84**	**0.16**
Pastures	0	0	0	0	2	1	3	0	0	1	122	9	0	0	0	0	138	**0.88**	**0.12**
Arable land	17	0	0	7	2	1	0	0	3	3	0	391	0	0	0	0	424	**0.92**	**0.08**
Permanent herbaceous	0	9	0	31	1	0	0	0	0	0	0	0	132	0	0	0	173	**0.76**	**0.24**
Water bodies	3	0	0	0	0	0	0	0	0	0	0	6	0	87	0	1	97	**0.90**	**0.10**
Permanent snow and ice	0	1	0	0	0	0	0	0	0	0	0	0	0	0	76	0	77	**0.99**	**0.01**
Wetlands	1	1	0	1	0	0	0	0	0	0	0	3	3	1	0	75	85	**0.88**	**0.12**
Total	159	107	100	386	162	100	119	77	103	130	130	441	168	91	77	77	2427		
Producer's Accuracy (%)	**0.83**	**0.82**	**0.85**	**0.91**	**0.96**	**0.86**	**0.94**	**0.84**	**0.89**	**0.83**	**0.93**	**0.93**	**0.83**	**0.95**	**0.79**	**0.79**		**0.9**	
Omission error(%)	**0.17**	**0.18**	**0.15**	**0.09**	**0.04**	**0.14**	**0.06**	**0.16**	**0.11**	**0.17**	**0.07**	**0.07**	**0.17**	**0.05**	**0.21**	**0.21**			

Land cover

Analysing the first classification level of the 2012 land cover map (Table 32), over 88 % of the national surface is occupied by vegetation, followed by abiotic surfaces (9.83 %) and water bodies and wetlands (1.46 and 0.17 %). At the second classification level, in the abiotic class the artificial component prevails (6.98%) followed by bare rocks. Regarding vegetation, woody and herbaceous vegetation cover comparable surfaces (45.76% and 42.78% respectively). In the woody vegetation trees prevail, which occupies 38.91% of the national surface.

Table 32. Land cover classes 2012 (first and second classification level)

	ha	% Total	% Class
Abiotic surfaces	**2,964,151**	**9.83**	
Artificial abiotic surfaces	2,102,288	6.98	70.92
Natural abiotic surfaces	861,864	2.86	29.07
Biotic surfaces	**26,685,696**	**88.54**	
Woody vegetation	13,791,561	45.76	51.68
Herbaceous vegetation	12,894,135	42.78	48.32
Water surfaces	**439,830**	**1.46**	
Water bodies	402,830	1.34	91.59
Permanent snow and ice	37,000	0.12	8.41
Wetlands	**50,295**	**0.17**	

Considering the maximum thematic detail, class 22120 (arable land) prevail, which occupies 30.47% of the national territory, followed by broad-leaved trees (25.90%). All other classes occupy less than 10% of the territory and 11 out of 16 classes less than 5% (Table 33).

Table 33. Surface occupied by the land cover classes (2012)

LC code	Class name	ha	%
11000	Artificial abiotic surfaces	2,102,288	6.98
12100	Consolidated abiotic	802,539	2.66
12200	Unconsolidated abiotic	59,325	0.20
21110	Broad-leaved	7,805,217	25.90
21120	Needle-leaved	2,167,261	7.19
21131	Orchards	619,759	2.06
21132	Olive plantation	1,088,099	3.61
21133	Wood plantations	46,356	0.15
21210	Vineyards	689,746	2.29
21220	Shrubland	1,375,125	4.56
22110	Pastures	1,372,790	4.55
22120	Arable land	9,183,519	30.47
22200	Permanent herbaceous	2,337,826	7.76
31000	Water bodies	402,830	1.34
32000	Permanent snow and ice	37,000	0.12
40000	Wetlands	50,295	0.17
Total		**30,139,972**	**100.00**

The artificial abiotic surfaces are concentrated in the Po Valley: Lombardia and Veneto host about a quarter of the class, the value rises to 40% also considering Piemonte and Emilia Romagna (Table 34). The bare rocks are mainly in the Alpine area (Trentino-Alto Adige, Piemonte and Valle d'Aosta), while about 35% of the unconsolidated natural abiotic surfaces are in Friuli-Venezia Giulia (e.g. Tagliamento river) and in the "fiumare" of Calabria.

The 28.7% of the needle-leaved forests are in Trentino-Alto Adige, while almost a quarter of the broad-leaved forests are in Toscana (13.1%) and Piemonte (10.3%). Orchards and olive groves are concentrated in the south (Sicilia, Puglia, Calabria), and over half of the wood plantations are in Lombardy, near the Po river. The herbaceous is mainly in the regions of the Po valley and in the two main islands.

Perennial ice is concentrated in Valle d'Aosta and Trentino-Alto Adige, while permanent water bodies and wetlands have high values in Veneto, due to the presence of lagoons and Garda Lake.

Table 34. Land cover classes 2012, regional level (%)

Region	**Artificial abiotic surfaces**	**Consolidated abiotic**	**Unconsolidated abiotic**	**Broad-leaved**	**Needle-leaved**	**Orchards**	**Olive plantation**	**Wood plantations**	**Vineyards**	**Shrubland**	**Pastures**	**Arable land**	**Permanent herbaceous**	**Water bodies**	**Permanent snow and ice**	**Wetlands**
Piemonte	8.0	16.8	8.0	10.3	9.3	4.9	0.0	8.6	8.9	4.4	10.4	7.2	10.2	6.7	7.4	0.3
Valle d'Aosta	0.3	13.6	0.4	0.2	4.2	0.0	0.0	0.0	0.1	1.9	0.9	0.0	2.0	0.3	33.5	0.1
Lombardia	13.5	12.8	4.3	5.6	9.0	1.3	0.2	51.9	3.9	4.1	9.4	8.6	10.2	19.4	22.5	5.5
Trentino-Alto Adige	2.0	24.1	0.9	1.8	28.7	3.0	0.0	0.0	1.7	3.0	6.5	0.3	6.5	2.5	36.5	0.2
Veneto	10.1	5.3	5.6	3.4	9.2	3.5	0.1	2.4	9.8	2.1	5.6	7.6	4.6	22.4	0.1	36.5
Friuli-Venezia Giulia	2.9	2.9	17.9	2.7	6.1	0.6	0.0	4.5	1.8	1.7	1.4	2.4	1.9	4.5	0.0	5.8
Liguria	1.9	0.3	1.3	4.5	1.6	0.3	2.0	0.0	0.3	1.1	0.9	0.2	1.9	0.5	0.0	0.2
Emilia-Romagna	9.3	1.8	7.1	7.5	1.4	4.8	0.1	13.8	3.7	1.5	11.0	11.3	4.2	9.3	0.0	10.1
Toscana	6.7	1.0	3.2	13.1	5.0	6.2	4.9	0.1	8.9	3.6	9.5	6.4	3.4	3.5	0.0	8.7
Umbria	2.1	0.2	0.3	4.6	0.9	1.7	1.9	0.1	0.9	0.6	2.9	3.0	1.8	3.8	0.0	1.0
Marche	3.0	0.5	1.5	3.4	1.0	2.2	0.1	0.0	1.0	1.0	2.2	5.0	2.3	0.6	0.0	0.0
Lazio	6.5	2.3	1.7	7.1	1.1	6.9	7.9	0.8	3.8	4.2	7.5	5.6	5.5	6.7	0.0	1.2
Abruzzo	2.5	2.9	1.7	4.9	1.5	3.8	6.1	0.3	4.3	2.8	2.4	2.5	7.0	0.9	0.0	0.3
Molise	0.8	0.1	0.5	2.0	0.3	0.4	1.1	0.0	0.8	0.6	1 8	2.0	1.2	0.5	0.0	0.0
Campania	6.6	0.8	2.2	6.0	2.0	11.6	5.6	0.0	1.9	2.5	4.1	4.0	4.0	1.5	0.0	0.9
Puglia	7.3	0.5	5.7	1.7	1.6	9.9	34.4	0.1	17.1	2.5	7.1	8.7	4.4	3.8	0 .0	13.9
Basilicata	1.5	1.3	6.2	3.8	1.2	2.8	2.4	0.3	1.1	2.9	4.6	4.0	4.5	1.5	0.0	0.5
Calabria	3.5	2.3	17.1	6.5	7.0	11.5	15.5	1.2	2.7	5.4	3.2	3.2	2.9	1.7	0.0	0.1
Sicilia	7.8	6.8	7.3	3.7	3.5	21.7	14.8	0.0	25.2	13.8	1.7	10.6	13.3	2.8	0.0	0.4
Sardegna	3.7	3.7	7.0	7.2	5.4	2.9	3.0	16.0	2.1	40.3	6.8	7.4	8.1	7.1	0.0	10.1
Total	**100**	**100**	**100**	**100**	**100**	**100**	**100**	**100**	**100**	**100**	**100**	**100**	**100**	**100**	**100**	**100**

Comparison with the CLC

Table 35 shows the comparison between the 2012 land cover map and the CLC 2012.

Table 35. Comparison between CLC 2012 and land cover map 2012 (km^2). Values referring to changes lower than 0.5 km^2 do not appear in the matrix but contribute to the counts for the totals

CLC class	**Artificial abiotic surfaces**	**Consolidated abiotic**	**Unconsolidated abiotic**	**Broad-leaved**	**Needle-leaved**	**Orchards**	**Olive plantation**	**Wood plantations**	**Vineyards**	**Shrubland**	**Pastures**	**Arable land**	**Permanent herbaceous**	**Water bodies**	**Permanent snow and ice**	**Wetlands**	**Tot**
	11000	**12100**	**12200**	**21110**	**21120**	**21131**	**21132**	**21133**	**21210**	**21220**	**22110**	**22120**	**22200**	**31000**	**32000**	**40000**	
111	1,288	2	1	31	2	3	6	0	4	3	7	27	204	2	0	0	**1,580**
112	6,084	16	9	663	42	36	44	0	47	33	181	485	2,641	34	0	1	**10,317**
121	2,069	10	1	80	6	6	6	0	9	10	48	168	588	13	0	3	**3,017**
122	94	1	0	7	1	0	0	0	1	1	6	20	43	1	0	0	**175**
123	76	0	1	1	0	0	0	0	0	0	1	4	18	4	0	0	**106**
124	80	0	0	4	0	0	0	0	0	0	4	14	125	0	0	0	**228**
131	254	82	0	42	3	1	3	0	2	14	9	30	41	16	0	1	**498**
132	23	7	0	1	0	0	0	0	0	0	2	3	6	1	0	0	**44**
133	34	3	0	4	0	0	0	0	0	1	2	10	18	0	0	0	**74**
141	24	1	0	30	7	1	0	0	0	0	5	9	32	2	0	0	**110**
142	76	2	1	45	22	1	1	0	1	3	8	19	135	3	0	1	**317**
211	4,084	73	15	1,582	78	301	514	9	774	540	4,121	64,086	3,124	307	0	28	**79,636**
212	57	1	0	5	1	2	1	0	3	2	20	525	57	4	0	1	**679**
213	109	0	0	37	0	1	0	0	1	3	88	2,658	28	13	0	1	**2,940**
221	324	2	0	92	6	199	157	0	4,118	26	336	756	132	10	0	0	**6,158**
222	240	3	4	258	10	2,139	87	0	305	49	151	420	91	18	0	1	**3,774**
223	739	6	4	691	51	0	8,249	1	405	119	351	909	288	7	0	0	**11,820**
231	230	8	3	276	99	12	12	0	20	72	2,510	420	451	19	0	5	**4,136**
241	133	3	1	121	10	373	146	0	76	59	78	1,185	112	3	0	0	**2,300**
242	2,306	21	8	1,081	60	2,729	961	1	828	156	1,256	11,308	1,182	60	0	5	**21,962**
243	1,259	42	20	7,844	382	205	354	5	185	482	3,241	6,059	1,218	87	0	4	**21,387**
244	28	1	0	863	57	1	6	0	2	37	27	607	57	4	0	0	**1,692**
311	694	86	31	51,347	655	102	139	329	40	797	402	901	875	127	0	4	**56,530**
312	112	32	11	415	11,689	7	11	0	4	175	77	67	257	24	0	1	**12,883**
313	122	22	8	4,959	4,117	12	23	1	6	126	67	82	139	19	0	1	**9,704**
321	72	121	4	564	2,536	9	18	0	9	378	290	221	3,451	6	0	1	**7,678**
322	3	41	3	73	141	0	0	0	0	1,055	4	4	315	2	0	0	**1,640**
323	108	125	11	1,380	143	20	53	4	18	6,779	52	179	1,242	24	0	2	**10,138**
324	155	140	21	4,501	1,261	24	56	111	18	2,228	241	390	1,048	40	0	4	**10,239**
331	32	100	296	107	13	4	4	0	6	48	10	37	67	89	0	4	**819**
332	5	3,852	3	18	13	0	0	0	0	25	1	4	388	5	33	0	**4,347**
333	56	3,131	13	788	248	5	27	0	10	498	105	135	4,927	14	1	0	**9,959**
334	1	17	0	55	10	2	0	0	0	9	3	4	9	0	0	0	**111**
335	0	53	0	0	0	0	0	0	0	0	0	0	0	0	336	0	**390**
411	4	0	0	16	2	0	0	0	0	4	7	22	10	40	0	82	**188**
412	0	0	0	0	0	0	0	0	0	0	0	0	0	0	0	4	**4**
421	4	1	2	5	3	0	0	0	1	6	2	12	10	109	0	236	**390**
422	1	1	0	0	0	0	0	0	0	0	0	5	1	15	0	69	**92**
511	11	9	18	49	1	1	0	0	3	7	11	40	27	293	0	3	**473**
512	21	11	6	18	4	0	0	0	0	5	3	11	13	1,640	0	20	**1,753**
521	4	0	1	1	0	0	0	0	0	0	0	2	3	968	0	18	**998**
522	0	0	0	0	0	0	0	0	0	0	0	0	0	1	0	0	**1**
523	7	0	96	0	0	0	0	0	0	0	0	0	3	3	0	0	**110**
Tot	**21,023**	**8,025**	**593**	**78,052**	**21,673**	**6,198**	**10,881**	**464**	**6,897**	**13,751**	**13,728**	**91,835**	**23,378**	**4,027**	**370**	**503**	**301,397**

The integration of UA, RZ, N2000 and national data guarantees a higher geometric detail than the CLC, allowing the mapping of areas smaller than the MMU CLC, such as small urban agglomerations and roads, and to distinguish land cover classes in mixed CLC polygons. Furthermore, the map uses a land cover-only classification system while maintaining much of the thematic content of the input data.

11000 - Artificial abiotic surfaces

The class is mainly present in correspondence with class 11 and 12 CLC polygons (Figure 25). The correspondence is greater in densely built-up areas, such as 111 (continuous urban fabric), 121 (industrial or commercial units) and 123 (port areas). Less correspondence with classes 144 (artificial, non-agricultural vegetated areas).

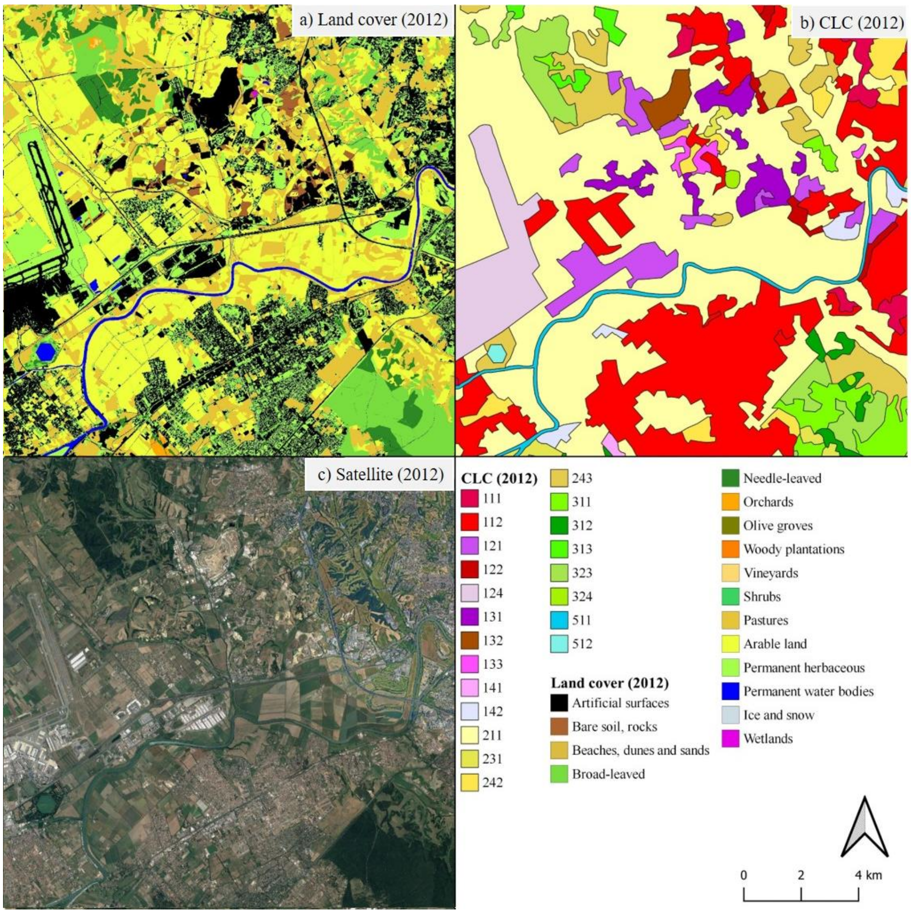

Figure 25. Comparison between land cover map for 2012 (a) and CORINE Land Cover (b) - Discontinuous urban fabric near Rome

The class is also very present in the CLC classes 211 (non-irrigated arable land), 242 (bomplex cultivation patterns) and 243 (land principally occupied by agriculture, with significant areas of natural vegetation). This is due to the large extent of these classes and because the map identifies isolated buildings or small groups of buildings and the road network, much present in these areas but smaller than the CLC MMU. The 14 CLC class largely falls into the land cover classes 21110 (broad-leaved trees) and 22200 (permanent herbaceous), due to the large natural surfaces.

12000 - Natural abiotic surfaces

Class 12100 corresponds above all with class CLC 332 (bare rocks) and maps bare soil areas of class 333 (sparsely vegetated areas). About half of the 12200 class (beaches, dunes, sands) falls into the CLC 331 class (beaches, dunes, sands), with which there is direct correspondence. The two data differ on the coastal area and near the river banks. In coastal area most of the 12200 class is classified by CLC as 523 (sea and ocean) due to the different geometry of the coastline used by the two data (the land cover map uses ISTAT limits). Near rivers and streams, the 12200 class fall into the CLC classes 2, 31 and 32 due to the differences of resolution between RZ and CLC, as CLC often does not map water courses or consider polygons wider than reality to reach MMW (Figure 26).

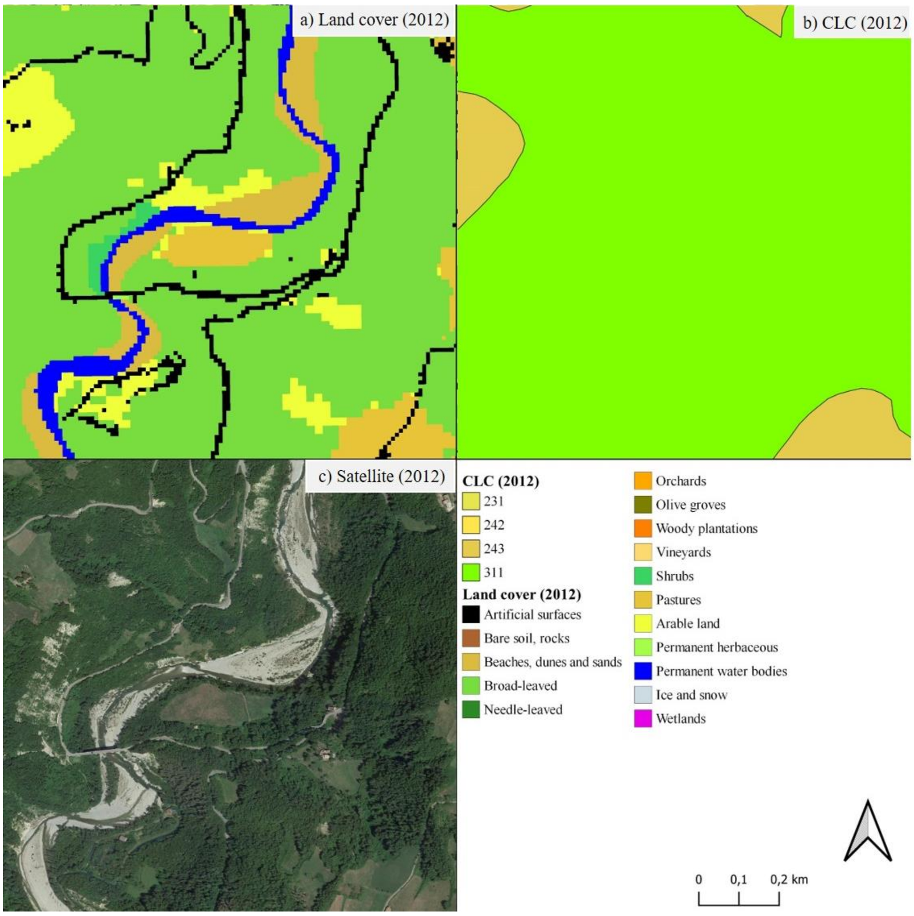

Figure 26. Comparison between land cover map for 2012 (a) and CORINE Land Cover (b) – River banks and broad-leaved trees

20000 – Biotic-vegetated surfaces

The classes of herbaceous vegetation for agricultural purposes of the land cover map (classes 2211, pastures and 2212, arable land) coincide for more about 70% with the corresponding

CLC classes (class 21, arable land and class 23, pastures). The natural herbaceous vegetation (class 2220) of the land cover map corresponds only for 15% with the homonymous CLC class (321, natural grasslands), while the rest is distributed among different classes: about 20% falls in correspondence with class 333 (sparsely vegetated areas), where the herbaceous component is mapped, about 15% in class 211 (arable land) and in class 1 (artificial surfaces, where the green urban areas are mapped). The broad-leaved and needle-leaved classes coincide for about 3/4 with the homologous CLC classes (311, 312, 313). Also about 2/3 of the permanent crops (land cover classes 21131, 21132 and 2121) have a good correspondence with CLC class 22. The main differences occur in the transition areas at the edges of the forest and in the heterogeneous agricultural and agroforestry areas, due to the difference in spatial detail between the two data. The definition of land cover classes relating to trees, shrubs, permament crops and herbaceous vegetation, together with the higher spatial resolution of the land cover map, allows a much more accurate description of the mixed CLC classes (24, heterogeneous agricultural areas and 32, scrub and/or herbaceous vegetation associations) (Figure 27, Figure 28).

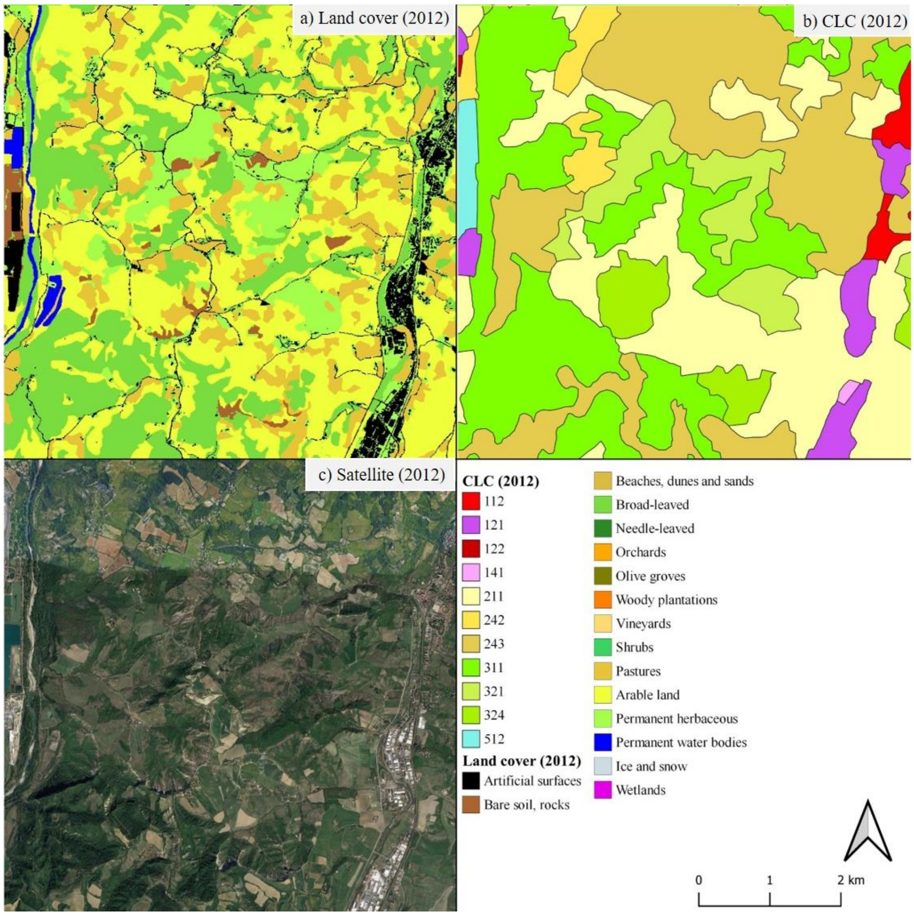

Figure 27. Comparison between land cover map for 2012 (a) and CORINE Land Cover (b) – arable land, trees, scrub and/or herbaceous vegetation associations

The land cover map also improves the geometric description of the areas near water bodies and agricultural areas. The accuracy of the distinction between arable land and pastures is difficult to evaluate, while the distinction between periodically herbaceous and other classes is accurate.

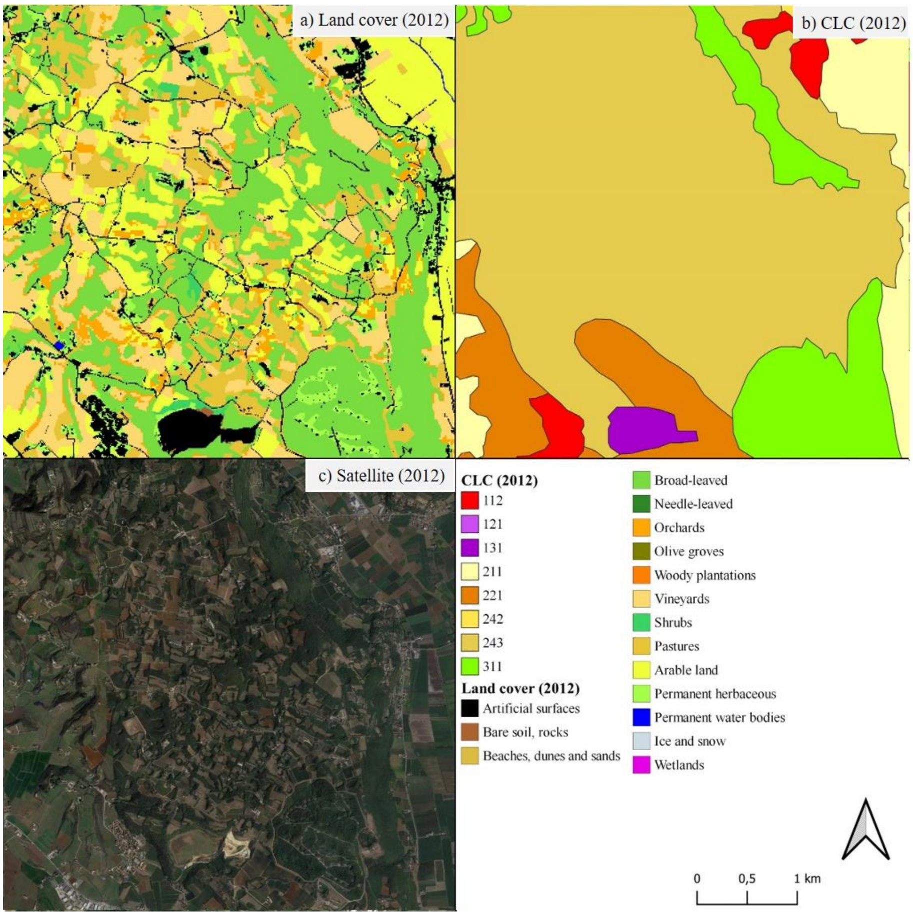

Figure 28. Comparison between land cover map for 2012 (a) and CORINE Land Cover (b) - heterogeneous agricultural areas

30000 - Water surfaces

About ¾ of the areas classified as 31000 coincide with water bodies of class 5 CLC. In class 511 (water courses) the correspondence is lower due to the geometric difference between the data. The CLC does not map small rivers, while it maps larger rivers with wider boundaries, to meet the minimum requirements in terms of MMU and MMW. In the first case, water bodies often fall into CLC vegetation classes, in the second case vegetated areas are included in the CLC water bodies polygons. This is visible in the 31000 areas that the CLC maps as 311 (broad-leaved forest), 331 (beaches, dunes, sands) and 243 (land principally occupied by agriculture, with significant areas of natural vegetation) and in the biotic classes of the land cover map which fall on CLC classes 4 (wetlands) and 5 (water bodies) (Figure 29).

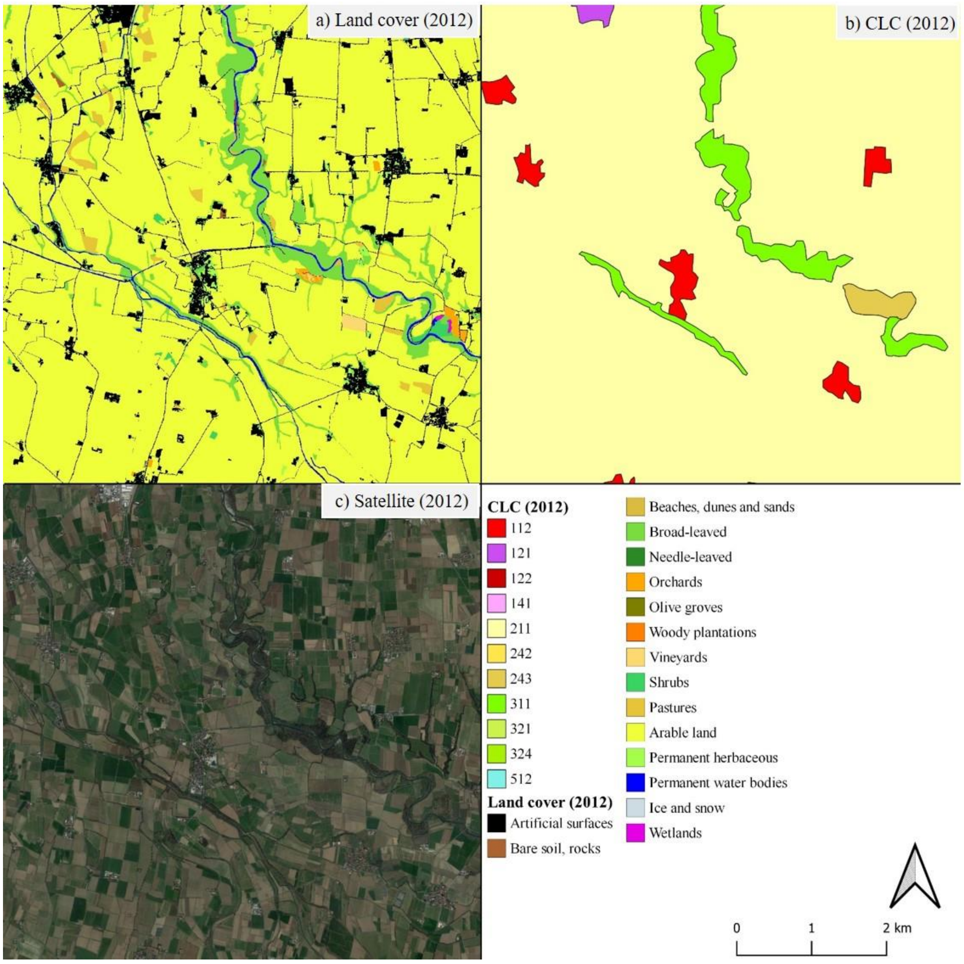

Figure 29. Comparison between land cover map for 2012 (a) and CORINE Land Cover (b) – arable land, small rivers, roads and low density urban areas

Class 32000 and 335 CLC (glaciers and perpetual snow) coincide almost completely, since the data used to make the map have little coverage in high elevation alpine areas, so the data largely coincides with the CLC one. The few differences are related to the areas where N2000 is present, in particular above Garda lake.

40000 - Wetlands

The class mainly coincides with the CLC 412 (peat bogs) and 422 (salines) classes. The correspondence is less exact with CLC class 421 (salt marshes) and 411 (inland marshes), since RZ and UA allowed to distinguish the wetland from the water body. The areas indicated as a water bodies by one of the two data and as wetland by the other and vice versa are linked to this geometric difference.

Discussion of the results

This activity made it possible to analyse in detail the main data available for the Italian territory at national and European level and highlighted the problems related to their updating frequency and the comparison between their classification systems.

The CLC is still one of the few data able to guarantee information on land cover and land use for the entire national territory and is a reference for studies on a national scale, thanks to the long historical series and the high thematic detail. However, the new monitoring needs in terms of updating frequency and level of detail have revealed the limits of the project. Other Copernicus data offer a higher geometric detail (UA, RZ, N2000) but are limited to specific territorial areas and are updated with low frequency.

The land cover and land use maps available at regional level in Italy are often based on CLC data and are updated in a few cases (Lombardia, updated to 2018, Toscana 2016, Liguria 2018, Lazio 2016), while other maps are less up to date (2012 for Sicilia and Puglia, 2013 for Abruzzo and Basilicata, 2006 for Calabria and 2009 for Campania).

Furthermore, all the aforementioned data also present some critical issues from a thematic point of view. CLC has a classification system based on land cover and land use characteristics, with numerous mixed classes. The classification system of the other Copernicus data is very similar in approach to the CLC one, and carries its limitations. It is therefore complex to compare different data to conduct studies at different levels of detail. More recently, HRLs have introduced a 3-year refresh rate and 10-20 m detail coverage for a limited number of land cover classes. In this context, there is a need to introduce products with a higher update frequency and above all more easily comparable and interoperable from a thematic point of view.

4.1.2 Automatic land cover classification of the Italian territory

The land cover classification methodology analysed below takes up the results published in the "Land" journal with the title "Multispectral Sentinel-2 and SAR Sentinel-1 Integration for Automatic Land Cover Classification" (De Fioravante *et al.*, 2021) , adding a comparison between the land cover map and the CLC for 2018 and an analysis of the main surface statistics on a regional scale. These analysis allow to deepen the potential and criticality of the land cover product obtained from the application of the methodology. The land cover map of Figure 30 shows the 8 land cover classes for 2018 and the 4 land cover change classes for 2017-2018 described above.

Figure 30. Land cover map (2018)

Accuracy assessment

Accuracy assessment was conducted by photointerpreting the sample of 2,400 points (Figure 31) and provides the results shown in Table 36.

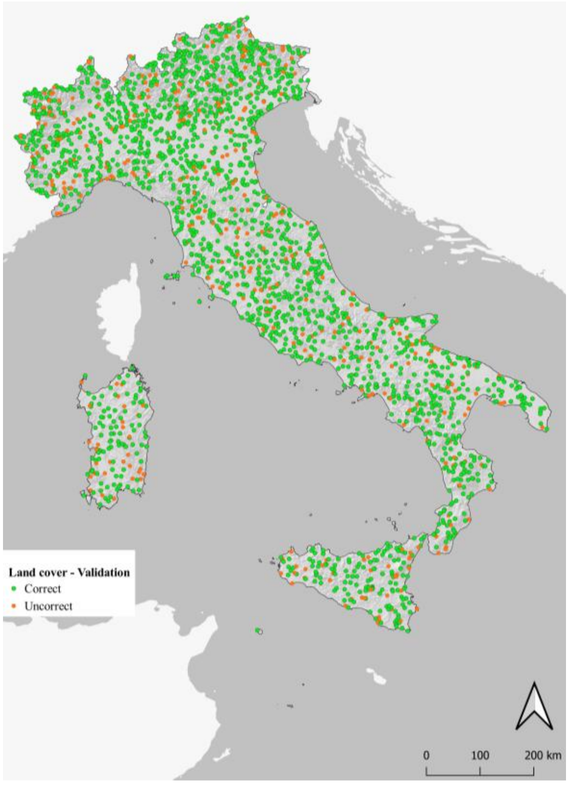

Figure 31. Result of the accuracy assessment with reference to the sample of 2,400 points.

Table 36. Confusion matrix obtained from the accuracy assessment

		Reference data														
		Other disturbance	Burned areas	Land consumption	Renaturation	Abiotic artificial surfaces	Abiotic natural surfaces	Water bodies	Permanent snow and ice	Broad-leaved	Needlelaved	Permanent herbaceous	Periodically herbaceous	Total	**User's Accuracy**	**Commission error**
Classified data	Other disturbance	36	0	0	0	0	1	0	0	25	10	8	23	103	**0.35**	**0.65**
	Burned areas	11	67	0	0	0	2	1	0	5	4	6	4	100	**0.67**	**0.33**
	Land consumption	0	0	81	0	3	1	0	0	2	0	4	9	100	**0.81**	**0.19**
	Renaturation	0	0	0	50	8	3	1	0	4	0	9	25	100	**0.5**	**0.5**
	Abiotic artificial surfaces	0	0	0	0	172	1	0	0	1	0	1	11	186	**0.92**	**0.08**
	Abiotic natural surfaces	0	0	0	0	5	114	5	0	3	0	2	9	138	**0.83**	**0.17**
	Water bodies	0	0	0	0	0	2	111	0	0	0	0	0	113	**0.98**	**0.02**
	Permanent snow and ice	0	0	0	0	2	13	0	89	0	0	0	0	104	**0.86**	**0.14**
	Broad-leaved	3	0	0	0	0	3	3	0	501	2	25	41	578	**0.87**	**0.13**
	Needlelaved	0	0	0	0	0	0	0	0	12	148	3	1	164	**0.9**	**0.1**
	Permanent herbaceous	0	0	0	0	1	1	0	0	6	0	101	1	110	**0.92**	**0.08**
	Periodically herbaceous	1	0	0	0	5	6	3	0	57	5	5	522	604	**0.86**	**0.14**
	Total	51	67	81	50	196	147	124	89	616	169	164	646	2400		
	Producer's Accuracy	**0.71**	**1**	**1**	**1**	**0.88**	**0.78**	**0.9**	**1**	**0.81**	**0.88**	**0.62**	**0.81**		**0.83**	
	Omission error	**0.29**	**0**	**0**	**0**	**0.12**	**0.22**	**0.1**	**0**	**0.19**	**0.12**	**0.38**	**0.19**			

The map has 83% overall accuracy. This value offers a general estimation of the accuracy, but it is influenced by the distribution of the error between the classes, especially those of land cover change.
Water bodies (98%), abiotic artificial surfaces (92%) and permanent herbaceous (92%) have best user accuracy, while the land cover change classes show the lowest values, except for "land consumption" which presents a user accuracy of 81%.
As regard producer's accuracy, 4 classes have values of 100%, and 9 out of 12 greater than 81%. The lowest values affect the land cover change class of "other forest disturbances" (71%) and the land cover class of permanent herbaceous (62%).

Land cover

Analysing the land cover data for 2018 and land cover change occurred between 2017 and 2018 (Table 37), 10.22% of the Italian territory is represented by the abiotic surfaces, of which about 70% are artificial surfaces. The rest of the territory is divided between woody vegetation (45.17%, with a prevalence of broad-leaved trees) and herbaceous vegetation (42.79%, especially periodically herbaceous). The remaining 1.49% is represented by water bodies (1.12%) and perennial ice and snow (0.37%). Land cover change classes occupy 0.32% of the national territory and about 90% are forest disturbances.

Table 37. Distribution of land cover classes for 2018 and land cover change for 2017-2018 on the Italian territory

		ha	% Total	% Class
Abiotic surfaces		**3,081,573**	**10.22**	
	Artificial surfaces	2,127,999	7.06	69.06
	Natural surfaces	953,574	3.16	30.94
Woody vegetation		**13,614,064**	**45.17**	
	Broad-leaved	12,006,482	39.84	88.19
	Needle-leaved	1,607,582	5.33	11.81
Herbaceous vegetation		**12,897,724**	**42.79**	
	Periodically	12,657,890	42.00	98.14
	Permanent	239,834	0.80	1.86
Water and ice		**449,510**	**1.49**	
	Water bodies	337,737	1.12	75.13
	Permanent snow and ice	111,773	0.37	24.87
Land cover change		**97,102**	**0.32**	
Italy		30,139,974	100.00	

The artificial abiotic surfaces (Figure 32) and the changes related to land consumption (Figure 33) were mapped using the National Land Consumption Map produced and updated by ISPRA. Data has high accuracy, due to periodically updates and improvements through photointerpretation.

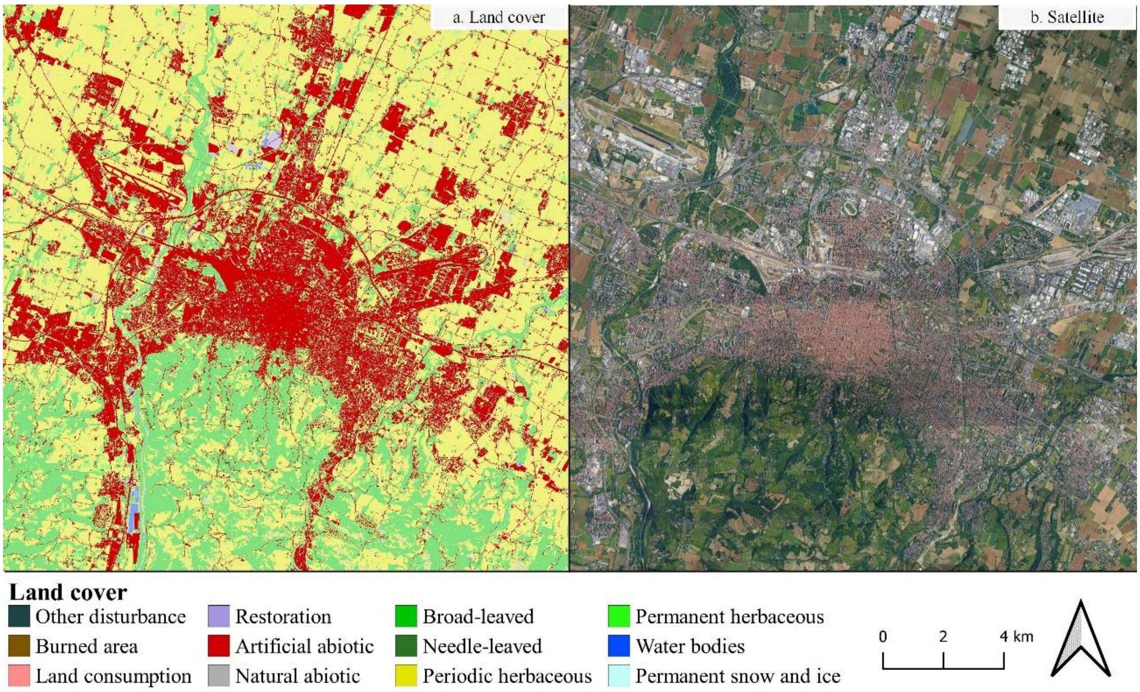

Figure 32. Abiotic artificial surfaces

The use of ancillary data allowed to overcome the issue related to spectral similarity between the natural abiotic surfaces and the artificial ones using Sentinel-2 images. Hyperspectral images (such as PRISMA) could be used in the future to improve the distinction of abiotic surfaces exploiting the bands in the SWIR region (Pepe *et al.*, 2020).

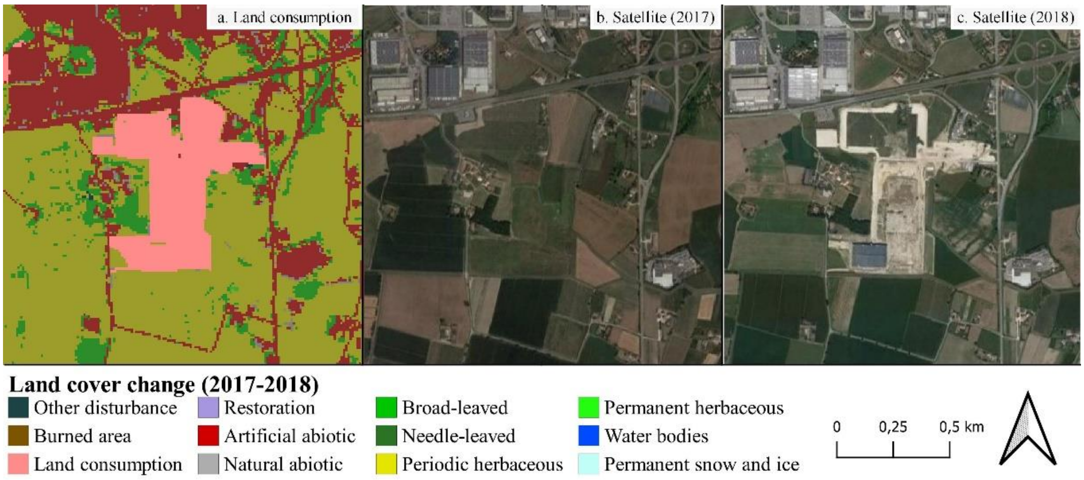

Figure 33. Land consumption

Permanent water bodies has an accuracy of over 90%, as the characteristics of the class can be well discriminated through the optical and radar instruments used in this research (Figure 34). Few omission errors concern boundary areas between water bodies and other land cover classes, such as river and lake banks, and some wetlands.

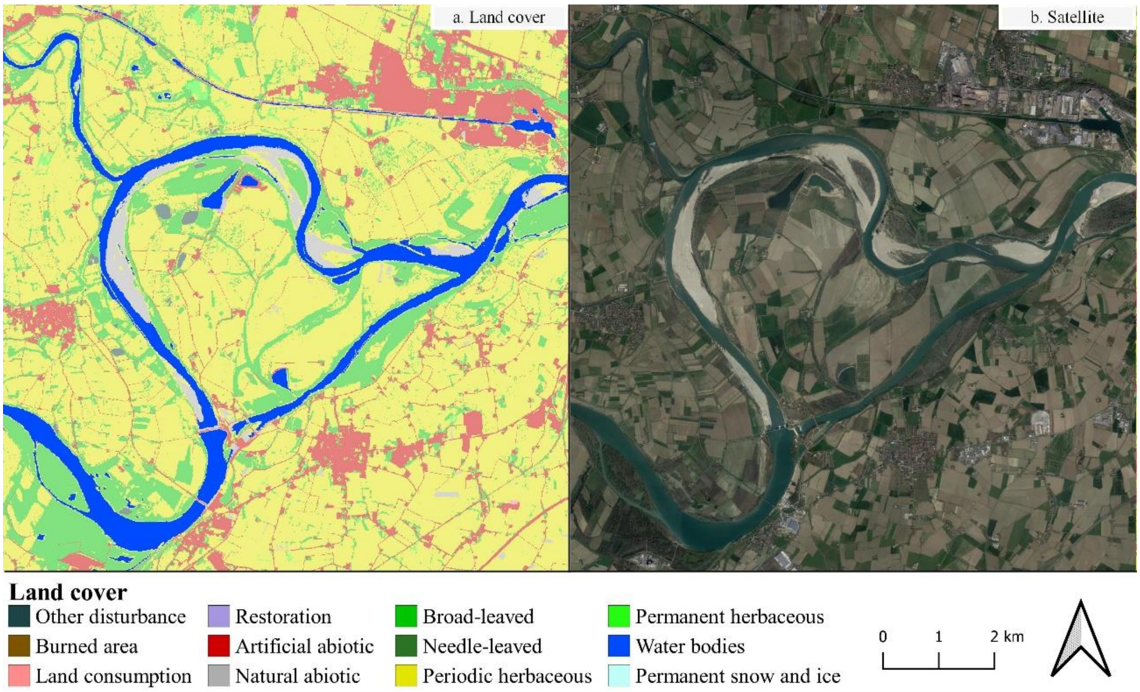

Figure 34. Water bodies

Perennal snow and ice has high accuracy (Figure 35), although it is slightly lower than permanent water bodies (86%), due to commission errors on natural abiotic class linked to the variation of snow cover in mountain areas.

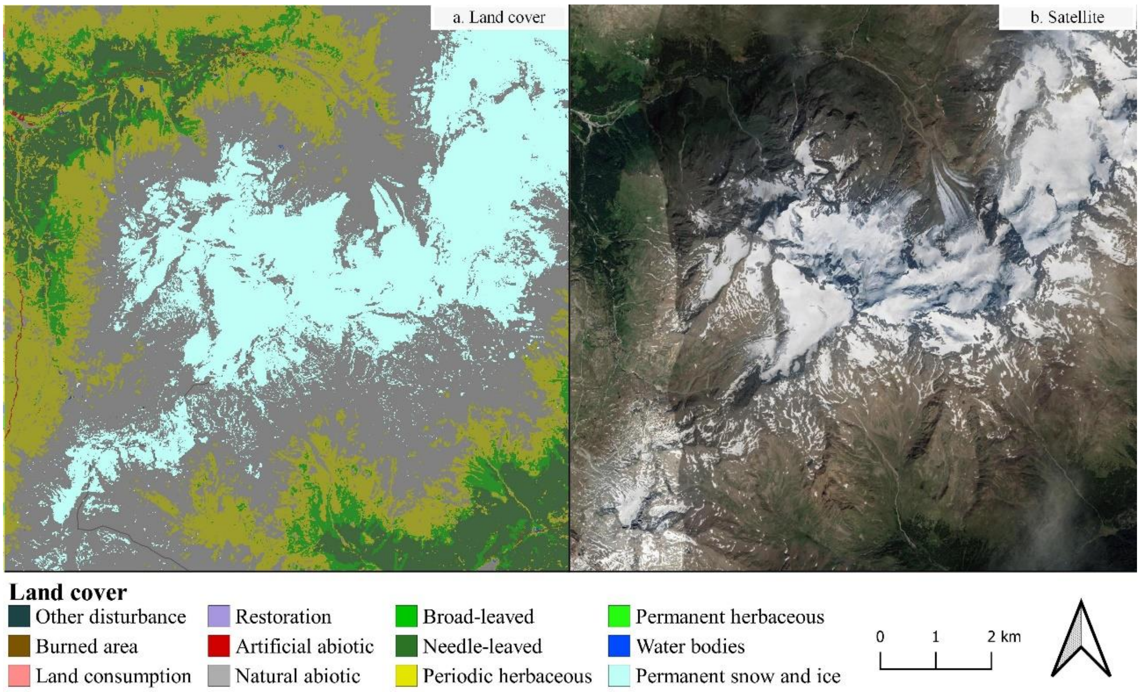

Figure 35. Permanent snow and ice

Woody vegetation correctly identified broad-leaved and needle-leaved trees in areas with homogeneous coverage (Figure 36).

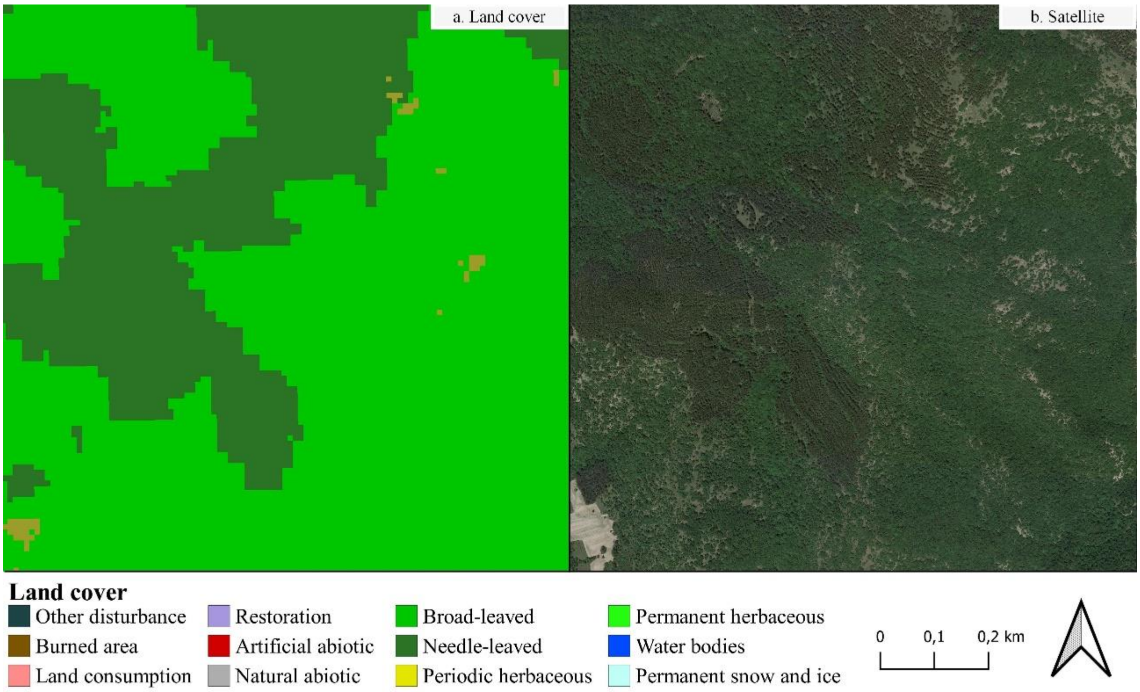

Figure 36. Woody vegetation

There are classification errors in the mixed forest pixels related to the spatial resolution of the data and to the spectral similarity between the different types of trees (Kuenzer *et al.*, 2014; del Río-Mena *et al.*, 2020; Modzelewska *et al.* 2020).

The results obtained for the herbaceous cover are related to the definition adopted for distinguish periodically and permanent herbaceous, which consider the persistence of the herbaceous cover in the pixel during the year.

In detail, pixels showing herbaceous cover in at least 95% of valid observations were classified as permanent herbaceous. This threshold is conservative and aligned with the definitions of CLC+ products (Kleeschulte *et al.*, 2019), but it could be adapted to different temporal definitions (Figure 37).

Figure 37. Periodically herbaceous

Land cover change – forest disturbances

The decrease in vegetation caused by forest disturbances affects 89,596 hectares (Table 38). The 12.4% (11,106 ha) of forest disturbances are burnt areas, while 87.6% (78,490 ha) had other causes. The "other disturbances" class was further analysed, showing that more than half of the disturbance are attributable to forest harvesting.

Table 38. Distribution of forest disturbances occurred between 2017 and 2018 among woody vegetation classes

	2017-2018	ha	%
	Total	**11,106**	**12.4**
Burnt areas	Broad-leaved	6,610	59.5
	Needle-leaved	4,496	40.5
	Total	**78,490**	**87.6**
Other disturbances	Broad-leaved	71,096	90.6
	Needle-leaved	7,394	9.4
Total		**89,596**	**100.0**

The forest disturbances classes (Figure 38) have mainly commission errors, due to the adoption of wide thresholds. The commissions mainly concern permanent crops, since they have a spectral behavior similar to forest disturbances during the year. The mapping of burned areas (Figure 39) shows results aligned with the European Forest Fire Information System[12] (EFFIS) database.

[12] https://effis.jrc.ec.europa.eu/

The user accuracy of the class of "other disturbances" is also low because it has been validated assimilating the class to "forest harvesting" only; the choice was made to evaluate the algorithm's effectiveness in identifying this type of disturbance. Recently, several studies refer to the use of Sentinel data for monitoring forest disturbances, even if for limited areas (Puletti and Bascietto, 2019). The size of the study area conditioned the identification of changes, since forest harvesting are done with different techniques which vary according to the geographical area, therefore in some cases it is not possible to clearly associate the spectral variations to a certain type of disturbance.

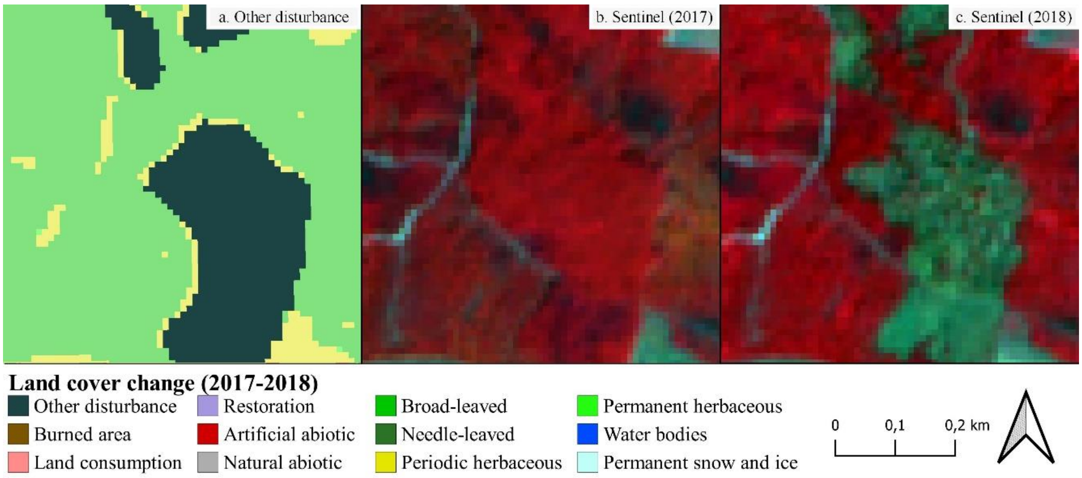

Figure 38. Other disturbances – Forest harvesting

The detection of forest harvesting is more effective in central Italy, while there are classification errors where selective logging method is practiced, such as the Alps.

The observation of the areas of potential disturbance over a longer period can allow the improvement of the data (Banskota *et al.*, 2014; Giannetti *et al.*, 2020).

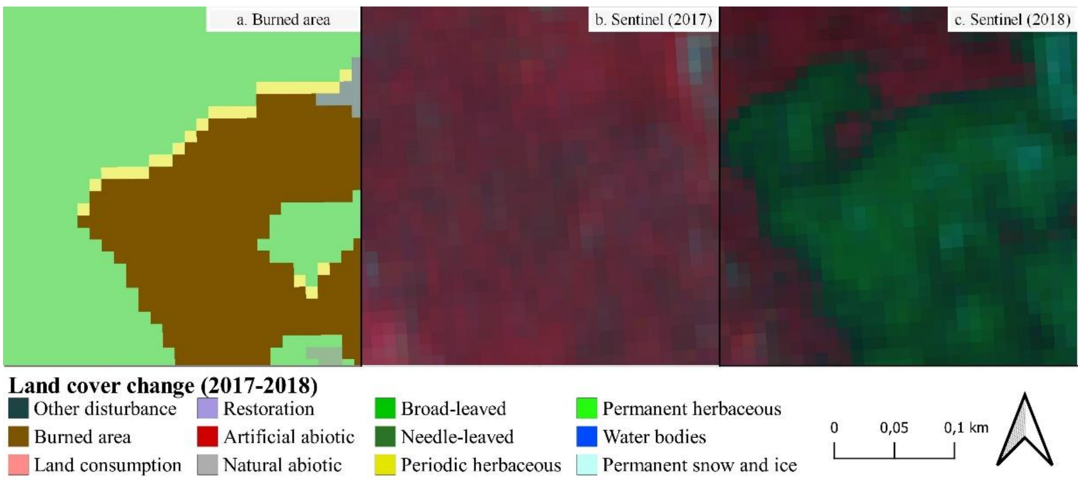

Figure 39. Other disturbances – Burned area

Land cover change – land consumption

Between 2017 and 2018 land consumption and restorations mainly occurred in the periodically herbaceous class (4,231 ha and 636 ha respectively). The results in Table 39 refer to the National Land Consumption Map, which is updated through photointerpretation by ISPRA.

Table 39. Distribution of land consumption between 2017 and 2018 among land cover classes

	Land consumption			Restoration		
	ha	%	m^2chg/ha	ha	%	m^2chg/ha
Abiotic surfaces	**1,311**	**19.9**	**4.2**	**91**	**10.0**	**0.3**
Artificial surfaces	-	-	-	-	-	-
Natural surfaces	1,311	19.9	13.6	91	10.0	0.9
Woody vegetation	**1,049**	**15.9**	**0.8**	**169**	**18.6**	**0.1**
Broad-leaved	1,019	15.4	0.8	166	18.3	0.1
Needle-leaved	30	0.5	0.2	3	0.3	0.0
Herbaceous vegetation	**4,240**	**64.2**	**3.3**	**647**	**71.4**	**0.5**
periodically	4,231	64.1	3.3	636	70.2	0.5
permanent	9	0.1	0.3	11	1.2	0.3
Water and ice	**0**	**0.0**	**0.0**	**0**	**0.0**	**0.0**
Water bodies	0	0.0	0.0	0	0.0	0.0
Permanent snow and ice	0	0.0	0.0	0	0.0	0.0
Italy	6,600	100.0	2.2	906	100.0	0.3

The change detection methodology for potential land consumption analysed below takes up the results published on "Remote Sensing" journal with the title "Land consumption monitoring with SAR data and multispectral indices" (Luti et al., 2021). The methodology is part of the land consumption monitoring activities conducted by ISPRA for the whole Italian territory, therefore the project requirements influenced this methodology. The update must ensure very high accuracy values, since the current LCM has an overall accuracy of 99.7% (Munafò, 2020), therefore it was conducted by manual inspection of the entire national territory and photointerpretation of the changes. The extent of the study area and, in particular, the required level of accuracy were constraint in the development of a change detection methodology based on photointerpretation.

Many methodologies based on supervised classification, as machine learning methods, allow for obtaining excellent accuracy, but they are still lower than the required values. Furthermore, the application of these methodologies on a large scale require a huge number of training areas.

The proposed methodology is based on photointerpretation, identifying areas with potential changes and thus reducing the extent of the area that must be inspected by the photointerpreter. In this sense, a set of rules based on conservative thresholds has been defined, in order to prefer the presence of commission errors and limit omissions. This method is therefore time-effective, as well as cost-effective, by significantly reducing costs for the purchase of VHR images.

The additional project requirement of reference period conditioned the definition of the thresholds. The updating institutionally must be referred to a flexible time range between March and July (e.g. in order to detect changes occurred between the nominal year and the previous one). It is worth highlighting that this flexible period allows for overcoming the unavailability of very high resolution images (with a precise acquisition date) during the photointerpretation of changes performed by ISPRA-SNPA.

This period centered in May influenced several choices of the present methodology, because of the impact of seasonality on the vegetation and therefore on the spectral characteristics of land before and after land consumption.

The methodology was applied to the whole Italian territory (about 301,000 km^2), the three approaches were performed in sequence as indicated in the previous chapter.

The first approach yielded about 5 million polygons of potential change, covering about 3,200 km^2 (1.1% of the national territory). The second approach produced fewer polygons of possible change, about 1 million polygons extending for 200 km^2 (0.1% of the national territory). The third approach led to about 13 million polygons, involving 7,300 km^2 (2.4% of the national territory), although many of the changes are related to the additional NDVI range, especially in Southern Italy.

As expected, the addition of the condition on arable land led to a strong reduction of possible change surface detected. Whilst the time-frame extension, with the additional observation period (shift period) caused, on the other hand, a massive increase in the number and in the extension of detected changes. Nevertheless, this additional period allowed for the detection of even large changes that were not detected by the other approaches.

The three approaches results were compared to the land consumption map produced by ISPRA-SNPA for the period 2018-2019. About 33,000 real changes were classified by ISPRA-SNPA by photointerpretation, covering about 57 km^2 of land consumed between 2018 and 2019 (Munafò, 2020). It should be noted that the photointerpretation was performed for the whole Italian territory, in order to classify all the real changes and assess errors, for each approach, due to the variability of geographical conditions.

The correspondence between real and potential changes was assessed both quantitatively and qualitatively. The assessment was also carried out at pixel level, since the purpose of the methodology is to highlight the presence of potential change to the photointerpreter, which is in charge of outlining geometries.

The accuracy of three detection approaches when compared to photointerpreted changes is shown in Table 40. The highest overall accuracy was achieved by the third approach (59.8% of real changes deteceted), followed the first (50.7) while the worst performance was obtained by the second experiment (31%).

Table 40. Count of real changes identified by at least one pixel

Approach	Undetected changes	Detected changes	Total	Percentage of detection
First	16,245	16,702	32,947	50.7
Second	22,742	10,205	32,947	31.0
Third	13,257	19,690	32,947	59.8

Filtering changes by their extension and considering only those above a threshold of 100 m^2 (i.e. one pixel), the first approach detection improved, reaching 58.9% of changes (Table 41). In the same way, the second approach resulted in 37.6% of changes detected. The highest percentage of detection was provided by the third approach (70.4%). Therefore, as can be seen from the comparison between Table 40 and Table 41, the exclusion of single isolated pixels can lead to an improvement, justified by mixed pixel abundance, which is common, especially in coarse spatial resolution data. Single pixel omission however, does not affect large area detection that are usually highlighted by more than one pixel.

Table 41. Count of real changes with surface >100 m^2 identified by at least one pixel

Approach	Not detected changes	Detected changes	Total	Percentage of detection
First	10,163	14,572	24,735	58.9
Second	15,426	9,309	24,735	37.6
Third	7,332	17,403	24,735	70.4

To better understand the relation between detected changes and change area, changes were grouped in classes based on the surface (i.e. ≤ 100 m^2, between 100 m^2 and 500 m^2, between 500 m^2 and 1,000 m^2, between 1,000 m^2 and 1,500 m^2, between 1,500 m^2 and 2,000 m^2, > 2,000 m^2). Table 42 illustrates the changes identified by the third approach. The number of changes detected by the masks exceeds 90% for changes larger than 500 m^2, reaching over 98% for the largest changes. The resumed results are also good for small changes (i.e. between 1 and 5 pixels), which are detected at almost 85%.

Table 42. Count of real changes identified in the third approach, by at least one pixel, grouped by class of area

Class of area	Not detected changes	Detected changes	Percentage of detection
≤ 100 m^2	11,983	11,304	48.5
between 100 m^2 and 500 m^2	1,126	6,236	84.7
between 500 m^2 and 1,000 m^2	113	1,205	91.4
between 1,000 m^2 and 1,500 m^2	22	420	95.0
between 1,500 m^2 and 2,00 0m^2	3	188	98.4
> 2,000 m^2	10	337	97.1

The omissions are mainly related to the smallest changes, which are less than one pixel in size. This is partly due to the reflectance of the mixed pixels. The larger omissions mainly concern photovoltaic fields, in which the NDVI does not reach the set thresholds. Main causes can be intuitively identified in mixed cover (bare soil under the panels) and light-absorbing material behavior. Their detection is a further research direction proposal, as they are an important source of land consumption, especially in areas with significant irradiation values.

The third approach generated the largest number of changes and the largest surface to be investigated, due to the greater presence of false positives. In this sense, the use of the masks produced by the third approach requires the inspection of a 56% larger surface than that detected with the first approach (7,300 km^2, against 3,200 km^2).

The introduction of the shift period has made it possible to increase the percentage of changes detected in the northern regions, but has introduced numerous false changes especially in the South of Italy. Actually, the use of two ranges of NDVI (“main range” and “additional range”) allows to distinguish the less probable changes during the photointerpretation process.

The NDVI method causes false positive in agricultural fields that were vegetated in the first year and permanently plowed in the second year, resulting, visually as exposing bare soil. Analogue issues were found with the method for detecting land consumption related to buildings and infrastructures using SAR data, due to the movement of large vehicles such as trucks or bus in parking lots.

However, the third approach is preferable, as it identifies most of the large changes, keeping the area to be inspected at 2.4% of the total national surface.

Land cover map 2018 - Regional level

The artificial abiotic surfaces mainly affect Lombardia, Veneto, Emilia Romagna and Piemonte, due to the presence of the Po Valley in their territory. About half of the natural abiotic surfaces are in the Alps (Piemonte, Lombardia, Valle d'Aosta, Veneto, Trentino-Alto Adige and Friuli-Venezia Giulia). The class is almost absent in Molise and Liguria, both with 0.6% (Table 43).

The woody vegetation is present mainly in Trentino-Alto Adige, Piemonte and Toscana. These two regions are also the richest in broad-leaved trees (here we find respectively 9.6% and 10.2% of the total broad-leaved trees). Needle-leaved are mainly concentrated in Trentino-Alto Adige (31.8%).

The herbaceous is mainly in Sicilia and Sardegna and in the regions of the Po Valley.

Permanent water bodies, whose extent and presence is linked to the spatial resolution of the data and the periodicity of the water bodies, are concentrated in the northern regions, in particular in Veneto (25.1%, due to the presence of Garda Lake and of the Lagoon of Venice) and Lombardia (20%, mainly linked to the presence of large lakes and the Po river). Valle d'Aosta, Trentino-Alto Adige, Liguria, Marche Abruzzo, Molise, Campania, Basilicata and Calabria have values below 2%. The perennial ice and snow are concentrated in the Alps and in particular in Trentino-Alto Adige (35.9%) and Valle d'Aosta (28.9%). Regarding forest disturbances, about half of the fires (49.2%) detected in the period 2017-2018 are in 4 regions: Piemonte (15.9% of the total), Calabria and Sicilia (in these two regions one quarter of the total fires are concentrated, respectively 12.5% and 12.4%) and Toscana (8.4%). The regions least affected by the phenomenon are Valle d'Aosta (0.3%), Marche (0.3%) Molise (0.5%) and Basilicata (0.9%) where less than 1% of the fires detected occurred.

In Piemonte and Calabria the presence of other disturbances is also notable (respectively 11.3% and 12% of the total). As with fires, about half of the other disturbances are concentrated in a few regions: Piemonte, Calabria, Puglia, Toscana and Sicilia. The regions least affected by the phenomenon are Valle d'Aosta (0.6%), Sardegna (0.7%) and Marche (0.8%). Veneto is the most dynamic region regarding land consumption (17.1% of the total) and restorations (31.0% of the total).

Table 43. Land cover at regional level (2018)

Region	Artificial abiotic surfaces	Natural abiotic surfaces	Broad-leaved	Needle-leaved	Periodically herbaceous	Permanent herbaceous	Water bodies	Permanent snow and ice	Burned areas	Other disturbances	Land consumption	Restoration
Piemonte	8.0	11.8	9.6	8.5	7.2	3.3	5.3	12.1	15.9	11.3	8.2	15.8
Valle d'Aosta	0.3	7.3	0.4	3.9	0.8	0.0	0.1	28.9	0.3	0.6	0.4	1.4
Lombardia	13.5	11.2	6.4	11.0	7.2	19.0	20.0	13.1	2.4	6.6	10.8	8.2
Trentino-Alto Adige	2.0	14.1	2.9	31.8	2.2	0.3	1.7	35.9	7.8	5.3	2.2	4.9
Veneto	10.1	5.3	4.8	8.9	5.7	14.4	25.1	7.3	8.1	6.2	17.2	31.0
Friuli-Venezia Giulia	3.0	3.1	3.0	4.5	1.9	3.6	6.1	1.3	2.4	3.6	4.2	3.8
Liguria	1.8	0.6	3.3	3.0	0.4	0.6	0.2	0.0	1.0	1.1	0.6	0.3
Emilia-Romagna	9.3	3.0	6.9	1.3	8.8	11.1	7.6	0.0	1.3	3.9	9.3	12.0
Toscana	6.6	4.2	10.2	4.7	6.1	10.5	3.0	0.0	8.4	8.6	4.4	3.1
Umbria	2.1	0.9	3.7	1.8	2.3	2.9	4.1	0.0	1.7	3.6	1.9	4.7
Marche	3.0	1.5	3.3	1.5	3.4	2.4	0.3	0.1	0.3	0.8	2.8	0.9
Lazio	6.5	2.3	6.7	2.4	5.3	9.6	7.2	0.0	7.8	5.4	6.9	6.2
Abruzzo	2.5	2.9	4.7	2.9	3.0	2.5	0.8	0.3	1.8	2.1	4.7	0.9
Molise	0.8	0.6	1.9	0.5	1.4	1.6	0.4	0.0	0.5	2.3	0.7	0.1
Campania	6.6	2.0	5.6	0.7	4.0	4.2	0.8	0.1	3.8	3.9	3.7	0.4
Puglia	7.3	6.9	5.0	1.5	8.4	0.3	5.7	0.0	6.0	10.3	7.5	0.9
Basilicata	1.5	2.8	3.8	0.8	3.6	1.9	1.0	0.1	0.9	4.0	2.8	1.7
Calabria	3.6	3.0	6.6	5.9	3.9	3.4	1.2	0.5	12.5	12.0	1.5	1.3
Sicilia	7.8	10.9	5.8	3.3	12.2	0.7	2.6	0.2	12.4	7.6	7.2	1.7
Sardegna	3.7	5.7	5.7	1.3	12.1	7.5	6.9	0.1	4.7	0.7	3.0	0.8
Tot	100	100	100	100	100	100	100	100	100	100	100	100

The analysis of forest disturbances with respect to total woody vegetation was expressed in terms of square meters of disturbance per hectare of forest area, due to the limited extent of the phenomena (Table 44).

Burned areas in Italy affected 8.1 m^2 for each hectare of forest between 2017 and 2018. The highest values are in Sicilia (18.3 m^2/ha), Calabria (15.5 m^2/ha), Piemonte (13.6 m^2/ha) and Veneto (12.4 m^2/ha). Trentino-Alto Adige, Lazio and Puglia have values close to 10 m^2/ha, while the other regions remain below the national average, with a minimum in the Marche (0.8 m^2/ha).

The national average value for other disturbs is 57.3 m^2/ha. In 9 of the 20 regions there are higher values, with a maximum in Puglia (128.6 m^2/ha) and Calabria (105.3 m^2/ha). The lowest value is in Sardegna, with 7.7 m^2/ha, followed by Marche (14.7 m^2/ha) while all the other regions have values over 20 m^2/ha.

Table 44. Distribution of forest disturbances

Region	Burnt areas	Other disturbances	Broad-leaved	Needle-leaved	Tot. woody vegetation	Burned areas	Other disturbances
	ha					m^2/ha	
Piemonte	1,770	8,831	1,157,932	136,813	1,294,745	13.6	67.7
Valle d'Aosta	38	499	53,897	61,956	115,853	3.2	42.9
Lombardia	265	5,193	768,043	176,606	944,649	2.8	54.7
Trentino-Alto Adige	867	4,193	342,644	511,337	853,981	10.1	48.8
Veneto	898	4,837	573,044	143,067	716,112	12.4	67.0
Friuli-Venezia Giulia	262	2,838	356,062	72,265	428,327	6.1	65.8
Liguria	116	875	396,604	48,118	444,722	2.6	19.6
Emilia-Romagna	145	3,064	826,497	21,610	848,107	1.7	36.0
Toscana	934	6,751	1,225,335	75,297	1,300,632	7.1	51.6
Umbria	189	2,851	443,803	28,639	472,442	4.0	60.0
Marche	34	614	392,767	24,675	417,442	0.8	14.7
Lazio	869	4,213	798,444	37,800	836,244	10.3	50.1
Abruzzo	205	1,610	560,228	45,890	606,118	3.4	26.5
Molise	50	1,780	223,942	8,381	232,323	2.1	76.0
Campania	418	3,089	667,795	10,687	678,482	6.1	45.3
Puglia	671	8,093	597,026	23,566	620,592	10.7	128.6
Basilicata	100	3,174	457,011	12,593	469,604	2.1	67.1
Calabria	1,387	9,439	791,248	94,217	885,465	15.5	105.3
Sicilia	1,372	6,003	690,752	53,377	744,129	18.3	79.9
Sardegna	518	545	683,407	20,687	704,095	7.3	7.7
Tot	**11,106**	**78,490**	**12,006,481**	**1,607,582**	**13,614,063**	**8.1**	**57.3**

Comparison with the CLC

The 2018 land cover map was compared with the 2018 CLC to analyse common aspects and differences (Table 45).

10000 - Abiotic surfaces

About half of the 11000 class (artificial abiotic surfaces) falls under CLC class 1. The same considerations made in the comparison between CLC and land cover map 2012 of the previous paragraph are valid, since both data use the LCM to map the artificial abiotic surfaces.

Table 45. Comparison between CLC 2018 and land cover map 2018. Table does not consider land cover change classes, since the CLC 2018 waas photointerpreted on 2017 images, so comparing the two data about the 2017-2018 changes would not be representative. Values referring to changes lower than 0.5 km^2 do not appear in the matrix but contribute to the counts for the totals

CLC	Artificial abiotic surfaces	Natural abiotic surfaces	Broad-leaved	Needle-leaved	Periodically herbaceous	Permanent herbaceous	Water bodies	Permanent snow and ice	Tot
	11000	**12000**	**21110**	**21120**	**22100**	**22200**	**31000**	**32000**	
111	1,292	56	74	2	153	0	1	0	1,580
112	6,129	384	1,499	30	2,227	51	12	0	10,335
121	2,131	104	252	3	576	10	4	0	3,082
122	108	8	24	0	58	1	0	0	202
123	77	10	4	0	10	0	3	0	106
124	8	7	8	0	125	4	0	0	228
131	263	28	69	2	121	1	13	0	501
132	25	2	3	0	12	0	0	0	44
133	24	2	4	0	13	0	0	0	45
141	24	2	42	6	31	3	0	0	109
142	78	11	76	16	109	24	2	0	319
211	4,162	1,287	11,101	79	61,419	1,218	84	0	79,502
212	58	72	46	0	512	4	1	0	696
213	110	7	397	0	2,410	6	3	0	2,942
221	331	284	2,698	11	2,802	46	3	0	6,211
222	244	6	2,107	25	1,254	26	4	0	3,759
223	750	249	4,911	82	5,727	77	1	0	11,815
231	234	37	1,455	9	2,144	150	6	0	4,135
241	136	66	635	7	1,436	13	0	0	2,300
242	2,347	474	7,360	79	11,337	316	15	0	21,975
243	1,272	188	11,706	290	7,646	218	19	0	21,375
244	28	6	387	1	1,244	22	0	0	1,692
311	698	129	50,158	1,758	3,272	63	25	5	56,377
312	114	98	2,271	8,696	1,588	11	15	0	12,881
313	123	36	6,052	2,744	670	9	18	0	9,700
321	72	158	2,556	225	4,574	24	5	6	7,655
322	2	90	632	338	543	0	6	1	1,639
323	108	226	4,227	207	5,167	46	7	0	10,002
324	158	212	6,312	1,115	2,383	25	15	1	10,278
331	32	392	145	4	214	1	33	0	825
332	4	2,950	90	12	592	0	15	681	4,350
333	58	1,555	2,373	217	5,645	11	15	98	10,007
334	3	8	113	13	167	0	0	0	321
335	0	65	0	0	3	0	0	319	387
411	4	11	69	0	73	0	30	0	190
412	0	0	2	0	1	0	0	0	4
421	4	53	55	2	111	0	163	0	391
422	1	24	0	0	7	0	59	0	92
511	11	34	94	1	88	0	235	0	467
512	2	69	33	2	68	0	1,557	0	1,753
521	4	24	6	0	25	0	936	0	996
522	0	0	0	0	0	0	0	0	1
523	7	34	1	0	10	0	55	0	110
Tot	**21,346**	**9,536**	**120,066**	**16,075**	**126,585**	**2,398**	**3,377**	**1,117**	**301,399**

Figure 40 shows how the land cover map better distinguishes the natural component in the 112 CLC (discontinuous urban fabric), 124 (airports), 131 (mineral extraction sites) and 132 (dump sites) class areas.

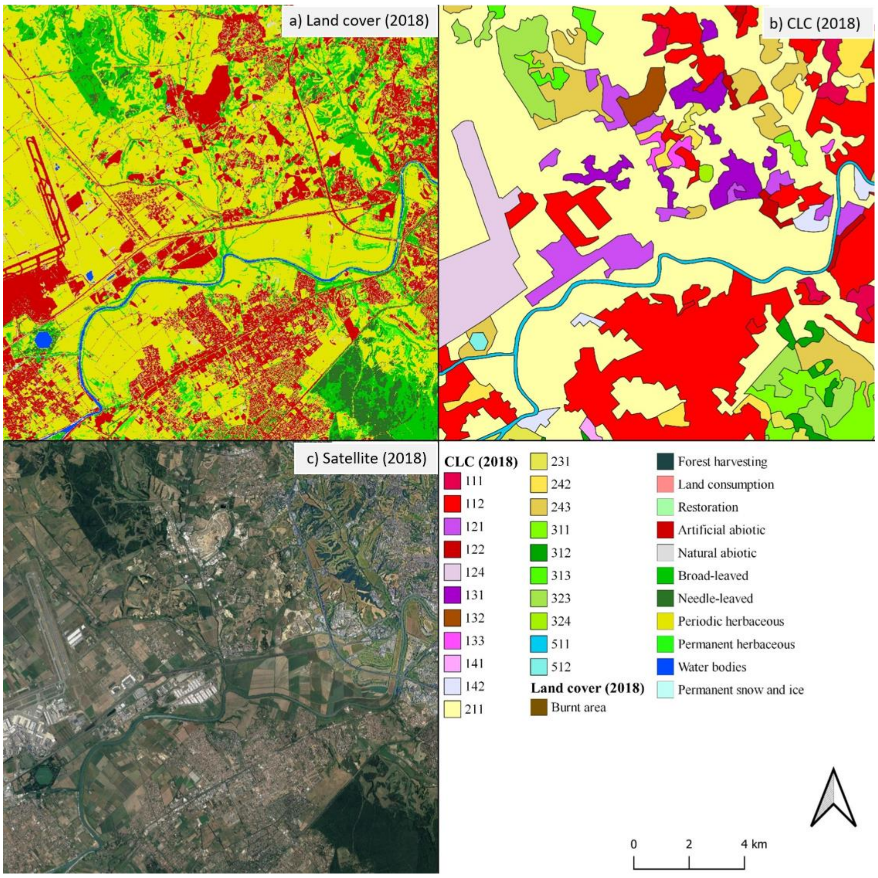

Figure 40. Comparison between land cover map and CLC for 2018 – Discontinuous urban area in Rome

About half of the natural abiotic surfaces coincide with the CLC classes 331 (beaches, dunes, sands), 332 (bare rocks) and 333 (sparsely vegetated), especially in mountain areas.

Natural abiotic surfaces are present in some agricultural classes CLC (211, 221, 223 and 242), due to the presence of greenhouses or arable lands, whose spectral signature is associated with that of bare soil due to factors connected with materials, arrangement of crops or tillage. The natural abiotic surface is also present near water bodies and beaches, the geometry of which is described more accurately than the CLC.

20000 - Biotic-vegetated areas

The classes of broad-leaved (21110) and needle-leaved (21120) trees have a good correspondence with the analogous CLC classes (311, 312 and 313). The broad-leaved of the land cover also includes the CLC classes referring to permanent crops. For olive groves, the accuracy is influenced by the density of the coverage. In fact, in the presence of very spaced trees, the soil below the trees influences the spectral signature of the pixel, making it

similar to herbaceous spectral signature. Vineyards are included in this class despite being shrubs. Their identification is accurate but requires refinements. The class is difficult to identify due to its spectral signature, which is similar to that of the sparse forest in the period of maximum vegetative stage, and to that of the herbaceous in the period of quiescence.
The land cover classes are useful in distinguishing the arboreal and herbaceous component in the heterogeneous CLC classes (class 24, 324) (Figure 41, Figure 42).

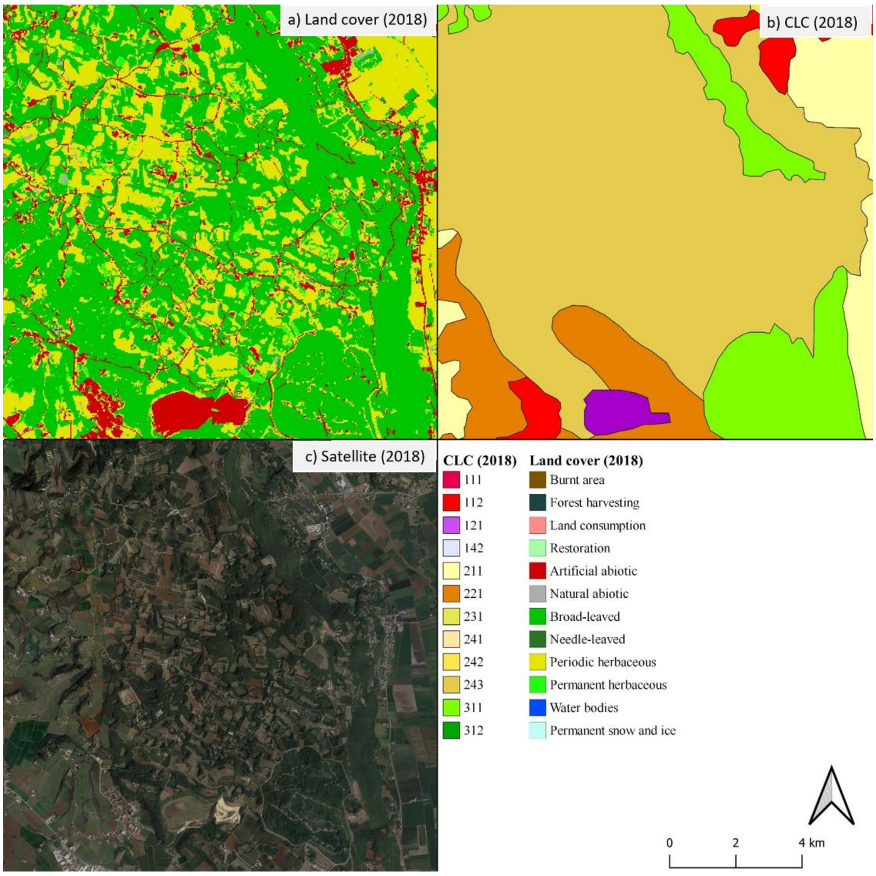

Figure 41. Comparison between land cover map and CLC for 2018 - Heterogeneous agricultural areas

The herbaceous vegetation corresponds for about half to the CLC 21 class (arable land).
As previously illustrated with reference to olive groves, sometimes the herbaceous class of the land cover map is placed in correspondence with CLC permanent crops, in relation to the influence that the configuration of the crop exerts on the spectral signature of the pixels. With reference to the distinction between periodic and permanent herbaceous, it is not possible to establish a clear correspondence with the same CLC classes, due to the different definitions. Actually, in the CLC the distinction follows criteria based on land use, while in the land cover map reference is made to the spectral response during the year.

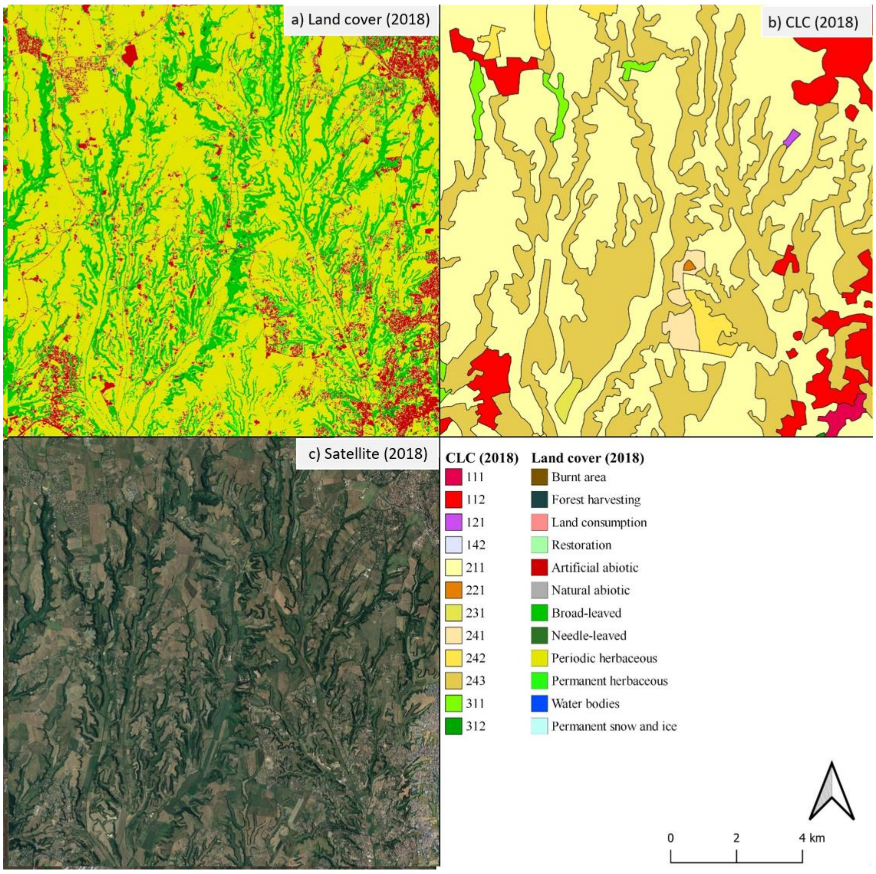

Figure 42. Comparison between land cover map and CLC for 2018 - land principally occupied by agriculture, with significant areas of natural vegetation and discontinuous urbana areas

The use of land cover classes is also important in class CLC 323 (sclerophyllous vegetation) and 333 (sparsely vegetated areas), where bare soil is distinguished from the herbaceous component.

30000 – Water surfaces

The two data show good correspondence in the mapping of lakes, while rivers are mapped with more precision by the land cover map, thanks to the higher spatial resolution. Numerous wetlands also fall into the class, in particular the salt pans.

The permanent snow and ice class corresponds to the CLC classes 332, 333 and 335. The class is very dynamic and the correspondence between the two data is influenced by the reference period, since the land cover map is based on annual images relating to 2018, while the CLC is photointerpreted on 2017 images. Overall, the class still maps transition areas at high elevations, located near the glaciers and in any case above the tree line.

Discussion of the results

The classification of vegetated areas would improve with the introduction of a land cover class for shrubs. This allowing a better description of Mediterranean macchia, permanent crops, such as vineyards, transition areas and woodland boundaries.

In this sense is necessary an indepth analysis of the spectral behavior of shrubs, which are similar to scattered trees or to a mixed herbaceous and arboreal cover.

A further improvement in the classification of vegetation is also linked to the adoption of variable thresholds based on elevation, latitude and phytoclimatic characteristics of the territory. In this way it is possible to better analyse the phenological evolution of vegetation in order to improve the distinction between broad-leaved and needle-leaved trees and the identification of the different types of herbaceous conver and forest disturbances.

A characteristics of the proposed method consists in the definition of thresholds and set of rules, which can be modified and adapted to different conditions. Therefore, future research will focus on selecting the optimal thresholds for the different phytoclimatic regions that characterize Italy.

Also, the classification system based on EAGLE, allows for the introduction of new classes, such as shrubs, or can be modified for specific purposes, for example with land use attributes to identify agricultural areas in the herbaceous vegetation. Of course, additional classes would require additional methodologies, in the implementation of which the integration of hyperspectral data will be fundamental. The new HyperSpectral Precursor of the Application Mission (PRISMA) sensor, developed by the Italian Space Agency, has shown encouraging results in the distinction of forest types (Vangi *et al.*, 2021). This technology will be particularly useful with the launch of the “Hyperspectral Imaging Mission for the Environment” (CHIME) (Rast *et al.*, 2019), whose data will be freely accessible in the coming years.

The versatility of the algorithm and of the classification system make the methodology suitable for future integrations and for adaptation for specific purposes, while remaining consistent with the requirements proposed at European level.

4.2 Land consumption in Italy and related phenomena

The analysis on a national scale shows an increase in land consumption, fragmentation and degradation especially in the plains and coastal areas. The expansion of artificial surfaces mainly affects areas near large metropolitan centers and major infrastructures. Protected areas are less affected by the analysed phenomena, although they are not immune to them.

The analysis of urban areas shows uneven trends from a demographic point of view and in any case an expansion of cities, especially in peripheral areas, where sprawl occurs. The SDGs have provided a good description of the degradation and of the relationship between population and urban growth, although the definition of the most suitable input data is still a fundamental aspect. Analysis were included in the ISPRA-SNPA report “Land Consumption, territorial dynamics and ecosystem services” (Munafò, 2018, 2019, 2020), “Report on Urban Environment Quality” (ISPRA, 2018c, 2019c) and “Environmental Data Yearbook” (ISPRA, 2018a, 2018b, 2019b, 2019a), in the “Rapporto sullo Stato del Capitale Naturale in Italia” (Comitato per il Capitale Naturale, 2018, 2019), in the publication “Land Consumption in Italy” of Journal of Maps (Strollo *et al.*, 2020), in the publication “Land consumption in Itanian coastal area” (Riitano *et al.*, 2020).

4.2.1 Spatial distribution and evolution of land consumption

4.2.1.1 Land consumption at the third classification level

The analysis of changes at the third classification level primarily regards a study on the main flows of change that occurred in the three considered periods, which are analysed in terms of land consumption, restoration, and soil sealing. Particular attention was paid to the presence of prevailing third-level classes and to the main flows. This approach was used for the interpretation of total changes at national level and referring to specific territorial areas (EUAP protected areas, elevation and slope).

Land consumption at national level

The highest land consumption is recorded between 2017 and 2018 (6,600 ha) while in the following period it drops to 5,750 ha. Restorations follow a similar trend, with a maximum value which occurs in 2017-2018 (906 ha), and a minimum of 564 ha in 2018-2019 (Table 46) (Figure 43).

Table 46. Land consumption and restoration in Italy (2016-2019)

Reference period	**Land consumption (ha)**	**Restoration (ha)**	**Net land consumption (ha)**
2016 - 2017	5,991	665	5,326
2017 - 2018	6,600	906	5,694
2018 - 2019	5,750	564	5,186
Total 2016 - 2019	**18,341**	**2,135**	**16,206**

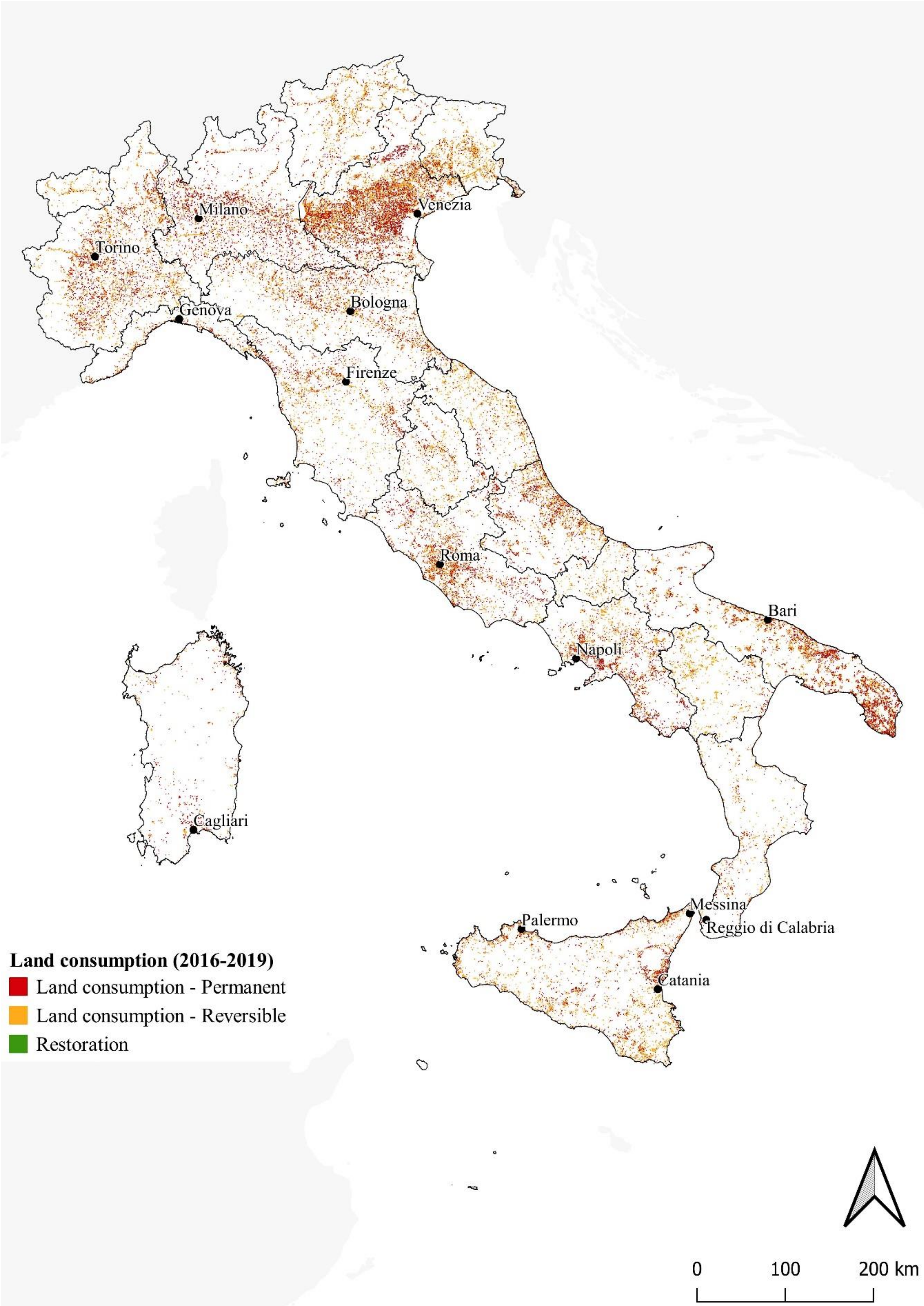

Figure 43. Land consumption in Italy (2016-2019)

Over 90% of the land consumption that took place between 2016 and 2019 in Italy was mapped to the third classification level (95.9% in the period 2016 - 2017, 90.9% in 2017 - 2018 and 94.5% in 2018 - 2019). The second classification level referred 2.0% of the changes for the period 2016 - 2017, 3.9% for 2017 - 2018 and 5.3% for 2018 - 2019 (Table 47).

Table 47. Percentage of total national changes mapped to the three classification levels, for each period analysed.

Classification level	**Reference period**		
	2016 - 2017	**2017 - 2018**	**2018 - 2019**
I	2.0	6.4	0.2
II	2.0	3.9	5.3
III	95.9	90.9	94.5

Analysing the changes mapped at the second and third classification level, reversible land consumption prevails (Table 48). This class affects 69.1% of the changes in the 2016 - 2017 and increases to 71.4% in 2017 - 2018 and 76.4% in 2018 - 2019.

Table 48. Distribution between reversible and permanent land consumption of the total changes mapped at the second and third classification level.

Classification level	**Reference period**		
	2016 - 2017	**2017 - 2018**	**2018 - 2019**
Permanent	**28.8**	**22.2**	**23.5**
II level	3.3	1.6	0.3
III level	96.7	98.4	99.7
Reversible	**69.1**	**71.4**	**76.4**
II level	1.5	3.3	6.9
III level	98.5	96.7	93.1

The analysis of the third classified level shows that the most dynamic class is 122 “construction sites and other clay areas” (Table 49) (Figure 45), both in terms of consumption and restoration. Almost 60% of the land consumption is within this class. The percentage increased from 57.8% in 2016 - 2017 to 58.0% in 2017 - 2018 and 59.6% in 2018 - 2019. The value in hectares is similar in 2016 - 2017 and 2018 - 2019 (3,461 ha and 3,427 ha respectively) and higher of about 400 ha in the period 2017 - 2018 (3,829 ha) (Table 49). The restorations (green area in Table 49) in 2017 involved 356 ha which in 2016 was classified as class 122. The value increases to 565 hectares in the period 2017-2018 and drops to 462 in 2018 - 2019.

Another dynamic reversible class is 123 (non-renaturalized quarries) (Figure 46), with a lot of territory affected by restorations (with a maximum of 203 ha in 2017 - 2018) and land consumption (between 427 ha in 2017 - 2018 and 330 ha in 2018 - 2019). About 6% of the land consumption in the observed periods fall into this class (Table 50).

Table 49. Changes in the three considered periods (ha). Values referring to changes lower than 0.5 ha do not appear in the matrix but contribute to the counts for the totals. Soil sealing is highlighted in gray, land consumption in red and restoration in green.

	2017																		
2016	1	11	111	112	113	114	115	116	117	118	12	121	122	123	124	125	126	2	
1		4	86	8			1	156			12	39	403	8	29	17		68	834
11			11	2				14			2		76			2		5	112
111		2		6				3					24					7	43
112		1	3					2				3	7					3	20
113																			
114																			
115																			
116		1	6			1							14					4	27
117																			
118													18						18
12		5	19	10				6				4	25	2	4			43	119
121			1	27				2		1			5					8	44
122	1	6	169	61		2		181		11	2	7		16	1		8	356	823
123													26		1			157	185
124													3	28				14	44
125											2		1		12				16
126			1					2					2					1	6
2	122	57	948	158	1	7	1	494	34	29	64	124	3461	353	46	74	19		5991
TOT	124	76	1244	272	1	10	3	861	35	42	81	177	4067	407	95	93	28	665	

	2018																		
2017	1	11	111	112	113	114	115	116	117	118	12	121	122	123	124	125	126	2	
1		1	10	1				24	1			1	71	8	3	11		77	207
11			3	1				3			6		4					3	20
111		2						5					31					5	43
112			6					10				1	16					7	40
113																			1
114																			
115																			
116			21						2				16					4	44
117																		14	14
118					18							1		1					20
12		1	2					6					6					7	22
121			1	22									2	2				7	35
122	3	14	421	102				266		12	16	10		11	4		2	565	1427
123													1		4			203	210
124														19				12	31
125																			
126											3		4					2	9
2	426	23	821	118	1	3	8	476	8	8	155	171	3829	427	41	65	23		6600
TOT	429	41	1285	244	20	3	8	791	11	20	181	184	3983	467	52	76	25	906	

	2019																		
2018	1	11	111	112	113	114	115	116	117	118	12	121	122	123	124	125	126	2	
1													2			2		3	6
11													1						2
111				1				2			2	1	17					2	24
112			1					5					3					2	10
113	8									18									26
114																			
115																			
116			7										13					2	24
117								2											2
118								5					1						6
12			1										2					4	8
121				22				1					2					7	34
122		2	341	146	1	7	3	310	3	7	40	4		1		19	1	462	1345
123								16					17		2			79	115
124													1					3	4
125																			
126			1	1									1					1	3
2	10	5	734	97		17	4	473	10	8	302	127	3427	330	22	176	9		5750
TOT	19	7	1085	267	1	24	7	814	13	33	345	131	3488	331	23	197	10	564	

Table 50. Distribution of land consumption at the national level among the classes at the third classification level for the three reference periods

	Land consumption (%)																
Classes	**1**	**11**	**111**	**112**	**113**	**114**	**115**	**116**	**117**	**118**	**12**	**121**	**122**	**123**	**124**	**125**	**126**
2016-2017	2.0	1.0	15.8	2.6	0.0	0.1	0.0	8.2	0.6	0.5	1.1	2.1	57.8	5.9	0.8	1.2	0.3
2017-2018	6.5	0.3	12.4	1.8	0.0	0.0	0.1	7. 2	0.1	0.1	2.3	2.6	58.0	6.5	0.6	1.0	0.3
2018-2019	0.2	0.1	12.8	1.7	0.0	0.3	0.1	8.2	0.2	0.1	5.3	2.2	59.6	5.7	0.4	3.1	0.2

The most dynamic permanent land consumption classes are 111 "buildings" (Figure 44) and 116 "other non-built waterproof/paved areas" (Figure 48). About 1/6 of the land consumption falls into 111 class, but the value decreases from 948 ha (15.8% of the total) in 2016 - 2017 to 734 ha in 2018 - 2019 (12.8% of the total) (red area in Table 49, Table 50).

There are also numerous new paved roads, especially in the Po Valley and along the Adriatic (Figure 47), while the new unpaved roads are concentrated in Veneto, Puglia and in the inland areas of the south (Figure 49). Soil sealing linked to the transformation of a class of reversible consumed land or of a natural area into permanent consumed land (gray area in Table 49) affects almost exclusively class 122. The conversion of reversible consumed land into permanent has almost doubled in terms of extension between the period 2016 - 2017 and the following, changing from 430 ha to 815 ha and then settling down. Soil sealing in natural areas mainly affects classes 111, 112 and 116.

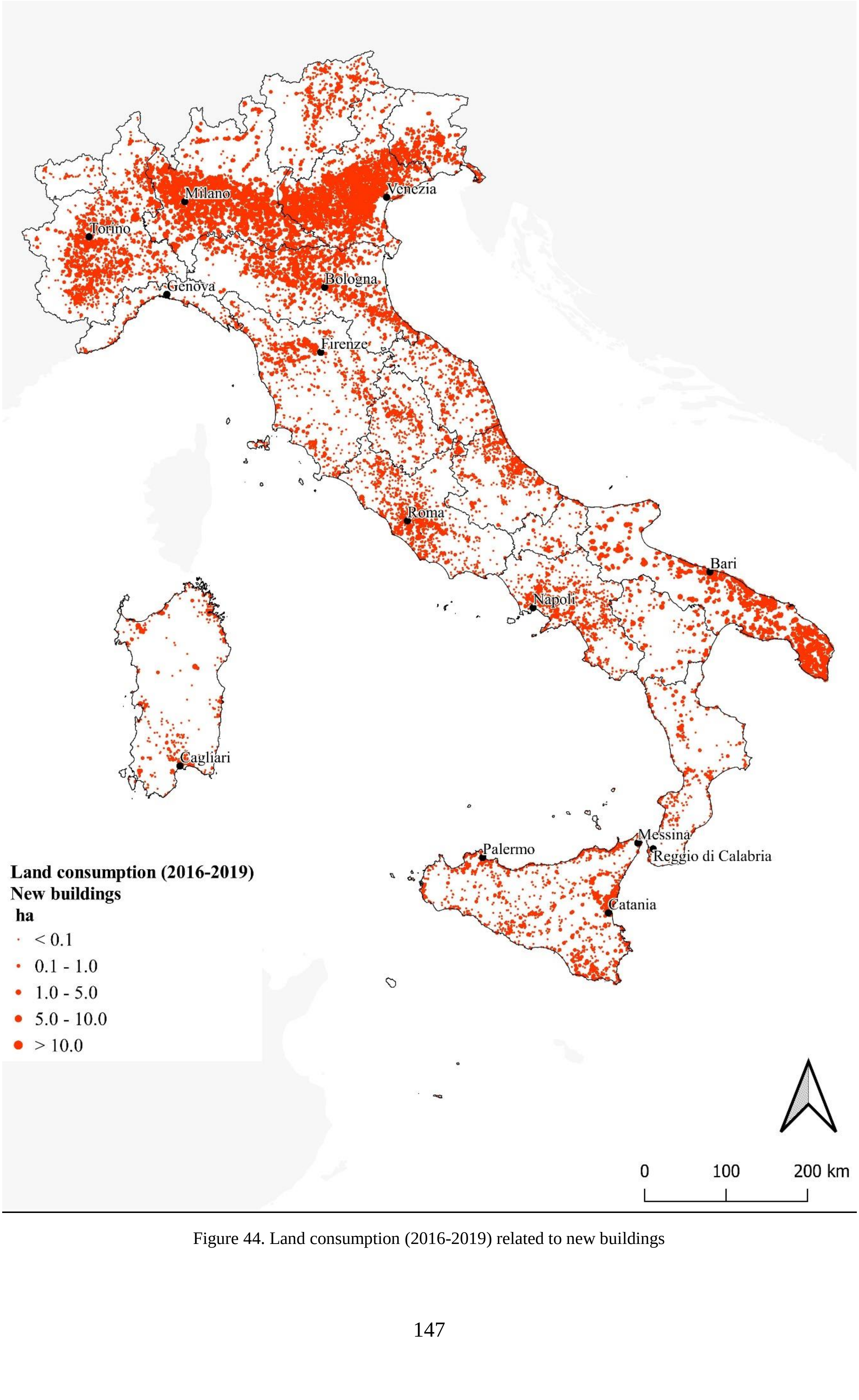

Figure 44. Land consumption (2016-2019) related to new buildings

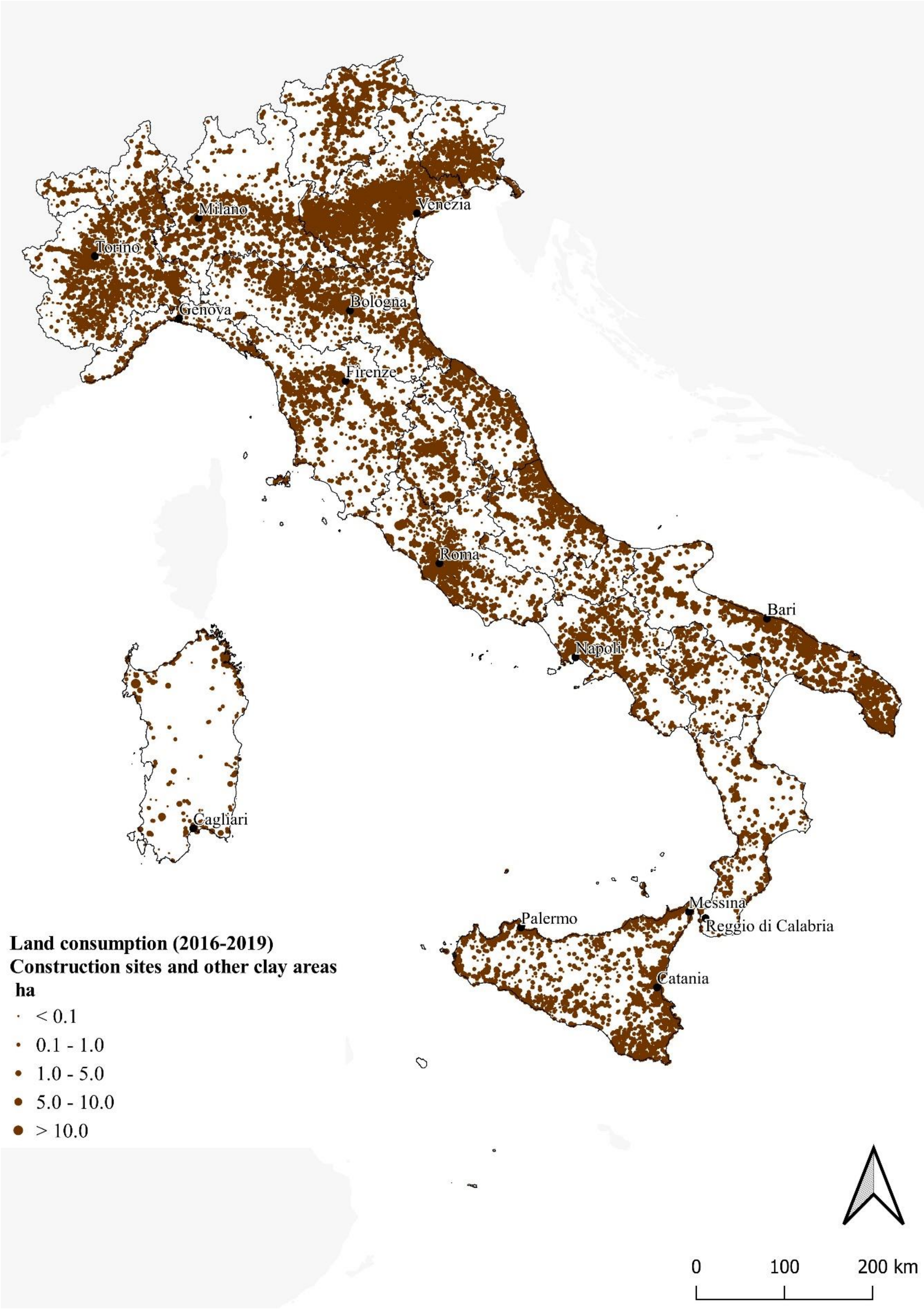

Figure 45. Land consumption (2016-2019) related to construction sites and other clay areas

Figure 46. Land consumption (2016-2019) related to non-renaturalized quarries

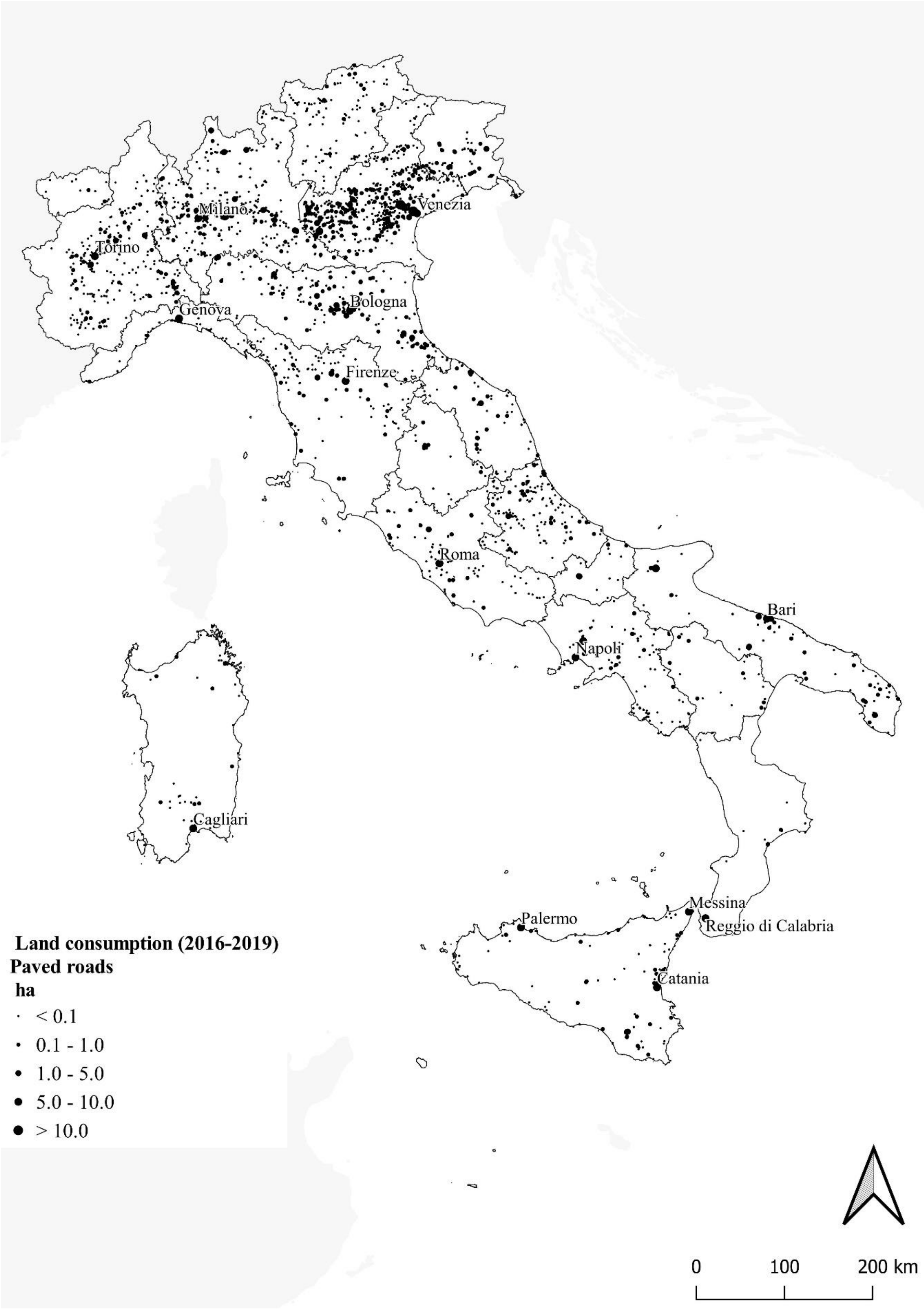

Figure 47. Land consumption (2016-2019) related to paved roads

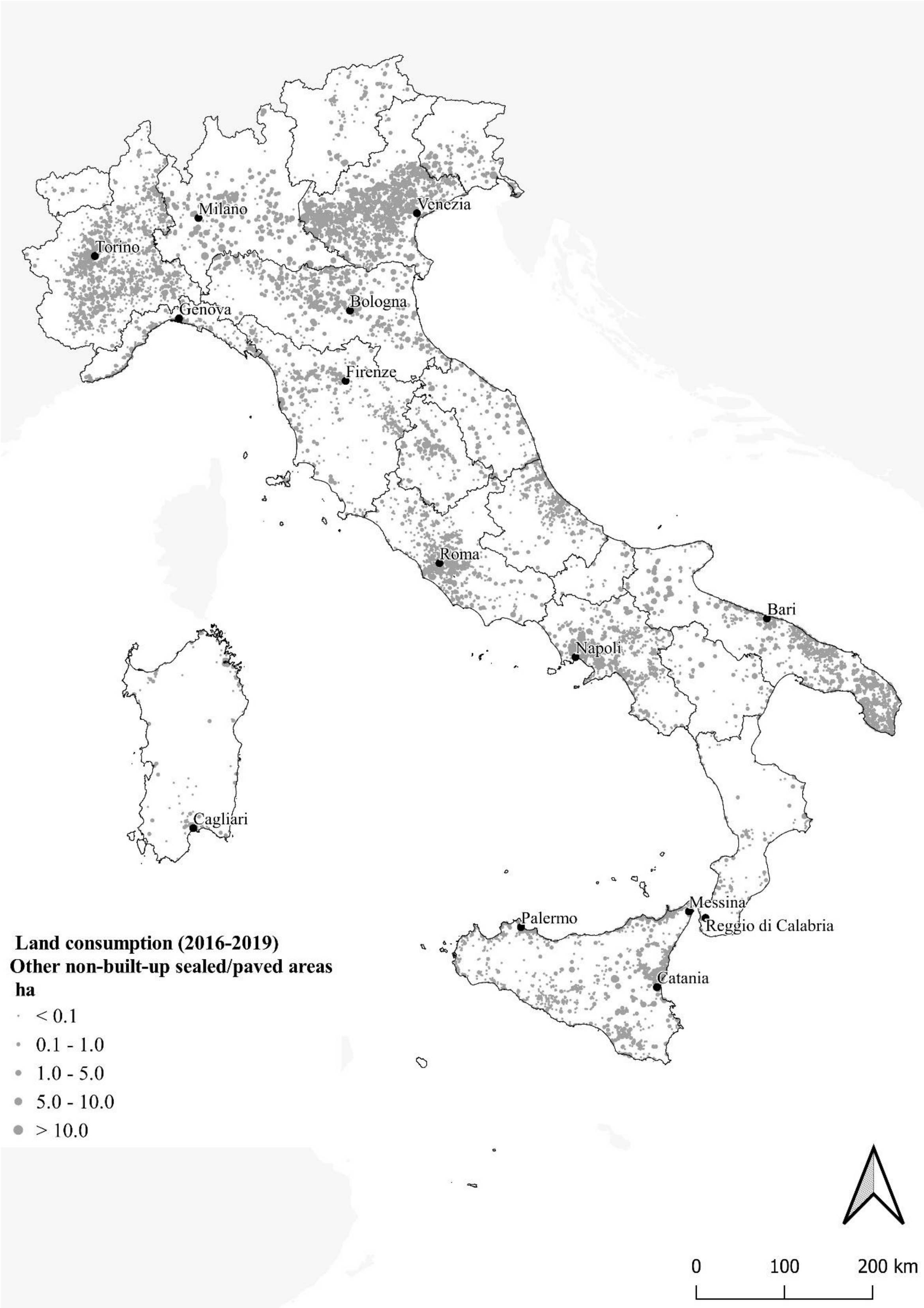

Figure 48. Land consumption (2016-2019) related to other sealed non-built-up/paved areas

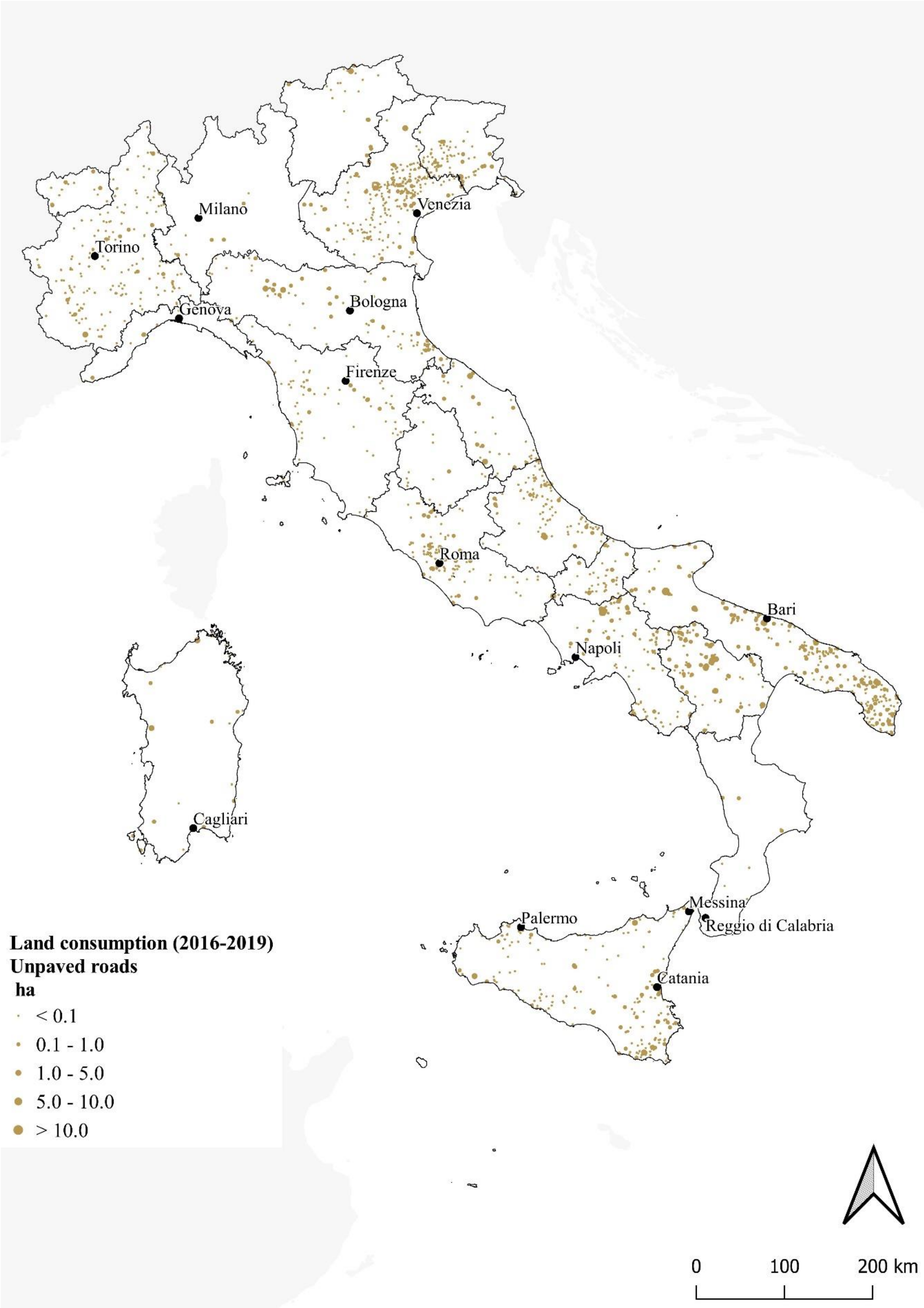

Figure 49. Land consumption (2016-2019) related to unpaved roads

Land consumption in EUAP protected areas

EUAP protected areas occupy 3,135,601 ha (10.4% of the national surface) (Table 51). Within the EUAP areas there is 2.7% of the total consumed land (58,391 ha). Compared to the total extension of the protected areas, consumed land affects 1.9% (Table 51), a value significantly lower than the national average of 7.1% (Munafò, 2020).

Table 51. Total surface and consumed land in EUAP areas compared with non-protected areas and the entire national territory.

	Surface		**Consumed land 2019**		
	ha	%	ha	%	% on class surfaces
EUAP	3,135,601	10.4	58,391	2.7	1.9
Not EUAP	27,004,373	89.6	2,081,395	97.3	7.7
Italy	**30,139,974**	**100.0**	**2,139,786**	**100.0**	**7. 1**

Land consumption in EUAP areas (Table 52) were mainly affected the period 2017 - 2018 and then halved in the following year. However, land consumption in EUAP areas remain lower than 2% of the total national value between 2016 and 2019.

Table 52. Land consumption, restoration and net land consumption in EUAP protected areas

Reference period	**Land consumption**		**Restoration**		**Net land consumption**	
	ha	% on total L.C.	ha	% on total restoration	ha	% on total net L.C.
2016 - 2017	105	1.8	5	0.7	101	1.9
2017 - 2018	145	2.2	7	0.8	138	2.4
2018 - 2019	73	1.3	12	2.1	62	1.2
Total 2016 - 2019	**324**	1.8	**24**	1.1	**300**	1.9

Changes at the third classification level in EUAP areas are concentrated in class 122, with a maximum of 62.9 ha in 2017 - 2018 (Table 53). Class 122 affects 47.0% of the total changes at the third classification level in EUAP areas for 2016 - 2017 (Table 54), the value drops slightly in the other periods and rises to 73.5% in 2018 - 2019.

Class 111 is the second most dynamic class in 2016 - 2017 and 2018 - 2019 (respectively 19 and 6 ha of land consumption, equal to 17.9% and 7.6% of the total changes in the period) and the third most dynamic class for the 2017 - 2018 (13 hectares, equal to 8.6% of the total changes), even though it shows a decreasing trend. Class 123 is highly dynamic, going from 8 ha of land consumption for 2016-2017 to 19 ha for 2017 - 2018, and then drastically falling to 1 ha for 2018 - 2019.

The restorations involved a few hectares in all the observed periods and mainly affect the 122 class.

Soil sealing is limited to a few hectares, especially in the period 2017 - 2018, which involves classes 111 and 116.

Table 53. Changes in EUAP areas in the three considered periods (ha). Soil sealing is highlighted in gray, land consumption in red and restoration in green.

		2017																		
		1	**11**	**111**	**112**	**113**	**114**	**115**	**116**	**117**	**118**	**12**	**121**	**122**	**123**	**124**	**125**	**126**	**2**	**TOT**
2016	**1**		0.94	8.37	0.56			0.07	12.3		0.11	0.6	10.1	15.4	4.54				0.04	52.94
	11			0.43	0.12				0.15					0.01					0.05	0.76
	111		0.1		0.06	0.01			0.11					0.23						0.51
	112											0	0.23	0.01					0.01	0.27
	113																			0
	114																			0
	115																			0
	116			0.02										0.23						0.25
	117								0.09											0.09
	118																			0
	12												0.49	1.07					0.18	1.74
	121				0.38				0.08					0.03					0.01	0.5
	122	0.08		0.77	0.21				1.91			0.2			0.06				0.9	4.13
	123													6.45					3.46	9.91
	124																			0
	125																			0
	126								0.23										0.08	0.31
	2	1.37	3.35	18.9	0.92				16	1.3		3	2.7	49.5	8.06		0.01	0.3		105.32
	TOT	1.45	4.39	28.5	2.25	0.01	0	0.07	30.9	1.3	0.11	3.7	13.5	72.9	12.7	0	0.01	0.3	4.73	0

		2018																		
		1	**11**	**111**	**112**	**113**	**114**	**115**	**116**	**117**	**118**	**12**	**121**	**122**	**123**	**124**	**125**	**126**	**2**	**TOT**
2017	**1**			0.08					0.03				0.06	0.19	1.07				0.93	2.36
	11													0.97						0.97
	111		0.01																	0.01
	112			0.02					0.13				0.42	0.8						1.37
	113			0.01																0.01
	114																			0
	115																			0
	116			0.43				0.14		0				0.76					0.03	1.39
	117																			0
	118												0.02							0.02
	12			0.08									0.02							0.1
	121				0.14									0.01					3.27	3.42
	122	0.16		4.69	7.77				5.32	0.1									2.52	20.54
	123			0.03										0.03					0.36	0.42
	124																			0
	125																			0
	126								0.11					0.21						0.32
	2	27.7	0.17	12.6	3.36	0.09			7.03	0.2	0.06	1.5	10.2	62.9	19	0.5		0.2		145.44
	TOT	27.86	0.18	18	11.3	0.09	0	0.14	12.6	0.3	0.06	1.5	10.7	65.9	20.1	0.5	0	0.2	7.11	0

		2019																		
		1	**11**	**111**	**112**	**113**	**114**	**115**	**116**	**117**	**118**	**12**	**121**	**122**	**123**	**124**	**125**	**126**	**2**	**TOT**
2018	**1**																			0
	11													0.16						0.16
	111				0.03	0.01		0.02	0.12					0.2				0		0.39
	112													0.27						0.27
	113																			0
	114																			0
	115																			0
	116			0.4																0.4
	117										0.01									0.01
	118																			0
	12																			0
	121				1.36				0.16											1.52
	122		0.03	2.49	0.53				2.97				0.04						11.44	17.5
	123																		0.24	0.24
	124																			0
	125																			0
	126			0.21					0.01											0.22
	2	0.03		5.57	1.05			1.25	5.42	0		2.4	1.69	53.8	1.02	0.2		0.7		73.23
	TOT	0.03	0.03	8.67	2.97	0.01	0	1.27	8.68	0	0.01	2.4	1.73	54.4	1.02	0.2	0	0.8	11.68	0

Table 54. Distribution of land consumption in EUAP areas among the classes at the third level for the three reference periods

	Land consumption (%)																
Classes	**1**	**11**	**111**	**112**	**113**	**114**	**115**	**116**	**117**	**118**	**12**	**121**	**122**	**123**	**124**	**125**	**126**
2016 - 2017	1.3	3.1	17.9	0.8	0.0	0.0	0.0	15.1	1.2	0.0	2.8	2.5	46.9	7.6	0.0	0.0	0.2
2017 - 2018	19.0	0.1	8.6	2.3	0.0	0.0	0.0	4.8	0.1	0.0	1.0	7.0	43.2	13.0	0.3	0.0	0.1
2018 - 2019	0.0	0.00	7.6	1.4	0.0	0.0	1.7	7.4	0.0	0.0	3.3	2.3	73.4	1.3	0.2	0.0	1.0

The analysis conducted on the 5 types of terrestrial EUAP areas show that the National Parks (PNZ) are those with the lowest percentage of consumed land surface compared to the total surface (Table 55) but also those with the highest land consumption in the period 2016 - 2019 (153 hectares), according with the trend underlined in other analisys of IUTI data (Sallustio *et al.*, 2013). Land consumption is also high in Regional Parks (PNR). The other classes are affected by an almost negligible land consumption between 2016 and 2019.

Table 55. Subdivision of EUAP areas: Land consumption, restoration and soil sealing for the period 2016-2019, total area, consumed land in hectares and as a percentage of the total area for the years 2016 and 2019. The values related to land consumption cannot be summed up due to the overlap between some protected areas. Acronyms: National Parks (PNZ), State Natural Reserves (RNS), Regional and Interregional Natural Parks (PNR), Regional Natural Reserves (RNR), Other Regional Protected Natural Areas (AAPR)

	Land consumption	**Restoration**	**Soil sealing**	**Total surface**	**Consumed land 2016**		**Consumed land 2019**	
	ha	**ha**	**ha**	**ha**	**ha**	**%**	**ha**	**%**
RNS	11	3	3	128,892	2,067	1.6	2,078	0.4
RNR	29	1	5	238,011	4,956	2.1	4,985	0.6
PNZ	153	7	61	1,606,092	24,586	1.5	24,738	0.6
AAPR	6	1	2	42,974	1,310	3.1	1,317	0.4
PNR	125	14	36	1,266,318	25,521	2.0	25646	0.4

Changes were distinguishing in permanent and reversible land consumption (Table 56).

Table 56. Changes in the 5 types of terrestrial EUAP protected areas (ha). Soil sealing is highlighted in gray, land consumption in red and restoration in green.

PNZ

	2019				
2016	1	11	12	2	**Tot**
1	-	14,15	20	0,04	**35**
11	0	-	1	0	**1**
12	0,16	12	-	7	**19**
2	25,29	49	78	-	**153**
Tot	**25,45**	**75**	**99**	**7**	

RNS

	2019				
2016	1	11	12	2	**Tot**
1	-	0	0	0	**0**
11	0	-	0	1	**1**
12	0	2	-	2	**4**
2	0	1	10	-	**11**
Tot	**0**	**3**	**10**	**3**	

AANP

	2019				
2016	1	11	12	2	**Tot**
1	-	3,75	0	0	**4**
11	0	-	1	1	**2**
12	0	1	-	0	**1**
2	0,4	1	5	-	**6**
Tot	**0,4**	**6**	**7**	**1**	

PNR

	2019				
2016	1	11	12	2	**Tot**
1	-	6,11	9	0,92	**16**
11	0	-	3	0	**3**
12	0,08	14	-	13	**27**
2	3,11	22	100	-	**125**
Tot	**3,19**	**42**	**112**	**14**	

RNR

	2019				
2016	1	11	12	2	**Tot**
1	-	0,31	2	0,01	**2**
11	0	-	1	0	**1**
12	0	1	-	1	**1**
2	0,3	5	24	-	**29**
Tot	**0,3**	**6**	**26**	**1**	

Reversible classes are the most dynamic in all types of EUAP areas, both in terms of land consumption and restoration. Changes in reversible land consumption classes are 5 to 7 times greater than the permanent ones. National parks (PNZ) are an exception, as reversible land consumption flows are only 1.5 times greater than permanent ones. PNZ and PNR are the most dynamic types also in terms of soil sealing.

Specifically, land consumption in National Parks is concentrated for a third (33.9%) in Sibillini Mountains Park and for 23.5% in Cilento and Vallo di Diano National Park (Table 57). However, the latter is also the one with more restorations (5.7 ha, equal to 82.5% of the total of the National Parks). Land consumption in the Monti Sibillini National Park is associated with reconstruction activities following the seismic events that hit the area around 2016 (Figure 50 c), while in the Gran Sasso National Park the changes are concentrated in Norcia (Figure 50 d). In Cilento and Vallo di Diano National Park and in Gargano National Park land consumption affects the coastal area (Figure 50 a and b). 15 out of 25 National Parks were affected by less than 5 ha of land consumption and in another 4 the phenomenon was absent in the considered period.

Table 57. Land consumption and restoration between 2016 and 2019 in Italian National Parks.

	Land consumption (2016-2019)		**Restoration (2016-2019)**	
	ha	%	ha	%
Asinara National Park	-	-	-	-
Golfo di Orosei e del Gennargentu National Park	-	-	-	-
Gran Paradiso National Park	1.4	0.9	0.1	1.7
Val Grande National Park	0.0	0.0	-	-
Stelvio National Park	2.5	1.6	0.0	0.4
Dolomiti Bellunesi National Park	0.1	0.1	-	-
Cinque Terre National Park	0.1	0.1	-	-
Appennino Tosco-Emiliano National Park	0.2	0.1	-	-
Foreste Casentinesi, Monte Falterona e Campigna National Park	0.3	0.2	-	-
Monti Sibillini National Park	51.8	33.9	0.1	1.2
Gran Sasso e Monti della Laga National Park	25.8	16.9	-	-
Maiella National Park	7.1	4.7	-	-
Abruzzo, Lazio e Molise National Park	1.4	0.9	0.0	0.3
Circeo National Park	0.1	0.0	0.2	2.9
Vesuvio National Park	1.6	1.0	-	-
Cilento e Vallo di Diano National Park	35.9	23.5	5.7	82.5
Gargano National Park	11.7	7.7	0.0	0.1
Alta Murgia National Park	1.9	1.2	-	-
Appennino Lucano. Val d'Agri Lagonegrese National Park	1.5	1.0	-	-
Pollino National Park	7.4	4.9	0.7	10.8
Sila National Park	-	-	-	-
Aspromonte National Park	0.2	0.1	-	-
Arcipelago di La Maddalena National Park	1.1	0.7	-	-
Arcipelago Toscano National Park	0.7	0.5	-	-
Isola di Pantelleria National Park	-	-	-	-
Total	**152.7**	**100.0**	**6.9**	**100.0**

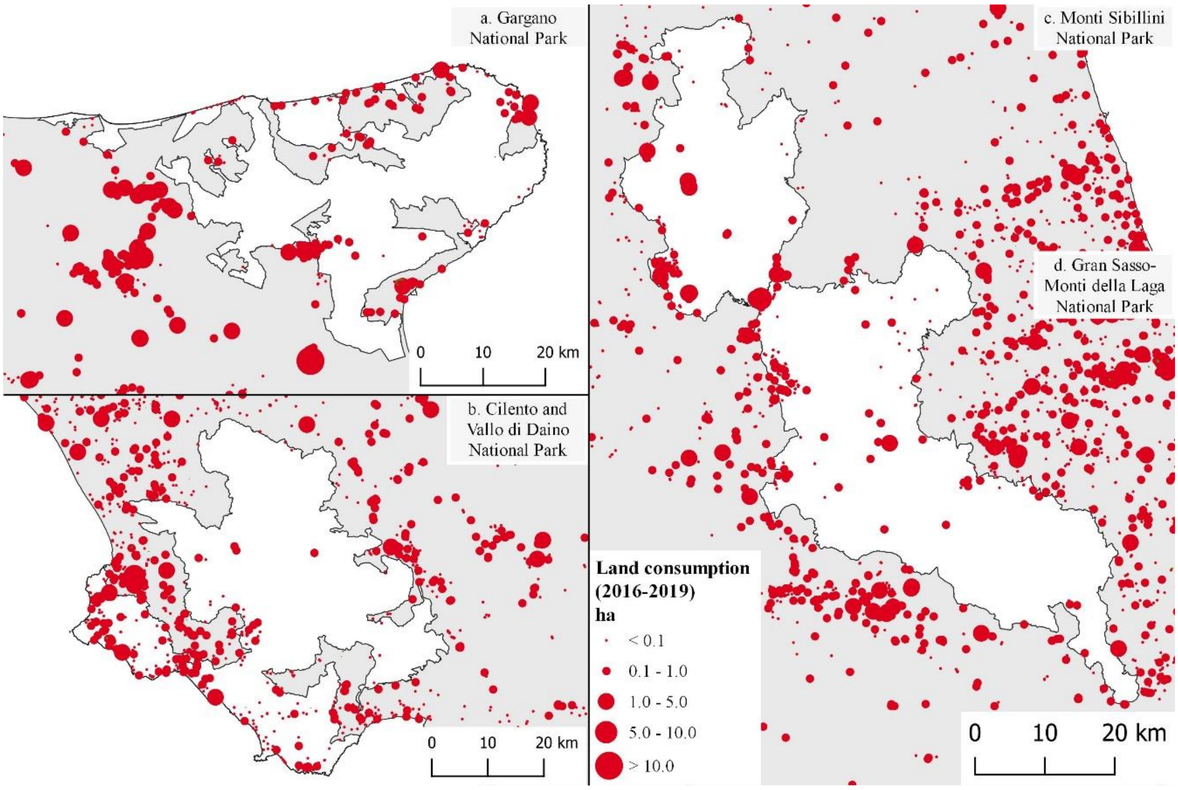

Figure 50. Land consumption (2016-2019) in the four national parks most affected by land consumption. Areas in white indicate the extent of the protected area.

Land consumption in relation to the elevation and slope

The composition of the Italian territory, with reference to elevation and slope, is characterized by a prevalence of low elevation and low slope areas (37.0% of the national surface) and high elevation and high slope areas (26.5% of the total) (Table 58).

Table 58. Extension of the slope and elevation classes, expressed in hectares and as a percentage of the national surface.

		Slope		
		< 10 %	> 10 %	**Tot. Italy**
Elevation	< 300 m	11,163,590 (37.0)	2,885,656 (9.6)	**14,049,246 (46.6)**
	300 - 600 m	2,618,640 (8.7)	4,057,868 (13.5)	**6,676,507 (22.2)**
	> 600 m	1,421,066 (4.7)	7,993,155 (26.5)	**9,414,221 (31.2)**
	Tot. Italy	**15,203,296 (50.4)**	**14,936,679 (49.6)**	**30,139,974 (100.0)**

The low-slope areas located at an elevation lower than 600 m a.s.l. occupy just over 46% of the national territory (Table 58) but they host more than 3/4 of the total consumed land in 2019 (68.4% and 10.8% respectively) (Table 59).

Table 59. Consumed land in the slope and elevation classes, expressed in hectares and as a percentage of the total national consumed land (2019).

		Slope < 10 %	Slope > 10 %	Tot. Italy
Elevation	< 300 m	1,462,676 (68.4)	123,270 (5.8)	**1,585,946 (74.1)**
	300 - 600 m	231,726 (10.8)	127,165 (5.9)	**358,891 (16.8)**
	> 300 m	81,798 (3.8)	113,151 (5.3)	**194,949 (9.1)**
	Tot. Italy	**1,776,200 (83.0)**	**363,586 (17.0)**	**2,139,786 (100.0)**

The percentage of consumed land in 2019, with reference to the total class area is more than triple in low slope areas compared to those with high slope. Among the low slope areas, the plain one (elevation < 300 m a.s.l.) is the most affected by the presence of consumed land with 13.1%. The value is more than 50% higher than the national average (Table 60).

Table 60. Percentage of consumed land in each class of slope and elevation, with respect to the total surface of the class (2019)

		Slope < 10 %	Slope > 10 %	Tot. Italy
Elevation	< 300 m	13.1	4.3	**11.3**
	300 - 600 m	8.8	3.1	**5.4**
	> 300 m	5.8	1.4	**2.1**
	Tot. Italy	**11.7**	**2.4**	**7.1**

Land consumption between 2016 and 2019 is concentrated in low elevation and low slope areas (75.5%). Areas with a slope lower than 10% occupy 50.4% (Table 58) of the national territory hosting just 88.6% of land consumption (Table 61).

Table 61. Land consumption in the slope and elevation classes, expressed in hectares and as a percentage of the total national land consumption (2016 – 2019)

		Slope < 10 %	Slope > 10 %	Tot. Italy
Elevation	< 300 m	13,853 (75.5)	843 (4.6)	**14,696 (80.1)**
	300 - 600 m	1,544 (8.4)	550 (3.0)	**2,094 (11.4)**
	> 300 m	852 (4.6)	700 (3.8)	**1,552 (8.5)**
	Tot. Italy	**16,248 (88.6)**	**2,093 (11.4)**	**18,342 (100.0)**

Restorations between 2016 and 2019 have a distribution similar to land consumption with reference to elevation and slope bands. 71.3% is in low-elevation and lowslope areas, which are confirmed as the most dynamic (Table 62).

Table 62. Restoration in the slope and elevation classes, expressed in hectares and as a percentage of the total national restoration (2016-2019).

		Slope		
		< 10 %	> 10 %	**Tot. Italy**
Elevation	< 300 m	1,523 (71.3)	135 (6.3)	**1,658 (77.6)**
	300 - 600 m	153 (7.2)	106 (5.0)	**259 (12.1)**
	> 300 m	106 (5.0)	113 (5.3)	**218 (10.2)**
	Tot. Italy	**1,782 (83.4)**	**353 (16.6)**	**2,135 (100.0)**

The analysis of changes at the third classification level was done for the portion of the national territory with low slope and low elevation since it is the most dynamic and the most affected by the phenomenon (Figure 51).

The changes at the third level in the low elevation and low slope areas reflect the national trend, with a clear prevalence of class 122 (Table 63, Table 64) which collects about 60% of land consumption in the reference period. Class 111 is the second most present, even if it shows a decreasing trend. Class 122 is also the most prevalent in terms of restoration, followed by class 123 which shows a sharp decrease in the period 2018 - 2019.

Soil sealing dynamics are aligned with the national trend and are mainly related to the sealing of natural areas and secondly to the conversion into permanent consumed land (especially buildings) of class 122 areas. The contribution linked to natural areas is more than double than 122 areas, while other classes are marginal.

With reference to the transformations of class 122, soil sealing affects a surface approximately 50% higher than the restoration in all three periods analysed.

Figure 51. Land consumption (2016-2019) in low slope and low elevation areas

Table 63. Changes in the three periods considered for different elevation ranges (ha). The values referring to changes lower than 0.5 ha do not appear in the matrix but contribute to the counts for the totals. Soil sealing is highlighted in gray, land consumption in red and restoration in green. The classes that have not undergone any changes are not shown in the table.

	2017																		
2016	**1**	**11**	**111**	**112**	**113**	**114**	**115**	**116**	**117**	**118**	**12**	**121**	**122**	**123**	**124**	**125**	**126**	**2**	**Tot**
1		3	57	3			1	125			6	19	201	6	16	16		66	**520**
11			7	1				11			1		67			1		2	**90**
111		1		1				3					18					6	**30**
112			2					1				1	6					3	**13**
116		1	4			1							11					4	**21**
118													17						**17**
12		2	5	6				3				2	14		4			24	**60**
121				22				2		1			4					4	**32**
122	1	4	136	51		2		153		11	2	4		15	1		8	279	**668**
123													8		1			96	**105**
124													3	28				7	**37**
125											1		1		12				**15**
126			1					1					2					1	**5**
2	69	37	779	128		7	1	398	31	27	28	80	2597	180	36	73	11		**4,483**
Tot	**70**	**49**	**991**	**213**	**0**	**10**	**2**	**697**	**31**	**39**	**39**	**106**	**2949**	**229**	**71**	**90**	**18**	**491**	

	2018																		
2017	**1**	**11**	**111**	**112**	**113**	**114**	**115**	**116**	**117**	**118**	**12**	**121**	**122**	**123**	**124**	**125**	**126**	**2**	**Tot**
1		1	3	1				21	1			1	53	5	3	10		57	**154**
11			3	1				3			6		3					3	**19**
111		1						4					27					3	**35**
112			1					9				1	3					5	**19**
116			13										13					4	**31**
117																		14	**14**
118					1							1		1					**2**
12		1	2					6					3					5	**16**
121			1	14									1	1				4	**22**
122	2	9	353	82				221		12	10	8		9	4		1	401	**1,112**
123															4			120	**124**
124														18				12	**30**
126											3		4					2	**8**
2	189	15	697	87	1	3	8	396	7	6	110	66	2949	226	37	64	8		**4,868**
Tot	**190**	**27**	**1072**	**185**	**2**	**3**	**8**	**661**	**8**	**18**	**128**	**77**	**3055**	**259**	**47**	**74**	**8**	**631**	**6,453**

	2019																		
2018	**1**	**11**	**111**	**112**	**113**	**114**	**115**	**116**	**117**	**118**	**12**	**121**	**122**	**123**	**124**	**125**	**126**	**2**	**Tot**
1													2			1,5			**3**
11													1						**1**
111				1				1			1		14					2	**20**
112								5					2					1	**8**
113	3									1									**4**
116			5										12					2	**19**
118													1						**1**
12			1										2					1	**4**
121				16				1					1					6	**24**
122		2	292	122	1	7	3	246	3	5	31	2		1		18		340	**1,071**
123													9		2			45	**56**
124																		3	**3**
2	2	3	639	86		17	4	393	10	7	261	71	2,598	213	17	173	7		**4,502**
Tot	**5**	**5**	**937**	**225**	**1**	**24**	**7**	**647**	**12**	**14**	**294**	**73**	**2,641**	**214**	**19**	**193**	**7**	**399**	**5,715**

Table 64. Distribution of land consumption in low slope and low elevation areas among the classes at the third level for the three reference periods

	Land consumption (%)																
Classes	**1**	**11**	**111**	**112**	**113**	**114**	**115**	**116**	**117**	**118**	**12**	**121**	**122**	**123**	**124**	**125**	**126**
2016 - 2017	1.5	0.8	17.3	2.8	0.0	0.1	0.0	8.9	0.7	0.6	0.6	1.8	57.9	4.0	0.8	1.6	0.2
2017 - 2018	3.8	0.3	14.3	1.7	0.0	0.0	0.1	8.1	0.2	0.1	2.2	1.4	60.6	4.6	0.8	1.3	0.2
2018 - 2019	0.0	0.0	14.2	1.9	0.0	0.3	0.1	8.7	0.2	0.2	5.8	1.6	57.7	4.7	0.4	3.8	0.2

4.2.1.2 Land consumption in Italian coastal area

The percentage of consumed land near the coast (Table 65) is above the national average (7.6%, (Munafò, 2020)) in all the examined buffer zones. The highest value occurs between 100 and 300 m from the coastline, with 29.4% of consumed land while it stays above 20% in the 500 m buffer zone.

As for land consumption, about 23% of what occurred between 2012 and 2018 in Italy falls within the buffer zone of 10 km, which occupies just over 16% of the national surface. Considering the density of changes (ratio between the land consumption and the surface of each distance band), it is interesting to highlight that it is more intense between 300 and 500 m, in the first unrestricted portion of land by law, with a value of 21.9 m^2 of land consumption for each hectar of territory in that band.

Table 65. Consumed Land (2018) in hectares and as percentage of the band surface, land consumption (2012-2018) in hectares, percentage of change (cha %) and annual land consumption for the observation period

Bands				Consumed land (2018)		Land consumption (2012-2018)		
Range		Area						
m		ha	%	ha	%	ha	m^2 cha/ ha band	%
0	100	82,612	0.3	20,534	24.8	112	13.6	0.3
100	300	137,183	0.5	40,407	29.4	279	20.3	0.8
300	500	125,494	0.4	31,868	25.3	275	21.9	0.8
500	1,000	287,114	1.0	56,376	19.6	593	20.7	1.8
1,000	10,000	4,165,111	14.0	378,211	9.0	6,169	14.8	19.0
> 10000		24,962,381	83.9	1,607,203	6.4	24,884	10.0	77.0
Italy		29,759,895	100.0	2,134,599	7.2	32,312	10.9	100.0

The analysis of the land consumption with reference to the types of coast takes into consideration a band within 300 m from the coastline and shows that the consumed land affects 29.2% of the areas with low coast (which represents 55.41% of the Italian coastline). These areas are also the most dynamic, with 250 ha of land consumption between 2012 and 2018 (Table 66).

The “other” class includes port areas and heavily built-up areas which occupy 21% of the coastline and which are consumed for 45.1% of their extension.

Table 66. Distribution of land consumption in coastal typologies, consumed land (2018) in hectares, percentage on the band surface, and land consumption (2012-2018) in hectares

Typology	% of the coastline	Consumed land within 300 m (2018)		Land consumption within 300 m (2012-2018)
		ha	%	ha
high	23.5	2,081,158	8.6	27.3
low	55.4	3,565,524	29.2	250.4
other	21.0	447,520	45.1	113.5

The analysis of consumed land on a regional scale (Table 67) shows a trend similar to the national one in 13 of the 15 regions, with a peak between 100 and 300 m. The maximum value occurs in the Marche (50.2%). In the first 100 m, consumed land affects more than 20% of the buffer zone surface in 12 of the 15 regions, with a maximum of 50.0% in Liguria. The total consumed land in the first 1,000 m from the coastline is higher than the national average in fourteen regions (except for Basilicata). Sicilia is the region with the largest amount of consumed land in all areas (179,482 ha), followed by Puglia (117,157 ha) and Calabria (81,041 ha).

Table 67. Consumed land (2018) in the coastal area of the 15 Italian non-landlocked regions, expressed in hectares and percentage of the buffer zone surface

Consumed land (ha) / Percentage on buffer zone surface (%)	Distance Bands (m)					
	0-100	100-300	300-500	500-1,000	1,000-10,000	0-10,000
Abruzzo	378	1,578	2,649	4,516	17,309	26,430
	(25.2)	(43.5)	(39.7)	(28.7)	(11.0)	(13.39)
Basilicata	33	124	184	332	2,336	3,009
	(5.0)	(7.5)	(5.1)	(5.3)	(3.8)	(4.03)
Calabria	1,869	6,647	10,452	16,384	45,688	81,041
	(24.2)	(33.1)	(27.1)	(17.2)	(5.1)	(7.02)
Campania	1,623	4,680	7,300	12,411	51,667	77,681
	(34.6)	(37.2)	(34.2)	(28.7)	(16.3)	(18.48)
Emilia-Romagna	449	1,844	3,021	5,037	19,579	29,930
	(28.9)	(50.1)	(44.1)	(32.9)	(14.2)	(16.95)
Friuli-Venezia G.	704	1,735	2,475	3,758	12,349	21,022
	(29.2)	(29.1)	(25.5)	(21.8)	(12.9)	(15.22)
Lazio	1,121	3,301	4,867	7,667	33,030	49,985
	(30.2)	(33.8)	(27.5)	(20.6)	(10.7)	(12.43)
Liguria	2,107	5,389	7,804	11,873	30,874	58,048
	(50.0)	(48.2)	(38.3)	(27.5)	(8.3)	(11.85)
Marche	795	2,597	3,988	6,229	23,358	36,967
	(39.8)	(50.2)	(39.9)	(26.2)	(12.0)	(14.58)
Molise	68	247	409	676	2,386	3,787
	(15.9)	(23.0)	(21.5)	(14.7)	(5.3)	(6.63)
Puglia	2,683	7,613	11,553	18,694	76,614	117,157
	(29.1)	(31.4)	(27.0)	(20.9)	(10.2)	(11.98)
Sardegna	1,752	5,006	7,486	11,823	42,146	68,214
	(9.9)	(11.7)	(10.2)	(8.2)	(4.5)	(5.27)
Sicilia	3,998	12,598	19,634	33,161	110,090	179,482
	(25.9)	(31.7)	(27.8)	(23.7)	(10.4)	(12.74)
Toscana	1,265	3,620	5,380	8,601	29,918	48,783
	(20.0)	(22.4)	(18.7)	(15.3)	(8.8)	(10.38)
Veneto	1,609	3,876	5,524	7,938	29,966	48,913
	(37.0)	(40.9)	(37.3)	(25.8)	(15.3)	(17.88)

Land consumption increases with distance (Table 68) in 14 of the 15 regions, in accordance with the national trend. Friuli-Venezia Giulia is an exception; here the peak of land consumption occurred between 100 and 300 m (1.5%), due to some major changes, involving almost 15 ha in the municipalities of Grado and Monfalcone, as already mentioned by ISPRA (Munafò, 2019). In Sicilia (1687.6 ha) and Puglia (1292.2 ha) there are the greatest number of changes. Basilicata is the region with fewer changes but with the greatest percentage increase, especially in the first 100 m and between 500 and 1,000 m.

Table 68. Land consumption (2012-2018) in the coastal area of the 15 Italian non-landlocked regions, expressed in hectares and percentage increase compared to the consumed land 2012

Land Consumption (Ha) / Percentage of Change in Consumed Land (%)	**Distance Bands (m)**				
	0-100	**100-300**	**300-500**	**500-1,000**	**1,000-10,000**
Abruzzo	2.1 (+0.6%)	3.6 (+0.3%)	3.8 (+0.4%)	8.1 (+0.4%)	215.9 (+1.7%)
Basilicata	1.3 (+4.2%)	2.0 (+2.3%)	1.3 (+2.3%)	7.2 (+5.1%)	24.1 (+1.2%)
Calabria	12.1 (+0.6%)	48.0 (+1.0%)	51.8 (+1.4%)	107.8 (+1.8%)	517.5 (+1.8%)
Campania	3.0 (+0.2%)	11.6 (+0.4%)	6.0 (+0.2%)	19.9 (+0.4%)	466.8 (+1.2%)
Emilia-Romagna	0.2 (+0.1%)	3.8 (+0.3%)	6.1 (+0.5%)	8.2 (+0.4%)	151.7 (+1.1%)
Friuli-Venezia G.	9.4 (+1.4%)	14.9 (+1.5%)	9.0 (+1.2%)	10.8 (+0.8%)	236.6 (+2.8%)
Lazio	4.4 (+0.4%)	7.2 (+0.3%)	9.6 (+0.6%)	29. (+1.1%)	494.3 (+2.0%)
Liguria	3.8 (+0.2%)	11.1 (+0.3%)	18.1 (+0.7%)	34.6 (+0.8%)	144.7 (+0.8%)
Marche	1.2 (+0.2%)	7.3 (+0.4%)	7.4 (+0.5%)	19.2 (+0.9%)	359.0 (+2.1%)
Molise	0.7 (+1.1%)	0.8 (+0.5%)	0.7 (+0.4%)	1.6 (+0.6%)	33.4 (+2.0%)
Puglia	20.2 (+0.7%)	46.4 (+0.9%)	53.9 (+1.4%)	86.9 (+1.2%)	1084.6 (+2.0%)
Sardegna	8.1 (+0.5%)	15.9 (+0.5%)	13.4 (+0.5%)	45.9 (+1.2%)	524.1 (+1.7%)
Sicilia	35.9 (+1.0%)	86.6 (+1.0%)	62.0 (+0.9%)	131.4 (+1.0%)	1371.3 (+1.8%)
Toscana	2.6 (+0.2%)	4.7 (+0.2%)	3.8 (+0.2%)	21.7 (+0.7%)	181.8 (+0.9%)
Veneto	5.8 (+0.4%)	14.5 (+0.6%)	27.2 (+1.7%)	59.9 (+2.5%)	362.4 (+1.7%)

In the study area, there was a population growth of +503,837 inhabitants (+3.08%), in line with the Italian trend (+1.83%). Considering the 6,416 ha of land consumption between 2012 and 2018, it can be calculated for comparative purposes a value of 127 m^2 for each new inhabitant which is surprisingly lower compared to the same value calculated for the rest of the municipalities of Italy (442 m^2 for each new inhabitant) where 25,896 ha were consumed for 585,929 new inhabitants.

4.2.2 The fragmentation of the territory

The analysis focused on the distribution of the five classes of fragmentation and their evolution, with reference to the national and regional level and with respect to the presence of protected areas, elevation, slope and distance from the coastline. The results obtained from the application of the methodology were used in the ISPRA report "Land Consumption, territorial dynamics and ecosystem services" (Munafò, 2018, 2019, 2020), in the ISPRA "Environmental Data Yearbook" (ISPRA, 2018a, 2019a) and they were also presented in two poster communications at the "World Forum on Urban Forests" in Mantua (Italy) and at the ISTAT 13th national Statistics Conference.

Fragmentation in Italy

One third of the national territory falls in areas with high or very high fragmentation in 2019 (Table 69), with a significant increase in the surfaces of both classes compared to 2012 (+6.9% and +15.4% respectively). The medium fragmentation class has undergone a limited reduction, while the extent of the low and very low fragmentation classes has significantly reduced. Very low fragmentation areas have undergone a reduction (-6.5%) lower than those of low fragmentation areas (-10.4%) since the morphological characteristics (Alps) of these areas limit the development of fragmenting elements (settlements, infrastructures, etc.).

Table 69. Fragmentation (S_{eff}) in Italy, in terms of hectares and percentage of the territory occupied by each class, with reference to the years 2012, 2019 and the variation 2012 - 2019.

	S_{eff} (2012)		**S_{eff} (2019)**		**S_{eff} (2012 - 2019)**	
Class	**ha**	**%**	**ha**	**%**	**ha**	**%**
1	3,621,154	12.0	3,384,799	11.2	-236,355	-6.5
2	6,200,196	20.6	5,553,856	18.4	-646,340	-10.4
3	10,348,497	34.3	10,315,645	34.2	-32,853	-0.3
4	7,276,406	24.1	7,776,113	25.8	499,707	6.9
5	2,693,720	8.9	3,109,561	10.3	415,841	15.4
Tot.	30,139,973	100.0	30,139,973	100.0	0	0.0

Fragmentation in the Italian regions

At the regional level, in Trentino-Alto Adige and, above all, in Valle d'Aosta the low and very low fragmentation classes prevail (Figure 52). In the northern regions, the contextual presence of the Po Valley and the Alps leads to a greater concentration of territory in the extreme classes (high and low fragmentation), while in the south and on the islands medium fragmentation areas prevail (Figure 53).

Regarding the variations on a regional scale between 2012 and 2019 (Table 70), the high and very high fragmentation classes are increasing in all regions, especially in the south and in the islands, while low and very low fragmentation classes are decreasing. In Piemonte, Valle d'Aosta, Friuli-Venezia Giulia and Lombardia the low fragmentation class has increased considerably, due to the sharp decrease in very low fragmentation areas (Table 70) (Figure 54).

Table 70. Change in fragmentation (S_{eff}) in the regions between 2012 and 2019, in hectares and as a percentage change compared to 2012.

	Very low		Low		Medium		High		Very High	
	ha	%	ha	%	ha	%	ha	%	ha	%
Piemonte	-137,286	-14.0	100,165	122.3	-54,982	-11.3	50,413	6.4	41,690	20.2
Valle d'Aosta	-2,244	-0.9	1,644	2.9	300	13.0	200	6.5	100	3.8
Lombardia	-47,565	-6.0	31,314	37.2	-49,610	-11.4	18,016	2.8	47,844	10.9
Trentino-Alto Adige	92,513	12.3	-100,790	-22.9	4,277	4.0	2,400	5.4	1,600	9.0
Veneto	-6,706	-3.0	-13,847	-4.2	-12,449	-4.4	-4,694	-0.8	37,696	8.5
Friuli-Venezia Giulia	-113,592	-38.5	99,146	143.5	5,375	5.2	-582	-0.3	9,653	7.6
Liguria	-10,102	-26.1	-3,642	-5.7	-4,166	-1.5	9,518	8.5	8,393	19.1
Emilia-Romagna	0	-	-45,660	-14.4	-17,051	-1.7	34,516	5.0	28,195	13.1
Toscana	0	-	-62,556	-10.6	21,529	2.0	18,218	3.7	22,809	17.5
Umbria	0	-	-33,576	-13.5	11,072	3.0	15,665	8.3	6,840	19.5
Marche	0	-	-9,625	-7.1	-29,432	-7.5	19,287	5.9	19,770	23.8
Lazio	0	-	-59,323	-12.1	-11,659	-1.9	46,557	10.5	24,425	13.5
Abruzzo	0	-	-50,444	-12.0	10,674	3.4	20,376	7.7	19,394	23.4
Molise	0	-	-11,790	-21.7	1,752	0.8	7,039	4.9	2,998	21.7
Campania	0	-	-33,207	-12.1	-8,919	-1.8	8,971	2.3	33,155	17.7
Puglia	0	-	-31,787	-18.6	-57,283	-6.6	58,709	8.2	30,361	16.3
Basilicata	0	-	-49,787	-17.8	29,966	5.4	15,485	10.0	4,336	34.4
Calabria	100	0.1	-46,632	-12.2	14,780	2.2	18,586	5.8	13,165	22.9
Sicilia	-10,973	-7.4	-243,713	-36.5	80,759	7.7	121,724	23.5	52,203	28.7
Sardegna	-500	-0.8	-82,230	-7.9	32,214	3.3	39,304	14.0	11,212	23.5

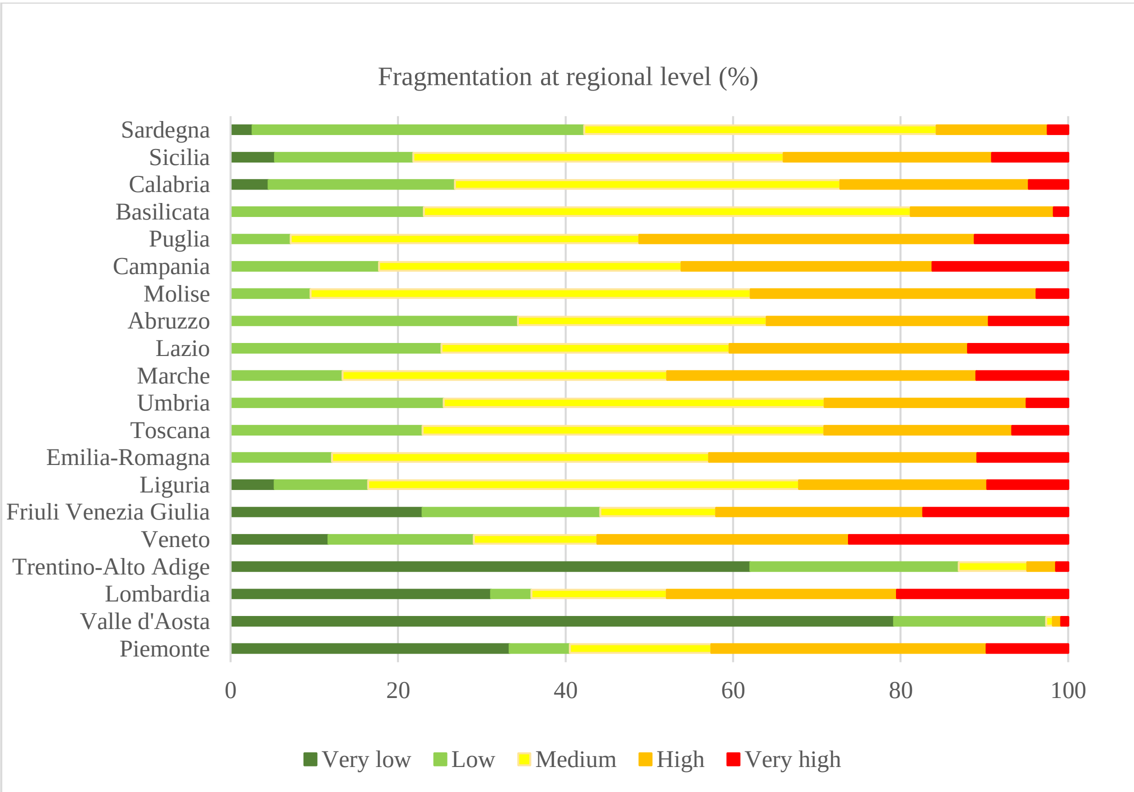

Figure 52. Fragmentation at the regional level, in terms of percentage of the territory occupied by each class of fragmentation

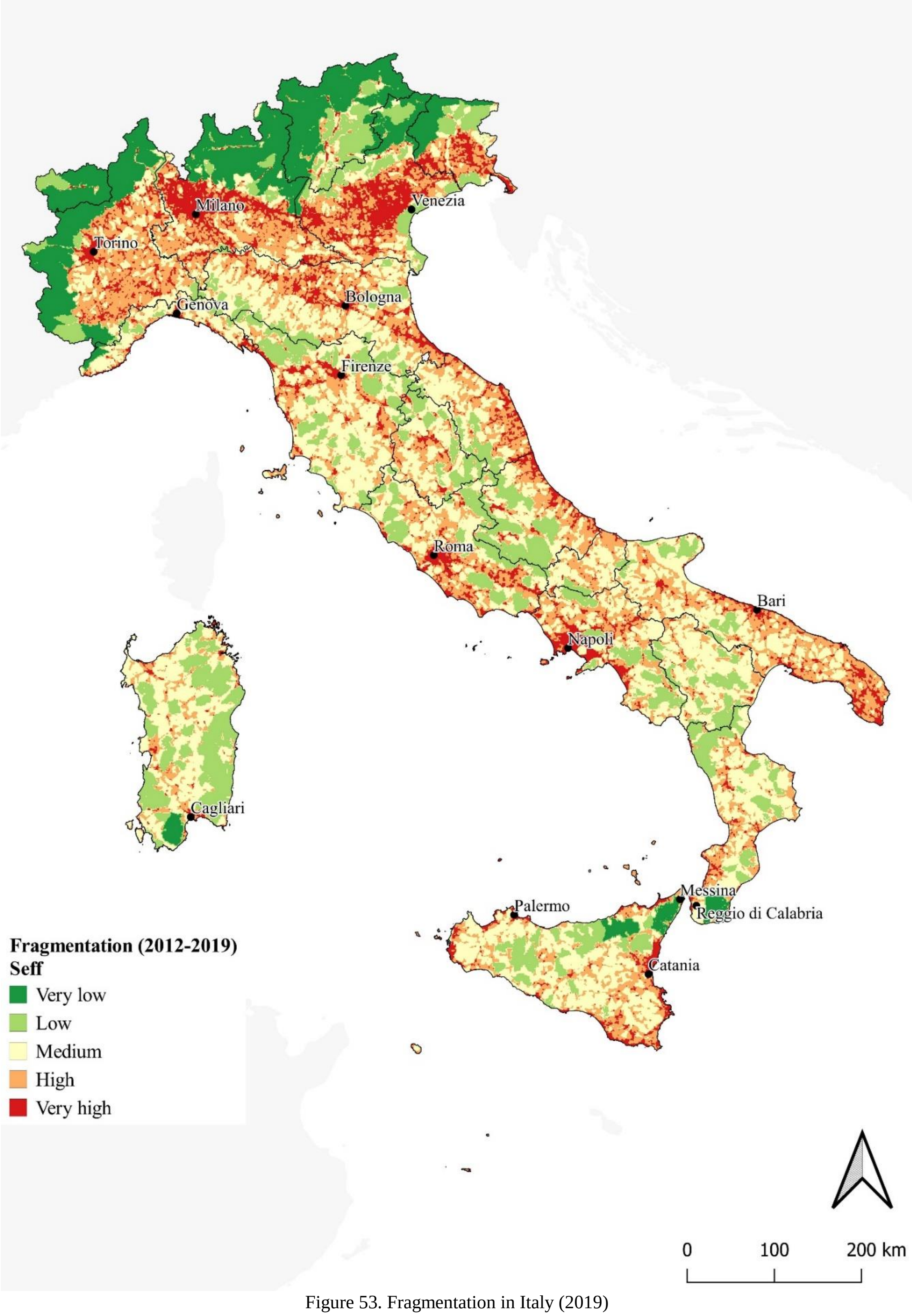

Figure 53. Fragmentation in Italy (2019)

Figure 54. Increase in fragmentation between 2012 and 2019, with reference to the increase in number of classes of fragmentation occurred each the pixel

Fragmentation in EUAP protected areas

Fragmentation within the EUAP protected areas is considerably lower than the national average (Figure 55). The classes with low and very low fragmentation occupy a percentage of the territory of the EUAP areas double compared to the national level, while high and very high fragmentation classes are just limited to over 10% of the territory, against an average value of 35% for the Italian territory.

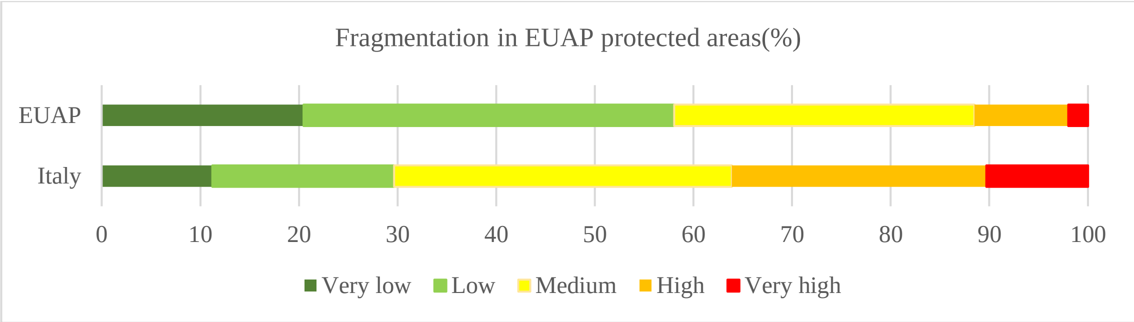

Figure 55. Fragmentation in EUAP protected areas, in terms of percentage of the territory occupied by each class of fragmentation

Changes in EUAP areas are considerably lower than the national value (Table 71), with a limited reduction in low and very low fragmentation areas and an equally limited increase in high and very high fragmentation areas

Table 71. Change in fragmentation (S_{eff}) in EUAP protected areas between 2012 and 2019, in hectares and as a percentage change compared to 2012.

	Very low		**Low**		**Medium**		**High**		**Very High**	
	ha	**%**	**ha**	**%**	**ha**	**%**	**ha**	**%**	**ha**	**%**
EUAP	-41,742	-1.3	-34,522	-1.1	39,942	1.3	28,169	0.9	8,152	0.3
Italy	-236,355	-6.5	-646,340	-10.4	-32,853	-0.3	499,707	6.9	415,841	15.4

Fragmentation with respect to elevation and slope

Fragmentation decreases when elevation and slope increase (Figure 56). In the low elevation and sloping areas, over 60% of the territory has high and very high fragmentation values, while the low and very low fragmentation areas are limited to a small percentage of the territory. The distribution of classes is opposite in the high elevation and sloping areas, less affected by anthropogenic activity. Here, the areas with low and very low fragmentation occupy 70% of the territory, while those with high and very high fragmentation do not reach 10%.

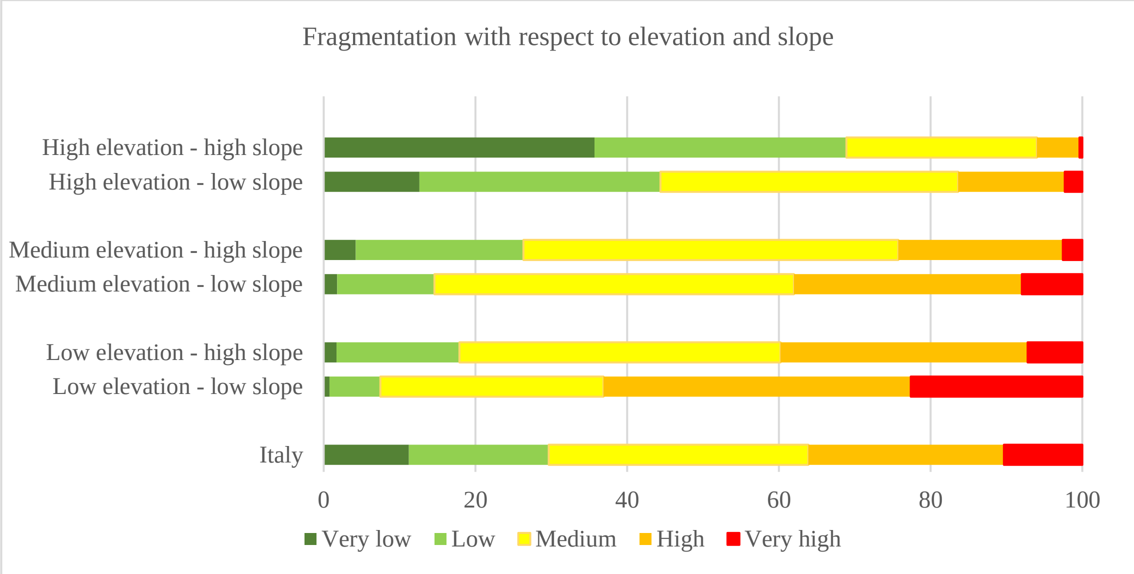

Figure 56. Fragmentation with respect to elevation and slope, in terms of percentage of the territory occupied by each class of fragmentation

More than half of the areas with very high fragmentation are concentrated in areas with a low slope and elevation (Figure 57). The value rises to almost 75% if we also consider the areas with low elevation and high slope. The very low fragmentation class is concentrated for more than 60% in mountain areas with high elevation and slope.

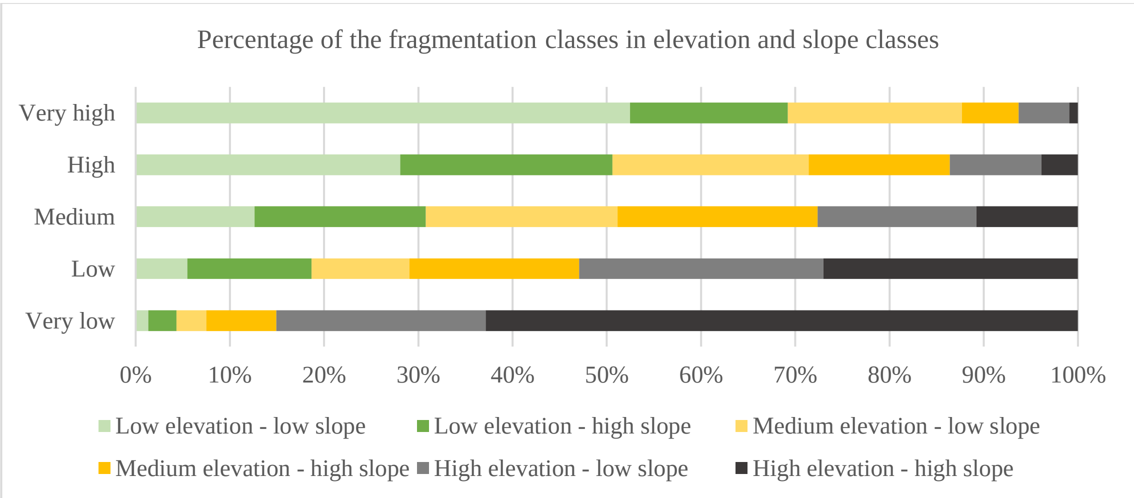

Figure 57. – Distribution of fragmentation classes in elevation and slope classes

Analysing the variations between 2012 and 2019, the areas with low and very low fragmentation decreased and those with high and very high fragmentation increased in all classes of slope and elevation (Table 72). In detail, high elevation and sloping areas have the highest decrease in the very low fragmentation class (decreased by 147,174 ha against a national decrease of about 236,355 ha) and with the highest increase in the medium fragmentation class (increased by 168,928 ha). The low elevation and slope areas have the greatest increase in the classes with high and very high fragmentation and the greatest decrease in those with medium and low fragmentation. Hills, with medium and low slopes are those less affected by variations.

Table 72. Change in fragmentation (S_{eff}) with respect to elevation and slope between 2012 and 2019, in hectares and as a percentage change compared to 2012.

	Very low		**Low**		**Medium**		**High**		**Very High**	
	ha	**%**	**ha**	**%**	**ha**	**%**	**ha**	**%**	**ha**	**%**
Low elevation Low slope	-14,004	-14.1	-154,911	-17.1	-269,897	-7.6	136,566	3.1	302,244	13.6
Low elevation High slope	-7,861	-13.8	-87,854	-15.8	515	0.0	57,240	6.5	37,960	22.3
Med elevation Low slope	-19,875	-29.8	-105,295	-23.9	2,232	0.2	87,942	12.6	34,995	20.2
Med elevation High slope	-38,336	-18.3	-140,233	-13.5	43,121	2.2	111,718	14.6	23,730	29.3
High elevation Low slope	-9,103	-4.8	-47,735	-9.6	22,246	4.2	26,552	15.3	8,039	32.2
High elevation High slope	-147,174	-4.9	-110,311	-4.0	168,928	9.2	79,686	21.7	8,870	38.9
Italy	**-236,355**	**-6.5**	**-646,340**	**-10.4**	**-32,853**	**-0.3**	**499,707**	**6.9**	**415,841**	**15.4**

Fragmentation in coastal area

The coastal area is highly fragmented (Figure 58). In the first 300 m from the coastline over 40% of the territory is in the very high fragmentation class. The value exceeds 70% considering both high and very high fragmentation classes. In the first 1,000 m from the coastline, the areas with very low fragmentation are almost absent, while those with low fragmentation slightly exceed 10% of the territory.

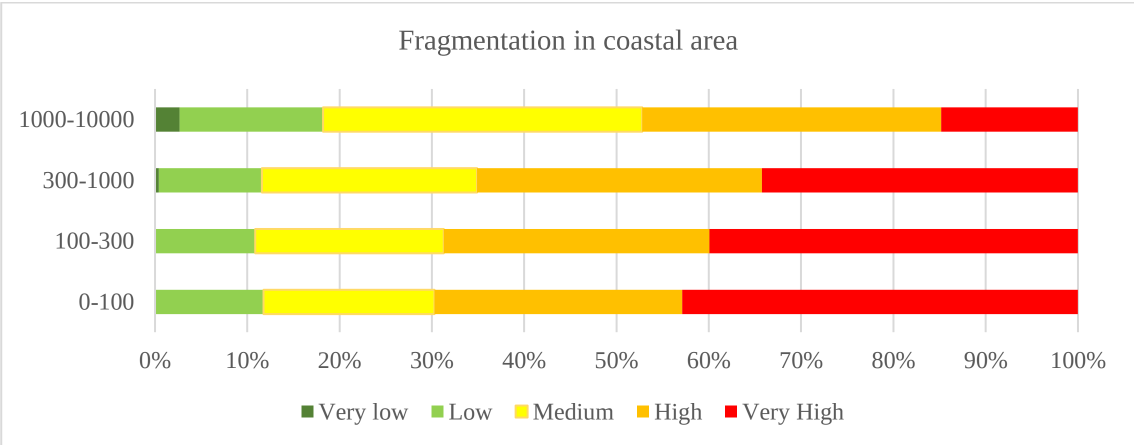

Figure 58. Fragmentation with respect to the distance from coastline, in terms of percentage of the territory occupied by each class of fragmentation

About the evolution of the phenomenon between 2012 and 2019 (Table 73), all the classes have undergone a reduction in the first 10,000 m from the coast, the only increasing class is the very high fragmentation class.

Table 73. Change in fragmentation (S_{eff}) with respect to the distance from coastline, between 2012 and 2019, in hectares and as a percentage change compared to 2012.

	Very low		**Low**		**Medium**		**High**		**Very High**	
	ha	**%**	**ha**	**%**	**ha**	**%**	**ha**	**%**	**ha**	**%**
0-100	-24	-77.1	-2,138	-18.3	-68	-0.4	-706	-3.1	2,936	9.2
100-300	-84	-44.7	-3,781	-20.4	-275	-1.0	-1,274	-3.1	5,414	11.0
300-1,000	-580	-26.0	-11,453	-19.9	-2,409	-2.5	-3,384	-2.6	17,826	14.5
1,000-10,000	-10,311	-8.5	-85,818	-11.7	-42,688	-2.9	48,689	3.8	90,129	17.2
Italy	-236,355	-6.5	-646,340	-10.4	-32,853	-0.3	499,707	6.9	415,841	15.4

4.2.3 Urbanization forms and the type of settlement

Urban expansion is characterized by phenomena to be monitored, such as diffusion and dispersion. Diffusion is the growth of a city through creation of small to medium-sized centres outside the main metropolitan areas. Dispersion implies fragmentation of inhabited centres, with the consequent loss of borders between urban and rural territory.

Widespread and dispersed urbanization produces loss of landscapes, soils and related ecosystem services but it is also an energy-intensive settlement model that encourages private mobility.

The analysis was conducted on 112 Italian provincial capitals which are among the most dynamic urban areas due to their size and the role they play in the territory (Table 74).

Diffusion in urban areas is observed analysing LCPI and RMPS:

The LCPI has values above 80% in 26 cities and above 90% in 8 cities. The highest values are in Savona (95.48%) (Figure 59 a) and Monza (95.12%). The lowest value is in Ascoli Piceno (18.24%) (Figure 59 b), while there is a total of ten capitals where the main urban centre includes less than 30% of the total built-up area of the municipality.

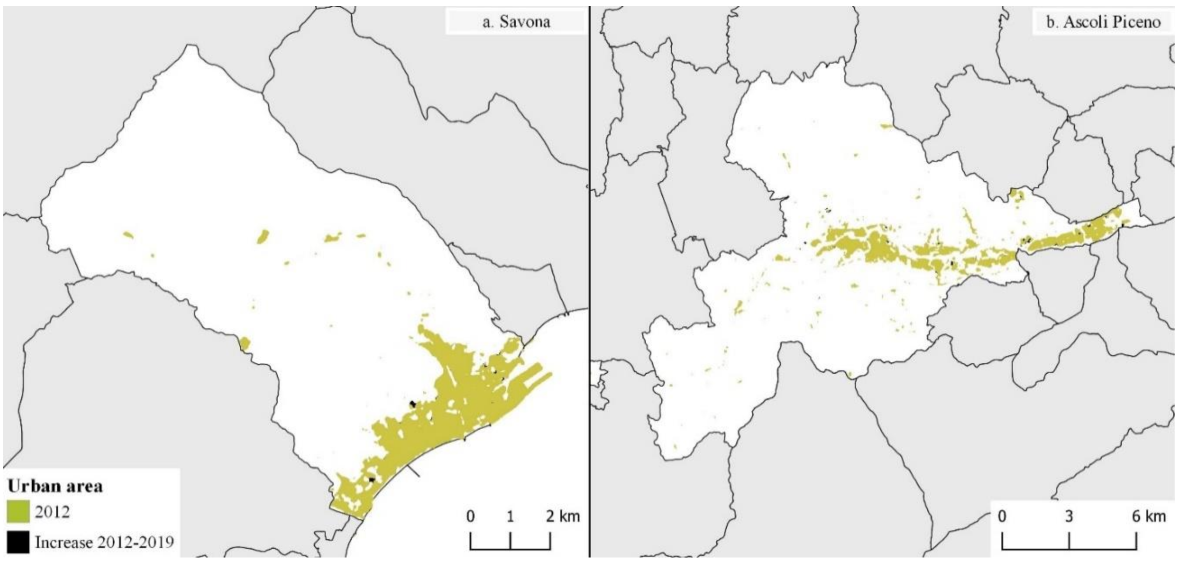

Figure 59. Urban area in Savona and Ascoli Piceno

As for variations in 2012 - 2019, Catanzaro (Figure 60 a) has an increase of 58.03% of LCPI, followed by Rieti (+46.01%), Messina (+19.88%) and Catania (+16.51%). Overall, 41 municipalities have an increase in the indicator. This trend indicates an expansion that has affected the main centre more than the peripheral areas. In these cities the urbanization along the main roads has led to merging of the main patch with one or more surrounding patches, enlarging the main city core. The remaining 71 cities have negative LCPI values, with a minimum of - 6.67% in Caltanissetta and Viterbo (- 5.33%) (Figure 60 b). This indicates that the expansion has affected the peripheral areas, reducing the overall percentage of the territory covered by the main patch.

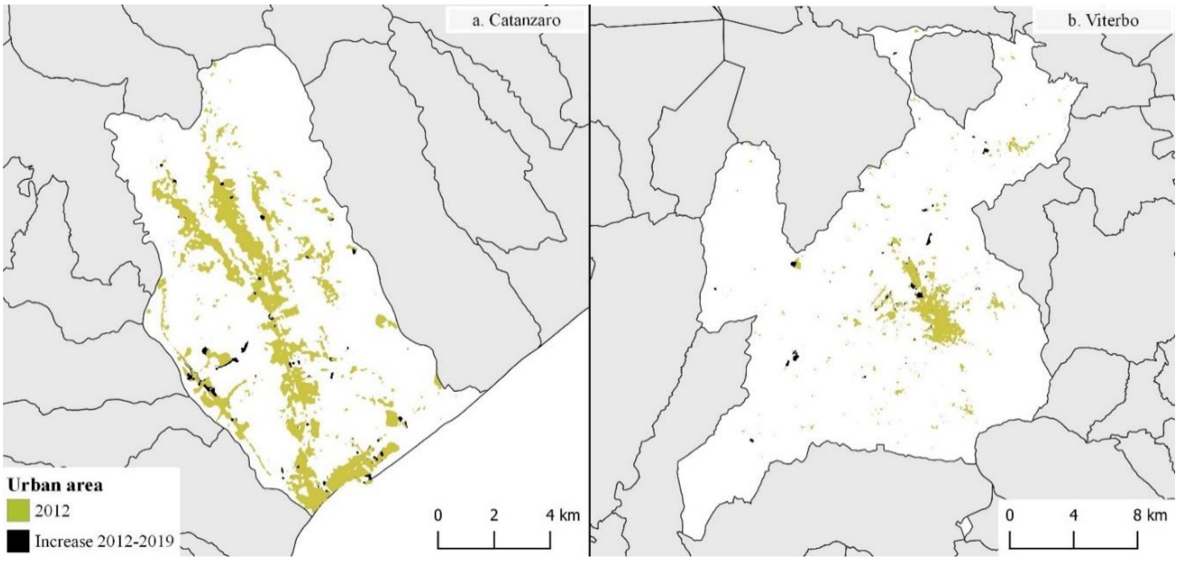

Figure 60. Urban area in Catanzaro and Viterbo

The RMPS shows values over 5 ha in 10 cities: one with more than 500,000 inhabitants (Torino) and three with more than 100,000 inhabitants (Bolzano, Taranto, Bari). In these cities the peripheral urban fabric is less widespread. In six provincial capitals the value is less than 1 ha, with a minimum of 0.47 ha in Savona.

In 5 cities, the RMPS increased by over 10%, with a maximum in Vercelli (+18.58%) (Figure 61 b), followed by Udine (+17.0%), Caltanissetta (+14.97%) (Figure 61 a), Pordenone (+13.64%) and Viterbo (+11.45%). Vercelli, Caltanissetta and Crotone are also among the cities with the highest decrease in LCPI, indicating an urban development that has affected the peripheral areas rather than the main centre. In Caltanissetta the variation is linked to the appearance of a large road construction site, while in Vercelli the increase is related to the expansion of an industrial area in the southern part of the municipality.

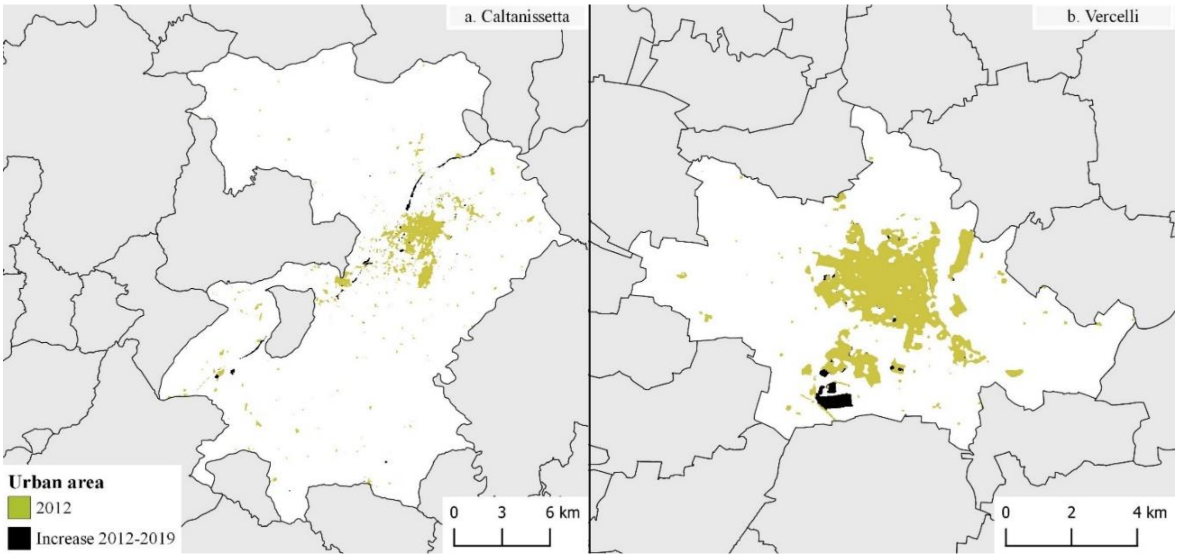

Figure 61. Urban area in Caltanissetta and Vercelli

Fragmentation and dispersion determined by the forms of urbanization and their evolution are described through an analysis of the built density with the use of two other indicators: the Edge Density (ED) and the dispersion index.

The Edge Density (ED) is closely linked to the morphological characteristics and allows to describe the dispersion of urban boundaries, intended as an interface between built and non-built areas. Regular borders (low ED values) refer to compact cities or, in the case of multipolarized realities, to urban centres defined and delimited by regular borders (McGarigal, 1995). The urban dispersion index (IDU) has the opposite character to compactness, with high values in low-density fabrics and low values in more compact areas. In 29 capitals ED exceeds 1,000 m/ha, with a maximum of 1,553.7 m/ha in Urbino (Figure 62 a). Such high values describe highly fragmented urban areas. In 9 capitals there are values below 500 m/ha, with a minimum of 190.45 m/ha in Torino (Figure 62 b), which is the most compact capital, followed by Napoli that has a double value compared to Torino (366.1 m/ha). Among the cities with the lowest values, four over six have more than 500,000 inhabitants. Low values are characteristic of very compact cities or cities where built-up area approximates the saturation of territory within the municipal limit. This second case describes situations like conurbations, where tendency to fragmentation develops mainly outside the administrative boundaries of the considered municipalities.

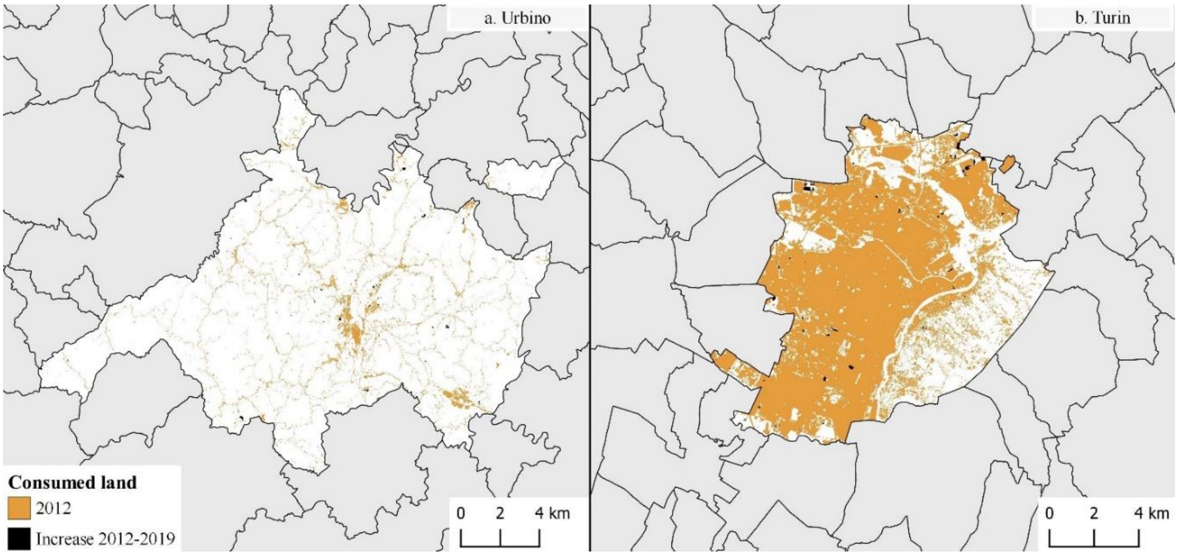

Figure 62. Urban area in Urbino and Torino

Between 2012 and 2019 the ED increased in 3 municipalities (Ancona, Carrara and Pistoia), while it decreased in all the others. The maximum decrease occurs in Vercelli (-4.03%), followed by Viterbo (-3.45%) and Caltanissetta (-3.36%). Decreasing values indicate a development of new buildings close to already built areas.

Figure 63 shows how in the six cities with over 500,000 inhabitants the central nucleus is highly compact, while in the neighbouring areas there is a greater diffusion of urban fabric as well as a greater density of changes.

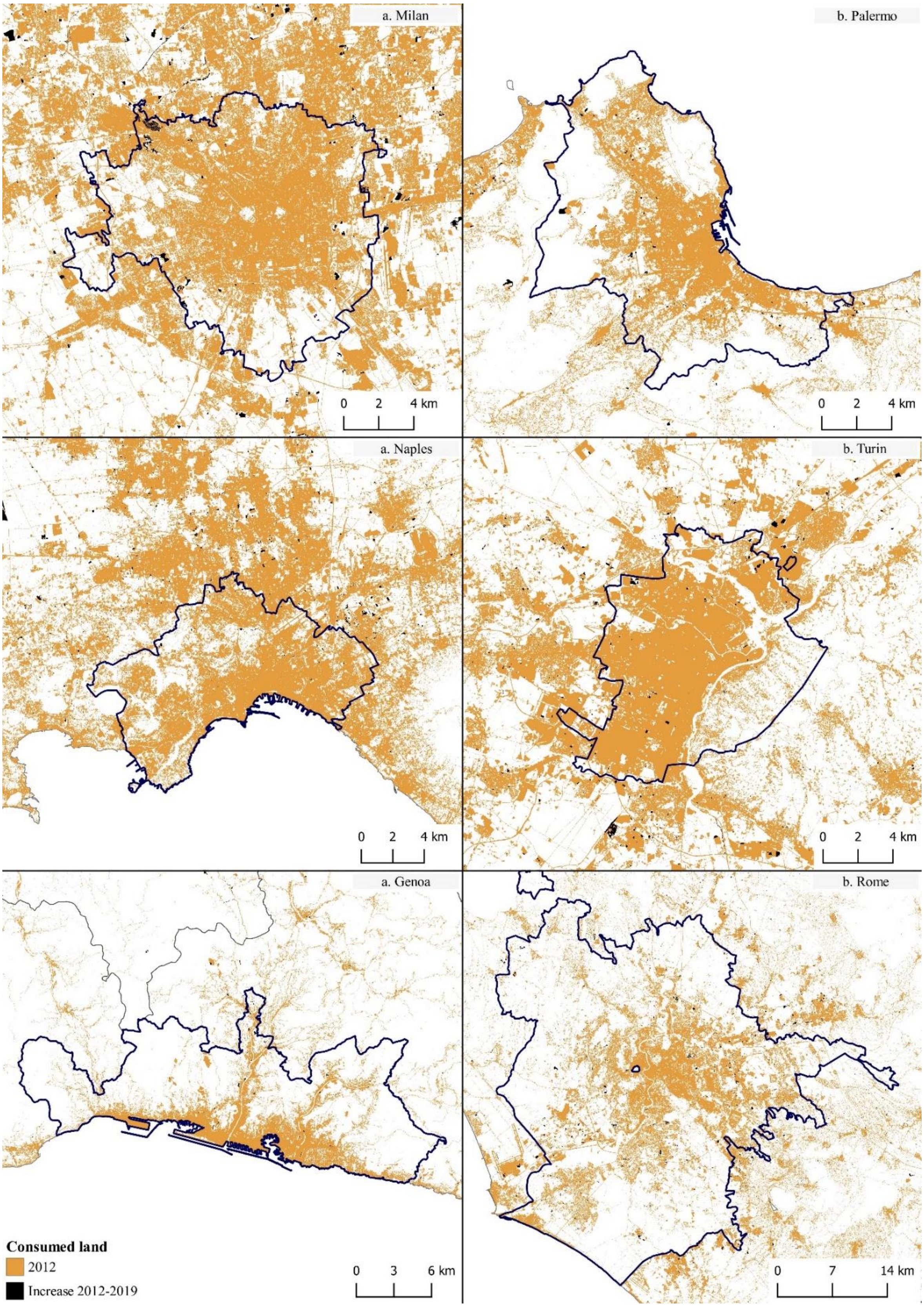

Figure 63. Consumed land in the cities with over 500,000 inhabitants

Table 74. Landscape metrics for the Italian provincial capitals. LCPI=Largest Class Patch Index, RMPS= Residual Mean Patch Size, ED=Edge Density, IDU=Dispersion Index

Municipality	LCPI (%)	RMPS (ha)	ED (m^2/ha)	IDU	Δ LCPI (%)	Δ RMPA (%)	Δ ED (%)
Bolzano	40,07	8,74	583,97	56,65	0,17	2,55	-2,56
Pordenone	48,74	7,49	517,63	54,19	-1,66	13,64	-1,84
Taranto	43,15	7,15	521,63	57,38	-0,07	-1,43	-0,82
Bari	50,48	7,09	537,01	51,32	1,09	4,65	-1,72
Mantova	36,41	6,09	549,26	64,09	-2,4	3,48	-1,49
Carrara	56,36	6,01	509,34	51,32	0,61	-2,55	0,33
Pisa	35,35	5,95	745,52	67,32	-0,05	0,97	-1,18
Roma	33,59	5,82	724,71	65,26	-0,09	4,09	-1,52
Torino	81,09	5,42	190,45	27,93	-0,21	1,87	-0,61
Brindisi	31,56	5,38	589,64	72,28	0,15	-0,87	-0,44
Venezia	65,19	4,63	413,48	55,35	-0,42	6,33	-2,16
Catania	74,00	4,49	505,99	52,23	16,51	-28,49	-2,79
Vercelli	65,88	4,46	551,93	60,35	-4,54	18,58	-4,03
Catanzaro	34,66	4,03	745,07	79,01	58,03	-14,17	-1,72
Verona	54,86	4,02	580,57	63,28	-1,09	0,36	-1,17
Ravenna	23,44	3,93	859,49	77,77	-1,84	2,76	-1,27
Vibo Valentia	33,57	3,86	768,99	76,25	0,21	1,15	-0,5
Cremona	63,86	3,83	506,37	62,41	-0,46	0,29	-0,37
Verbania	32,70	3,73	734,80	72,84	-0,04	2,73	-0,92
Firenze	63,38	3,70	600,17	55,92	-0,12	2,53	-0,34
Ascoli Piceno	18,24	3,69	1052,50	81,22	-0,93	2,45	-0,39
Salerno	61,67	3,65	501,64	59,41	0,05	2,15	-0,47
Trani	47,90	3,56	737,80	76,41	5,19	-1,84	-1,09
Ancona	48,98	3,51	733,12	65,91	-0,1	-0,82	0,33
Caserta	73,02	3,33	650,03	60,63	-0,51	8,21	-1,7
Terni	46,19	3,17	945,43	76,96	-2,5	2,73	-1,17
Napoli	88,97	3,14	366,07	30,72	0,01	1,85	-0,16
Trento	66,64	3,12	780,91	69,67	-0,19	1,26	-0,52
Agrigento	24,13	3,10	1020,55	86,05	-1,04	0,16	-0,52
Brescia	85,30	3,07	496,71	43,77	-0,14	1,8	-0,73
Nuoro	70,28	3,01	1279,88	68,67	-0,66	0,41	-1,37
Bergamo	81,79	2,91	542,40	44,10	-1,13	5,36	-1,05
Pavia	74,51	2,85	708,43	68,65	-0,17	0,92	-0,2
Alessandria	39,38	2,82	673,59	82,35	-1,01	3,82	-1,76
Pesaro	58,98	2,81	760,07	73,45	-0,24	0,95	-0,35
Prato	80,82	2,80	524,74	50,73	-0,82	2,52	-0,59
Udine	88,63	2,77	598,29	52,56	-1,13	17,01	-1,82
Crotone	29,40	2,76	1040,70	82,92	-5	9,26	-2,89
Lodi	64,25	2,72	602,82	70,45	-1,06	3,15	-1,17
Perugia	23,56	2,71	1111,85	85,69	-0,96	0,02	-0,64
Padova	79,62	2,70	498,58	50,60	2,44	-7,22	-1,09
Chieti	50,03	2,70	922,44	78,41	-0,5	4,86	-0,92
Siracusa	43,74	2,60	890,47	79,57	-1,25	2,45	-0,97
Matera	55,06	2,57	1130,24	79,42	-3,17	6,18	-2,86
Teramo	23,80	2,56	1101,82	82,75	-1,07	-0,48	-0,92
Macerata	47,14	2,50	1161,68	82,44	-0,55	3,21	-0,64
Messina	66,88	2,50	785,04	72,85	19,88	-24,54	-0,5
Novara	81,91	2,49	497,62	62,31	0,11	5,06	-2,42
Reggio di Calabria	64,42	2,43	780,51	71,22	-0,56	1,41	-0,56
Lecce	51,44	2,41	855,22	75,54	-0,89	1,07	-1,65
Fermo	27,78	2,41	998,29	87,88	-4,37	6,1	-1,92
Frosinone	52,41	2,39	811,04	75,64	0,06	1,15	-0,26
Rovigo	51,16	2,38	799,36	77,92	-0,24	1,68	-0,79
Trieste	79,39	2,33	668,05	57,23	0,51	1,34	-0,37
Parma	51,20	2,33	684,95	75,90	0,38	4,3	-2,98

Milano	93,16	2,29	409,11	29,29	-0,13	4,41	-1,89
Cesena	31,32	2,26	958,28	85,96	-1,58	1,84	-1,21
Oristano	63,63	2,25	1064,23	76,92	0,47	-0,41	-0,49
Grosseto	38,04	2,22	1071,98	79,65	-1,18	0,58	-0,66
Cuneo	29,27	2,20	817,05	83,06	-2,08	3,94	-2,13
Vicenza	74,65	2,12	550,90	66,32	-0,65	3,2	-0,24
Piacenza	78,54	2,09	512,90	61,91	0,43	0,7	-1,14
Foggia	51,91	2,08	877,43	80,67	-0,24	1,1	-1,86
Carbonia	47,01	2,06	1272,67	87,78	2,64	-1,31	-0,41
Forl•	54,47	2,03	846,57	77,53	-1,79	4,64	-1,16
Imperia	39,10	2,00	1102,24	84,53	-1,08	2,59	-0,18
Como	81,27	1,99	718,18	62,83	1,17	-3,59	-0,28
Rimini	60,52	1,98	672,85	70,59	0,29	-0,25	-0,68
L'Aquila	38,33	1,98	1198,86	87,37	-2,13	1,7	-1,4
Gorizia	79,95	1,96	799,80	62,49	-0,11	-1	-0,2
Trapani	57,48	1,92	758,46	80,15	-1,45	2,6	-0,61
Livorno	87,70	1,85	479,50	47,04	0,44	0,6	-1,06
Viterbo	44,55	1,83	1253,08	87,02	-5,33	11,45	-3,45
Genova	83,70	1,82	590,51	55,89	-0,2	0,72	-0,43
Bologna	85,74	1,76	730,45	51,56	0,44	-2,41	-1,05
Modena	73,75	1,74	649,97	68,26	0,03	0,3	-0,68
Benevento	34,97	1,73	883,99	85,19	-2,83	3,34	-1,87
Reggio nell'Emilia	61,84	1,69	780,58	77,16	-0,59	3,42	-1,35
Pescara	90,78	1,68	514,90	42,47	-0,02	3,04	-0,63
Palermo	90,15	1,67	452,18	43,64	-0,15	2,37	-0,32
Latina	40,39	1,66	1024,22	87,68	-1,33	2,8	-0,92
Massa	81,09	1,65	829,00	59,21	-1,5	8,65	-1,65
Enna	24,45	1,64	1386,05	92,97	-4,1	4,1	-1,43
Avellino	76,77	1,64	790,67	70,18	1,06	-0,07	-0,36
Lecco	94,39	1,62	520,08	49,74	0,01	3,57	-0,05
Andria	59,62	1,59	1065,23	81,02	-0,29	2,53	-1,02
Cagliari	88,93	1,57	677,18	46,42	0,85	-0,51	-0,71
Varese	81,56	1,57	850,12	68,75	-0,47	0,42	-0,4
Aosta	87,98	1,56	642,67	55,82	-0,39	-2,95	-0,11
Ragusa	53,68	1,50	1117,76	80,42	1,42	-1,33	-1,17
Ferrara	59,50	1,50	891,67	78,85	5,43	-5,02	-1,18
Sondrio	80,81	1,48	788,11	70,67	1,84	-3,52	-0,46
Arezzo	54,74	1,45	1177,02	85,92	0,32	-3,14	-0,49
Lucca	60,71	1,42	984,88	83,80	0,02	-0,27	-0,35
Sassari	44,31	1,42	1200,73	86,93	-1,67	3,66	-1,25
Treviso	87,12	1,41	603,24	57,82	5,79	-23,95	-1,06
Belluno	62,89	1,39	1209,23	84,74	-1,18	0,8	-0,33
Barletta	78,72	1,36	770,89	67,80	-1,07	4,48	-1,07
Caltanissetta	49,88	1,24	1279,58	89,00	-6,67	14,97	-3,36
Biella	81,89	1,21	658,04	66,38	0,08	1,58	-0,23
Pistoia	57,46	1,21	1089,16	87,34	-0,83	1,04	0,04
Urbino	24,51	1,18	1553,66	94,86	-2,1	0,58	-0,82
Campobasso	60,08	1,17	1094,78	81,60	-0,25	1,63	-0,77
Siena	64,78	1,06	1024,55	84,58	0,23	-0,32	-0,09
Rieti	61,66	1,06	1411,69	86,25	46,01	-32,44	-0,87
Asti	68,11	1,01	872,44	80,77	2,61	-1,56	-1,31
Isernia	64,31	0,99	1197,53	89,11	-1,39	4,35	-0,51
Monza	95,12	0,97	571,58	32,24	2,06	-29,26	-0,54
La Spezia	92,92	0,81	606,25	56,35	0,02	0,67	-0,61
Cosenza	90,07	0,77	630,84	62,01	1,23	-6,57	-1,13
Potenza	72,34	0,71	1135,05	83,15	-1,61	5,74	-1,2
Savona	95,48	0,47	804,61	55,40	0,15	-0,97	-0,29

4.2.4 Sustainable Development Goals

4.2.4.1 SDG indicator 11.3.1 Ratio of land consumption rate to population growth rate

Calculation of the RLCRPGR using different input data

The first results refer to the comparison between the values and the indicator obtained using different data for the calculation of the land consumption rate (LCR) (Figure 64). The results for the Copernicus Urban Atlas (UA) and CORINE Land Cover Accounting layer (CLCA) data consider the entire class 1 “Artificial surfaces”.

In Trieste and Napoli the CLCA data do not show variations in land consumption, leading to zero values of the Ratio of Land Consumption Rate to Population Growth Rate (RLCRPGR) indicator, while in the same city the two higher resolution data (UA and LCM) show an increase in land consumption associated with demographic decrease. In Venezia, the value obtained for the CLCA is aligned with the LCM, while in Bologna it is aligned with UA.

Milano is the municipality where there is greater alignment between the three data and the only one where the values obtained with UA are higher than those calculated with LCM. In Roma there is the biggest difference between the LCM data and Copernicus data.

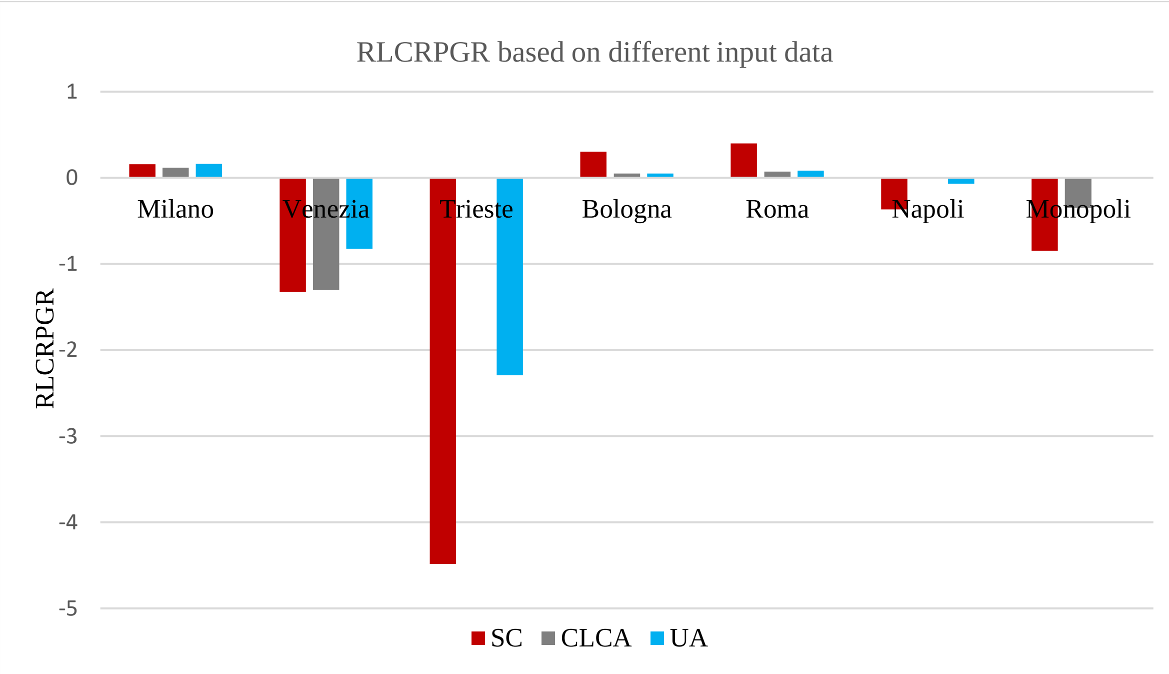

Figure 64. Ratio of Land Consumption Rate to Population Growth Rate (RLCRPGR), using different input data for Land Consumption Rate (LCR) calculation.

Table 75 shows RLCRPGR values and its two components, the LCR and the PGR. The PGR is common to all data and shows population increase in Roma, Milano and Bologna. On the contrary, population is decreasing in the other cities, where the PGR indicator gets negative values. The LCR shows an increase in land consumption in all cities. In detail, the LCR calculated with LCM and UA data assumes positive values in all the municipalities considered. The results obtained with the CLCA show null values in Trieste and Napoli and positive in the other cities. The null values are connected with the spatial resolution of the CLCA that did not allow to consider small changes while the LCM and UA data keep track of. Venezia is the city with the highest LCR value based on Copernicus data, while for the LCM data the city with the highest value is Monopoli.

Table 75. Ratio of Land Consumption Rate to Population Growth Rate (RLCRPGR) indicator, Population Growth Rate (PGR) and Land Consumption Rate (LCR) in the 5 cities, using three different input data for the description of land consumption

	LCM			CLCA		UA	
	PGR	**LCR**	**RLCRPGR**	**LCR**	**RLCRPGR**	**LCR**	**RLCRPGR**
Milano	0.0125	0.0019	0.158	0.0014	0.117	0.0020	0.161
Venezia	-0.0025	0.0033	-1.326	0.0033	-1.303	0.0021	-0.826
Trieste	-0.0002	0.0007	-4.483	0.0	0.0	0.0004	-2.295
Bologna	0.0057	0.0017	0.302	0.0003	0.051	0.0003	0.050
Roma	0.0057	0.0022	0.399	0.0004	0.074	0.0004	0.083
Napoli	-0.0014	0.0005	-0.365	0.0	0.0	0.0001	-0.071
Monopoli	-0.0048	0.0041	-0.847	0.0017	-0.348	-	-

The analysis shows a strong influence of the input data on the RLCRPGR values. The availability of data with high spatial resolution allows to monitor land consumption in detail and to obtain more reliable LCR values.

Green urban areas in the calculation of the RLCRPGR

Table 76 shows consumed land and land consumption in class 14 “Artificial, non-agricultural vegetated areas” based on UA data. In all the cities, class 14 occupy an extension close to 10% of the total consumed land, with a minimum of 8.8% in Trieste and a maximum of 15.1% in Milano. The role of this class is also important in terms of land consumption, as in three cities (Milano, Napoli and Trieste) almost 20% of land consumption is related to the passage of natural areas to class 14 areas. The value drops to 5% in Roma, while in Venezia and Bologna it is zero.

The transformations from class 14 to other classes of consumed land involve smaller extensions than the transition from natural areas to 14, in all cities except Venezia. Here there were 5 hectares of change from class 14 to other consumed land classes and no change from natural areas to 14.

Class 14 has a double impact on the calculation of the RLCRPGR indicator. Including this class in the definition of consumed land increases the extent of the consumed land, consequently LCR will be lower for the same land consumption value.

Secondly, class 14 affects land consumption values, since these change whether or not included in the definition of land consumption.

Table 76. Land consumption e consumed land related to class 14 “Artificial, non-agricultural vegetated areas”.

	Land consumption 2012-2018				Consumed land 2012			Consumed land 2018		
	Total	From natural to class 14		From 14 to other 1	Total	Class 14		Total	Class 14	
	ha	ha	%	ha	ha	ha	%	ha	ha	%
Bologna	21	0	0.0	0	7478	887	11,9	7491	887	11,8
Milano	183	32	17.6	13	14349	2145	14,9	14523	2193	15,1
Napoli	26	5	19.6	1	9860	923	9,4	9866	928	9,4
Roma	535	28	5.3	8	50773	6168	12,1	50919	6205	12,2
Trieste	9	2	19.1	1	3726	327	8,8	3734	328	8,8
Venezia	116	0	0.0	5	8113	833	10,3	8215	828	10,1

If we consider class 14 as consumed land, the transformations of a natural area into class 14 represent land consumption. If, on the other hand, class 14 is considered as a natural surface, land consumption will be the transition from class 14 to other classes of consumed land, while changes from other classes of natural land to 14 will be excluded. In four of the six cities, the exclusion of class 14 from the definition of land consumption causes a decrease in the LCR values (and consequently those of RLCRPGR) (Figure 65, Figure 66). This is because the decrease in land consumption affects the indicator more than the decrease in the total area of consumed land. Bologna and Venezia are an exception. In Bologna there are no variations in class 14 between 2012 and 2018, consequently the variation in the LCR (and so in the RLCRPGR) are only linked to the decrease in the overall extent of the consumed land. Venezia is the only one where excluding class 14 brings both a decrease in consumed land and an increase in land consumption, and therefore both contributions increase LCR.

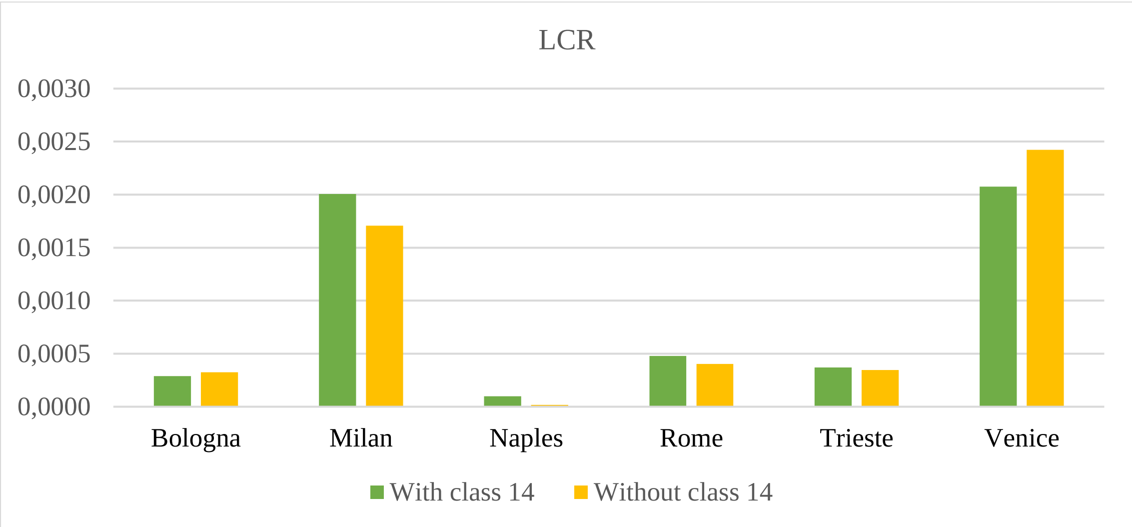

Figure 65. Land Consumption Rate (LCR) values referred to Urban Atlas data, including and excluding class 14 from the definition of land consumption.

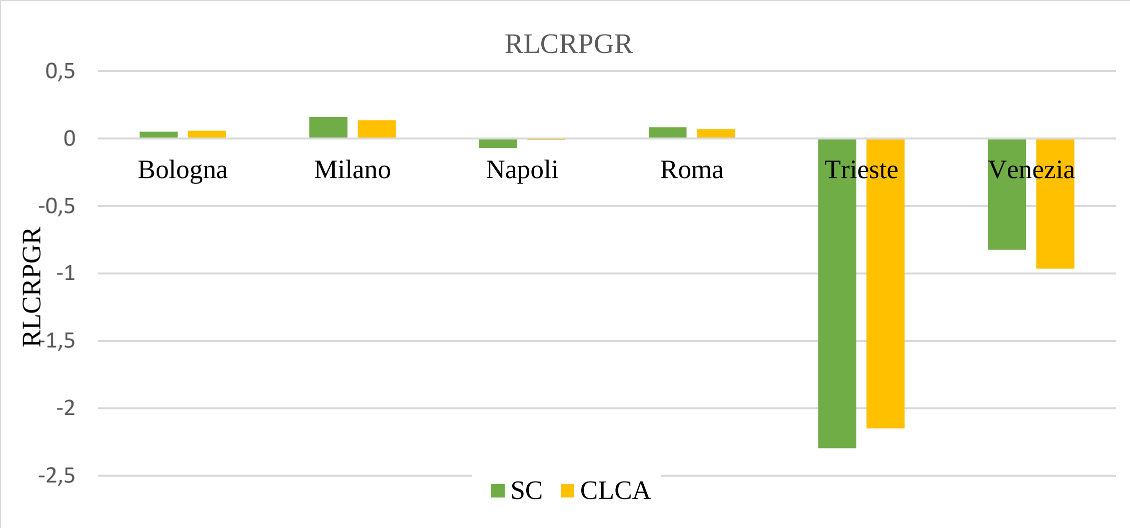

Figure 66. Ratio of Land Consumption Rate to Population Growth Rate RLCRPGR values referred to Urban Atlas data, including and excluding class 14 from the definition of land consumption.

The comparison between UA class 14 and LCM is reported in Table 77. Class 14 polygons have an average land consumption value of 38.1% of the surface, with a median value of 30.4%. Just over 30% of the polygons are affected by land consumption for over 50% of the surface.

Table 77. Percentage of the surface area of class 14 Urban Atlas polygons affected by the presence of consumed land (referred to Land Consumption Rate)

UA class	Consumed land (%)					
	Mean	Median	0-25	25-50	50-75	75-100
141	30.2	22.0	55.3	25.9	9.9	9.0
142	52.7	55.4	23.0	21.5	26.4	29.1
TOT	**38.1**	**30.4**	**43.9**	**24.3**	**15.7**	**16.1**

Class 14 was analysed with reference to its sub-categories at the third classification level. Polygons of class 141 have a percentage of consumed land higher than those 142, with an average of 52.7% of the surface, against 30.2% of class 141. Less than 20% of polygons 141 have more than half of the territory affected by land consumption, while for class 142 this condition occurs in over 55% of the polygons. Polygons with less than 1% of the territory affected by land consumption are just over 3% for both class 141 and 142 (Figure 67, Figure 68), while polygons with over 99% of land consumed exceed 3.5% for the 142 class and stop at just over 2% for the 141. Overall, low land consumption values prevail in both classes.

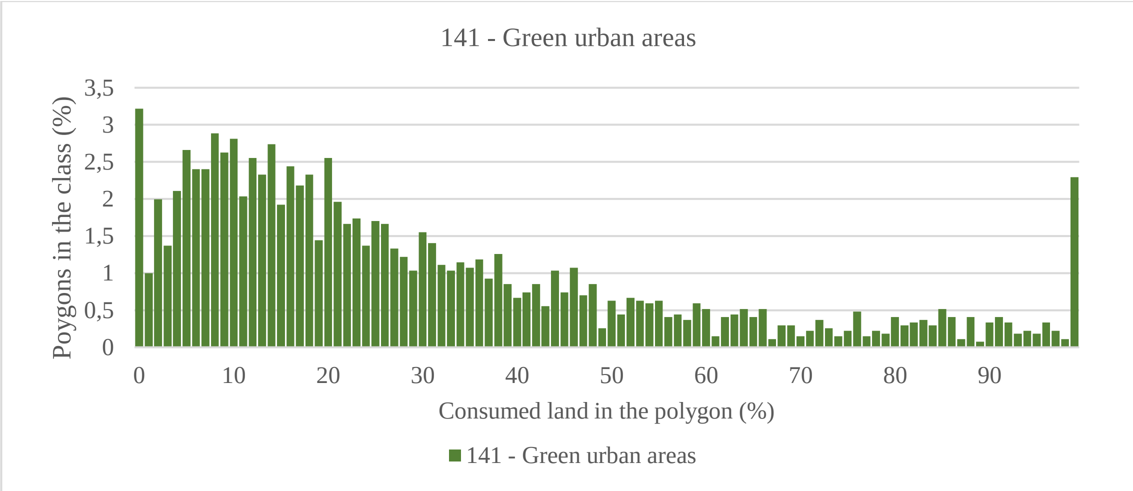

Figure 67. Percentage of the surface of the 141 Urban Atlas polygons covered by consumed land (based on National Land Consumption Map).

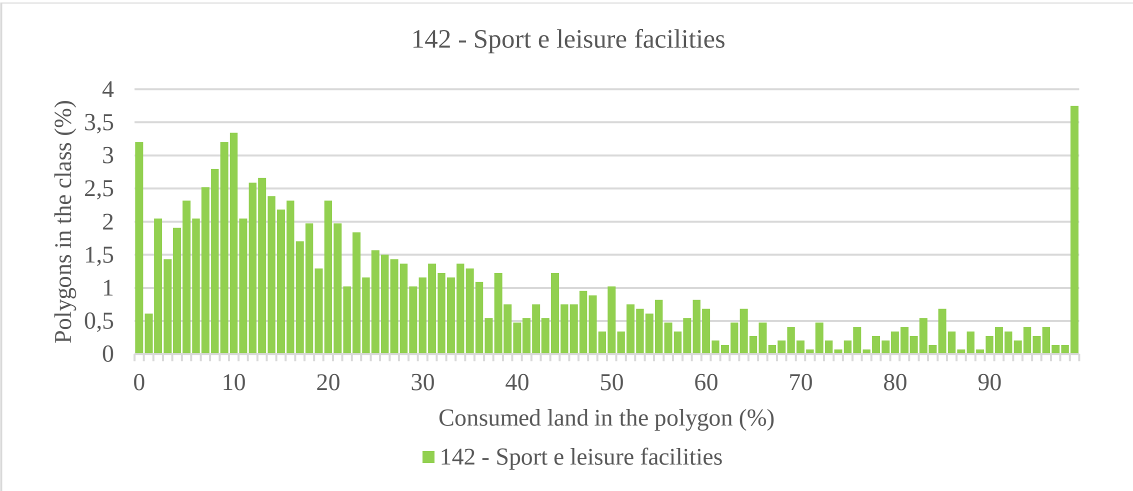

Figure 68. Percentage of the surface of the 142 Urban Atlas polygons covered by consumed land (based on National Land Consumption Map).

The analysis on green urban areas shows that the definition of land consumption must be linked to land cover criteria. In the Copernicus data classification systems, the 14 "artificial, non-agricultural vegetated areas" class is defined according to land use criteria. Consequently, both artificial and natural areas are associated with this class. For example, the 141 "green urban areas" class includes historic villas, where the artificial surface is not negligible, but also urban parks. The 142 "sport and leisure facilities" class includes totally artificial areas, such as auditoriums, but also natural areas, such as golf courses. It is important to distinguish the fraction of class 14 areas covered by artificial surfaces from natural ones, in order to make monitoring of the latter easier and more targeted. In this sense, including classes 14 in the definition of land consumption limits the possibilities of protecting the natural areas still present in that class, which are important since they are often included in urban contexts with little presence of green and natural areas (Fares *et al.*, 2020).

This study demonstrates how significant discrepancies can occur when different definition are compared. Defining land consumption from a land cover perspective could definitely solve ambiguous issues in urban land use classes such as green urban areas and sport and leisure facilities. Besides the fact that a land cover approach would be more appropriate to consider comprehensively soil issues. Whereas, land use classes involved in land consumption could be investigated as additional insight.

Analysis of the evolution of the provincial territory starting from the RLCRPGR

The analysis at the provincial level shows LCR values increasing in all the municipalities of the province of Venezia and Napoli, while in the other provinces there are four municipalities with negative LCR: Monrupino in the province of Trieste, Melzo in the province of Milano, Zola Predosa and Monterenzio in the province of Bologna, Civitella San Paolo in the province of Roma. Furthermore, 16 out of 451 municipalities have LCR = 0 (from Figure 69 to Figure 74).

The sign of the RLCRPGR in municipalities with positive LCR depends on the PGR value. The population variation shows different trends. In Bologna, Milano and Roma population increases in the capital and in the neighbouring municipalities, while it decreases in the peripheral ones. In Roma, population increases in the coastal area, while in Napoli it decreases. In Napoli and Venezia there is an opposite trend compared to other cities, with a decrease in population near the capital and an increase in the neighbouring municipalities of the hinterland.

When LCR > 0 and PGR > 0, RLCRPGR assumes sustainable values between 0 and 1, since the increase in population is greater than the increase in land consumption. This condition occurs in the municipalities of Milano Roma and Bologna. In the other provincial capitals, the increase in land consumption is associated with a decrease in the population.

The province of Milano shows a strong increase in population even in the suburbs. The RLCRPGR values are therefore sustainable (between 0 and 1) in most municipalities, despite the strong increase in land consumption (Figure 69).

The province of Bologna has sustainable values of RLCRPGR in the capital and in the adjacent municipalities, while in the south many municipalities have RLCRPGR values between 0 and -1, since the increase in land consumption is accompanied by a high decrease in population (LCR > PGR) (Figure 70).

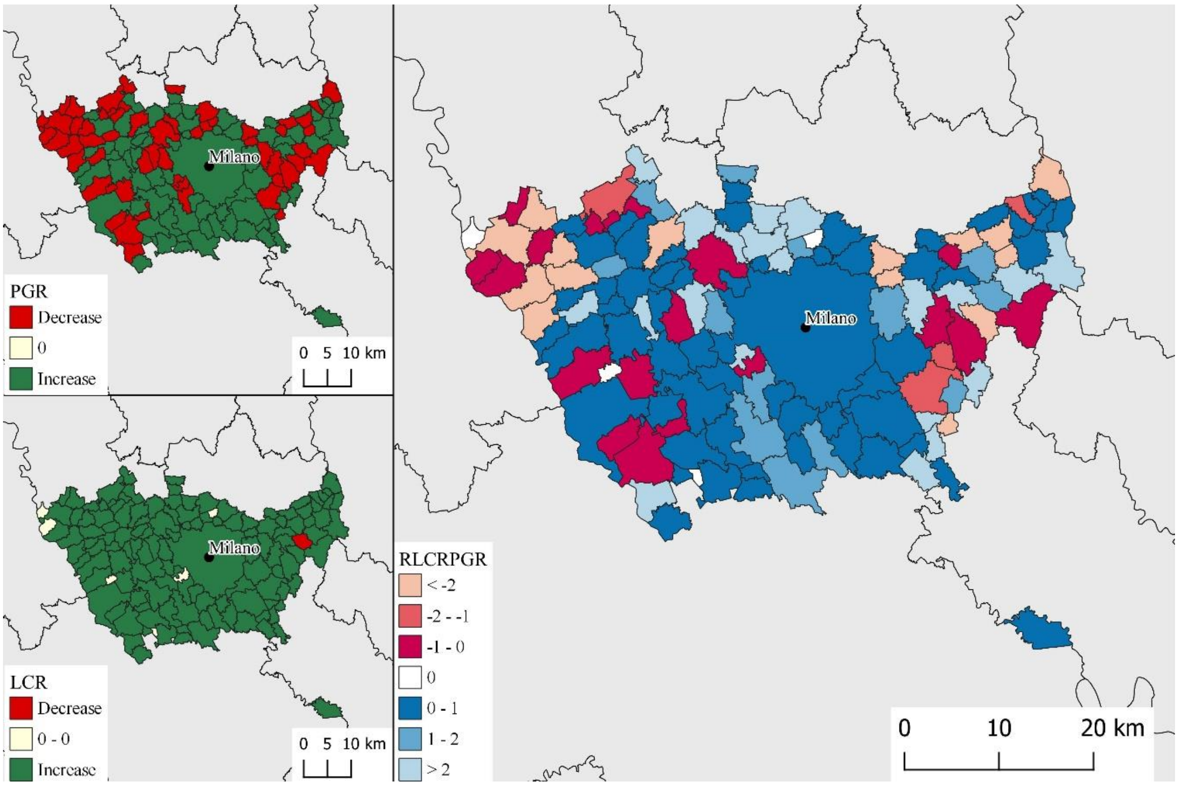

Figure 69. Ratio of Land Consumption Rate to Population Growth Rate (RLCRPGR), Land Consumption Rate (LCR), Population Growth Rate (PGR) in the province of Milano

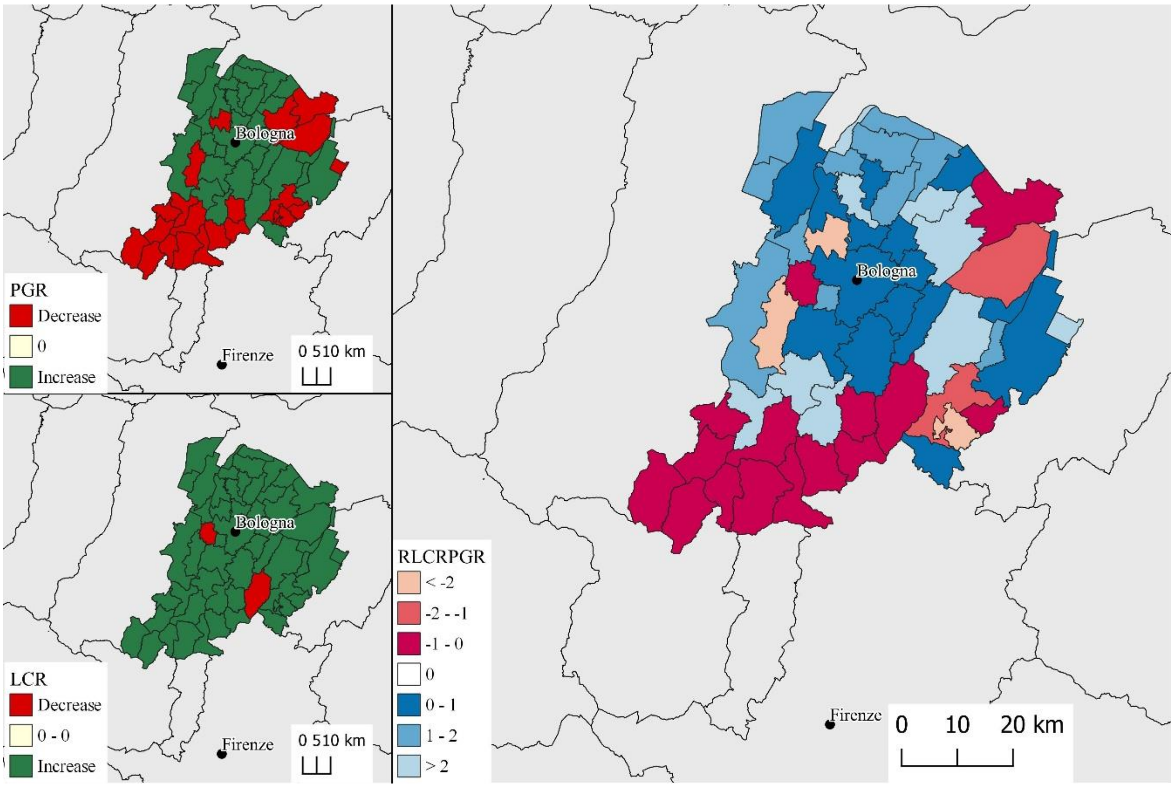

Figure 70. Ratio of Land Consumption Rate to Population Growth Rate (RLCRPGR), Land Consumption Rate (LCR), Population Growth Rate (PGR) in the province of Bologna

Venezia and Trieste have few municipalities with sustainable values of RLCRPGR (just one in Trieste), while most have values between 0 and -1, presenting a strong decrease in population and an increase in land consumption (Figure 71, Figure 72).

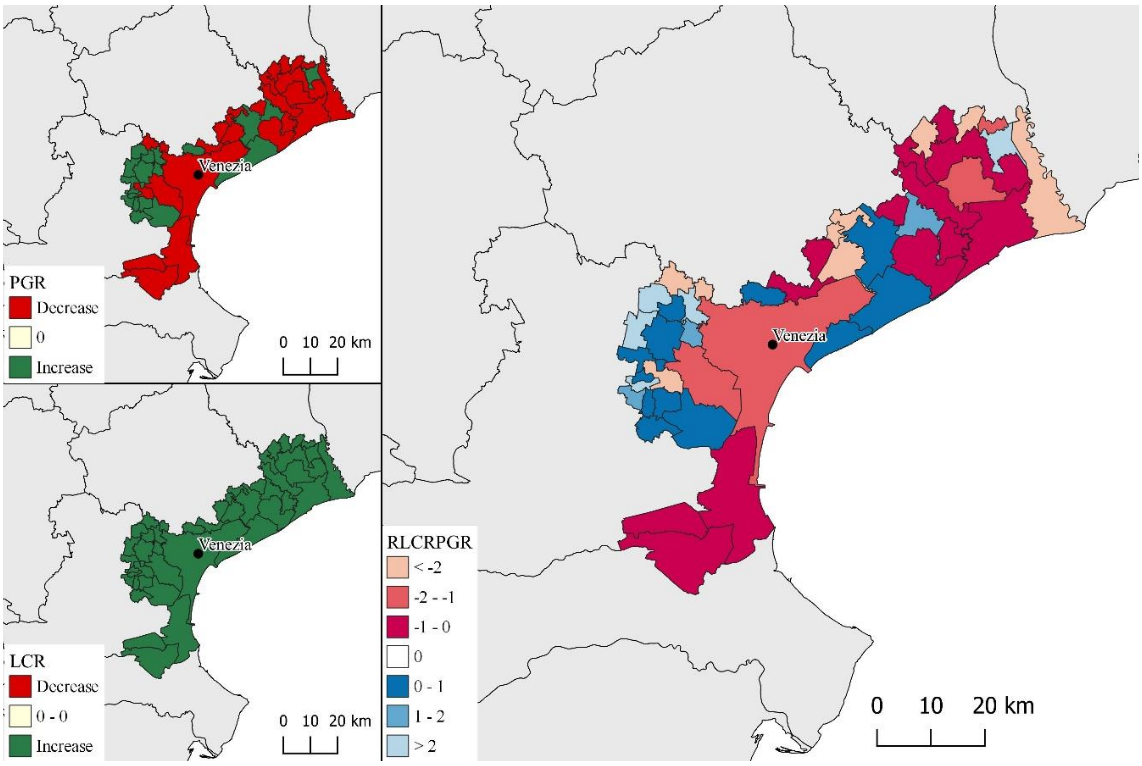

Figure 71. Ratio of Land Consumption Rate to Population Growth Rate (RLCRPGR), Land Consumption Rate (LCR), Population Growth Rate (PGR) in the province of Venezia

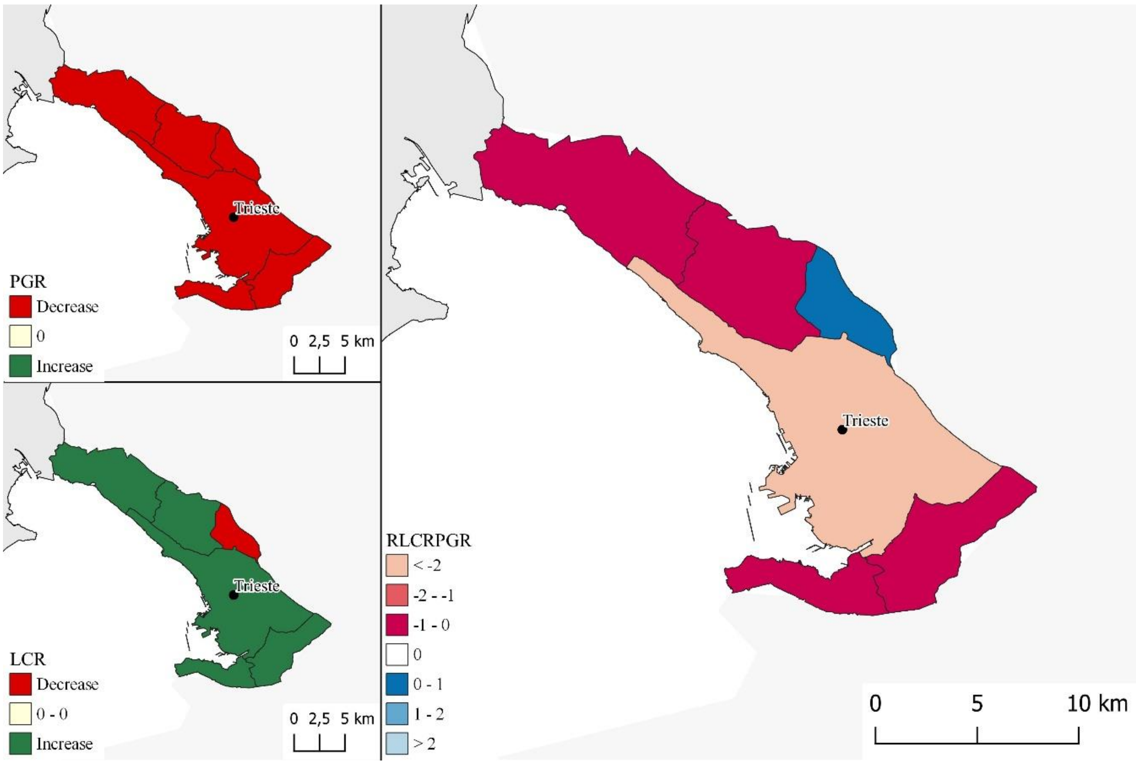

Figure 72. Ratio of Land Consumption Rate to Population Growth Rate (RLCRPGR), Land Consumption Rate (LCR), Population Growth Rate (PGR) in the province of Trieste

In the province of Roma there is a strong increase in population in the coastal area and in the municipalities located northeast and southeast of Roma. In these areas, the increase in population balances land consumption. In the east, the sharp decrease in population, associated with the increase in land consumption leads to value the indicator between 0 and -1 (Figure 73).

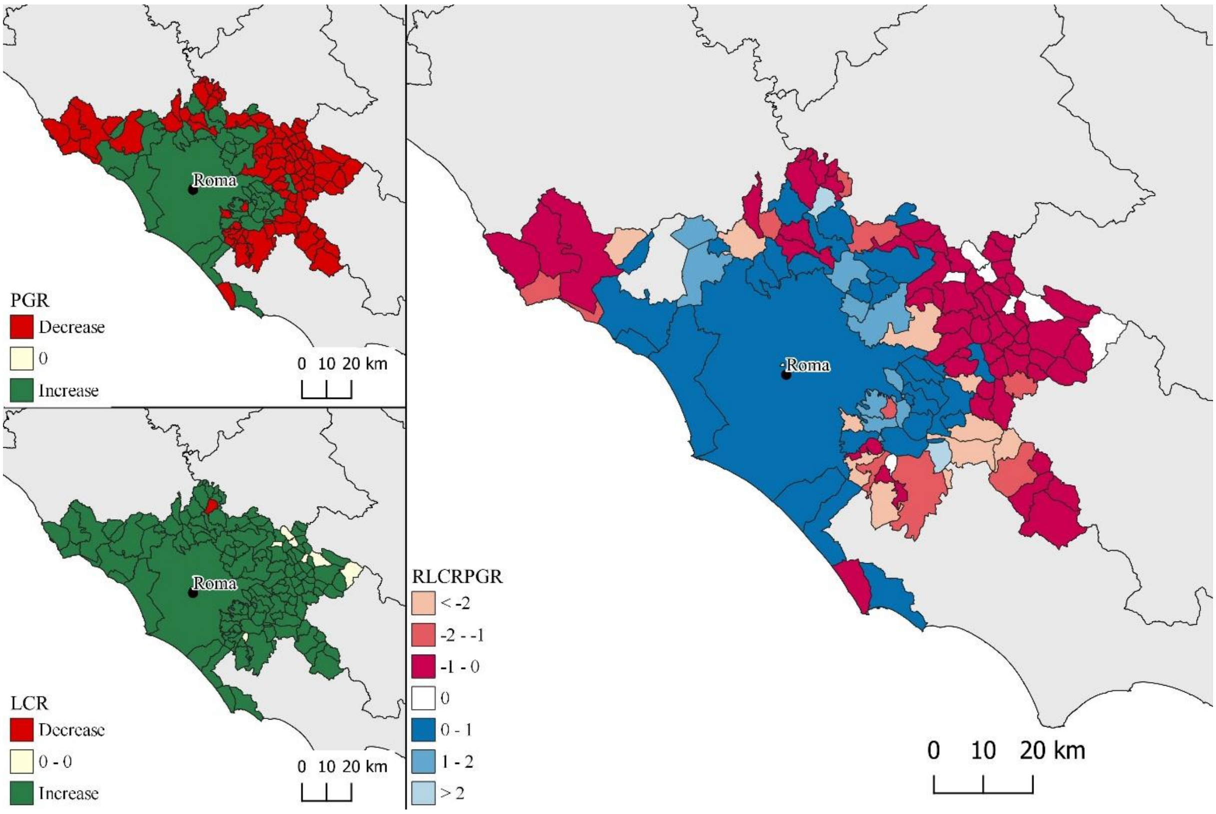

Figure 73. Ratio of Land Consumption Rate to Population Growth Rate (RLCRPGR), Land Consumption Rate (LCR), Population Growth Rate (PGR) in the province of Roma

In Napoli there is a decrease in population in the capital, along the coast and in the municipalities surrounding Vesuvius, while there are sustainable values of the indicator in the municipalities to the east (Figure 74).

The SDG indicator 11.3.1 measures how efficiently cities use land and shows the importance to increase the awareness of limiting land consumption. The indicator helps decision makers to monitor urban growth also because its value is comparable and scalable at different levels. In order to achieve the comparability a collective effort to homogenize the definitions is necessary, especially in territories involved in international community policies about soil protection, biodiversity conservation and the fight against climate change.

This indicator is categorized under Tier II, meaning it is conceptually clear and an established methodology exists, but data on many countries are not yet available and in many cases the resolution is too coarse to perceive changes in LU or LC.

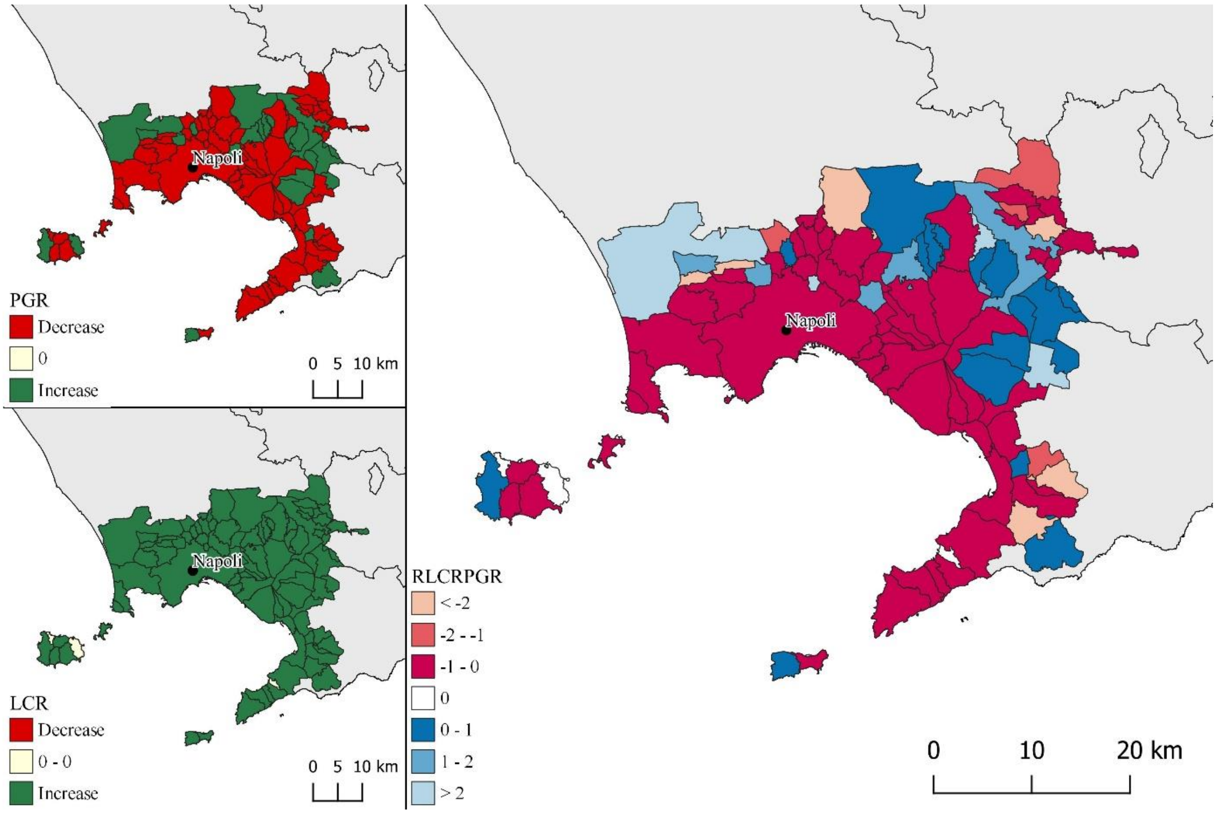

Figure 74. Ratio of Land Consumption Rate to Population Growth Rate (RLCRPGR), Land Consumption Rate (LCR), Population Growth Rate (PGR) in the province of Napoli

Increasing spatial resolution on land consumption data while maintaining adequate accuracy could result in increased ability in change detection. However, the difficulties in spatializing the population data in dasymetric maps with compatible resolutions represents a bottleneck in the improvement and deepening of this indicator. Administrative limits are now obsolete boundaries and they are unable to interpret the actual demographic dynamics of the new conurbations, that on the other hand, should be the new territorial units in which to adopt spatial planning policies.

The computation of the indicator is not always feasible considering that it strongly depends on the temporal availability of the data as well as on their distribution and spatial accuracy. Furthermore the interpretation of its results often needs the support of ancillary information in order to be practical and effectively used. Considering the incidence of commuting people, seasonal inhabitants or tourists could outline new biases in the sustainability assessment, therefore it would be of academic but also practical interest to isolate these components to analyse the actual relationship between new inhabitants and new buildings.

This research has highlighted land consumption and population variation decoupled trend, which occurs in many Italian municipalities. As stated in the metadata the major limitation for this indicator lies in its interpretation, which must consider the values of LCR and PGR, as their sign is strictly related to the meaning of the values of RLCRPGR.

Even if in some cases there is a balance between population growth and land consumption, many results illustrate the opposite trend: despite a population decrease land consumption increases, both in capital and neighboring municipalities: this trend has to be reasonably considered as a non-virtuous behavior.

On the other hand a land consumption decrease should always be considered environmentally sustainable, excluding socio-economic implications of overcrowding or depopulation, which differently from land consumption are not plannable, even if they can be predicted in short and middle term.

When both indices are positive: if LCR is lower than PGR, the new consumed land is coherent with the demographic needs, otherwise it is to be considered logically unsustainable.

4.2.4.2 SDG indicator 15.3.1 Proportion of land that is degraded over total land area

Land degradation at national level

The increase in degradation due to the different subindicators is reported in Table 78. Areas affected by individual contributions cannot be summed up due to the presence of overlaps.

Table 78 Area affected by land degradation increase for each of the subindicators, expressed in km^2 and percentage of the national territory (2012-2019).

Subindicator	New land degradation (2012-2019)	
	km^2	**% on national surface**
Land Cover change	777	0.26
Land Productivity dynamics	19,813	6.56
Soil organic carbon stock	528	0.18
Fragmentation	45,836	15.21
Soil erosion	540	0.18
Reduction in size of natural spaces	19	0.006
Potential impact area (60 m)	520	0.17
Expansion of high and medium density artificial areas	1,138	0.38
Burned areas	2,374	0.8
Loss of habitat quality	34,930	11.57

The main causes of degradation in the period 2012-2019 are linked to the increase in fragmentation (15.21% of the national territory), the loss of habitat quality (11.57%) and the loss of soil productivity (6.56%).

With reference to the land degradation associated with land cover variations, 299 km^2 are linked to the transition from a natural land cover class to an artificial one, while the remaining 478 km^2 derive from transitions between natural land cover classes.

This assessment is a preliminary result, obtained through subindicators mainly related to land cover changes, which confirm the necessity of improved national indicators to enhance compliance with the official UNSDG reporting system. More accurate results could be obtained by improving subindicators related with climate conditions such as drought and rainfall, and physical (compaction, water erosion) and chemical (contamination, salinization) degradation phenomena.

The total land degradation was calculated combining the binary degradation maps related to the single subindicators. The areas affected by an increase in land degradation between 2012 and 2019 are mapped in Figure 75.

The areas are distinguished according to the number of causes of degradation which are present at the same time. The increase in degradation affected 89,232 km^2 (29.56% of the national territory), mainly due to a single cause of degradation (Table 79). The surface area affected by the presence of two causes of degradation is 14,142 km^2 (4.68% of the territory), while over 1,600 km^2 are touched by three or more causes of deterioration.

Table 79. Surface affected by 1, 2 or at least 3 causes of degradation, expressed in km^2 and percentage of the national territory (2012-2019).

Causes of degradation	**New land degradation (2012-2019)**	
	km^2	**% of National surface**
1	73,446	24.33
2	14,142	4.68
≥3	1,643	0.54
Total	89,232	29.56

The increase in degradation due to the presence of at least one of the seven factors considered affects over 25% of the territory in 7 of the 20 regions (Table 80). In Sicilia and Veneto the value exceeds 30% of the regional territory. Veneto is also the region with the largest portion of territory affected by the presence of two causes of degradation at the same time and it is in third place by extension of the areas affected by at least three causes of degradation, following Campania (1.3% of the territory) and Puglia (1.1%).

Molise (12.7%), Basilicata (16.9%) and Sardegna (16.4%) are the regions with the lowest percentage of territory affected by new degradation. Molise is also the least affected region by the coexistence of multiple sources of degradation, followed by Trentino-Alto Adige.

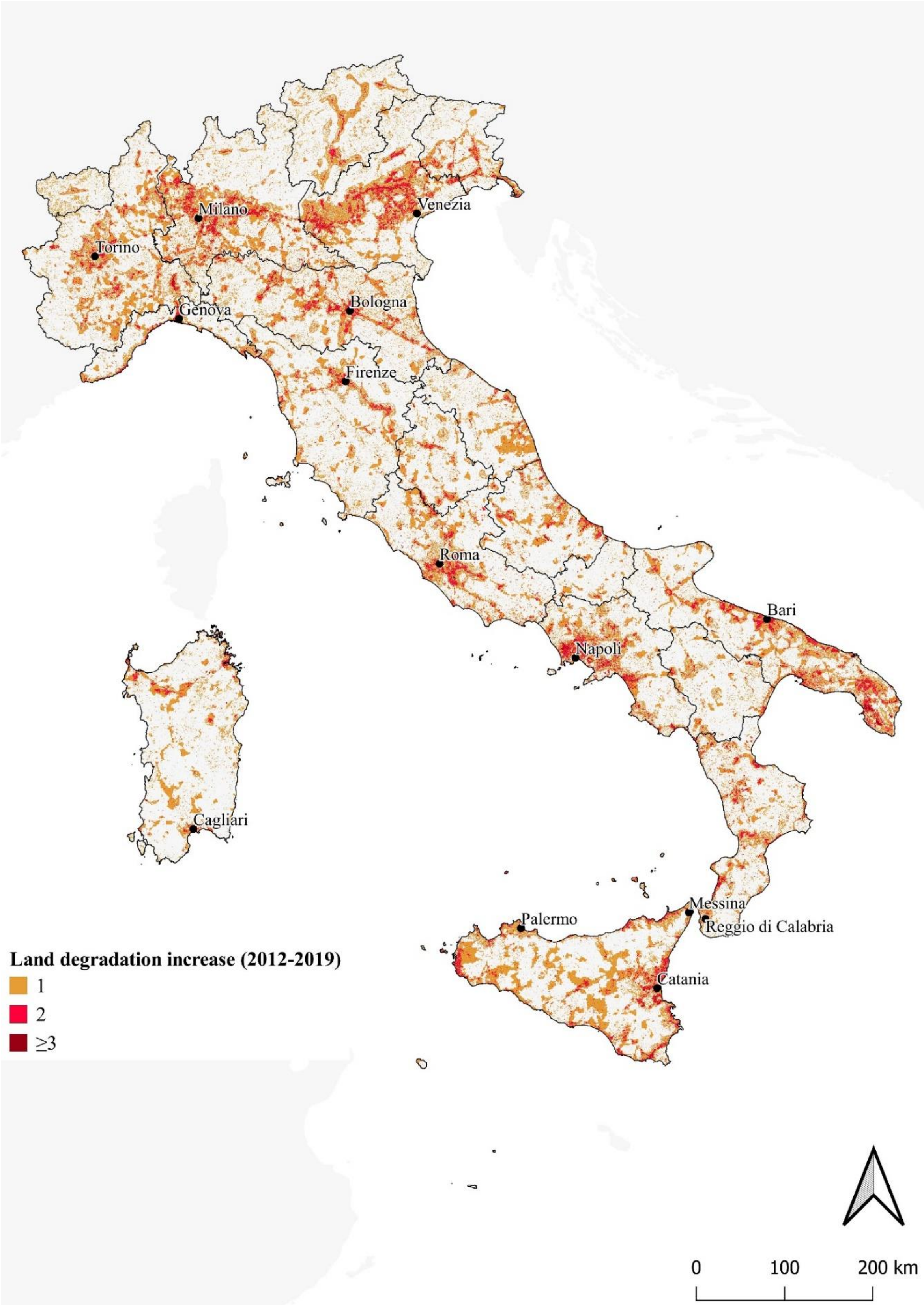

Figure 75. Increasing degradation between 2012 and 2019 due to one or more causes of degradation

Table 80. Surface affected by 1, 2 or at least 3 causes of degradation at regional scale, expressed in km^2 and percentage of the national territory (2012-2019).

	1		2		≥3		Unchanged	
	km^2	**%**	**km^2**	**%**	**km^2**	**%**	**km^2**	**%**
Piemonte	6,964	27.4	1,036	4.1	91	0.4	17,310	68.1
Valle d'Aosta	724	22.2	22	0.7	2	0.1	2,515	77.1
Lombardia	6,623	27.7	1,471	6.2	194	0.8	15,591	65.3
Trentino-Alto Adige	2,728	20.0	243	1.8	20	0.1	10,614	78.0
Veneto	5,626	30.7	1,675	9.1	173	0.9	10,863	59.2
Friuli-Venezia Giulia	1,674	21.1	333	4.2	34	0.4	5,878	74.2
Liguria	1,222	22.5	244	4.5	17	0.3	3,937	72.6
Emilia-Romagna	5,732	25.5	1,082	4.8	129	0.6	15,501	69.1
Toscana	4,423	19.2	573	2.5	50	0.2	17,943	78.1
Umbria	1,641	19.4	226	2.7	24	0.3	6,563	77.6
Marche	2,254	24.0	232	2.5	26	0.3	6,871	73.2
Lazio	4,157	24.2	985	5.7	87	0.5	11,974	69.6
Abruzzo	2,339	21.7	428	4.0	47	0.4	7,984	73.9
Molise	562	12.7	51	1.1	5	0.1	3,823	86.1
Campania	3,846	28.3	1,058	7.8	181	1.3	8,515	62.6
Puglia	5,579	28.8	1,537	7.9	208	1.1	12,032	62.2
Basilicata	1,685	16.9	196	2.0	22	0.2	8,088	80.9
Calabria	3,419	22.7	720	4.8	87	0.6	10,857	72.0
Sicilia	8,286	32.2	1,617	6.3	195	0.8	15,621	60.7
Sardegna	3,967	16.4	413	1.7	52	0.2	19,686	81.6
Italy	**73,449**	**24.4**	**14,142**	**4.7**	**1,643**	**0.5**	**212,165**	**70.4**

Land degradation in EUAP protected areas

The EUAP areas have a surface subject to degradation below the national average (Figure 76). In percentage, about 10% of the territory is affected by an increase in degradation and the areas subject to 2 or more forms of degradation are less than half the national value.

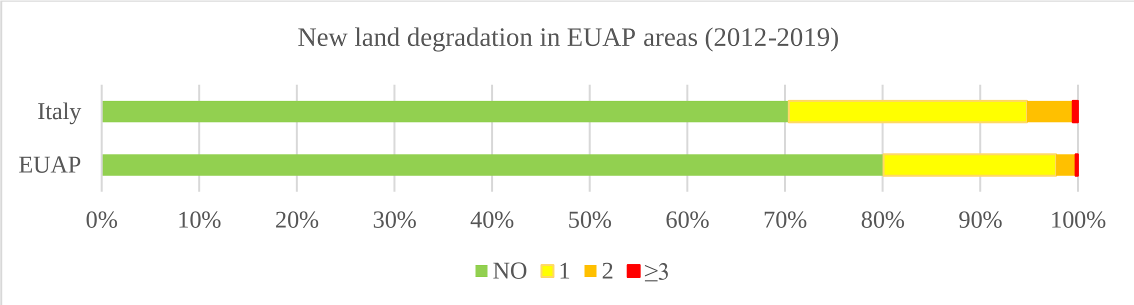

Figure 76. Percentage of the territory of the EUAP areas affected by increased land degradation, due to one (yellow), two (orange) or at least three (red) causes of degradation (2012-2019).

Land degradation in relation to elevation and slope

The distribution of the new degraded areas is strongly linked to the conformation of the territory. In mountain areas (with high elevation and slope) about 15% of the territory is affected by an increase in degradation. The value rises to over 30% in areas with low slope and medium elevation and in those with high slope and low elevation and exceeds 40% in lowland areas (at low elevation and slope) (Figure 77).

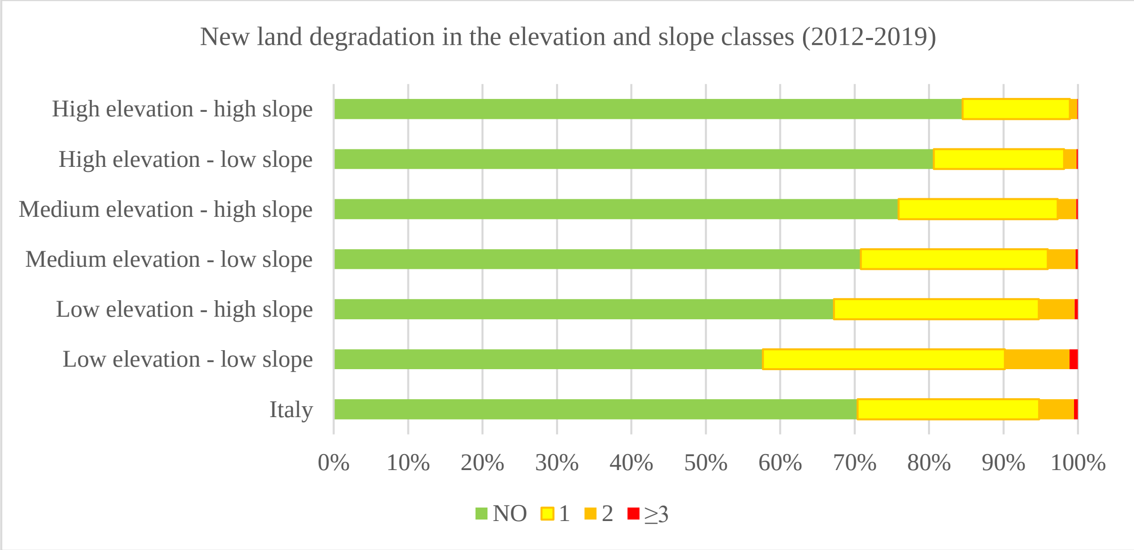

Figure 77. Percentage of the different elevation and slope classes affected by new land degradation, due to one (yellow), two (orange) or at least three (red) causes of degradation (2012-2019).

The areas with low elevation and slope are also those with higher coexistence of different causes of degradation, here fall almost 70% of the areas with two causes of degradation and almost 80% of those with 3 or more causes of degradation (Figure 78).

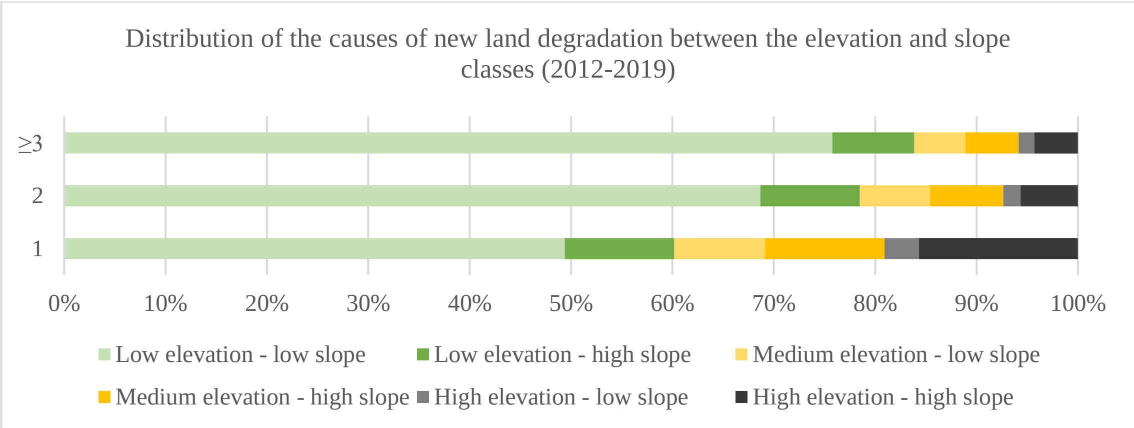

Figure 78. Distribution of the causes of new land degradation between the elevation and slope classes (2012-2019).

Land degradation in coastal area

The increase in degradation in the coastal area is higher than the national average in all the considered buffer zones (Figure 79). In the first 100 m from the coast, the percentage of territory affected by 3 or more degradation factors is quadruple compared to the national average, while in the first 1000 m the percentage of the area affected by two sources of degradation is three times the national average. The areas not affected by degradation are just over 40%, compared to a national value of about 70%.

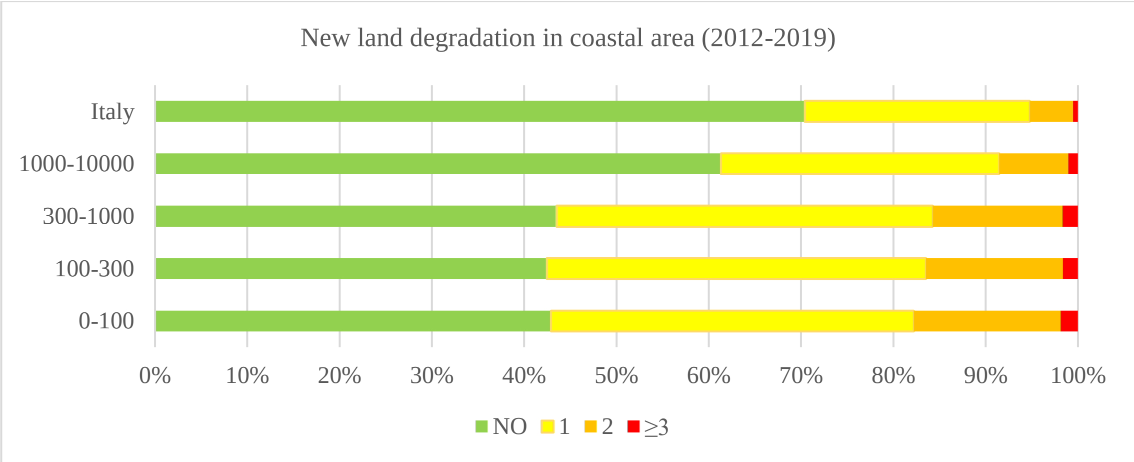

Figure 79. Distribution of the causes of new land degradation in coastal area, due to one (yellow), two (orange) or at least three (red) causes of degradation (2012-2019).

The analysis of the spatial distribution of land degradation shows that the areas most affected by the phenomenon are the most accessible: the coastline, the lowland areas, the areas near large cities and the main communication routes. In the protected areas there are increases of degradation lower than the national average, but not negligible especially in the protected areas near the large centers and the coast.

5 Conclusions and future perspectives

Land cover monitoring is a fundamental activity to provide spatial data for comprehensive assessment and mapping of ecosystem services, thus offering a helpful tool to support decision-making activities (Maes *et al.*, 2013).
The analysis carried out in the previous paragraphs shows how in recent years the Copernicus Programme has guaranteed the introduction of numerous spatial data useful for environmental monitoring and planning. Currently, however, these products have limitations in terms of spatial resolution, extension, update frequency and compatibility between different classification systems. These problems are even clearer if we analyse the products available in Italy on a national and regional level. Conducting analyses that involve the integration or the comparison of different data is often complex, due to the heterogeneity of the available informations. For studies on a national or interregional scale, the homogeneous data available for Italy are reduced to CORINE Land Cover, the High Resolution Layers and, for artificial surfaces, the National Land Consumption Map.

In Europe, numerous initiatives have been launched aiming at making spatial data homogeneous from a topological and thematic point of view and modular from the point of view of information content. In this sense, tools such as the INSPIRE directive, the EAGLE model and the CLC+ constitute essential references in defining the specifications of future products.

Conducting research related to the study of land cover in this historical period cannot ignore the aforementioned factors. So, the developed classification methodology seeks to provide a tool to allow overcoming the limits of current spatial data on one hand and, on the other hand, to be as aligned as possible with the European and national initiatives in the field of land monitoring.

The first goal of the research was creating a land cover classification methodology able of providing nationwide products with high spatial resolution and accuracy. The application of this methodology allowed producing a map for the whole Italian territory, with a spatial resolution of 10 m, a minimum mapping unit of 100 m^2 and an overall accuracy of 83%.

The approach based on decision rules guarantees controlling the choices adopted for the classification, and a high level of modularity. So, the rules can be refined inserting variable thresholds according to the characteristics of the area, such as latitude and phytoclimatic zone, but it is also possible to modify the rules or define new ones, allowing the classification to be improved each time new information is acquired, for example introducing new classes or considering new input data. The versatility of the algorithm and classification system make the methodology suitable for future integrations and to adapt to specific purposes, while keeping consistency with the requirements proposed at European level.

A first future development of the methodology involves introducing a specific class to describe shrubland. This will allow to increase the accuracy and get a more precise delimitation of forest areas, transition areas and Mediterranean vegetation. Even the vineyards, which are currently included in the broad-leaved class, would also be better placed in the shrubs class. This requires an in-depth analysis of the spectral behaviour of shrubs, which is easily confused with sparse trees or with herbaceous vegetation mixed with trees. The inclusion of this class would also prove useful for many applications (change detection studies) and to analyse ecosystem transformation. A further future development foresees a more detailed distinction of forest types, exploiting the new data of "Hyperspectral Imaging Mission for the Environment" (CHIME).

The methodology also includes rules for change detection monitoring. Classes characterized by clearly distinguishable changes within a year were considered, due to the availability of a limited historical series of Sentinel data at the time of the research. In detail, forest disturbances and land consumption classes were considered, however in the future we could be able to test the algorithm on a larger historical series of Sentinel data and refine change detection systems for other land cover classes as well. The identification of forest disturbances on a national scale shows difficulties related to the spatial variability of the phenomenon. In Mediterranean coppice forests, the recovery of vegetation activity takes place rapidly after cutting, therefore, to highlight these changes it is necessary to monitor them shortly after the cut (Chirici *et al.*, 2020). In the alpine forests of northern Italy selective felling is additionally applied and it is characterized by a different spectral response compared to coppice woods.

When fully operational, it will be possible to update the map annually or even more frequently, defining a basic land cover map and updating it integrating new changes. A similar approach allows to reduce errors associated with spectral variability, atmospheric disturbances and geometric errors that would arise from the comparison of two land cover maps for the extraction of changes.

The proposed method uses completely free tools and data. The whole process was developed using the Google Earth Engine platform, open source GIS tools and Sentinel data.

The characteristics of products obtainable applying the methodology meet the institutional needs indicated in the Mirror Copernicus initiative of the Space Economy Strategic Plan. This plan is promoted by the Italian Ministry of Economic Development and provides frequently updated products at a national scale and with Sentinel resolution, for monitoring as well as for government of the territory.

The map is also compatible with the CLC+ project and can be included among the national products to create instances within the Core component of CLC+. Compared to the HRL data, a product of this type would allow to identify detailed subclasses, specific to national needs.

These data can also be used as ancillary data to develop algorithms to monitor and characterize specific classes, such as detailed distinction of forest types, characterization of agricultural areas or a more detailed analysis of forest disturbances. It can be a useful support in producing forest map, as per Article 15 of Legislative Decree 03/04/2018 n. 34.

The methodology is therefore promising, thanks to the simplicity of the approach and the ability to apply it to large areas, while maintaining high spatial resolution and accuracy levels. In this sense, it is unique in the panorama of European and national land cover monitoring products.

The second part of the research involved the analysis of a set of indicators to describe the state and evolution of urban areas. In recent decades, these areas have been found to be characterized by the greatest dynamism and associated to the greatest impacts.

The analysis of the SDG indicators has highlighted the importance of having updated and homogeneous input data to develop reliable and comparable indicators among different countries.

The need for a monitoring tool with high update frequency and high spatial resolution is necessary to analyse other phenomena related to land consumption, such as the degree of fragmentation and the spatial evolution of settlement types. The emerging picture is characterized by a constant increase in land degradation, sprawl and fragmentation of natural areas which are well described through the National Land Consumption Map.

Land consumption, land degradation and loss of ecosystem functions go on unsustainably and protection and restoration of the ecosystems will be the key to a new plan for recovery and resilience of our country. This path should take place especially in the most degraded areas and in urban environments where the majority of population is concentrated and will have to be supported by the definition of a homogeneous policy framework at national level.

The innovations introduced by the Copernicus Programme in terms of data, analysis tools and new standards for sharing and classifying spatial information, offer new perspectives in producing data with high spatial detail, high updating frequency and strong interoperability. The novelty of these products and infrastructures can make producing new methodologies complex but there is plenty of new chances, thanks to the wide range of subjects involved, also at a national level, such as the investment planned for the Mirror Copernicus initiative as part of the "Space Economy" plan. These factors are essential in defining consistent and reliable monitoring systems that allow to produce effective responses to environmental pressures and to define a solid development model based on sustainability.

References

Alberti M (2005) The effects of urban patterns on ecosystem function, *International regional science review*, 28(2), pp. 168–192.
Anderson JR (1977) Land use and land cover changes-A framework for monitoring. *J. Res. US Geology Survey*, 5, 142-152.
Arnold S, Kosztra B, Banko G, Smith G, Hazeu G, Bock M (2013) The EAGLE concept – A vision of a future European Land Monitoring Framework, *EARSeL Symposium proceedings 2013, Towards Horizon 2020*, pp. 551–568.
Ballère M, Bouvet A, Mermoz S, Le Toan T, Koleck T, Bedeau C, André M, Forestier E, Frison PL, Lardeux C (2021) SAR data for tropical forest disturbance alerts in French Guiana: Benefit over optical imagery, *Remote Sensing of Environment*, 252, pp. 112-159.
Ban Y, Yousif O (2016) Change detection techniques: A review, *Multitemporal Remote Sensing*, pp. 19–43.
Banskota A, Kayastha N, Falkowski MJ, Wulder MA, Froese RE, White JC (2014) Forest Monitoring Using Landsat Time Series Data: A Review, *Canadian Journal of Remote Sensing*. Taylor & Francis, pp. 362–384. DOI: 10.1080/07038992.2014.987376.
Barbano A, Corsini S, Mandrone S, Rotunno M, La Mantia CBV (2006) Tecniche e metodi di studio dello stato delle coste in ambiente GIS. Available at: https://www.amazon.it/Tecnichemetodistudiodelloambiente/dp/B07RT6QJSX.
Baret F, Weiss M (2018) Gio Global Land Component - Lot I "Operation of the Global Land Component" Algorithm Theoretical Basis Document, pp. 1–41.
Belgiu M, Drăguţ L (2016) Random forest in remote sensing: A review of applications and future directions, *ISPRS Journal of Photogrammetry and Remote Sensing*, 114, pp. 24–31.
Berhane TM, Lane, CR, Wu Q, Autrey BC, Anenkhonov OA, Chepinoga VV, Liu H (2018) Decision-tree, rule-based, and random forest classification of high-resolution multispectral imagery for wetland mapping and inventory, *Remote Sensing*, 10(4). DOI: 10.3390/rs10040580.
Bovolo F, Bruzzone L (2007) A split-based approach to unsupervised change detection in large-size multitemporal images: Application to tsunami-damage assessment, *IEEE Transactions on Geoscience and Remote Sensing*, 45(6), pp. 1658–1670.
Bovolo F, Bruzzone L, Marconcini M (2008) A novel approach to unsupervised change detection based on a semisupervised SVM and a similarity measure, *IEEE Transactions on Geoscience and Remote Sensing*, 46(7), pp. 2070–2082.
Breiman L, Friedman J, Stone CJ, Olshen RA (1984) Classification and regression trees. *CRC press*.
Breiman L (2001) Random forests, *Machine learning*, 45(1), pp. 5–32.
Büttner G, Kostztra B, Soukup T, Sousa A, Langanke T (2017) CLC2018 Technical Guidelines, (3436), pp. 0–60.
Camps-Valls G, Tuia D, Gómez-Chova L, Jiménez S, Malo J (2011) Remote sensing image processing, *Synthesis Lectures on Image, Video, and Multimedia Processing*, 5(1), pp. 1–192.
Cao Y, Su C, Yang G (2014) Detecting the number of buildings in a single high-resolution SAR image, *European Journal of Remote Sensing*, 47(1), pp. 513–535.
Ceccarelli T, Bajocco S, Perini L, Salvati L (2014) Urbanisation and land take of high quality

agricultural soils-exploring long-term land use changes and land capability in Northern Italy. *International Journal of Environmental Research*, 8(1), pp. 181-192. DOI: 10.22059/ijer.2014.707

Celik N (2018) Change detection of urban areas in Ankara through Google Earth engine, in *2018 41st International Conference on Telecommunications and Signal Processing (TSP)*. IEEE, pp. 1–5.

Chang CI (2003) Hyperspectral imaging: techniques for spectral detection and classification. *Springer Science & Business Media*.

Chen Y, Gong P (2013) Clustering based on eigenspace transformation - CBEST for efficient classification, *ISPRS Journal of Photogrammetry and Remote Sensing*, 83, pp. 64–80. DOI: 10.1016/j.isprsjprs.2013.06.003.

Chirici G, Giannetti F, Mazza E, Francini S, Travaglini D, Pegna R, White JC (2020) Monitoring clearcutting and subsequent rapid recovery in Mediterranean coppice forests with Landsat time series. *Annals of Forest Science*, 77, pp. 1–14.

Clark DA, Brown S, Kicklighter DW, Chambers JQ, Thomlinson JR, Ni J, Holland EA (2001) Net primary production in tropical forests: An evaluation and synthesis of existing field data, *Ecological Applications*, 11(2), pp. 371–384. DOI: 10.1890/1051-0761(2001)011[0371:NPPITF]2.0.CO;2.

Clevers JGPW, Gitelson AA (2013) Remote estimation of crop and grass chlorophyll and nitrogen content using red-edge bands on Sentinel-2 and-3, *International Journal of Applied Earth Observation and Geoinformation*, 23, pp. 344–351.

Cochran WG, William G (1977) Sampling Techniques. New York: John Wiley& Sons. Inc.

Colditz RR (2015) An evaluation of different training sample allocation schemes for discrete and continuous land cover classification using decision tree-based algorithms, *Remote Sensing*, 7(8), pp. 9655–9681.

Coluzzi R, Imbrenda V, Lanfredi M, Simoniello T (2018) A first assessment of the Sentinel-2 Level 1-C cloud mask product to support informed surface analyses, *Remote sensing of environment*, 217, pp. 426–443.

Comitato per il Capitale Naturale (2018) *Secondo rapporto sullo stato del capitale naturale in Italia*, Roma.

Comitato per il Capitale Naturale (2019) *Terzo rapporto sullo stato del capitale naturale in Italia*, Roma.

Congedo L (2016) Semi-automatic classification plugin documentation, *Release*, 4(0.1), p. 29.

Conservation International (2020) Trends Earth Documentation. Available at: http://trends.earth/docs/en/pdfs/Trends.Earth.pdf.

Coppin P, Jonckheer I, Nackaerts K, Muys B, Lambin E (2004) Review ArticleDigital change detection methods in ecosystem monitoring: a review, *International journal of remote sensing*, 25(9), pp. 1565–1596.

Costanza R, D’Arge R, De Groot R , Farberll S, Grassot M, Hannon B, Limburg K, Naeem S, Neilltt RVO, Paruelo J, Raskin RG, Sutton P (1997) The value of the world’s ecosystem services and natural capital, *Nature*, 387115(May), pp. 253–260, DOI: 10.1038/387253a0.

De Fioravante P, Luti T, Cavalli A, Giuliani C, Di Chicco P, Marchetti M, Chirici G, Congedo L, Munafò M (2021) Multispectral Sentinel-2 and SAR Sentinel-1 integration for automatic land cover classification. Land, 10(6), 611, https://doi.org/10.3390/land10060611.

Dozier J (1989) Spectral signature of alpine snow cover from the Landsat Thematic Mapper, *Remote sensing of environment*, 28(1), pp. 9–22.

Drusch M, Del Bello U, Carlier S, Colin O, Fernandez V, Gascon F, Hoersch B, Isola C,

Laberinti P, Martimort P, Meygret A, Spoto F, Sy O, Marchese F, Bargellini P (2012) Sentinel-2: ESA's optical high-resolution mission for GMES operational services, *Remote sensing of Environment*, 120, pp. 25–36.
EAGLE (2020) Explanatory Documentation of the EAGLE Concept, May.
EEA (2015) Copernicus Land Monitoring Service - High Resolution Layer Small Woody Features – 2015 Product Specifications, pp. 1-30. Available at: land.copernicus.eu.
EEA (2017a) HRL Forest 2018 Product User Manual. Available at: https://www.eea.europa.eu/data-and-maps/data/copernicus-land-monitoring-service-eu-dem.
EEA (2017b) HRL Grassland 2018 Product User Manual. Available at: https://www.eea.europa.eu/data-and-maps/data/copernicus-land-monitoring-service-eu-dem.
EEA (2017c) HRL Imperviousness 2018 Product User Manual. Available at: https://www.eea.europa.eu/data-and-maps/data/copernicus-land-monitoring-service-eu-dem.
EEA (2017d) HRL Water & Wetness 2018 Product User Manual. Available at: https://www.eea.europa.eu/data-and-maps/data/copernicus-land-monitoring-service-eu-dem.
EEA (2017e) Landscape fragmentation indicator effective mesh density (Seff). Available at: https://sdi.eea.europa.eu/catalogue/srv/eng/catalog.search#/metadata/98d63709-5a79-44a8-ac5b-fd9a08466bf1.
EEA (2017f) Landscapes in transition: An account of 25 years of land cover change in Europe. Report 10/2017. Luxemburg. DOI:10.2800/81075.
EEA (2018a) Land systems at European level - analytical assessment framework. Available at:https://www.eea.europa.eu/themes/landuse/land-systems#:~:text=Land%20systems%20at%20European%20level%20%E2%80%94%20analytical%20assessment%20framework,-PDF&text=Land%20and%20soil%20provide%20vital,provide%20cultural%20and%20spiritual%20benefits.
EEA (2018b) Nomenclature And Mapping Guideline. Copernicus Land Monitoring Service Local Component: Natura 2000 Mapping, (1.3).
EEA (2019) Land take - Indicator specification. Available at: https://www.eea.europa.eu/data-and-maps/indicators/land-take-3 (Accessed: 24 April 2021).
EEA (2020) Explanatory Documentation of the EAGLE Concept. Copenhagen.
ESA (2021) Level-2A Algorithm Overview. Available at: https://sentinels.copernicus.eu/web/sentinel/technical-guides/sentinel-2-msi/level-2a/algorithm.
European Commission (2002) Communication From The Commission To The Council, The European Parliament, The Economic And Social Committee And The Committee Of The Regions "Toward s a Thematic Strategy for Soil Protection", COM(2002) 179 final, Brussels, 16.4.2002.
European Commission (2011) Roadmap to a Resource Efficient Europe. Communication from the Commision to the European Parliament, the Council and the European Economic and Social Committee and the Committee of the Regions, *European Commission*, pp. 1–26.
European Commission (2013) Guidelines on best practice to limit, mitigate or compensate soil sealing, 01(01), pp. 1689–1699.
European Commission (2016) Mapping Guide Urban Atlas, pp. 1–39, available at: https://land.copernicus.eu/user-corner/technical-library/urban-atlas-mapping-guide.

European Commission (2020) Communication From The Commission To The European Parliament, The Council, The European Economic And Social Committee And The Committee Of The Regions "EU Biodiversity Strategy for 2030", COM(2020) 380 final, Brussels, 20.5.2020.

European Council (2020) Special meeting of the European Council (17-21 July 2020) - Conclusions, 2020(EUCO 10/20). Available at: https://www.consilium.europa.eu/media/45109/210720-euco-final-conclusions-en.pdf.

European Council (2020) European Council meeting (10 and 11 December 2020) – Conclusions (EUCO 22/20) Brussels, 11 December 2020.

European Union (2013) Decision No 1386/2013/EU of the European Parliament and of the Council of 20 November 2013 on a General Union Environment Action Programme to 2020 “Living well, within the limits of our planet”, *Official Journal of the European Union*, (1600), pp. 171–200. Available at: http://eur-lex.europa.eu/legal-content/EN/TXT/PDF/?uri=CELEX:32013D1386&from=EN.

FAO (2016) Map accuracy assessment and area estimation : a practical guide, *National forest monitoring assessment working paper*, E(46).

FAO and ITPS (2020) Global Soil Organic Map V1.5: Technical Report. Rome, FAO. DOI: https://doi.org/10.4060/ca7597en.

Fares S, Sanesi G, Vacchiano G, Salbitano F, Marchetti M (2020) Le foreste urbane ai tempi del COVID-19 ci proteggono dalle polveri sottili, *Forest@-Journal of Silviculture and Forest Ecology*, 17(1), p. 48.

Flores-Anderson AI, Herndon KE, Thapa RB, Cherrington E (2019) The SAR Handbook: Comprehensive Methodologies for Forest Monitoring and Biomass Estimation. DOI: 10.25966/nr2c-s697.

Foody GM, Mathur A (2006) The use of small training sets containing mixed pixels for accurate hard image classification: Training on mixed spectral responses for classification by a SVM, *Remote Sensing of Environment*, 103(2), pp. 179–189.

Formaggio AR, Epiphanio JCN, Simões M dos S. (2001) Radarsat backscattering from an agricultural scene, *Pesquisa Agropecuária Brasileira*, 36(5), pp. 823–830.

Giannetti F, Pegna R, Francini S, McRoberts RE, Travaglini D, Marchetti M, Scarascia Mugnozza G, Chirici G (2020) A New Method for Automated Clearcut Disturbance Detection in Mediterranean Coppice Forests Using Landsat Time Series, *Remote Sensing*, 12(22), p. 3720.

Goldblatt R, Deininger K, Hanson G (2018) Utilizing publicly available satellite data for urban research: Mapping built-up land cover and land use in Ho Chi Minh City, Vietnam, *Development Engineering*, 3, pp. 83–99.

Gómez C, White JC, Wulder M (2016) ‘Optical remotely sensed time series data for land cover classification: A review, *ISPRS Journal of Photogrammetry and Remote Sensing*, 116, pp. 55–72. DOI: 10.1016/j.isprsjprs.2016.03.008.

Gulácsi A, Kovács F (2020) Sentinel-1-imagery-based high-resolutionwater cover detection on wetlands, aided by google earth engine, *Remote Sensing*, 12(10), pp. 1–20. DOI: 10.3390/rs12101614.

Haas J, Ban Y (2017) Sentinel-1A SAR and sentinel-2A MSI data fusion for urban ecosystem service mapping’, *Remote Sensing Applications: Society and Environment*, 8, pp. 41–53.

Haines-Young R (2009) Land use and biodiversity relationships, *Land use policy*, 26, pp. S178–S186.

Hansen MC, Loveland TR (2012) A review of large area monitoring of land cover change using Landsat data, *Remote sensing of Environment*, 122, pp. 66–74.

Herold M (2009) Essential Climate Variables - Assessment of the Status of the Development

of the standards for the Terestrial Essential Climate Variables, Roma: GTOS Segretariat.
Holloway J, Helmstedt KJ, Mengersen K, Schmidt M (2019) A decision tree approach for spatially interpolating missing land cover data and classifying satellite images, *Remote Sensing*, 11(15). DOI: 10.3390/rs11151796.
Holtgrave AK, Röder N, Ackermann A, Erasmi S, Kleinschmit B (2020) Comparing Sentinel-1 and -2 data and indices for agricultural land use monitoring, *Remote Sensing*, 12(18). DOI: 10.3390/RS12182919.
Hoskera AK, Nico G, Irshad Ahmed M, Whitbread A (2020) Accuracies of soil moisture estimations using a semi-empirical model over bare soil agricultural croplands from sentinel-1 SAR data, *Remote Sensing*, 12(10), p. 1664.
Houhoulis PF, Michener WK (2000) Detecting wetland change: A rule-based approach using NWI and SPOT-XS data, *Photogrammetric Engineering and Remote Sensing*, 66(2), pp. 205–211.
Huang X, Liu J, Zhu W, Atzberger C, Liu Q (2019) The optimal threshold and vegetation index time series for retrieving crop phenology based on a modified dynamic threshold method, *Remote Sensing*, 11(23), pp. 1–22. DOI: 10.3390/rs11232725.
Hussain M, Chen D, Cheng A, Wei H, Stanley D (2013) Change detection from remotely sensed images: From pixel-based to object-based approaches, *ISPRS Journal of photogrammetry and remote sensing*, 80, pp. 91–106.
ISPRA (2015) Il consumo di suolo in Italia - Edizione 2015. *Rapporti 218/2015*. Roma: ISPRA. ISBN: 978-88-448-0703-0.
ISPRA (2018a) Annuario dei dati ambientali - Biosfera. *Stato dell'Ambiente 84/2019*. Roma: ISPRA. ISBN: 978-88-448-0939-3.
ISPRA (2018b) Annuario dei dati ambientali - Geosfera. *Stato dell'Ambiente 84/2019*. Roma: ISPRA. ISBN: 978-88-448-0939-3.
ISPRA (2018c) Qualità dell’ambiente urbano - XIV Rapporto. *Stato dell'Ambiente 82/2018*. Roma: ISPRA. ISBN: 978-88-448-0926-3.
ISPRA (2018d) Territorio- Processi e trasformazioni in Italia. *Rapporti 296/2018*. Roma: ISPRA. ISBN: 978-88-448-0921-8.
ISPRA (2019a) Annuario dei dati ambientali - Biosfera. *Stato dell'Ambiente 89/2020*. Roma: ISPRA. ISBN: 978-88-448-0975-1.
ISPRA (2019b) Annuario dei dati ambientali - Geosfera. *Stato dell'Ambiente 89/2020*. Roma: ISPRA. ISBN: 978-88-448-0975-1.
ISPRA (2019c) Qualità dell’Ambiente Urbano – XV Rapporto. *Report SNPA n. 13/2020*. Roma: ISPRA. ISBN: 978-88-448-0973-7
ISTAT (2014) Principali Dimensioni Geostatiche e grado di urbanizzazione del Paese. Available at: https://www.istat.it/it/archivio/137001.
ISTAT (2018) Italian statistical yearbook, National Institute of Statistics. Available at: https://www.istat.it/it/files/2018/12/Asi2018.pdf.
ISTAT (2020) Popolazione Residente. Available at: http://demo.istat.it/.
Jacobson CR (2011) Identification and quantification of the hydrological impacts of imperviousness in urban catchments: A review, *Journal of environmental management*, 92(6), pp. 1438–1448.
Jaeger JAG (2000) Landscape division, splitting index, and effective mesh size: new measures of landscape fragmentation, *Landscape Ecology*, 15, pp. 115–130.
Jaeger JAG, Tappeiner (2007) Article in press for the journal Landscape Ecology Modification of the effective mesh size for measuring landscape fragmentation to solve the boundary problem, *Landscape Ecology*, March. DOI: 10.1007/s10980-006-9023-0.
JARAS (1993) Remote Sensing Note. *Japan Association on Remote Sensing*. Available at: https://books.google.it/books?id=rar2GgAACAAJ.

Jarvis A, Guevara E, Reuter HI, Nelson AD (2008) Hole-filled SRTM for the globe: version 4: data grid.

Johnson RD, Kasischke ES (1998) Change vector analysis: A technique for the multispectral monitoring of land cover and condition, *International Journal of Remote Sensing*, 19(3), pp. 411–426.

Key CH, Benson NC (1999) The Normalized Burn Ratio (NBR): A Landsat TM radiometric measure of burn severity, *United States Geological Survey, Northern Rocky Mountain Science Center*, Bozeman, MT.

Kleeschulte S (2019) Technical specifications for implementation of a new land-monitoring concept based on EAGLE. D5: Design concept and CLC+ Backbone, technical specifications, CLC+ Core and CLC+ Instances draft specifications, including requirements review Version 5.4.

Koppel K, Zalite K, Voormansik K, Jagdhuber T (2017) Sensitivity of Sentinel-1 backscatter to characteristics of buildings, *International Journal of Remote Sensing*, 38(22), pp. 6298–6318. DOI: 10.1080/01431161.2017.1353160.

Kotsiantis SB, Zaharakis I, Pintelas P (2007) Supervised machine learning: A review of classification techniques, *Emerging artificial intelligence applications in computer engineering*, 160(1), pp. 3–24.

Kuenzer C, Ottinger M, Wegmann, Guo H, Wang C, Zhang J, Dech S, Wikelski M (2014) Earth observation satellite sensors for biodiversity monitoring: potentials and bottlenecks, *International Journal of Remote Sensing*, 35(18), pp. 6599–6647. DOI: 10.1080/01431161.2014.964349.

Kulkarni AD, Lowe B (2016) Random Forest Algorithm for Land Cover Classification International Journal on Recent and Innovation Trends in Computing and Communication Random Forest Algorithm for Land Cover Classification, *International Journal on Recent and Innovation Trends in Computing and Communication*, 4(3).

Lary D J, Alavi AH, Gandomi AH, Walker AL (2016) Machine learning in geosciences and remote sensing, *Geoscience Frontiers*, 7(1), pp. 3–10. DOI: 10.1016/j.gsf.2015.07.003.

Liu Y, Gong W, Hu X, Gong J (2018) Forest type identification with random forest using Sentinel-1A, Sentinel-2A, multi-temporal Landsat-8 and DEM data, *Remote Sensing*, 10(6), pp. 1–25. DOI : 10.3390/rs10060946.

Liu K, Shi W, Zhang H (2011) A fuzzy topology-based maximum likelihood classification, *ISPRS Journal of Photogrammetry and Remote Sensing*, 66(1), pp. 103–114. DOI: 10.1016/j.isprsjprs.2010.09.007.

Lu D, Mausel P, Brondizio E, Moran E (2004) Change detection techniques, *International journal of remote sensing*, 25(12), pp. 2365–2401.

Luti T, De Fioravante P, Marinosci I, Strollo A, Riitano N, Falanga V, Mariani L, Congedo L, Munafò M (2021) Land Consumption Monitoring with SAR Data and Multispectral Indices. *Remote Sensing*, 13(1586), pp. 1–26. DOI: https://doi.org/10.3390/rs13081586.

Maes J, Teller A, Erhard M, Liquete C, Braat L, Berry P, Egoh B, Puydarrieus P, Fiorina C, Santos F, Paracchini ML, Keune H, Wittmer H, Hauck J (2013) An analytical framework for ecosystem assessments under action 5 of the EU biodiversity strategy to 2020, Publications office of the European Union, Luxembourg. DOI: 10.2779/12398.

Magnaghi A (1990) Il territorio dell'abitare, Lo sviluppo locale come alternativa strategica. Milano: Franco Angeli.

Mansaray LR, Huang W, Zhang D, Huang J, Li J (2017) Mapping rice fields in urban Shanghai, southeast China, using Sentinel-1A and Landsat 8 datasets, *Remote Sensing*, 9(3). DOI: 10.3390/rs9030257.

Mather PM, Koch M (2011) Computer processing of remotely-sensed images: an introduction. John Wiley & Sons.

Maxwell AE, Warner TA, Vanderbilt BC, Ramezan CA (2017) Land cover classification and feature extraction from national agriculture imagery program (NAIP) Orthoimagery: A Review, *Photogrammetric Engineering & Remote Sensing*, 83(11), pp. 737–747.

McFeeters SK (1996) The use of the Normalized Difference Water Index (NDWI) in the delineation of open water features, *International Journal of Remote Sensing*, 17(7), pp. 1425–1432. DOI: 10.1080/01431169608948714.

McFeeters SK (2013) Using the normalized difference water index (ndwi) within a geographic information system to detect swimming pools for mosquito abatement: A practical approach, *Remote Sensing*, 5(7), pp. 3544–3561. DOI: 10.3390/rs5073544.

McGarigal K, SA Cushman, and EE (2012) FRAGSTATS v4: Spatial Pattern Analysis Program for Categorical and Continuous Maps. Computer software program produced by the authors at the University of Massachusetts, Amherst. Available at: http://www.umass.edu/landeco/research/fragstats/fragstats.html.

Modzelewska A, Fassnacht F. E, Stereńczak K (2020) Tree species identification within an extensive forest area with diverse management regimes using airborne hyperspectral data, *International Journal of Applied Earth Observation and Geoinformation*, 84, p. 101960.

Moreira A, Prats-Iraola P, Younis M, Krieger G, Hajnsek I, Papathanassiou KP (2013) A tutorial on synthetic aperture radar, *IEEE Geoscience and remote sensing magazine*, 1(1), pp. 6–43.

Moser G, Serpico SB (2006) Generalized minimum-error thresholding for unsupervised change detection from SAR amplitude imagery, *IEEE Transactions on Geoscience and Remote sensing*, 44(10), pp. 2972–2982.

Munafò M (2018) Consumo di Suolo, dinamiche territoriali e servizi ecosistemici - Edizione 2018. *Rapporti 288/2018.* Roma: ISPRA. ISBN: 978-88-448-0902-7.

Munafò M (2019) Consumo di suolo, dinamiche territoriali e servizi ecosistemici. Edizione 2019. Report SNPA n. 8/2019. Roma: ISPRA. ISBN: 978-88-448-0964-5.

Munafò M (2020) Consumo di suolo, dinamiche territoriali e servizi ecosistemici. Edizione 2020. Report SNPA n. 15/2020. Roma: ISPRA. ISBN: 978-88-448-1013-9.

Nemmour H, Chibani Y (2006) Multiple support vector machines for land cover change detection: An application for mapping urban extensions, *ISPRS Journal of Photogrammetry and Remote Sensing*, 61(2), pp. 125–133.

Nezry E (2014) Adaptive speckle filtering in radar imagery, *Land Applications of Radar Remote Sensing; IntechOpen: London, UK*, pp. 1–55.

Nielsen MA (2015) Neural networks and deep learning. *Determination press* San Francisco, CA.

Olofsson P, Foody GM, Herold M, Stehman SV, Woodcock CE, Wulder MA (2014) Good practices for estimating area and assessing accuracy of land change, *Remote Sensing of Environment*, 148, pp. 42–57. DOI: 10.1016/j.rse.2014.02.015.

Otukei JR, Blaschke T (2010) Land cover change assessment using decision trees, support vector machines and maximum likelihood classification algorithms, *International Journal of Applied Earth Observation and Geoinformation*, 12(SUPPL. 1), pp. 27–31. DOI: 10.1016/j.jag.2009.11.002.

Panagos P, Ballabio C, Borrelli P, Meusburger K, Klik A, Rousseva S, Tadić MP, Michaelides S, Hrabalíková M; Olsen P; Aalto J; Lakatos M; Rymszewicz A; Dumitrescu AC (2015) Rainfall erosivity in Europe, *Science of the Total Environment*, 511, pp. 801–814. DOI: 10.1016/j.scitotenv.2015.01.008.

Panagos P, Borrelli P, Meusburger K, Alewell C, Lugato E, Montanarella L (2015)

Estimating the soil erosion cover-management factor at the European scale, *Land Use Policy*, 48, pp. 38–50. DOI: 10.1016/j.landusepol.2015.05.021.

Panagos P, Borrelli P, Meusburger K (2015) A new European slope length and steepness factor (LS-factor) for modeling soil erosion by water, *Geosciences (Switzerland)*, 5(2), pp. 117–126. DOI: 10.3390/geosciences5020117.

Panagos P, Borrelli P, Poesen J, Ballabio C, Lugato E, Meusburger K, Montanarella L, Alewell C (2015) The new assessment of soil loss by water erosion in Europe, *Environmental Science and Policy*, 54, pp. 438–447. DOI: 10.1016/j.envsci.2015.08.012.

Panagos P, Meusburger K, Ballabio C, Borrelli P, Alewell C (2014) Soil erodibility in Europe: A high-resolution dataset based on LUCAS, *Science of the Total Environment*, 479–480(1), pp. 189–200. DOI: 10.1016/j.scitotenv.2014.02.010.

Pepe M, Pompilio L, Gioli B Busetto L, Boschetti M (2020) Detection and Classification of Non-Photosynthetic Vegetation from PRISMA Hyperspectral Data in Croplands, *Remote Sensing*, 12(23), p. 3903.

Persson M, Lindberg E, Reese H (2018) Tree species classification with multi-temporal Sentinel-2 data, *Remote Sensing*, 10(11), pp. 1–17. DOI: 10.3390/rs10111794.

Pesaresi M, Corbane C, Julea A, Florczyk AJ, Syrris V, Soille P (2016) Assessment of the added-value of Sentinel-2 for detecting built-up areas, *Remote Sensing*, 8(4), p. 299.

Puletti N, Bascietto M (2019) Towards a tool for early detection and estimation of forest cuttings by remotely sensed data, *Land*, 8(4), p. 58.

Radke RJ, Andra S, Al-Kofahi O, Roysam B (2005) Image change detection algorithms: a systematic survey, *IEEE transactions on image processing*, 14(3), pp. 294–307.

Rast M, Ananasso C, Bach H, Dor E., Chabrillat S, Colombo R, Bello U, Feret J, Giardino C, Green R, Guanter L, Marsh S, Nieke J, Ong C, Rum G, Schaepman M, Schlerf M, Skidmore A, Strobl P (2019) Copernicus Hyperspectral Imaging Mission for the Environment-Mission Requirements Document, *European Space Agency, ESA-EOPSM-CHIM-MRD-3216*, (2.1).

Reba M, Seto KC (2020) A systematic review and assessment of algorithms to detect, characterize, and monitor urban land change, *Remote Sensing of Environment*, 242, p. 111739.

Renard KG (1997) Predicting soil erosion by water: a guide to conservation planning with the Revised Universal Soil Loss Equation (RUSLE). United States Government Printing.

Richards JA (1999) *Remote sensing digital image analysis*. Springer. DOI: 10.1007/978-3-642-30062-2.

Riitano N, Dichicco P, De Fioravante P, Cavalli A, Falanga V, Giuliani C, Mariani L, Strollo A, Munafò M (2020) Land consumption in italian coastal area, *Environmental Engineering & Management Journal (EEMJ)*, 19(10), p. 1857-1868. ISSN 1843-3707.

del Río-Mena T, Willemen L, Vrielin A, Nelson, A (2020) Understanding intra-annual dynamics of ecosystem services using satellite image time series, *Remote Sensing*, 12(4). DOI: 10.3390/rs12040710.

Rodriguez-Galiano VF, Chica-Olmo M, Abarca-Hernandez F, Atkinson PM, Jeganathan C (2012) Random Forest classification of Mediterranean land cover using multi-seasonal imagery and multi-seasonal texture, *Remote Sensing of Environment*, 121, pp. 93–107. DOI: 10.1016/j.rse.2011.12.003.

Rouse Jr JW (1973) Monitoring the vernal advancement and retrogradation (green wave effect) of natural vegetation.

Sallustio L, Marchetti M, Ottaviano M, Pazzagli R (2013) Consumo di suolo e analisi dei cambiamenti del paesaggio nei Parchi nazionali d'Italia. *Territorio: 66, 3, 2013*, pp.

121–131.
Sallustio L, Munafò M, Riitano N, Lasserre B, Fattorini L, Marchetti M (2016) Integration of land use and land cover inventories for landscape management and planning in Italy, *Environmental Monitoring and Assessment*, 188(1), pp. 1–20. DOI: 10.1007/s10661-015-5056-7.
Semikolennykh AA (2008) European thematic strategy for soil protection: a review of major documents, *Eurasian Soil Science*, 41(12), pp. 1349–1351.
Siedentop S, Meinel G (2004) CORINE Land Cover 2000 in nation-wide and regional monitoring of urban land use and land consumption, in *Berlin, UBA-Texte Workshop CORINE Land cover*, pp. 162–169.
Sims NC, Green C, Newnham GJ, England JR, Held A, Wulder MA Herold M, Cox SJD, Huete AR, Kumar L, Viscarra-Rossel RA, Roxburgh SH, McKenzie NJ (2017) Good Practice Guidance: SDG Indicator 15.3.1. Version 1.0, September, pp. 1–115. Available at: https://www.unccd.int/sites/default/files/relevant-links/2017-10/Good Practice Guidance_SDG Indicator 15.3.1_Version 1.0.pdf.
Singh A. (1989) Review article digital change detection techniques using remotely-sensed data, *International journal of remote sensing*, 10(6), pp. 989–1003.
Sinha P, Kumar L (2013) Independent two-step thresholding of binary images in inter-annual land cover change/no-change identification, *ISPRS Journal of Photogrammetry and Remote Sensing*, 81, pp. 31–43. DOI: 10.1016/j.isprsjprs.2013.03.010.
Spadoni GL, Cavalli A, Congedo L, Munafò M (2020) Analysis of Normalized Difference Vegetation Index (NDVI) multi-temporal series for the production of forest cartography, *Remote Sensing Applications: Society and Environment*, 20(August). DOI: 10.1016/j.rsase.2020.100419.
Stehman SV, Foody GM (2019) Key issues in rigorous accuracy assessment of land cover products, *Remote Sensing of Environment*, 231(June), p. 111199. DOI: 10.1016/j.rse.2019.05.018.
Stehman SV, Czaplewski RL (1998) Design and Analysis for Thematic Map Accuracy Assessment - an application of satellite imagery, *Remote Sensing of Environment*, 64(January), pp. 331–344.
Strollo A, Smiraglia D, Bruno R, Assennato F, Congedo L, De Fioravante P, Giuliani C, Marinosci I, Riitano N, Munafò M (2020) Land consumption in Italy, *Journal of Maps*, 16(1), pp. 113–123.
Sun Z, Xu R, Du W, Wang L, Lu D (2019) High-resolution urban land mapping in China from sentinel 1A/2 imagery based on Google Earth Engine, *Remote Sensing*, 11(7), p. 752. DOI: 10.3390/rs11070752.
Tamame M, Lorenzo A, Lindmayer A, Richter R, Ramminger G, Köpp W, Larsson K, Cristvall C, Ahlkrona E, Martin C, Risquez T, Cano F, Martinez A (2018) Riparian Zones Nomenclature Guideline Production, 2012(3464), p. 235.
Tarquini S, Isola I, Favalli M, Mazzarini F, Bisson M, Pareschi MT, Boschi E (2007) TINITALY/01: A new Triangular Irregular Network of Italy, *Annals of Geophysics*, 50(3), pp. 407–425. DOI: 10.4401/ag-4424.
Tewkesbury AP, Comber AJ, Tate NJ, Lamb A, Fisher PF (2015) A critical synthesis of remotely sensed optical image change detection techniques, *Remote Sensing of Environment*, 160, pp. 1–14.
Thanh Noi P, Kappas M (2018) Comparison of random forest, k-nearest neighbor, and support vector machine classifiers for land cover classification using Sentinel-2 imagery, *Sensors*, 18(1), p. 18.
Thonfeld F, Feilhauer H, Braun M, Menz G (2016) Robust Change Vector Analysis (RCVA) for multi-sensor very high resolution optical satellite data, *International Journal of*

Applied Earth Observation and Geoinformation, 50, pp. 131–140.
Torres R, Snoeij P, Geudtner D, Bibby D, Davidson M, Attema E, Potin P, Rommen B, Floury N, Brown M, Traver I, Deghaye P, Duesmann B, Rosich B, Miranda N, Bruno C, L'Abbate M, Croci R, Pietropaolo A, Huchler M, Rostan F (2012) 'GMES Sentinel-1 mission', *Remote Sensing of Environment*, 120, pp. 9–24.
UN (2012) The future we want. DOI: 10.1017/s0251107x00015583.
UN (2016) The 2030 Agenda for sustainable development, *Transforming the world: The 2030 agenda for sustainable development*, pp. 12–14. DOI: 10.1201/b20466-7.
UN (2017) *Transforming our world: the 2030 Agenda for Sustainable Development*, *Governing Through Goals: Sustainable Development Goals as Governance Innovation*. DOI: 10.1057/978-1-137-45443-0_24.
UN (2021) SDG indicator 11.3.1 metadata, March. Available at: https://unstats.un.org/sdgs/metadata/?Text=&Goal=&Target=11.3.
Vangi E, D'amico G, Francini S, Giannetti F, Lasserre B, Marchetti M, Chirici G (2021) The new hyperspectral satellite prisma: Imagery for forest types discrimination, *Sensors (Switzerland)*, 21(4), pp. 1–19. DOI: 10.3390/s21041182.
Verburg PH, Erb KH, Mertz O, Espindola G (2013) Land System Science: between global challenges and local realities, *Current opinion in environmental sustainability*, 5(5), pp. 433–437.
Volpi M, Tuia D, Bovolo F, Kanevski M, Bruzzone L (2013) Supervised change detection in VHR images using contextual information and support vector machines, *International Journal of Applied Earth Observation and Geoinformation*, 20, pp. 77–85.
Vrebos D, Bampa F, Creamer RE, Gardi C Ghaley BB, Jones A, Rutgers M, Sandén T, Staes J, Meire P (2017) The impact of policy instruments on soil multifunctionality in the European Union, *Sustainability*, 9(3), p. 407.
Wischmeier WH, Smith DD (1978) Predicting rainfall erosion losses: a guide to conservation planning. Department of Agriculture, Science and Education Administration.
Xin Q, Li J, Li Z, Li Y, Zhou X (2020) Evaluations and comparisons of rule-based and machine-learning-based methods to retrieve satellite-based vegetation phenology using MODIS and USA National Phenology Network data, *International Journal of Applied Earth Observation and Geoinformation*, 93(July), p. 102189. DOI: 10.1016/j.jag.2020.102189.
Zhou T, Pan J, Zhang P, Wei S, Han T (2017) Mapping winter wheat with multi-temporal SAR and optical images in an urban agricultural region, *Sensors (Switzerland)*, 17(6), pp. 1–16. DOI: 10.3390/s17061210.
Zhu Z, Gallant AL, Woodcock CE, Pengra B, Olofsson P, Loveland TR, Jin S, Dahal D, Yang Limin, Auch RF (2016) Optimizing selection of training and auxiliary data for operational land cover classification for the LCMAP initiative, *ISPRS Journal of Photogrammetry and Remote Sensing*, 122, pp. 206–221. DOI: 10.1016/j.isprsjprs.2016.11.004.
Zhu Z (2017) Change detection using landsat time series: A review of frequencies, preprocessing, algorithms, and applications, *ISPRS Journal of Photogrammetry and Remote Sensing*, 130, pp. 370–384.
Zhu Z, Woodcock CE (2014) Continuous change detection and classification of land cover using all available Landsat data, *Remote sensing of Environment*, 144, pp. 152–171.
Zitti M, Ferrara C, Perini L, Carlucci M, Salvati L (2015) Long-term urban growth and land use efficiency in Southern Europe: Implications for sustainable land management. *Sustainability*, *7*, 3359–3385. DOI:10.3390/su7033359.

List of papers

1. Congedo L, Assennato F, Bruno R, Ciocci C, De Fioravante P, Di Leginio M, Giuliani C, Luti T, Marinosci I, Milano G, Pellegrino P, Pranzo S, Soraci M, Strollo A, Raudner A, Trogu D, Munafò M (2018) Il consumo di suolo e la crescita urbana. In ISPRA (2018) *Consumo di suolo, dinamiche territoriali e servizi ecosistemici*, Edizione 2018, Roma: ISPRA, pp. 14-36.

2. Congedo L, De Fioravante P, Di Leginio M, Iadanza C, Marinosci I, Pranzo S, Strollo A, Trigila A, Munafò M (2018) La distribuzione territoriale del consumo di suolo. In ISPRA (2018) *Consumo di suolo, dinamiche territoriali e servizi ecosistemici*, Edizione 2018, Roma: ISPRA, pp. 37-50.

3. Strollo A, Assennato F, Braca G, Cavalli A, De Fioravante P, Di Leginio M, Marchetti M, Sallustio L, Soraci M, Munafò M (2018) La perdita di servizi ecosistemici. In ISPRA (2018) *Consumo di suolo, dinamiche territoriali e servizi ecosistemici*, Edizione 2018, Roma: ISPRA, pp. 59-61.

4. Munafò M, Marinosci I, Pranzo S, Bruno R, Congedo L, De Fioravante P, Strollo A (2018) Consumo di suolo e frammentazione. *Tredicesima conferenza nazionale di statistica,* Roma (Italy), July, 4-6.

5. Munafò M, Marinosci I, Bruno R, Congedo L, De Fioravante P, Strollo A (2018) Copertura del suolo. *Tredicesima conferenza nazionale di statistica,* Roma (Italy), July, 4-6.

6. Comitato Capitale Naturale (2018), *Secondo Rapporto sullo Stato del Capitale Naturale in Italia*. Roma.

7. ISPRA (2018), Territorio. Processi e trasformazioni in Italia. Edizione 2018, *Rapporti 296/2018*, Roma: ISPRA, ISBN 978-88-448-0921-8.

8. Angelini P, Arcangeli A, Capogrossi R, Carnevali L, De Fioravante P, Di Leginio M, Ercole S, Finocchiaro G, Genovesi P, Giacanelli V, Grignetti A, Laureti L, Licheri D, Marinosci I, Munafò M, Nardelli R, Piccini C, Pranzo S, Spina F (2019) Biosfera. In ISPRA (2019) *Stato dell'ambiente 84/2019,* Roma: ISPRA, pp. 2-8, ISBN 978-88-448-0939-3.

9. Araneo F, Bartolucci E, Carta R, Dacquino C, De Fioravante P, Di Leginio M, Fumanti F, Finocchiaro G, Cristina Giovagnoli MC, Teresa Lettieri MT, Luise A, Marinosci I, Martarelli L, Munafò M, Pascarella F, Patane'A (2019) Geosfera. In ISPRA (2019) *Stato dell'ambiente 84/2019*, Roma: ISPRA, pp. 2-8, ISBN 978-88-448-0939-3.

10. Munafò M, Assennato F, Congedo L, De Fioravante P, Di Leginio M, Marinosci I, Raudner A, Soraci M, Pranzo S, Strollo A (2018) Il consumo di suolo. In ISPRA (2018) *XIV Rapporto Qualità dell'ambiente urbano*, Edizione 2018, Roma: ISPRA, pp. 57-68, ISBN 978-88-448-0926-3.

11. Munafò M, De Fioravante P, Bruno R, Congedo L, Strollo A, Marinosci I, Giuliani C, Riitano N, Pecci A (2019) Monitoring of Land Cover in Italy through remote sensing. *XXIX Congresso Nazionale S.It.E (Società Italiana di Ecologia),* Ferrara (Italy), September, 10-12.

12. Soraci M, Assennato F, Bruno R, Congedo L, De Fioravante P, Di Leginio M, Marinosci I, Munafò M, Pranzo S, Strollo A, (2018) Soil Sealing and Urban Growth in Italy. *World Forum on Urban Forests*, Mantova (Italy).

13. Munafò (a cura di) (2019), Consumo di suolo, dinamiche territoriali e servizi ecosistemici. Edizione 2019, *Report SNPA 08/2019*, Roma:ISPRA, ISBN 978-88-448-0964-5.

14. Riitano N, Dichicco P, De Fioravante P, Cavalli A, Falanga V, Giuliani C, Mariani L, Strollo A, Munafò M, (2020) Land consumption in italian coastal area. *Environmental Engineering and Management Journal*. 19(10), p. 1857-1868. ISSN 1843-3707.

15. Strollo A, Smiraglia D, Bruno R, Assennato F, Congedo L, De Fioravante P, Giuliani C, Marinosci I, Riitano N, Munafò M (2019) Land Consumption in Italy. *Journal of Maps*, 16:1, pp. 113-123, DOI: 10.1080/17445647.2020.1758808.

16. Comitato Capitale Naturale (2019), *Terzo Rapporto sullo Stato del Capitale Naturale in Italia*. Roma.

17. ISPRA-SNPA (2020) Biosfera. In ISPRA (2020) *Stato dell'ambiente 89/2020*, ISBN 978-88-448-0975-1.

18. ISPRA-SNPA (2020) Geosfera. In ISPRA (2020) *Stato dell'Ambiente 89/2020* (ed.), ISBN 978-88-448-0975-1.

19. ISPRA-SNPA (2020) Consumo di suolo, dinamiche territoriali e servizi ecosistemici. Edizione 2020. *Report SNPA 15/2020*, ISBN 978-88-448-1013-9.

20. ISPRA-SNPA (2020). XV Rapporto sulla qualità dell'ambiente urbano. Edizione 2019 (2019). *Report SNPA 13/2020*, ISBN 978-88-448-0996-6.

21. Assennato F, Strollo A, D'Antona M, De Fioravante P, Cavalli A, Munafò M, (2019) Soil ecosystem services assessment to support land use planning - applications in Italy and a reflection for the future. *AESOP annual congress 2019 Planning for transition*, Venice, July, 9-13.

22. Munafò M, Assennato F, Congedo L, d'Antona M, De Fioravante P, Di Leginio M, Giuliani C, Marinosci I, Riitano N e Strollo A (2021) Indicatori e mappatura delle dinamiche urbane e del degrado del territorio - Sessione: Le statistiche ambientali per la ripartenza sostenibile dei territori. *AIQUAV 2020/21 – Libro degli Abstract*.

23. Luti T, De Fioravante P, Marinosci I, Strollo A, Riitano N, Falanga V, Marani L, Congedo L, Munafò M (2021) Land consumption monitoring with SAR data and multispectral indices. *Remote Sens*, 13, 1586, https://doi.org/ 10.3390/rs13081586.

24. De Fioravante P, Luti T, Cavalli A, Giuliani C, Di Chicco P, Marchetti M, Chirici G, Congedo L, Munafò M (2021) Multispectral Sentinel-2 and SAR Sentinel-1 integration for automatic land cover classification. *Land*, 10(6), 611, https://doi.org/10.3390/land10060611.

25. De Fioravante P, Luti T, Cavalli A, Giuliani C, Di Chicco P, Congedo L, Munafò M (2021) Monitoraggio del consumo e della copertura del suolo tramite immagini Sentinel-1 e Sentinel-2 a cura del Sistema Nazionale per la Protezione dell'Ambiente. In CRCS (2018) *Suolo, servizi ecosistemici e infrastrutture verdi*. Awaiting publication

26. De Fioravate P, Cimini A (2021) Multispectral Sentinel-2 and SAR Sentinel-1 integration for automatic land cover classification and land consumption monitoring with SAR data and multispectral indices. *Earth Technology Expo*, Florence (Italy), October, 13-16.